Universidade de Aveiro Departamento de Biologia
Ano 2013

Ana Luísa Mendes dos Santos

Stress induzido por UV no bacterioneuston: mecanismos e implicações ecológicas

UV-induced stress in bacterioneuston: mechanisms and ecological implications

Universidade de Aveiro Departamento de Biologia
Ano 2013

Ana Luísa Mendes dos Santos

Stress induzido por UV no bacterioneuston: mecanismos e implicações ecológicas

UV-induced stress in bacterioneuston: mechanisms and ecological implications

Tese apresentada à Universidade de Aveiro para cumprimento dos requisitos necessários à obtenção do grau de Doutor em Biologia, realizada sob a orientação científica da Professora Doutora Maria Ângela Sousa Dias Alves Cunha, Professora Auxiliar do Departamento de Biologia da Universidade de Aveiro e sob a coorientação científica do Professor Doutor António Carlos Matias Correia, Professor Catedrático do Departamento de Biologia da Universidade de Aveiro.

Apoio financeiro da FCT e do FSE no âmbito do III Quadro Comunitário de Apoio.

Referência da bolsa:
SFRH/BD/40160/2007

o júri

presidente

Prof. Doutor Fernando Joaquim Fernandes Tavares Rocha
professor catedrático do Departamento de Geociências da Universidade de Aveiro

Prof. Doutor António Carlos Matias Correia
professor catedrático do Departamento de Biologia da Universidade de Aveiro

Prof. Doutor Carlos Manuel Correia
professor associado da Escola de Ciências da Vida e do Ambiente da Universidade de Trás-os-Montes e Alto Douro

Prof. Doutora Paula Maria de Melim Vasconcelos de Vitorino Morais
professora auxiliar da Faculdade de Ciências e Tecnologia da Universidade de Coimbra

Prof. Doutora Célia Maria Manaia Rodrigues
professora auxiliar da Escola Superior de Biotecnologia da Universidade Católica Portuguesa

Prof. Doutora Maria Ângela Sousa Dias Alves Cunha
professora auxiliar do Departamento de Biologia da Universidade de Aveiro

Prof. Doutora Maria do Amparo Ferreira Faustino
professora auxiliar do Departamento de Química da Universidade de Aveiro

Doutor Newton Carlos Marcial Gomes
investigador auxiliar do CESAM e Departamento de Biologia da Universidade de Aveiro

agradecimentos

À Professora Doutora Ângela Cunha, orientadora desta tese, o meu profundo reconhecimento pelo excecional apoio e confiança no desenvolvimento deste trabalho.

Ao Professor Doutor António Correia, coorientador desta tese, o meu sincero agradecimento pelo interesse, envolvimento e ideias inspiradoras.

À Professora Doutora Isabel Henriques, pela permanente disponibilidade e incansável acompanhamento.

À Professora Doutora Ivonne Delgadillo, pelas muitas horas que conseguiu dispensar para colaborar num dos capítulos deste trabalho e pelo entusiasmo contagiante.

À Professora Doutora Adelaide Almeida e ao Doutor Newton C. M. Gomes pelo incentivo e colaboração.

À Doutora Alexandra Moura pelo apoio científico e pelos valiosos ensinamentos transmitidos.

Ao Doutor Thomas Jové pela abertura à colaboração e contributo enriquecedor para um dos capítulos deste trabalho.

À Professora Doutora Amparo Faustino e à Professora Doutora Rosário Correia pela revisão de dois dos capítulos incluídos nesta tese.

À Catarina Moreirinha, Inês Baptista, Sílvia Lopes e Susana Machado pela preciosa contribuição no trabalho laboratorial.

À minha amiga e colega Vanessa Oliveira, pelas viagens, aventuras e por todo o apoio, no laboratório e fora dele.

Aos elementos dos laboratórios de Microbiologia Ambiental e Aplicada, Microbiologia Molecular e Ecologia Molecular e Ambientes Marinhos, por contribuírem para um ambiente de trabalho agradável e intelectualmente estimulante.

À Universidade de Aveiro, por fornecer as instalações para a realização deste trabalho.

À Fundação para a Ciência e Tecnologia (FCT) e CESAM (Centro de Estudos do Ambiente e do Mar) pelo financiamento.

Aos meus pais e irmão, pelo apoio, compreensão e paciência.

palavras-chave

Radiação UV, microcamada superficial, bactéria, bacterioneuston, bacterioplâncton, espécies reativas de oxigénio (*reactive oxygen species* [ROS]), marcadores de *stress* oxidativo, reparação de lesões, filogenia molecular

resumo

As bactérias desempenham um papel chave na reciclagem de energia e matéria nas teias tróficas aquáticas. No entanto, as suas pequenas dimensões, curto tempo de geração e o facto de os seus genomas constituírem uma grande porção do seu volume celular, tornam as bactérias mais suscetíveis às alterações ambientais que os organismos superiores. O aumento dos níveis de radiação UVB (280-320 nm) constitui uma ameaça particularmente importante para as comunidades bacterianas dos sistemas aquáticos, uma vez que a radiação consegue penetrar até profundidades consideráveis. No entanto, os mecanismos através dos quais a radiação causa danos nas bactérias ainda não são claros, o que impede a modelação precisa dos efeitos da radiação UV nas comunidades bacterianas naturais. O bacterioneuston habita a microcamada superficial (primeiro milímetro da coluna de água), estando naturalmente exposto a níveis de radiação UV superiores aos que o bacterioplâncton está exposto. Deste modo, a microcamada superficial pode ser vista como um nicho ecológico modelo para estudar as interações entre as bactérias e a radiação UV.

Os objetivos deste trabalho foram (i) avaliar a influência do nível de exposição natural à radiação das comunidades bacterianas na sua sensibilidade à radiação UV, através da comparação das respostas fotobiológicas do bacterioneuston e bacterioplâncton; (ii) aprofundar o conhecimento acerca dos mecanismos através dos quais a radiação UV causa danos, bem como dos fatores que afetam a interação entre a radiação UV e as bactérias; e (iii) avaliar o potencial da proteína RecA, que medeia a resposta SOS das bactérias, para ser usada como marcador de danos induzidos por UV nas comunidades bacterianas.

Verificou-se que o bacterioneuston é mais resistente à radiação UVB que o bacterioplâncton e recupera de modo mais eficiente dos danos induzidos por UV, particularmente em condições de escassez de nutrientes, indicando assim que o nível de exposição natural das comunidades bacterianas à radiação afeta a sua sensibilidade à radiação UV. Os resultados das análises independentes do cultivo revelaram o potencial da radiação UV para afetar a estrutura das comunidades bacterianas ao selecionar bactérias resistentes. A análise do perfil de utilização de fontes de carbono usando o sistema de Ecoplacas Biolog ® e a determinação das taxas de incorporação de leucina e timidina permitiu também verificar que a radiação UV modifica o funcionamento das comunidades bacterianas. Os resultados obtidos indicam a possibilidade do bacterioneuston conter um conjunto de estirpes resistentes a UV que, mediante as condições meteorológicas apropriadas, podem ser selecionadas aquando da exposição à radiação.

A determinação dos efeitos da radiação UV de diferentes comprimentos de onda na abundância e atividade bacterianas, bem como nos níveis de vários marcadores de *stress* oxidativo (produção de ROS, quebra de cadeias do DNA, peroxidação lipídica e carbonilação proteica), permitiu verificar que a sobrevivência aquando da exposição à radiação UVA (320-400 nm), UVB e UVC (100-280 nm) é determinada pela extensão dos danos ao nível do DNA, oxidação lipídica e níveis intracelulares de ROS, respetivamente. Adicionalmente, estudos de espetroscopia do infravermelho revelaram uma variedade de modificações oxidativas, composicionais e estruturais nos lípidos e proteínas das bactérias com a irradiação.

Usando diferentes antioxidantes, verificou-se que o oxigénio singleto desempenha um papel crucial na inativação das bactérias durante a exposição à radiação UVB, potencialmente devido à sua participação na oxidação lipídica. Verificou-se também que a adição de metais, particularmente ferro, cobre e manganês, acentua a inativação das bactérias durante a exposição à radiação UVB, o que sugere que a homeostasia dos níveis de metais na célula durante a irradiação é crucial para atenuar os efeitos nocivos dos ROS. Experiências conduzidas com estirpes bacterianas incubadas a diferentes temperaturas (15 ºC e 25 ºC), em diferentes fases de crescimento (fase exponencial e estacionária) e diferentes meios de cultura (rico e pobre em nutrientes) revelaram que as condições de crescimento são determinantes cruciais da extensão dos danos oxidativos induzidos pela exposição à radiação UVB nas bactérias. Verificou-se também que o ambiente abiótico (conteúdo em nutrientes e qualidade do meio de suspensão) das comunidades bacterianas influencia a sua sensibilidade à radiação UVB.

O estudo da filogenia da proteína RecA revelou grande coerência com a filogenia do gene 16S rRNA, demonstrando uma elevada conservação da proteína, e não qualquer adaptação particular à resistência ao *stress*. Vários plasmídeos contendo homólogos do gene *recA* ainda não descritos na literatura foram identificados e a análise do contexto genómico revelou a possibilidade dos genes *recA* presentes nos plasmídeos poderem complementar os genes *recA* cromossomais na resposta SOS.

No seu conjunto, os resultados obtidos neste trabalho fornecem novas perspetivas acerca da fotobiologia ambiental das comunidades bacterianas. Novas informações acerca dos mecanismos e fatores que influenciam os efeitos inibitórios da radiação UV nas bactérias foram também obtidas. Esta informação poderá ajudar a uma melhor compreensão da interação entre as bactérias e radiação UV no contexto das alterações globais, bem como o desenvolvimento de tecnologias de desinfeção baseadas em UV mais eficientes.

keywords

UV radiation, surface microlayer, bacteria, bacterioneuston, bacterioplankton, reactive oxygen species (ROS), oxidative stress markers, lesion repair, molecular phylogeny.

abstract

Bacteria play a key role in the cycling of energy and matter in aquatic food webs. However, their small size, short generation time and the fact that their genomes make up a large portion of their cellular volume, make bacteria more susceptible to environmental changes than higher organisms. Increased UVB radiation (280-320 nm) levels pose a particularly important threat to bacterial communities in aquatic systems, due to the ability of radiation to penetrate to considerable depths. However, the mechanisms of UV-induced damage to bacteria are still not clear, preventing the accurate modelling of the effects of UV radiation on natural bacterial communities. Located at the sunlit surface microlayer (SML, top millimetre of the water column), bacterioneuston is naturally exposed to higher levels of UV radiation than the bacterioplankton bellow. Therefore, the SML can be viewed as a model ecological niche to study the interaction between bacteria and UV radiation.

The objectives of this work were (i) to study the influence of the light history of bacterial communities in their UV sensitivity, by comparing the photobiological responses of bacterioneuston and bacterioplankton; (ii) to gain further insights into the mechanisms of UV-induced damage, as well as the factors that affect the interaction between UV radiation and bacteria; and (iii) to assess the potential role of the SOS response mediator RecA protein as a marker of UV-induced damage in bacteria.

Bacterioneuston was found to be more resistant to UVB radiation than bacterioplankton and to recover more efficiently from UV-induced damage, particularly under nutrient depleted conditions, thus indicating that the light history of bacterial communities influences their UV sensitivity. Results from culture-independent analysis suggest that UV radiation can affect bacterial community structure by selecting for UV-resistant bacteria. UV radiation was also found to modify the functioning of bacterial communities, as indicated by sole-carbon-source use profiling with Biolog EcoPlates^{TM}, as well as leucine and thymidine incorporation measurements. The results obtained indicate the possibility that bacterioneuston may contain a pool of UV resistant strains that, under appropriate meteorological conditions, may be selected for upon UV exposure.

By measuring the effects of UV radiation of different wavelengths in bacterial abundance, activity, as well as several oxidative stress markers (ROS generation, DNA strand breakage, lipid peroxidation and protein carbonylation), survival under UVA (320-400 nm), UVB and UVC (100-280 nm) wavelengths was found to be best explained by the extent of DNA damage, oxidative damage to lipids, and intracellular ROS levels, respectively.

Additionally, mid-infrared spectroscopy revealed an array of oxidative, compositional and structural modifications in the lipids and proteins of bacteria following irradiation.

Singlet oxygen was found to play a pivotal role in UVB-induced cell inactivation, potentially due to its effects in lipid peroxidation, as revealed by using specific ROS scavengers. Metal amendment, particularly with iron, copper and manganese, was found to enhance bacterial inactivation during UVB exposure, thus suggesting that metal homeostasis during irradiation is crucial to attenuate the detrimental effects of ROS. Experiments with bacterial strains grown at different temperatures (15 ºC and 25 ºC), growth phases (exponential and stationary) and growth media (nutrient-rich and nutrient-poor) revealed that growth conditions preceding irradiation are pivotal in determining the extent of the oxidative damage induced by UVB exposure. The abiotic environment (nutrient content and quality of the suspension medium) of bacterial communities was also found to influence their UVB sensitivity.

The study of the phylogeny of the RecA protein revealed high coherence with that of the 16S rRNA gene, reflecting high evolutionary conservation of the protein, rather than particular adaptations to stress resistance. Several plasmids containing *recA* homologs not yet reported in the literature were identified, and gene context analysis suggested that plasmid-encoded *recA* genes could complement the activity of chromosome-encoded *recA* genes in the bacterial SOS response.

Taken together, the results obtained in the present work provide new insights into the environmental photobiology of bacterial communities. New information regarding the mechanisms and factors influencing the inhibitory effects of UV radiation on bacteria was also acquired. This information may contribute for a better understanding of the interaction between UV radiation and bacteria in the context of environmental changes, as well as the development of more efficient UV-based disinfection technologies.

"It's clear to me that if you wiped all multicellular life-forms off the face of the Earth, microbial life might shift a tiny bit; if microbial life were to disappear, that would be it - instant death for the planet."

Carl Woese, *The New York Times*, 1996

Stress induzido por UV no bacterioneuston: mecanismos e implicações ecológicas

UV-induced stress in bacterioneuston: mechanisms and ecological implications

List of Original Publications

This thesis includes results which have already been published in the journals listed below:

Santos, A. L., Lopes, S., Baptista, I., Henriques, I., Gomes, N. C. M., Almeida, A., Correia, A. & Cunha, A. 2011. Diversity in UV sensitivity and recovery potential among bacterioneuston and bacterioplankton isolates. *Letters in Applied Microbiology*, 52, 360-366.

Santos, A. L., Baptista, I., Lopes, S., Henriques, I., Gomes, N. C. M., Almeida, A., Correia, A. & Cunha, A. 2012. The UV responses of bacterioneuston and bacterioplankton isolates depend on the physiological condition and involve a metabolic shift. *FEMS Microbiology Ecology*, 80, 646-658.

Santos, A. L., Gomes, N. C. M., Henriques, I., Almeida, A., Correia, A. & Cunha, Â. 2012. Contribution of reactive oxygen species to UVB-induced damage in bacteria. *Journal of Photochemistry and Photobiology B: Biology*, 117, 40-46.

Santos, A. L., Oliveira, V., Baptista, I., Henriques, I., Gomes, N. C. M., Almeida, A., Correia, A. & Cunha, A. 2012. Effects of UVB radiation on the structural and physiological diversity of bacterioneuston and bacterioplankton. *Applied and Environmental Microbiology*, 78, 2066-2069.

Santos, A. L., Oliveira, V., Baptista, I., Henriques, I., Gomes, N. C. M., Almeida, A., Correia, A. & Cunha, A. 2013. Wavelength dependence of biological damage induced by UV radiation on bacteria. *Archives of Microbiology*. 195, 63-74.

Santos, A. L., Gomes, N. C. M., Henriques, I., Almeida, A., Correia, A. & Cunha, A. Role of Transition Metals in UV-B Induced Damage to Bacteria. *Photochemistry and Photobiology* (accepted).

Santos, A. L., Gomes, N. C. M., Henriques, I., Almeida, A., Correia, A. & Cunha, A. Growth conditions influence UVB sensitivity and oxidative damage in an estuarine bacterial isolate. *Photochemical & Photobiological Sciences* (accepted).

Table of Contents

List of Figures 3

List of Tables 7

Abbreviation List 9

Thesis Outline 11

CHAPTER 1: Introduction 15

UV radiation 15

Depletion of the ozone layer 16

Effects of UV radiation on microorganisms 18

Mechanisms of UV-induced damage 19

Reactive oxygen species and the importance of metals 20

Cellular targets of UV radiation 22

Repair and protection strategies against UV-induced damage 25

Effects of UVR on bacterial communities 29

Factors influencing the responses of microorganisms to UVR 33

The surface microlayer (SML) as a model system for environmental photobiology studies 35

Objectives of this thesis 36

CHAPTER 2: Effects of UVB Radiation on the Structural and Physiological Diversity of Bacterioneuston and Bacterioplankton 39

CHAPTER 3: Diversity in UV-Sensitivity and Recovery Potential among Bacterioneuston and Bacterioplankton Isolates 45

CHAPTER 4: The UV Responses of Bacterioneuston and Bacterioplankton Isolates Depend on the Physiological Condition and Involve a Metabolic Shift 57

CHAPTER 5: Wavelength Dependence of Biological Damage Induced by UV Radiation on Bacteria 77

CHAPTER 6: Effects of UV Radiation on the Lipids and Proteins of Bacteria Studied by Mid-Infrared Spectroscopy 95

CHAPTER 7: Contribution of Reactive Oxygen Species to UVB-Induced Damage in Bacteria 113

CHAPTER 8: Role of Transition Metals in UVB-Induced Damage to Bacteria 129

CHAPTER 9: Influence of Water Properties on UVB Effects in Estuarine Bacteria 147

CHAPTER 10: Growth Conditions Influence UVB Sensitivity and Oxidative Damage in an Estuarine Bacterial Isolate 165

CHAPTER 11: The recA Gene on Bacterial Genomes: When one Chromosomal Gene is not a Universal Rule 187

CHAPTER 12: Discussion 207

Bacterioneuston as a model community for environmental photobiology studies 207

Effects of UVB radiation on bacterioneuston and bacterioplankton 208

Experimental considerations 210

Isolation of UV-resistant bacterioneuston and bacterioplankton 211

New insights into the mechanisms of UV-induced damage 212

Wavelength-dependence of UV-induced damage 213

Identity and targets of ROS in UVB-induced damage 216

Role of metals in UVB-induced damage 217

Factors influencing UVB-induced inactivation and their mechanisms of interaction 219

The role of RecA as an indicator of UV repair potential 222

CHAPTER 13: Conclusions 225

REFERENCES 227

APPENDIX 261

List of Figures

Fig. 1.1. Main types of DNA photoproducts resulting from exposure to UVB radiation: cyclobutane pyrimidine dimers (CPDs) and pyrimidine (6-4) pyrimidone photoproducts (6-4 PPs).. 23

Fig. 1.2. Main mechanisms involved in the repair of UV-induced DNA damage.. 26

Fig. 1.3. Catalytic cycle of the repair of bipyrimidine photoproducts by DNA photolyase.. 27

Fig. 2.1. UVB dose-dependent variation of (A) the abundance of culturable bacteria and (B) total prokaryote abundance. 40

Fig. 2.2. Representative DGGE gel of bacterioneuston and bacterioplankton exposed to different UVB doses (0, 12, 24, 36, 48, 60 kJ m^{-2}). 41

Fig. 2.3. Mean relative abundance (expressed as the percentage of total DAPI counts) of specific bacterial groups detected by FISH before and after exposure of bacterioneuston and bacterioplankton communities to a total dose of 60 kJ m^{-2} of UVB radiation. 42

Fig. 2.4. UVB dose-dependent variation of (A) leucine incorporation (protein synthesis) and (B) thymidine incorporation (DNA synthesis).. 43

Fig. 2.5. Mean relative consumptions of different substrate categories present in Biolog EcoPlates™ before and after exposure of bacterioneuston and bacterioplankton communities to a total dose of 60 kJ m^{-2} of UVB radiation. 44

Fig. 3.1. Effects of UVB radiation and reactivation under different light regimes on the culturability and activity (protein synthesis) of UV-resistant bacterioneuston isolates. 50

Fig. 3.2. Effects of UVB radiation and reactivation under different light regimes on the culturability and activity (protein synthesis) of UV-resistant bacterioplankton isolates..... 51

Fig. 4.1. Variation in CFU counts during exposure of bacterioneuston and bacterioplankton to UVB radiation. 65

Fig. 4.2. Phylogenetic tree based on 16S rRNA gene sequences showing the phylogenetic position of isolated strains (indicated by arrows)..... 67

Fig. 4.3. Effects of UV radiation on CFU counts (A), rate of leucine incorporation (B) and rate of thymidine incorporation (C) averaged for the sets of bacterioneuston and bacterioplankton isolates, evaluated under nourished or starvation conditions.. 68

Fig. 4.4. Relative consumption rates of substrates in Biolog EcoPlates™ before and after UV exposure, averaged for the sets of bacterioneuston (A) and bacterioplankton (B) isolates..... 68

Fig. 4.5. Recovery of CFU counts under UVA (A), PAR (B), dark (C), leucine incorporation under UVA (D), PAR (E), dark (F), and thymidine incorporation under UVA (G), PAR (H), dark (I) averaged for the sets of bacterioneuston and bacterioplankton isolates, evaluated under nourished or starvation conditions. 69

Fig. 4.6. Induction of Nal^R (A) and Rif^R (B) mutant phenotypes averaged for the sets of bacterioneuston and bacterioplankton isolates, evaluated under nourished or starvation conditions. 70

Fig. 4.7. Effects of UV radiation on CFU counts during two periods of UV exposure, used to assess the potential for photoadaptation, averaged for the sets of bacterioneuston (A) and bacterioplankton (B) isolates, evaluated under nourished or starvation conditions 71

Fig. 5.1. UV sensitivity curves for the bacterial isolates under the different UV spectral regions.. 84

Fig. 5.2. Effects of exposure to the LD_{50} of different UV spectral regions on bacterial activity.. 85

Fig. 5.3. Effects of exposure to the LD_{50} of different UV spectral regions on (A) intracellular ROS generation, (B) DSB, (C) TBARS levels, (D) protein carbonyl levels, (E) CAT and (F) SOD activity.. 86

Fig. 5.4. Principal component analysis (PCA) score plot of data (activity, ROS levels, lipid oxidation, protein oxidation, DNA lesions, CAT and SOD activity) used to determine the parameters contributing the most for the separation of UVA, UVB and UVC treatments.. 88

Fig. 6.1. Original spectra of lipid extracts of (A) *Acinetobacter* sp. PT5I1.2G, (B) *Pseudomonas* sp. NT5I1.2B, and protein extracts of (C) *Acinetobacter* sp. PT5I1.2G, (D) *Pseudomonas* sp. NT5I1.2B.. 100

Fig. 6.2. Difference spectra (irradiated-minus-control) for the lipid extracts of *Acinetobacter* sp. PT5I1.2G under UVA (A), UVB (B) and UVC (C) and *Pseudomonas* sp. NT5I1.2B under UVA (D), UVB (E) and UVC (F).. 101

Fig. 6.3. Scores and loading plots for PCA analysis of lipid extracts irradiated with different UV spectral regions of *Acinetobacter* sp. PT5I1.2G (A, B) and *Pseudomonas* sp. NT5I1.2B (C, D). 104

Fig. 6.4. Difference spectra (irradiated-minus-control) for the protein extracts of *Acinetobacter* sp. PT5I1.2G under UVA (A), UVB (B) and UVC (C) and *Pseudomonas* sp. NT5I1.2B under UVA (D), UVB (E) and UVC (F).. 106

Fig. 6.5. Scores and loading plots for PCA analysis of protein extracts irradiated with different UV spectral regions of *Acinetobacter* sp. PT5I1.2G (A, B) and *Pseudomonas* sp. NT5I1.2B (C, D). 109

Fig. 7.1. Effects of UVB exposure in (A) colony forming units (CFU) and (B) total bacterial number, in the presence and absence of different ROS scavengers. 120

Fig. 7.2. Effects of UVB exposure in (A) glucose incorporation and (B) respiration in the presence and absence of different ROS scavengers. 121

Fig. 7.3. Effects of UVB exposure in ROS generation in the presence and absence of different ROS scavengers. 122

Fig. 7.4. Effects of UVB exposure in DSB levels in the presence and absence of different ROS scavengers. 122

Fig. 7.5. Effects of UVB exposure in TBARS levels in the presence and absence of different ROS scavengers. 123

Fig. 7.6. Effects of UVB exposure in protein carbonyls levels in the presence and absence of different ROS scavengers..... 123

Fig. 8.1. Influence of transition metals on UVB inactivation curves of (A) *Micrococcus* sp., (B) *Paracoccus* sp., (C) *Pseudomonas* sp. and (D) *Staphylococcus* sp..... 137

Fig. 8.2. Variation of (A) cell survival and (B) glucose incorporation upon UVB exposure in cell suspensions unamended and amended with 1 µM of the different transition metals.. 139

Fig. 8.3. Variation of (A) ROS, (B) DSB, (C) TBARS and (D) carbonyl levels upon UVB exposure in cell suspensions unamended and amended with 1 µM of the different transition metals.. 139

Fig. 8.4. Variation of (A) CAT activity and (B) SOD activity upon UVB exposure in cell suspensions unamended and amended with 1 µM of the different transition metals..... 140

Fig. 9.1. Schematic representation of the experimental setup used to test the influence of nutrients and suspension media on the UV sensitivity responses of bacterioneuston, bacterioplankton and bacterial isolates..... 150

Fig. 9.2. Effects of different nutrient concentrations on (A) abundance and (B) activity (expressed as leucine incorporation) of bacterioneuston and bacterioplankton of marine and brackish origin..... 155

Fig. 9.3. Effects of irradiation on different media (AMS – artificial mineral solution, SML – surface microlayer, and UW – underlying water) on (A) abundance and (B) activity (expressed as leucine incorporation) of bacterioneuston and bacterioplankton of marine and brackish origin.. 157

Fig. 9.4. Effects of irradiation on different media (AMS – artificial mineral solution, SML – surface microlayer, and UW – underlying water) on (A) abundance and (B) activity (expressed as leucine incorporation) in bacterial isolates.. 158

Fig. 10.1. Growth curve of *Pseudomonas* sp. NT5I1.2B cultivated at 15 ºC and 25 ºC in (A) TSB and (B) M9 medium..... 173

Fig. 10.2. UVB survival curves of *Pseudomonas* sp. NT5I1.2B grown at 15 ºC and 25 ºC in TSB and M9 medium in (A) mid-exponential, (B) late-exponential and (C) stationary phase.. 174

Fig. 10.3. Dose-dependent variation of TBARS levels in *Pseudomonas* sp. NT5I1.2B grown at 15 ºC and 25 ºC in TSB and M9 medium in (A) mid-exponential, (B) late-exponential and (C) stationary phase..... 175

Fig. 10.4. Dose-dependent variation of DNA strand breaks (expressed as strand scission factor, SSF) in *Pseudomonas* sp. NT5I1.2B grown at 15 ºC and 25 ºC in TSB and M9 medium in (A) mid-exponential, (B) late-exponential and (C) stationary phase.. 176

Fig. 10.5. Dose-dependent variation of the levels of DNA-protein cross-links (DPC) in *Pseudomonas* sp. NT5I1.2B grown at 15 ºC and 25 ºC in TSB and M9 medium in (A) mid-exponential, (B) late-exponential and (C) stationary phase.. 177

Fig. 10.6. Dose-dependent variation of carbonyl levels in *Pseudomonas* sp. NT5I1.2B grown at 15 ºC and 25 ºC in TSB and M9 medium in (A) mid-exponential, (B) late-exponential and (C) stationary phase.. 178

Fig. 10.7. Graphical representation of the temporal variation of survival and markers of oxidative stress in *Pseudomonas* sp. NT5I1.2B upon exposure to low UVB doses (0-10 kJ m^{-2}).. 184

Fig. 11.1. Relative distribution of *recA* sequences considered in this study by phylum.. 191

Fig. 11.2. Phylogenetic tree of RecA proteins in Bacteria.. 194

Fig. 11.3. Phylogenetic tree of *recA* (A) and 16S rRNA (B) genes in *Gammaproteobacteria*.. 196

Fig. 11.4. Phylogenetic tree of *recA* (A) and 16S rRNA (B) genes in *Deltaproteobacteria*.. .. 199

Fig. 11.5. Phylogenetic tree of *recA* (A) and 16S rRNA (B) genes in Firmicutes.. 201

Fig. 11.6. Genomic context of *recA* in the plasmids of (A) *Serratia marcescens* strain B-6493 (plasmid pSM22) and (B) *Thermomicrobium roseum*. 204

List of Tables

Table 3.1. Origin, phylogenetic affiliation, sequence similarity to the closest relative and NCBI accession number of the UV-resistant bacterial isolates used in this study.. 48

Table 4.1. Phylogenetic affiliation, accession numbers, similarity with database and microbial classification of isolated strains..... 66

Table 5.1. Bacterial strains used in the experiments, their accession number, phylogenetic affiliation, closest relatives, similarity with database, as well as bacterial group and growth rates.. 79

Table 5.2. Multiple stepwise regression analysis used to determine the parameters that explained bacterial inactivation under the different UV spectral regions.. 88

Table 6.1. Bacterial strains used in the experiments, their accession number, phylogenetic affiliation, closest relatives, similarity with database, as well as bacterial group.. 98

Table 7.1. Bacterial strains used in the experiments, their closest relatives, 16S rRNA gene accession number bacterial group and UVB LD_{50} values. 115

Table 8.1. Bacterial strains used in the experiments, their closest relatives, accession number and bacterial group and UVB LD_{50} values. 131

Table 8.2. Absolute values of the different stress markers in unirradiated metal-amended and unamended cell suspensions..... 138

Table 8.3. Multiple stepwise regression analysis used to infer the parameters contributing to bacterial inactivation (expressed as LD_{50}) under the different treatments.. 141

Table 9.1. Physical and chemical properties of original samples collected from the marine (CN) and brackish water (I6) stations.. 154

Table 9.2. One-way ANOVA results (p value, n = 9) for the comparisons between different nutrient treatments and suspension media in each community from the two estuarine sites.. .. 155

Table 9.3. One-way ANOVA results (p value, n = 9) for the comparisons between the responses of bacterioneuston and bacterioplankton to the different treatments.. 156

Table 9.4. One-way ANOVA results (p value, n = 9) for the comparisons between the responses of the different treatments in each bacterial strain tested.. 159

Table 10.1. Initial characteristics (time to achieve a certain growth phase, optical density at 600 nm, total bacterial abundance and biovolume) of *Pseudomonas* sp. NT5I1.2B cultures under the different growth conditions.. 173

Table 11.1. *recA* genes containing introns or inteins..... 193

Table 11.2. Bacterial genomes containing multiple copies of the *recA* gene and comparisons between different *recA* copies from the same genome..... 198

Table 11.3. Bacterial genomes on which the G+C content of the *recA* gene showed relevant deviation (over 1.5 times the standard deviation of the genome) in relation to the G+C content of the whole genome.. 202

Table 11.4. Plasmids encoding RecA homologs, with indication of the hosts and G+C content 205

Abbreviation List

2,4-DNPH – 2,4-Dinitrophenylhydrazine

6-4 PPs – Pyrimidine (6-4) Pyrimidone Photoproducts

ADP – Adenosine Diphosphate

AMS – Artificial Mineral Solution

ATP – Adenosine Triphosphate

BER – Base Excision Repair

BHT – Butylhydroxytoluene

CAT – Catalase

CFCs – Chlorofluorocarbons

CFU – Colony Forming Unit

CPDs – Cyclobutane Pyrimidine Dimers

DGGE – Denaturing Gradient Gel Electrophoresis

DNA – Deoxyribonucleic Acid

DOC – Dissolved Organic Carbon

DOM – Dissolved Organic Matter

DPC – DNA-Protein Cross-Links

DSB – DNA Strand Breaks

FISH – Fluorescence *In Situ* Hybridization

MDR – Mutagenic DNA repair

NADH – Nicotinamide Adenine Dinucleotide

NER – Nucleotide Excision Repair

OD – Optical Density

ODSs – Ozone-depleting Substances

PAR – Photosynthetically Active Radiation

PCA – Principal Component Analysis

PCR – Polymerase Chain Reaction

PER – Photoenzymatic Repair

PMSF – Phenylmethylsulfonyl Fluoride

POC – Particulate Organic Carbon

POM – Particulate Organic Matter

PSCs – Polar Stratospheric Clouds

RNA – Ribonucleic Acid

ROS – Reactive Oxygen Species

SML – Surface Microlayer

SOD – Superoxide Dismutase

TBARS – Thiobarbituric Acid Reactive Substances

UV – Ultraviolet

UVR – UV Radiation

UW – Underlying Water

WMO – World Meteorological Organization

Thesis Outline

Microorganisms are highly responsive to environmental changes since their large surface-to-volume ratio facilitates close contact with the surrounding environment. Furthermore, due to their relatively short generation times, microbial communities are among the fastest components of an ecosystem to respond to environmental changes. UV radiation, in particular, can be highly detrimental for microorganisms inhabiting aquatic systems, since UV radiation can penetrate to considerable depths.

The surface microlayer (SML) represents the top millimetre of the water column. Due to its location and exposure to high levels of UV radiation (UVR), the SML could be viewed as an interesting niche to investigate the interaction between UV radiation and bacteria that could provide valuable predictive information on how bacterial communities respond to enhanced levels of UV radiation, in terms of function and structure. However, information on the comparative responses of bacterioneuston and bacterioplankton to UV radiation are still scarce in the literature. Likewise, information on the mechanisms that are initiated at the cellular level upon exposure to UV radiation, particularly the more biologically relevant UVB (280-320 nm), in different bacteria is also absent from the literature, preventing a thorough understanding of the consequences of UV radiation to natural bacterial communities, as well as the development of more efficient UV-based disinfection technologies. This work aimed to address this lack of information.

In **Chapter 1** a brief contextualization of the known mechanisms of UV-induced cellular damage and protection/repair, the role of UVR as a driver of the functioning and structure of bacterial communities and the relevance of bacterioneuston in environmental photobiology studies is presented.

Chapter 2 addresses the comparative effects of UVB radiation on the structure and function of bacterioneuston inhabiting the SML and bacterioplankton inhabiting underlying waters (UW). The results revealed that bacterial abundance and DNA synthesis were more affected in bacterioplankton, while protein synthesis was more inhibited in bacterioneuston. UVB exposure led to a reduction in ribotype diversity, demonstrating the potential of UVR to affect community structure, probably by selecting UV-resistant bacteria most notably belonging to *Gammaproteobacteria*, particularly abundant in bacterioneuston. These observations raise the hypothesis that

bacterioneuston may contain a pool of UV-resistant strains that are selected for upon UV exposure.

The comparative analysis of the UV responses of bacterioneuston and bacterioplankton is extended in **Chapters 3 and 4** which describe the isolation of UVB-resistant bacterial strains from both communities that were then tested for their individual UVB sensitivity. Bacterial numbers were more reduced by UVB in bacterioplankton, while leucine incorporation was more inhibited in bacterioneuston. UVB irradiation was accompanied by a shift in sole-carbon source use profiles, assessed with Biolog EcoPlates^{TM}, characterized by a reduction in consumption of amines and amino acids and increased use of polymers, particularly in bacterioneuston isolates. Recovery from UV-induced damage under starvation was generally enhanced compared to nourished conditions, especially in bacterioneuston isolates.

Chapter 5 describes the study of the wavelength dependence of UV-induced cellular damage in a set of bacterial isolates, used as tentative biological models. Biological effects (survival and activity) and molecular markers of oxidative stress (DNA strand breakage, generation of reactive oxygen species [ROS], oxidative damage to proteins and lipids, and the activity of the antioxidant enzymes catalase and superoxide dismutase) were quantified and statistically analyzed in order to identify the main determinants of cell inactivation under the different wavelengths. The reduction in survival and activity was stronger for shorter wavelengths, as expected. DNA damage followed the same pattern. The generation of ROS, as well as protein and lipid oxidation, showed the inverse trend. Multiple stepwise regression analysis revealed that survival under UVA, UVB and UVC wavelengths was best explained by DNA damage, oxidative damage to lipids, and intracellular ROS levels, respectively. The wavelength dependence of biomolecule damage was further investigated by mid-infrared spectroscopy analysis of the effects of irradiation on the proteins and lipids of two representative bacterial isolates in **Chapters 6**. Mid-infrared spectroscopy was proven to be an excellent tool to study changes in bacterial components upon UV exposure, revealing an array of modifications in the lipids and proteins of bacteria following irradiation and providing critical clues to drive future studies concerning the mechanisms involved in the inactivation of bacteria by UV irradiation.

In **Chapter 7**, the investigation of the identity and targets of ROS produced during UVB exposure in a set of isolates displaying different UV susceptibilities is addressed. For that, specific exogenous ROS scavengers (catalase [CAT], superoxide dismutase

[SOD], sodium azide and mannitol) were used. Biological effects were assessed from colony counts and heterotrophic activity (glucose uptake and respiration). DNA strand breakage, ROS generation and oxidative damage to proteins and lipids were used as markers of oxidative stress. Sodium azide conferred a statistically significant protection in terms of survival and lipid oxidation, suggesting that singlet oxygen might play a pivotal role in UVB-induced cell inactivation. Mannitol exerted a significant protection against DNA strand breakage and protein carbonylation, assigning hydroxyl radicals to DNA and protein damage. The addition of exogenous CAT and SOD significantly protected the capacity of the cells for glucose uptake and respiration, suggesting that impairment of metabolic activity during UVB exposure has a contribution of superoxide and hydrogen peroxide.

Chapter 8 reports the investigation of the role of transition metals (cobalt, copper, iron, manganese, zinc) in UVB-induced damage to bacterial isolates. In general, UVB irradiation of metal-amended cell suspensions, particularly those with iron, copper and manganese, contributed synergistically to enhance bacterial inactivation. Amendment with iron exacerbated ROS generation, DNA damage and oxidative damage to lipids during irradiation. Additionally, lipid damage during UVB exposure was also enhanced after incubation with copper and cobalt. Despite attenuating the formation of protein carbonyls during irradiation, manganese decreased survival during irradiation. The results indicate that iron, copper, cobalt and manganese play a role in UVB-induced inactivation and that metal homeostasis may be crucial in limiting oxidative stress during UVB exposure.

Chapter 9 analyzes the influence of nutrients and water properties in the UVB-sensitivity of bacterioneuston and bacterioplankton, as well as in a set of representative bacterial strains. UVB-induced inhibition was generally attenuated upon inoculation in high nutrient medium, compared to unamended conditions. Under low nutrient conditions, bacterioneuston was less affected by UVB exposure than bacterioplankton in marine samples. For brackish water samples, nutrient conditions did not substantially affect inactivation, but a high nutrient concentration attenuated the reduction in activity. Resuspension in natural surface or subsurface estuarine water attenuated inactivation during irradiation, compared to suspensions prepared in an artificial mineral solution. These results indicate that the biological consequences of UV exposure are influenced by the composition of the suspension medium. Accordingly, the abiotic environment of

the surface microlayer and underlying water potentially influences the UV sensitivity of bacterioneuston and bacterioplankton, respectively.

Chapter 10 describes the influence of growth conditions, in particular, growth phase (mid-exponential, late-exponential and stationary), growth temperature (15 ºC and 25 ºC) and growth medium (nutrient-rich TSB and nutrient-poor M9) in UVB-induced cellular damage in a representative bacterial strain. In general, oxidative damage did not follow a linear dose-dependent variation, suggesting a dynamic interaction between damage induction and repair, particularly at high UVB doses, and/or saturation of oxidative damage. Stationary phase cells usually survived better and showed lower levels of oxidative damage than exponential phase cells. Oxidative damage, most notably in mid-exponential phase cells, was generally higher at 25 ºC than at 15 ºC, suggesting that ROS generation and/or ROS interaction with the cellular targets is temperature-dependent. Survival during UVB exposure was generally higher when cells were grown in nutrient-rich media, than under nutrient-deprived conditions. Growth conditions might influence bacterial UVB sensitivity by affecting the temporal progression and magnitude of biomolecule damage.

Chapter 11 examines the diversity of RecA proteins among completely sequenced bacterial genomes and the reliability of the *recA* gene as a molecular marker. The presence of multiple RecA copies in sequenced genomes and the frequency of plasmid-encoded *recA* genes were also examined. Phylogenetic analysis of the RecA protein revealed, in general, support for the phyla defined by 16S rRNA gene analysis. *recA* gene trees of *Deltaproteobacteria* and Firmicutes were in general agreement with 16S rRNA trees, but were more divergent in *Gammaproteobacteria*. Duplication of the *recA* gene was found to be a widespread feature in myxobacteria and frequent among Firmicutes. Sequence analysis revealed that the extra *recA* copy could, in some cases, have resulted from an endogenous duplication event. In other cases, divergence of the G+C content of the *recA* gene and the genome raises the possibility of horizontal transfer of the additional gene. The presence of *recA* homologs in plasmids and, in some cases, the presence of transposases in the vicinity of *recA* genes could support the possibility of plasmid-mediated mobility of the *recA* gene. Gene context analysis suggested that these plasmid-encoded *recA* genes could complement the activity of the chromosomal *recA* in the bacterial SOS response.

Chapter 12 briefly discusses the main results of this work in an integrated perspective. **Chapter 13** is a general conclusion of the thesis.

CHAPTER 1
Introduction

UV radiation

Ultraviolet (UV) radiation (100-400 nm) corresponds to the region of the electromagnetic spectrum located between visible light and X-rays (Iqbal, 1983) and, as a natural component of sunlight, it is part of the environment in which life evolved and to which it adapted. UV radiation has been proposed to be involved in the evolution of DNA base composition and sequence (Lesk, 1973; Boulikas, 1992), the ecology, biochemistry and evolution of the first life forms (Sagan, 1973) and the pattern of early evolution (Walker et al., 1976). The importance of solar UV radiation as an evolutionary driving force is reflected by the development of several protection mechanisms against the deleterious biological effects of UV radiation, including several partly redundant enzymatic pathways for the repair of UV-induced DNA damage, very early in evolution (DiRuggiero and Robb, 2004). The genotoxic effects of solar UV radiation are thought to have precluded the development of terrestrial life for two or three billion years, before the stratospheric ozone layer was formed.

The use of sunlight by cells was an achievement of utmost importance for life on Earth. The Sun not only provided an unlimited source of energy and assured a dependable supply of food but also drastically changed the Earth's atmosphere by helping to generate molecular oxygen through photosynthesis which, in turn, had a dramatic influence on the abundance and diversity of life forms on Earth (Falkowski, 2006; Holland, 2006; Payne et al., 2008). The interaction of sunlight with the increasing amounts of accumulating oxygen allowed the formation of the ozone molecule and subsequently the ozone layer, approximately 2 billion years ago (Canuto et al., 1982). The newly formed ozone layer altered the solar spectrum, preventing high energy radiation photons (short-wavelength UVC radiation, 100-280 nm) from reaching the lower troposphere, where life was developing. Once the ozone layer matured, survival was no longer dependent on protection against UV radiation by a layer of water or other physical shields. Life became possible on the top of the water column and eventually on the surface of the land (Goldblatt et al., 2006).

Depletion of the ozone layer

The first doubts about the effectiveness of the stratospheric ozone layer in protecting the Earth's surface from damaging solar wavelengths raised upon the observation of a latitudinal gradient in skin cancer incidence, correlating with UV radiation incidence (Urbach, 1969). In 1985, a paper published in Nature surveying the variation in total column ozone over the Antarctic for four seasons, unequivocally described massive ozone losses during the spring (Farman et al., 1985), an event which was latter dubbed as the "ozone hole". Further analysis of the ozone records retrieved from scientific bases in the Antarctic demonstrated a trend for decreasing thickness of the ozone layer since the 1970s, progressing at increasing rates (Crutzen, 1970). Ozone loss events were later also observed at mid-latitudes and in the Arctic, although not to the same extent as over Antarctica (W.M.O., 1988; W.M.O., 1991). The implications of massive ozone depletion stimulated the interest in the mechanisms of ozone degradation and the biological consequences of increased UV fluxes, particularly UVB (280-320 nm), the major known outcome of ozone depletion (Nolan and Amanatidis, 1995).

Molina and Rowland (1974) first proposed that chlorofluorocarbons (CFCs) released to the atmosphere by human activity were responsible for the depletion of the ozone layer, indisputably associating a global environmental change with anthropogenic activity. According to the authors, the photochemical breakdown of CFCs and other ozone-depleting substances (ODSs) in the stratosphere resulted in the release of chlorine (Cl) and bromine (Br) atoms, which catalyzed the destruction of ozone. The pioneer work of Molina and Rowland led to the Nobel Prize for the authors in 1995. Subsequently, the presence of polar stratospheric clouds (PSCs) was also identified as an important catalyst for large ozone loss in Polar Regions, by creating sites on which fast heterogeneous chemical reactions can occur, rapidly increasing ozone-destroying molecules in the stratosphere (Solomon, 1999).

The early prolific scientific research in the field of ozone depletion culminated in the first World Meteorological Organization (WMO)/United Nations Environment Program scientific assessment of ozone depletion in 1985 (WMO, 1985), which provided the scientific consensus that CFCs and halons posed a critical threat to the ozone layer. In response to the conclusions of the report, the landmark Montreal Protocol agreement was negotiated in 1987, which regulated the production of CFCs and other ODSs (Velders et al., 2007). Since 1987, 193 nations have signed the

Montreal Protocol leading to a worldwide decrease in the production of ODSs. Accordingly, the cumulative levels of chlorine and bromine from ODSs in the troposphere (Montzka et al., 1996) and stratosphere (Anderson et al., 2000; Froidevaux et al., 2006; Mäder et al., 2010) have shown a decreasing trend.

Based on the reduction of ozone depleting chemicals in the atmosphere, normal ozone levels were initially expected to be restored by around 2050 (Schrope, 2000). However, interactions between stratospheric ozone loss and other observed or potential atmospheric changes associated with global warming are expected to change the timeline. For example, increasing carbon dioxide (CO_2) levels are responsible for warming in the lower atmosphere (*i.e.*, troposphere), but have the opposite cooling effect on the stratosphere. Ozone loss in itself also cools the stratosphere since less radiation is absorbed. The cooling of the stratosphere results in an enhanced chance of PSCs forming and existing for more prolonged periods at high altitudes. This mediates further ozone loss processes, accelerating ozone depletion and cooling the stratosphere even more in a positive feedback effect. On the other hand, increases in greenhouse gas concentrations, by influencing the spatial distribution of ozone and its exchange between the stratosphere and the troposphere, can also potentially affect UV levels reaching the Earth's surface (Bais et al., 2011).

As a result of the interplay between climate change and changes in UV fluxes reaching the Earth, the most recent predictions indicate that the UV radiation index is expected to decrease by 9 % in northern high latitudes, but to increase by 4 % in the tropics and by up to 20 % in southern high latitudes in late spring and early summer, up to the year 2095 (Hegglin and Shepherd, 2009). These changes in tropospheric ozone budget and the ultraviolet index will likely have consequences for tropospheric radiative forcing (Velders et al., 2007), air quality (Wilson et al., 2007; Tang et al., 2011) and human and ecosystem health (Ballaré et al., 2011; Häder et al., 2011; Norval et al., 2011; Zepp et al., 2011; Thomas et al., 2012). Warming, acidification and changes in ocean stratification patterns are also expected to increase the penetration of UV radiation in the water column and enhance organism exposure to UVB in forthcoming years (Andrady et al., 2010). Besides these modelled, predicted effects, unpredicted events could also potentially affect the UV radiation index. For example, in 2011, an unprecedented Arctic ozone loss was recorded as a result of unusually long-lasting cold conditions in the Arctic lower stratosphere (Manney et al., 2011). Whether such Arctic ozone depletion events may be matched or exceeded in the future, is unknown. These

concerns continue to make the study of the effects of UV radiation on the Earth's biota a critical and timely subject.

Effects of UV radiation on microorganisms

The recognition of the involvement of UV radiation as a cause or contributing factor for skin cancer and eye cataracts, as well as its connection to the development of immune deficiencies, prompted the scientific interest on the biological effects of UV radiation (Kligman et al., 1985; Kraemer et al., 1987; Kripke, 1988; Taylor et al., 1988). The detrimental impact of UV radiation on ecosystem structure and function was also soon recognized, and is now known to include decreased primary productivity, altered species composition and potential consequences to biogeochemical cycles and food production (Caldwell et al., 1998; Zepp et al., 1998; Searles et al., 2001; Caldwell et al., 2003; Häder et al., 2003; Paul and Gwynn-Jones, 2003; Caldwell et al., 2007; Häder et al., 2007; Zepp et al., 2007; Ballaré et al., 2011; Häder et al., 2011).

UV radiation can be a particularly important selective force in aquatic systems, since radiation can penetrate to considerable depths (Fleischmann, 1989; Smith, 1989; Worrest and Häder, 1989; Smith et al., 1992; Tedetti and Sempéré, 2006). For example, in the subtropical open Atlantic, the 10 % radiation level for 320 nm, 340 nm and 380 nm wavelengths is at < 25, 35 and 60 m deep, respectively (Obernosterer et al., 1999) and UV penetration has been detected to a depth of 70 m in Antarctica (Smith et al., 1992). Early studies focused on the UV sensitivity responses of phytoplankton, due to its contribution to the primary productivity of ecosystems (Smith et al., 1980; Smith, 1989; Karentz et al., 1991; Helbling et al., 1992; Behrenfeld et al., 1993; Cullen and Neale, 1994; Helbling et al., 1994; Vernet et al., 1994; Häder et al., 1995). However, the short generation time, simple haploid genomes with little or no functional redundancy and small size, which might preclude effective cellular shading or protective pigmentation, make bacteria particularly susceptible to UV radiation (Garcia-Pichel, 1994). Considering the role of bacteria in the cycling of nutrients and energy in ecosystems (Azam et al., 1983), the knowledge of the effects of UV radiation on bacterial communities becomes of utmost importance, as demonstrated by the considerable number of reviews covering the effects of UV radiation in both freshwater and marine systems (Häder and Worrest, 1991; Karentz, 1994; Siebeck et al., 1994;

Herndl et al., 1997; Häder et al., 1998; Moran and Zepp, 2000; Vincent and Neale, 2000; Whitehead et al., 2000; Häder, 2001; Buma et al., 2003; Häder et al., 2003).

In the natural environment, UVR effects are generally attenuated by protection and repair strategies (Becker-Hapak et al., 1997; Cabiscol et al., 2000; Tedetti and Sempéré, 2006). The overall stress imposed by UV exposure thus reflects an equilibrium between damage, repair and the energetic costs of protection, which may affect energy consumption and the biochemical composition of the cellular material of individuals, ultimately resulting in decreased survival and growth rate (Moriarty, 1986; Vincent and Neale, 2000). Consequences at the organism level can, in turn, affect the microbial community, creating shifts in ecosystem carbon cycles, and in the fluxes of energy and nutrients (Schimel et al., 2007).

Mechanisms of UV-induced damage

At the cellular level, the toxic effects of UV radiation can be initiated by direct and indirect photochemical mechanisms (Moriarty, 1986; Vincent and Neale, 2000). The direct mechanism involves the absorption of UV photons by chromophores present in certain biomolecules, such as proteins and nucleic acids. Upon UV absorption, these molecules are photochemically degraded or transformed, resulting in impairment or even loss of biological function. The indirect mechanism involves the absorption of UV photons by a photosensitizer molecule inside or outside the cell (namely flavins, porphyrins, quinones, protein-bound tryptophan and also humic compounds present in environmental samples) (Curtis et al., 1992; Davies-Colley et al., 1994). Upon excitation, the photosensitizer is able to transfer energy in two different ways, often called type I and type II mechanisms (Foote, 1987; Foote, 1991). In the type I process, the electronically excited sensitizer reacts directly with the cellular component, subtracting one electron or hydrogen atom from the cellular target, resulting in the formation of reactive oxygen species (ROS), including free radicals (*e.g.*, superoxide ions and hydroxyl radicals) which initiate free-radical chain reactions. The type II mechanism involves energy transfer from the sensitizer to molecular oxygen with the consequent formation of an excited state of oxygen, singlet oxygen, which can then attack biomolecules (Hélène, 1987).

In the case of the direct pathway, the magnitude of the damage caused by UV exposure is determined by the amount of radiation absorbed and the quantum yield of photodestruction (*i.e.*, the number of molecules damaged per photon absorbed), which

in turn depends on the incident UV wavelength (Moriarty, 1986; Vincent and Neale, 2000). UVR can be divided in three wavelength ranges: UVA (320-400 nm), UVB (280-320 nm) and UVC (100-280 nm). Although, on a proton basis, UVA radiation contains less energy than UVB radiation, the greater fraction of solar UV radiation in the UVA (95 %) spectrum than in the UVB spectrum (5 %) makes it a potentially significant source of biological damage (Moan et al., 1999). DNA absorbs only weakly at longer UV wavelengths (Wells and Han, 1984). Therefore, the biological effects of UVA are usually considered to be mostly indirect, resulting from intracellular generation of ROS which cause oxidative damage to lipids, proteins and DNA (Tyrrell, 1973; Girotti, 1985; Chamberlain and Moss, 1987; Girotti, 1998; Pattison and Davies, 2006). The UVB component of solar radiation can directly induce the formation of DNA lesions that block DNA replication and RNA transcription and, left unrepaired, lead to cell death (Mitchell and Karentz, 1993). UVB-induced damage can also arise from increased production of intracellular ROS upon irradiation, as suggested by the enhanced expression of ROS scavenging systems following irradiation (Qiu et al., 2004; Matallana-Surget et al., 2009a; Di Capua et al., 2011). The resulting damage can be even more detrimental than the direct effects of UV radiation, since oxidative lesions are energetically expensive to prevent and very resource intensive to repair (Halliwell and Gutteridge, 1999; Lister et al., 2010).

Although almost entirely screened out by the ozone layer, high-energy UVC wavelengths remain useful in laboratorial experiments to assess UV sensitivity in bacteria that are highly tolerant or insensitive to elevated doses of UVB (Sundin and Jacobs, 1999). Additionally, UVC wavelengths are also well known for their potential to inactivate microorganisms in several settings, including hospitals (Andersen et al., 2006), the pharmaceutical/medical industry (Rastogi et al., 2007), water treatment plants (Høibye et al., 2008) and food products (Chun et al., 2009; Sommers et al., 2009).

Reactive oxygen species and the importance of metals

The autoxidation of flavoenzymes (*e.g.*, succinate dehydrogenase, fumarate reductase, NADH dehydrogenase I and II, glutamate synthase, lipoamide dehydrogenase, and sulfite reductase) is a key biological source of both superoxide ($O_2^{\bullet -}$) and H_2O_2 in the cell (Imlay, 2008; Spiro and D'Autreaux, 2012). Superoxide toxicity arises from its ability to directly oxidize and inactivate proteins containing iron-sulphur (4Fe-4S) clusters (*e.g.*, aconitases, fumarases, serine dehydratase, threonine

deaminase, isopropylmalate isomerase, 6-phosphogluconate dehydratase). The reaction results in inactive [3Fe-4S] clusters and releases free iron ions [Fe^{2+}] and H_2O_2, which can participate in Fenton and Haber-Weiss oxidative reactions that generate the potent hydroxyl radical ($OH^{\bullet}$) (see below). Superoxide can also participate in lipid peroxidation (Thomas et al., 1985).

While H_2O_2 is poorly reactive compared to other ROS, its long half-life and capability to diffuse across the cell membranes makes it significant in oxidative stress. H_2O_2 can also be produced as a result of the catalytic activity of superoxide dismutase (SOD) (McCord and Fridovich, 1969; Imlay, 2008) and from the photooxidation of tryptophan (McCormick et al., 1976). H_2O_2 is able to directly oxidize and inactivate the iron-sulphur clusters of key enzymes. H_2O_2 can also react with the intracellular pool of incorporated ferrous iron and thereby generate the highly reactive hydroxyl radical. As a consequence of its reactions with iron, H_2O_2 interferes with iron homeostasis and metabolism, diminishing the delivery of iron into new metalloproteins (Valko et al., 2006; Imlay, 2008).

The hydroxyl radical ($OH^{\bullet}$) is highly reactive with a half-life in aqueous solution of less than 1 ns (Liochev and Fridovich, 2002). The majority of hydroxyl radicals are produced from H_2O_2 and superoxides in a Haber-Weiss reaction (Bast et al., 1991; Kehrer, 2000; Koppenol, 2001):

$$H_2O_2 + O_2^{\bullet -} \rightarrow O_2 + OH^- + OH^{\bullet}$$

or in a transition metal-catalyzed Fenton reaction, involving Fe^{2+}:

$$Fe^{2+} + H_2O_2 \rightarrow Fe^{3+} + OH^- + OH^{\bullet}$$

Other metals, like Cu^+ and Co^{2+}, can also favour the generation of the hydroxyl radical but, since they are only present in very small amounts in the cell, the reaction is less favourable (Bucher et al., 1983). Additionally, the hydroxyl radical can also be formed by metal-independent processes, as a result of the decomposition of peroxynitrite, an oxidant formed by the combination between nitric oxide and the superoxide radical (Hogg et al., 1992).

The extremely short half-life of the hydroxyl radical limits its reactivity to the immediate vicinity from where it is formed, such as near iron-sulphur clusters or in enzymes using iron as a prosthetic metal (Imlay, 2006). Iron bound to DNA can also catalyze the formation of the hydroxyl radical which then attacks DNA bases or the deoxyribosyl backbone of DNA to produce damaged bases or strand breaks (Imlay et

al., 1988). A role for the hydroxyl radical in sunlight-induced damage in *Escherichia coli* has been proposed (Oppezzo, 2012).

Among different ROS, singlet oxygen ($^1O_2$) is the only electronically excited state of molecular oxygen. The relatively short lifetime of singlet oxygen (~ 4 µs) limits the distance it can diffuse in cells and, therefore, restricts its reactivity (Krasnovsky Jr, 1981; Egorov et al., 1989; Baker and Kanofsky, 1992; Gorman and Rodgers, 1992). Singlet oxygen readily reacts with DNA, lipids (mainly unsaturated fatty acids) and particularly with proteins (Davies, 2003; Miyamoto et al., 2007). Upon reaction of amino acids with singlet oxygen, short-lived endo- or hydroperoxides are formed which, in turn, decompose into reactive radicals in the presence of redox-reactive metal ions and can cause oxidative damage to other biomolecules (Miyamoto et al., 2007). Singlet oxygen has also been shown to induce the formation of protein carbonyls and modify the prosthetic groups of proteins (Davies, 2003). Interaction of singlet oxygen with unsaturated lipids can form lipid hydroperoxides, which are able to diffuse in cells and initiate chain oxidation reactions at sites distant from the site of initial photodamage (Howden and Faux, 1996). Additionally, in the presence of Fe^{2+} or Cu^{+}, lipid peroxides formed as a result of singlet oxygen attack can participate in Fenton-like reactions to produce oxy- and peroxy- radicals capable of inducing damage to DNA and proteins (Nowis and Golab, 2008). Singlet oxygen has been implicated in UVA-induced damage (Chamberlain and Moss, 1987; Baier et al., 2006).

Understanding the role of metals in UVB-induced damage is necessary for a realistic perspective of the interaction of bacteria with radiation in a natural context, where these metals can be enriched, particularly when industries and agricultural areas are located nearby (Zhou et al., 2008). Furthermore, information regarding the contribution of metals for UV-induced bacterial inactivation may help develop more efficient photocatalytic disinfection strategies (Sciacca et al., 2010).

Cellular targets of UV radiation

DNA

The most notable molecule affected by UV radiation is DNA. The absorbing centres within DNA are the purine and pyrimidine bases, which have absorption maxima at 260-265 nm (Diffey, 1991). Therefore, UVC and UVB wavelengths are able to cause direct damage to DNA, in an oxygen-independent manner, while DNA damage by UVA wavelengths generally arises as a result of photosensitized reactions involving

ROS (Ravanat et al., 2001; Cadet et al., 2005b). The main lesions induced by UVB and UVC wavelengths are the DNA photoproducts cyclobutane pyrimidine dimers (CPDs) and pyrimidine (6-4) pyrimidone photoproducts (6-4 PPs), resulting from the formation of covalent bonds between adjacent pyrimidines (Cadet et al., 2005b) (Fig. 1.1). CPDs are generally produced in higher amounts than 6-4 PPs upon UV irradiation of DNA. Formation of CPDs under UVA has also been observed (Ikehata et al., 2008). The generation of these lesions by UV radiation is influenced by the DNA sequence. For example, sequences that facilitate bending and unwinding are favourable sites for damage (Becker and Wang, 1989; Lyamichev, 1991). In bacteria, the distribution of bipyrimidine photoproducts within UVB-irradiated DNA has also been found to be profoundly affected by the G+C content of the genome (Matallana-Surget et al., 2008). Therefore, the pattern and amount of UV-induced damage to DNA is expected to be variable among bacterial strains.

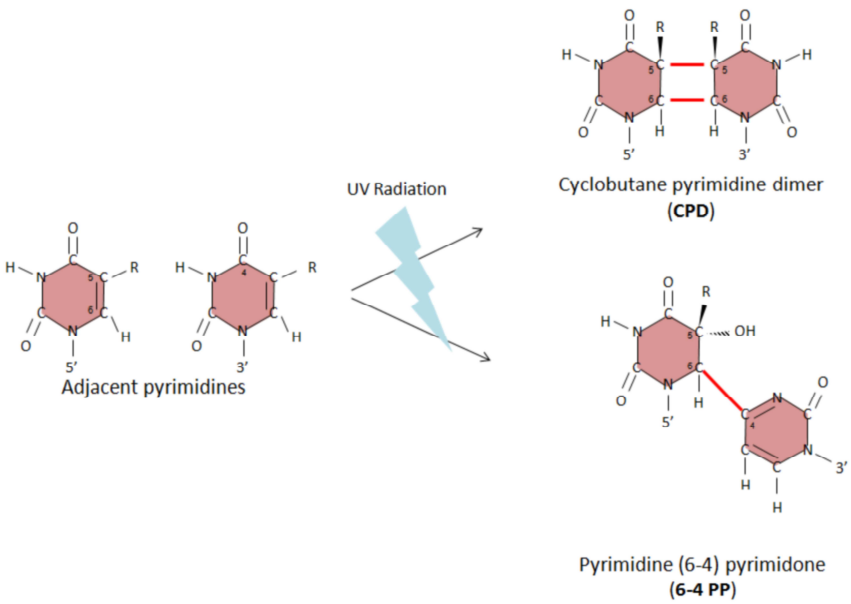

Fig. 1.1. Main types of DNA photoproducts resulting from exposure to UVB radiation: cyclobutane pyrimidine dimers (CPDs) and pyrimidine (6-4) pyrimidone photoproducts (6-4 PPs). CPD formation: upon UV exposure, a bond (red line) is formed between adjacent thymine (or cytosine) residues (C_5 and C_6). Since these bonds are shorter than the spacing between the planes of adjacent thymines, the DNA helix becomes distorted, causing the stalling of the DNA polymerase at the site of the lesion. 6-4 PPs are formed similarly to CPDs, but the covalent bond (red line) is established between the C_6 of the 5' pyrimidine and the C_4 of its adjacent 3' pyrimidine. R = H or CH_3 (Maloy et al., 1994).

Other DNA lesions that can occur to a smaller extent during UVB exposure include photohydration of cytosine, oxidation of guanine into 8-oxo-7,8-dihydroguanine and the formation of adducts between either two adjacent adenine bases or between adenine and a vicinal thymine (Cadet et al., 2005b). Additionally, reactive oxygen

species generated during photosensitized reactions can interact with DNA to form modified bases, strand breaks, alkali-labile sites and DNA-protein cross-links (Mitchell, 1995).

Lipids

The action spectrum for UV effects does not correlate with the absorption spectrum of lipids. Therefore, UV-induced damage to lipids is likely to be a result of photodynamic action (Girotti, 2001). ROS, most notably singlet oxygen, cause damage to lipids, particularly unsaturated ones, by directly oxidizing their double bonds or by initiating a chain of auto-catalyzed reactions of one oxidizing lipid reacting with another (lipid peroxidation) (Garmyn and Yarosh, 2007). Lipid peroxidation end products, such as malondialdehyde or 4-hydroxy-nonenal, induce a number of cellular responses, including changes in the electrical properties and ionic permeability of the membrane and, at higher concentrations, are cytotoxic (Girotti, 1998). Furthermore, these compounds can also interact with DNA (Park and Floyd, 1992) and proteins, potentially leading to loss of protein function (Esterbauer et al., 1991; Stadtman, 1992; Szweda et al., 1993; Berlett and Stadtman, 1997).

Proteins

The absorption maximum of proteins in the UV region is at approximately 280 nm due to absorption by the aromatic amino acids tyrosine (Tyr), phenylalanine (Phe) and tryptophan (Trp), as well as cysteine (Cys). These proteins can be direct targets of UVB, which can induce the scission of disulphide bridges between cysteine residues, important for the tertiary structure of many proteins, thus affecting protein structure and function (Creed, 1984). Direct UV photolysis of aromatic amino acids or disulphide bridges can also cause inactivation of proteins and enzymes, if the affected residues are included in the active site (Hollósy, 2002; Pattison and Davies, 2006).

Proteins are also key targets of photosensitized damage, which may cause functional changes in structural and enzymatic proteins. Oxidative reactions may result in modification of amino acid side chains, fragmentation of polypeptide chains and intra- and intermolecular cross-linking of proteins and peptides (Nowis and Golab, 2008). Proteins that contain iron as a prosthetic metal are particularly noteworthy targets of oxidation through Fenton reaction, being readily oxidizable by hydrogen peroxide (Beyer and Fridovich, 1991; Tamarit et al., 1998; Murakami et al., 2006). Lysine (Lys),

arginine (Arg), proline (Pro) and threonine (Thr) can be directly oxidized upon the absorption of UV radiation by the protein or bound chromophore groups through photosensitized reactions (Pattison and Davies, 2006). Upon oxidative attack of Pro, Arg, Lys and Thr, carbonyl (C = O) groups are introduced in the side chains of the protein, generating aldehydes or ketone products (Nyström, 2005). Quantitatively, the most prominent products of the carbonylation reaction are glutamic semialdehyde from Arg and Pro, and aminoadipic semialdehyde from Lys (Requena et al., 2001). In addition, carbonyl groups can be introduced into proteins by reaction with reactive carbonyl compounds produced by oxidation of carbohydrates and lipids (Nyström, 2005). Protein carbonyl levels have, therefore, been used as a marker of ROS-mediated protein oxidation (Dukan and Nyström, 1999; Hoerter et al., 2005a; Nyström, 2005; Daly et al., 2007; Bosshard et al., 2010b).

Repair and protection strategies against UV-induced damage

DNA repair

In response to UV-induced damage, bacteria have evolved several DNA repair mechanisms that can essentially be divided in dark repair and light-dependent repair. At least three dark repair mechanisms can be found in bacteria that are inducible to a greater or lesser extent as a part of the SOS regulon: (1) excision repair, which includes nucleotide excision repair (NER) and base excision repair (BER); (2) post-replication recombinational repair; and (3) error-prone or mutagenic DNA repair (MDR) (Simonson et al., 1990; Smith and Walker, 1998) (Fig. 1.2 A-C). Nucleotide excision repair involves the creation of dual incisions at the 5’ and 3’ extremities of the damaged site and removal of the section of the DNA containing the lesion, being the resulting gap subsequently filled by DNA polymerase, using the complementary strand as a template, and sealed by DNA ligase (Reardon and Sancar, 2005). In base excision repair, the enzyme DNA glycosylase removes the damaged or modified DNA base, generating an apurinic/apyrimidinic (AP) site which is then excised by an AP endonuclease or an AP lyase. The remaining deoxyribose phosphate residue is removed by a phosphodiesterase. The resulting gap is filled by a DNA polymerase, and the strand is sealed by DNA ligase (Sakumi and Sekiguchi, 1990; Seeberg et al., 1995). Recombinational repair is involved in the repair of double-strand breaks and single-strand breaks in damaged DNA, which cannot be directly repaired (Shinohara and Ogawa, 1995). In this process, the intact parental strand invades the other duplex containing the break allowing the

filling of the gap. The gap that is left in the previously intact strand is then filled by the DNA polymerase and sealed by DNA ligase (Kuzminov, 1999).

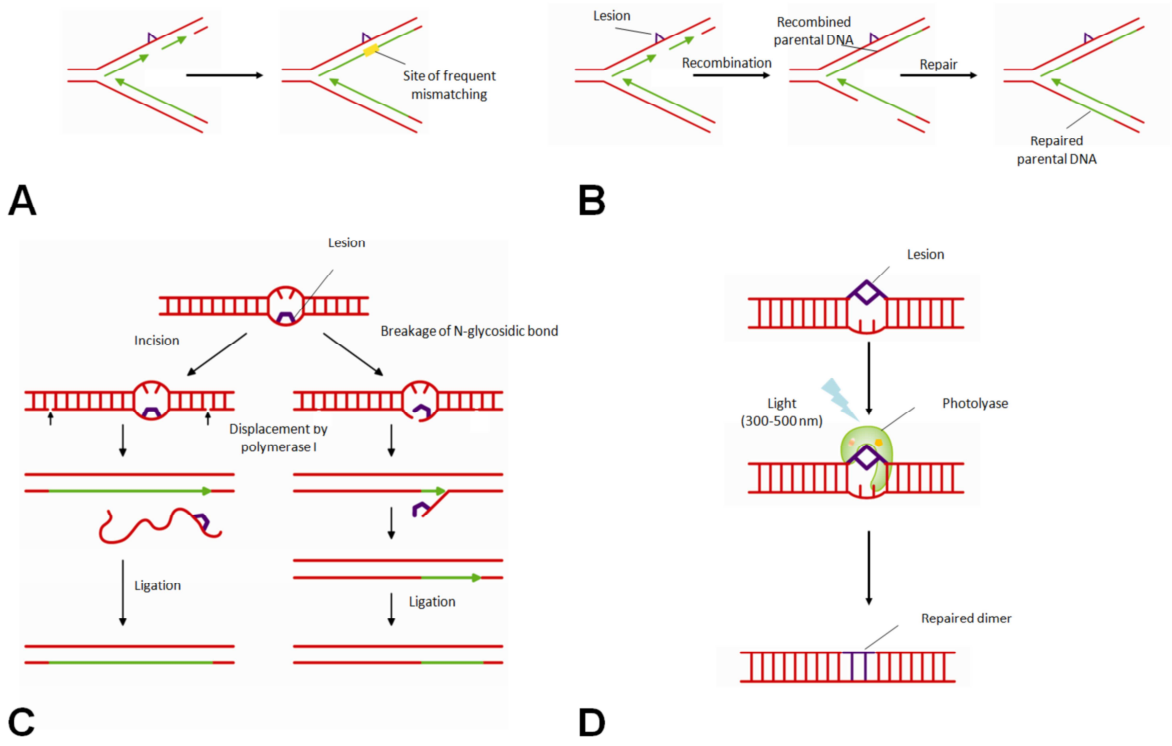

Fig. 1.2. Main mechanisms involved in the repair of UV-induced DNA damage. **(A) Mutagenic repair, SOS mutagenesis or error-prone repair.** In this process, a modified DNA polymerase is able to read through damaged DNA, misincorporating nucleotides in the section of the copy strand opposite the lesion. Mutagenic repair involves the *recA*, *umuD* and *umuC* (organized in the *umuDC* operon) genes. The RecA protein activates the cleavage of UmuD to an active form, UmuD'. While the exact contribution of UmuC and UmuD' to mutagenic repair is still unclear, it seems that the UmuC-UmuD' complex directly interacts with RecA and the stalled DNA polymerase, inhibiting its editing function, thus promoting error-prone replication. **(B) Recombinational repair.** During DNA synthesis, the DNA polymerase encounters a DNA lesion and leaves a gap in the copy strand opposite the lesion. To repair the gap, RecA-dependent recombination occurs whereby the good template copy strand is cleaved and invades the gap in the damaged copy strand. A crossover intermediate forms that, after cutting and sealing, results in filling the gap with the complementary DNA from the sister strand. The gap formed in the sister strand is filled by the DNA polymerase and the gaps are sealed by the DNA ligase. The lesion is then remover by nucleotide excision repair or simply diluted out during growth. **(C) Excision repair.** The excision repair mechanism is an ATP-dependent, multistep enzymatic process. The first step of the mechanism corresponds to an incision step, which can occur by two mechanisms. In *E. coli*, a repair endonuclease recognizes the distortion of the DNA helix produced by the DNA lesion and makes two cuts (at the 5' and 3' extremities of the lesion) in the sugar-phosphate backbone. At the 5' incision site, a 3'-OH group results which the DNA polymerase uses as a primer to synthesize a new strand while displacing the DNA segment that carries the lesion. In the final step the newly synthesized segment is joined to the original strand by DNA ligase. In other systems (*e.g.*, *Micrococcus luteus* and *E. coli* phage T4), the incision step occurs in two distinct stages. In the first step, the N-glycosidic bond is cleaved in the 5'-nucleotide of the dimer. The incision is completed by an endonuclease activity that recognizes a deoxyribose lacking a base. The enzyme makes a single cut at the 5' side of the remaining thymine in the dimer site. The deoxyribose is removed afterwards and the polymerase acts at the new 3'-OH group, displacing the strand and filling the gap. The displaced strand is subsequently excised enzymatically. **(D) Light-dependent repair, photoenzymatic repair or photoreactivation.** In this process, the enzyme DNA photolyase, encoded by the *phr* gene in *E. coli*, reverses the dimerization reaction induced by UV radiation upon absorbing blue light (300-500 nm). The enzyme uses the light energy absorbed to cleave the dimers (Maloy et al., 1994; White, 1995). Further details on the photoreactivation mechanism are provided in Fig. 1.3.

Mutagenic DNA repair (MDR) involves the activation of low fidelity repair polymerases, which are able to perform DNA synthesis across damaged regions of DNA (translesion DNA synthesis) in a template-independent manner, therefore rescuing stalled replication forks and allowing complete replication of the genome, but carrying the cost of an increased mutation rate (Goodman, 2002; Rattray and Strathern, 2003). MDR-mediated UV tolerance seems to provide a critical ecological advantage for microorganisms inhabiting UV-exposed habitats, such as epiphytic plant pathogens (Sundin and Murillo, 1999).

In bacteria, dark repair systems are regulated by the RecA protein. Exposure to UVA and UVB radiation has been shown to result in increased levels of the RecA protein in *Pseudomonas aeruginosa* (Elasri and Miller, 1998), *Vibrio natriegens* (Booth et al., 2001b) and *Photobacterium angustum* S14 (Matallana-Surget et al., 2012). Since RecA levels correlate with the cell's capacity to repair DNA damage (Miller, 2000), RecA induction levels have been used as a dosimeter of the repair potential in both isolates (Booth et al., 2001b) and bacterial communities (Booth et al., 2001a).

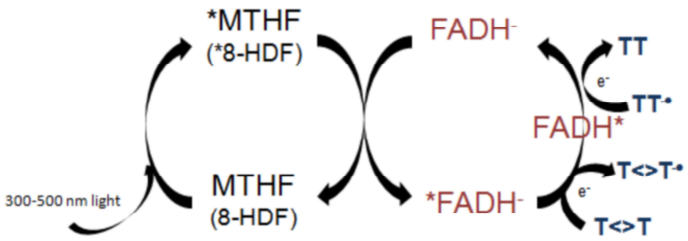

Fig. 1.3. Catalytic cycle of the repair of bipyrimidine photoproducts by DNA photolyase. The photolyase enzyme contains two types of cofactors: the redox-active cofactor flavine adenine dinucleotide (FAD) and the light harvesting factor, which can be 5,10-methenyltetrahydrofolylpolyglutamate (MTHF) or 8-hydroxy-5-deazaflavin (8-HDF). In the repair process, the DNA photolyase binds to its substrate. The light harvesting factor (MTHF or 8-HDF) absorbs light (300-500 nm) and the excitation energy is transferred to $FADH^-$. The flavin in its excited form ($*FADH^-$) transfers one electron to the pyrimidine dimer, generating a flavin/substrate radical pair. The excited pyrimidine dimer radical (T<>T*) suffers a bond rearrangement, which results in the cleavage of the carbon-carbon double bond of the pyrimidine dimer. The electron of the excited dimer is transferred back to the flavin radical (FADH*). $FADH^-$ and a repaired dinucleotide result from the process (Stochel et al., 2009).

Light-dependent repair, also known as photoenzymatic repair (PER) or photoreactivation, depends on the DNA photolyase enzyme that can be activated by blue light (300-500 nm) (Mitchell, 1995) (Fig. 1.2 D). Photolyases contain two chromophores, one of which (5,10-methenyltetrahydrofolylpolyglutamate or 8-hydroxy-5-deazaflavin) harvests light energy, transferring it to a reduced flavin chromophore that acts as the reaction centre in the reversal of the DNA lesion (Sancar, 1994) (Fig. 1.3).

During photoenzymatic repair, photolyase binds the DNA lesion (CPDs in the case of CPD photolyase or 6-4 PPs in the case of the 6-4 PP photolyase), reverses the lesion in a light-dependent step and dissociates from the repaired DNA (Kim et al., 1994; Sancar, 1994; Sancar, 1996; Thoma, 1999).

The importance of photoreactivation and dark repair for bacteria has been deduced from field and laboratorial studies of the kinetics of formation of DNA photoproducts in bacterioplankton (Jeffrey et al., 1996a; Jeffrey et al., 1996b; Meador et al., 2002). For example, the occurrence of PER in natural bacterial communities has been inferred from analyses of CPD kinetics in bacterioplankton samples obtained from the marine water column throughout the solar day (Jeffrey et al., 1996b). Similar field studies have also shown a reduction in the amount of CPDs from the day to the night period in bacterioplankton, suggesting that much of the DNA damage induced by UV exposure during the day is repaired at night, thus indicating that NER is an important repair mechanism as well (Lyons et al., 1998; Pakulski et al., 1998).

ROS scavenging systems

ROS are produced abundantly by a variety of metabolic pathways in cells (Halliwell, 2006). By increasing the activity of oxidases and peroxidases, UV exposure enhances ROS production in the cell (Apel and Hirt, 2004; Beak et al., 2004). Throughout the course of evolution, bacteria have evolved several defence mechanisms against oxidative stress, most notably antioxidant enzymes, such as superoxide dismutase (SOD) and catalase (CAT) (Imlay, 2003).

SOD is considered to be one of the primary antioxidant defences of the cell, because it catalyzes the dismutation of superoxide ($O_2^{\bullet -}$) to hydrogen peroxide (H_2O_2), preventing further generation of free radicals (McCord and Fridovich, 1969). The resulting H_2O_2 is then decomposed by CAT to oxygen and water.

The radioprotective effect of SOD is conferred not only by its ability to remove the potentially dangerous radical superoxide, but also by preventing the redox cycling of metals involved in the generation of the hydroxyl radical (Fridovich, 1995). However, SOD may actually sensitize organisms and enhance oxidative damage since H_2O_2 (scavenged by the photosensitive enzyme CAT), resulting from the activity of SOD, is a more oxidant species than superoxide (Scott et al., 1989).

Low UVA doses have been shown to result in substantial up-regulation of SOD activity (Hoerter et al., 2005a). High catalase activity also seems to play a role in UV

tolerance, in some bacterial strains (Di Capua et al., 2011). However, CAT has been shown to be inactivated by UV radiation (Wood and Schallreuter, 2006). A direct role of CAT in generating oxidants in response to UVB light has also been proposed (Heck et al., 2003). Therefore, reducing the levels of CAT activity upon exposure to UV radiation could be a protective mechanism to minimize damage. Decreased enzyme synthesis or altered assembly of enzyme subunits have been suggested to account for decreased CAT activity upon UV exposure (Hertwig et al., 1992).

Effects of UVR on bacterial communities

UV radiation affects microorganisms in natural communities both directly and indirectly. In the microbial loop, bacteria, viruses, phytoplankton and bacterivores interact closely (Azam et al., 1983). Therefore, it is expected that if one group of organisms is directly impacted by UV radiation (*e.g.*, DNA damage) this will indirectly affect carbon flow through the other groups (Moriarty, 1986; Vincent and Neale, 2000). For example, since systems dominated by different phytoplankton communities usually have different associated bacterial communities (Pinhassi et al., 2004) and bacterial communities are influenced by phytoplankton exudates (Van Hannen et al., 1999; Riemann et al., 2000), variations in the light regime that affect phytoplankton will indirectly influence the bacterial community. Predation by bacterivores is also influenced by UV-radiation which in turn can affect the outcome of UV exposure for bacteria (Sommaruga et al., 1996; Chatila et al., 1999).

Effects of UVR on bacteria are also influenced by the photochemical alteration of the bioavailability of dissolved organic carbon (DOC) to bacteria by radiation. On the one hand, irradiation of DOC can result in the production of low molecular weight compounds that are easily degradable by bacteria, stimulating bacterial growth (Kieber et al., 1989; Wetzel et al., 1995; Bertilsson and Tranvik, 1998). On the other hand, refractory products and ROS might also be formed in the process which could exert an overall inhibitory effect on bacteria (Obernosterer et al., 1999; Tranvik and Bertilsson, 2001).

Effects on bacterial abundance

Decreased bacterial abundance seems to be a common effect of exposure to solar UV radiation (Müller-Niklas et al., 1995; Joux et al., 1999; Maranger et al., 2002; Sinton et al., 2002; Hoerter et al., 2005a; Hoerter et al., 2005b; Berney et al., 2006d;

Bosshard et al., 2009; Santos et al., 2011a; Santos et al., 2011b; Santos et al., 2012a; Santos et al., 2012b). Detrimental effects of UV radiation on cell abundance can arise as a result of membrane dysfunction elicited by reactive oxygen species, eventually leading to increased membrane permeability and cell death (Berney et al., 2006b; Bosshard et al., 2010a). Genomic instability and mutagenesis as a result of UV-induced DNA damage (Friedberg et al., 2004) can also contribute to decrease cell abundance during irradiation. By disrupting the ability of bacteria to properly replicate, cyclobutane dimers formed upon UV exposure can contribute to the reduction in bacterial numbers during irradiation, as well (Karentz et al., 1994). Likewise, UV-induced lysogeny of virus-infected cells is also a contributing factor for decreased cell abundance during irradiation (Maranger et al., 2002). Finally, a detrimental effect of the photoproducts resulting from DOM (dissolved organic matter) irradiation on bacterial numbers has also been found (Ortega-Retuerta et al., 2007).

Some beneficial effects of UVR on bacterial abundance have also been reported (Lindell et al., 1995; Lindell et al., 1996; Mostajir et al., 1999; Chatila et al., 2001; De Lange et al., 2003), as a result of the release of exudates by UV-stressed phytoplankton and UV-induced photolysis of high molecular weight DOM into smaller molecules that can subsequently be incorporated by bacterioplankton, promoting bacterial growth. Additionally, negative effects of UV radiation on bacterivores can also account for enhanced bacterial numbers upon UV exposure (Sommaruga et al., 1996; Mostajir et al., 1999).

Effects on bacterial community structure

Variability in the UV responses and subsequent repair strategies of bacterial isolates (Joux et al., 1999; Arrieta et al., 2000; Fernández Zenoff et al., 2006b; Santos et al., 2011b; Santos et al., 2012a) have been considered indicative of the potential of UV radiation to affect microbial community structure. However, results on the effects of UV radiation on bacterial community composition are contrasting, with some studies reporting only minimal effects of UV radiation on the community structure (Winter et al., 2001; Norris et al., 2002; Piquet et al., 2010) and others indicating a substantial dependence of the bacterial community structure on radiation (Langenheder et al., 2006; Dobretsov et al., 2010; Santos et al., 2011a; Manrique et al., 2012; Pajares et al., 2012; Santos et al., 2012b). UV effects on bacterial community structure may involve the selection of phototolerant members of the community by radiation. For example,

members of *Gammaproteobacteria* have been found to dominate bacterial assemblages exposed to UV radiation (Alonso-Sáez et al., 2006; Santos et al., 2012b). Differences in the efficiency of the systems involved in the repair of damage induced by UV radiation can contribute for the variability in UV sensitivity among different bacteria (Joux et al., 1999; Arrieta et al., 2000; Fernández Zenoff et al., 2006b; Santos et al., 2011b; Santos et al., 2012a) and help to explain the effects of UV radiation on bacterial community structure.

Effects of UV radiation on bacterial community structure can, in turn, lead to shifts in the pathways of DOM use by bacteria (Morris et al., 2002), since different bacterial groups have different susceptibilities to UV radiation and also differ in their activities and patterns of DOM utilization (Cottrell and Kirchman, 2000). For example, *Alphaproteobacteria*, which are UV-sensitive, are responsible for a large part of low-molecular-weight-DOM uptake in the ocean, while Bacteroidetes, considered as more UV-resistant, are specialized in high-molecular-weight-DOM uptake (Cottrell and Kirchman, 2000; Alonso-Sáez et al., 2006).

Effects on bacterial metabolic activity

Field studies have indicate that, in general, exposure to UVR results in a decrease in amino acid uptake (Bailey et al., 1983), exoenzymatic activities (Herndl et al., 1993; Müller-Niklas et al., 1995; Santos et al., 2011a), oxygen consumption (Pakulski et al., 1998), leucine and thymidine incorporation (Aas et al., 1996; Lindell et al., 1996; Jeffrey et al., 1996a; Sommaruga et al., 1997; Visser et al., 2002; Santos et al., 2012b), as well as single-cell activity (Alonso-Sáez et al., 2006; Pérez and Sommaruga, 2007; Ruiz-González et al., 2012), in bacterioplankton. However, results are sometimes contrasting among studies and variable even between bacterial isolates tested in the same study (Joux et al., 1999; Arrieta et al., 2000; Fernández Zenoff et al., 2006b; Hörtnagl et al., 2011; Santos et al., 2011b; Santos et al., 2012a).

Monitoring diel cycles has been frequently used to infer the inhibitory potential of solar radiation on bacterioplankton activities, particularly leucine and thymidine incorporation, in the field. Leucine and thymidine incorporation have been found to be inhibited during the day and recover during the night period (Pakulski et al., 1998; Chróst and Faust, 1999; Visser et al., 1999; Visser et al., 2002; Hernández et al., 2007; Van Wambeke et al., 2009). However, leucine and thymidine incorporation do not seem

to follow the same pattern of inhibition and the extent of the photoinhibition of incorporation can also vary during the day (Pakulski et al., 1998; Visser et al., 2002).

Conclusions on the waveband of the solar spectrum most responsible for the inhibition of activity also seem to vary among studies. For example, while many studies identify UVB radiation as the main solar waveband contributing for the inhibition of leucine and thymidine (Herndl et al., 1993; Aas et al., 1996; Jeffrey et al., 1996a; Conan et al., 2008), others highlight the inhibitory potential of UVA and even PAR (Gourmelon et al., 1994; Sommaruga et al., 1997; Hernández et al., 2007). Some studies have also indicated that leucine and thymidine incorporation are affected differently by different UV wavelengths (Aas et al., 1996).

Solar radiation also affects bacterial activities at the single-cell level. For example, in the northwestern Mediterranean *Gammaproteobacteria* and Bacteroidetes seem to be highly resistant to solar radiation, displaying small changes in activity after irradiation, while *Alphaproteobacteria* are more sensitive to radiation (Alonso-Sáez et al., 2006). More recently, the seasonality of bacterial responses to solar radiation was also reported, with autumn and winter irradiances too low to cause changes in single-cell activity ([^{3}H]leucine uptake), and variable effects in spring and summer (Ruiz-González et al., 2012).

Stimulatory effects of UV exposure, particularly UVA wavelengths, on leucine and thymidine incorporation have been reported as a result of DOM phototransformation (Gustavson et al., 2000; Carrillo et al., 2002; Xenopoulos and Schindler, 2003; Pakulski et al., 2007; Piccini et al., 2009; Vähätalo et al., 2011). However, inhibitory effects of DOM phototransformation on bacterial activity have also been observed (Benner and Biddanda, 1998; Pérez and Sommaruga, 2007). DOM characteristics, such as its age and origin, seem to contribute to determine the effects of solar radiation on the availability of DOM for bacteria (Benner and Biddanda, 1998; Obernosterer et al., 1999; Anesio et al., 2000; Tranvik and Bertilsson, 2001). Freshly produced or autochthonous DOM is prone to become more recalcitrant for bacteria upon irradiation (Tranvik and Kokalj, 1998; Pausz and Herndl, 1999), while irradiation of old or allochthonous DOM produces readily usable products which stimulate bacterial growth (Benner and Biddanda, 1998; Anesio and Granéli, 2003). Furthermore, solar radiation is able to reverse the bioavailability of DOM to bacterioplankton, being the biological reactivity of irradiated DOM inversely related to its bioavailability prior to irradiation (Obernosterer et al., 2001). The effects of DOM phototransformation on

bacterial activity have been associated with the changes induced in bacterial community composition by the process (Pérez and Sommaruga, 2007; Piccini et al., 2009).

UVR also exerts a significant detrimental effect on the activity of extracellular enzymes (Herndl et al., 1993; Müller-Niklas et al., 1995). Aminopeptidase activity appears to be particularly susceptible to UV exposure (Wetzel et al., 1995; Lindell and Edling, 1996; Espeland and Wetzel, 2001; Santos et al., 2011a). While UVB contributes the most for the inhibition of extracellular enzyme activity upon exposure to natural solar radiation (Espeland and Wetzel, 2001), UVA exposure can also result in significant enzyme inhibition (Tank et al., 2005). Inhibition of extracellular enzymes by UVB exposure has been attributed to their direct photolytic cleavage (Müller-Niklas et al., 1995). However, direct photoinactivation of enzymes by natural sunlight, at least in lakes, has been considered negligible (Scully et al., 2003). Alternatively, inactivation might occur through photochemical processes whereby enzymes are inactivated through binding of Fe (III) resulting from the oxidation of Fe (II) by H_2O_2 (Scully et al., 2003).

Whether UV radiation can exert a stimulatory or inhibitory effect on bacterial metabolism seems, therefore, dependent on the physical, chemical and biological properties of the water body studied. However, despite the variability of the reported results, most studies are unanimous in concluding that UVR has the potential to alter the efficiency by which dissolved organic matter is transformed into bacterial biomass and, thus, affect global biogeochemical cycles.

Factors influencing the responses of microorganisms to UVR

The impact of solar UVR on marine microorganisms is complex and several factors, including species composition, environmental factors such as temperature, salinity and nutrients, as well as intrinsic properties, like DNA repair potential and cell size, are crucial in determining their sensitivity.

Temperature

Inactivation of bacteria by UVC and UVB radiation has been found to be either insensitive to temperature, suggesting that DNA damage arises as a result of a purely photochemical process (Severin et al., 1983; Abu-ghararah, 1994; Pakker et al., 2000), or increase with enhanced temperature (Takeuchi et al., 1996; Li et al., 2002; Waterworth et al., 2002; Li et al., 2004; Matallana-Surget et al., 2010). On the other

hand, the photoreactivity of isolated DNA has been reported to decrease with increasing temperature (Douki, 2006).

Consistent with enzyme-catalyzed reactions being temperature dependent, DNA repair rates in bacteria (Dorrell et al., 1995; Salcedo et al., 2007) and archaea (Eker et al., 1991) increase with temperature. Increased temperatures have also been found to reduce bacterioplankton sensitivity to UVR, as determined by [^{3}H]leucine incorporation (Bullock and Jeffrey, 2010), while the activity of antioxidant enzymes during exposure to UV radiation has been shown to decrease with temperature (Borgeraas and Hessen, 2000).

Nutrients

Organic and inorganic nutrients can influence the susceptibility of bacterial communities to UV radiation by affecting the penetration of radiation in the water body (Joux et al., 2009) or altering bacterial physiology (Steinberger et al., 2002). For example, nitrogen (N) limitation can potentially increase susceptibility to UVR by constraining the defences of the cell, since proteins involved in DNA repair require nitrogen (Lesser and Shick, 1989; Roy, 2000). Phosphorus (P) is a constituent of nucleic acids (DNA and RNA) and occurs in the phospholipids of cell membranes, as well as theichoic acids and teichuronic acids of the Gram-positive cell wall. Phosphate is also a component of ADP and ATP which is required, for example, for the activity of the nucleotide excision repair system (Moolenaar et al., 2000). Therefore, phosphorus and nitrogen availability could influence bacterial responses to UVR by affecting bacterial physiology (Pausz and Herndl, 1999; Medina-Sánchez et al., 2002; Pausz and Herndl, 2002).

Growth phase and growth rate

Cell specific growth rate is also a critical determinant of bacterial susceptibility to UV radiation (Berney et al., 2006c; Bucheli-Witschel et al., 2010). UV effects are also influenced by the growth phase, with stationary phase cells generally being more resistant and recovering faster from the lethal effects of UV radiation than exponential growing cells (Dantur and Pizarro, 2004). The influence of growth rate and growth phase on bacterial susceptibility to stress seems to be determined by the global regulator RpoS, controlling the general stress response in *E. coli*, whose expression increases with decreasing specific growth rate (Notley and Ferenci, 1996; Ihssen and Egli, 2004).

Intrinsic DNA repair potential

The intrinsic DNA repair potential of bacteria can also influence their susceptibility to UV radiation. For example, the enhanced UVB resistance of the marine bacterium *Photobacterium angustum*, compared to that of *Sphingopyxis alaskensis*, was assigned to the presence of three genes coding for DNA photolyase type I enzymes in *P. angustum* compared to only one in *S. alaskensis*. The presence of additional photolyase enzymes in *P. angustum* was proposed to not only enhance the efficiency for photoenzymatic repair but also for nucleotide excision repair (Matallana-Surget et al., 2009b). The presence of two *recA* genes was also proposed to account for UV resistance in *Myxococcus xanthus* (Nahrstedt et al., 2005), while two plasmid-encoded *recA* in *Deinococcus desertii*, in addition to the chromosomal *recA*, were suggested to provide higher levels of RecA protein for efficient error-free repair of DNA damage (Dulermo et al., 2009).

The surface microlayer (SML) as a model system for environmental photobiology studies

In the environment, the effects of UVR on aquatic organisms depend on the dose of harmful radiation to which individuals are exposed, which in turn depends on organism positioning in the water column (Sommaruga, 2003). Thriving at the top millimetre of the water column, also known as surface microlayer (SML), bacterioneuston is naturally exposed to high levels of solar radiation, including in the UV spectrum. However, enhanced bacterial abundance and microbial activity at the SML comparatively to underlying waters (Norkrans, 1980; Hardy, 1982; Agogué et al., 2004) suggest a possible adaptation of bacterioneuston to high levels of UV radiation. Several factors have been suggested to contribute to the enhanced resistance of bacterioneuston to high levels of solar radiation, including the accumulation of exopolysaccharides and chromophoric DOM and POM (particulate organic matter) at the air-water interface (Plane et al., 1997; Elasri and Miller, 1999; Whitehead and Vernet, 2000; Obernosterer et al., 2005).

Its location and exposure to high levels of UV radiation make the SML an interesting model compartment to investigate the interaction between UV radiation and bacteria that can provide relevant predictive information on how bacterial communities respond to enhanced levels of UV radiation, in terms of functioning and structure.

As the role of the SML in the regulation of global air-water gas exchange, and consequently in global biogeochemistry, has increasingly been recognized in recent years (Upstill-Goddard et al., 2003; Calleja et al., 2005; Ploug, 2008; Cunliffe and Murrell, 2009; Cunliffe et al., 2011; Dixon and Nightingale, 2012; Cunliffe et al., 2013), the assessment of the biological responses of bacterioneuston to UVR gains even further ecological relevance.

Objectives of this thesis

The understanding of the significance of UV radiation as a controlling factor of bacteria is still limited, since comprehensive mechanistic studies of the targets of UV radiation on bacterial cells are scarce. This, in turn, limits the knowledge of the potential effects of changes in environmental UV levels in the function and structure of microbial communities.

The following research questions were addressed in this thesis:

- Does the light history of the bacterial communities from the SML and UW influence their UV sensitivity?
- What are the cellular targets of UV radiation, how are they affected by irradiation and do they vary among bacteria?
- Which ROS are involved in UVB-induced damage to bacteria?
- Do metals play a role in UVB-induced damage to bacteria?
- How do extrinsic (quality of the irradiating medium) and intrinsic (growth phase and temperature) properties influence the UV sensitivity responses of bacterial communities and bacterial isolates?
- Does RecA evolution reflect an adaptation to withstand stress, including UV radiation, in particular bacterial groups?

These questions were addressed by:

- Studying the effects of UV radiation on natural bacterioneuston and bacterioplankton communities and the photobiological responses of bacterial isolates retrieved from the SML and UW in the laboratory (**Chapters 2, 3 and 4)**.

- Determining the cellular and biological effects of UV radiation of different spectral regions in selected environmental bacterial isolates, used as tentative biological models (**Chapters 5 and 6**).
- Studying the influence of amendment of cell suspensions with ROS scavengers and metals on UVB-induced damage (**Chapter 7 and 8**)
- Assessing the influence of resuspending bacterial cells in aqueous media with different nutrient content and origin in the UV-sensitivity responses of bacterial communities and representative isolates (**Chapter 9**) and studying the influence of growth conditions in UV-induced damage (**Chapter 10**).
- Studying the phylogeny of the RecA protein in order to infer the potential role of *recA* gene duplication or lateral gene transfer events in the adaptation to UV radiation during bacterial evolution (**Chapter 11**).

PÁGINA INTENCIONALMENTE DEIXADA EM BRANCO

CHAPTER 2

Effects of UVB Radiation on the Structural and Physiological Diversity of Bacterioneuston and Bacterioplankton

Santos A. L., Oliveira V., Baptista I., Henriques I., Gomes N. C. M., Almeida A., Correia A., Cunha A.

Applied and Environmental Microbiology (2012) **78**: 2066-2069

Abstract

The effects of UV radiation (UVR) on estuarine bacterioneuston and bacterioplankton were assessed in microcosms experiments. Bacterial abundance and DNA synthesis were more affected in bacterioplankton. Protein synthesis was more inhibited in bacterioneuston. Community analysis indicated that UVR has the potential to select resistant bacteria (*e.g., Gammaproteobacteria*), particularly abundant in bacterioneuston.

Introduction

Global changes over the next decades are expected to increase the exposure of aquatic organisms to damaging UV wavelengths, particularly UVB (280-320 nm), with far reaching ecological consequences (Andrady et al., 2010). Therefore, a thorough understanding of the effects of UV radiation (UVR) on the diversity and function of bacterial communities, key players in nutrient cycling in aquatic ecosystems, is necessary.

The effects of UVB on aquatic organisms depend on the dose of harmful radiation to which they are exposed that is, in turn, determined by the positioning of the organism in the water column (Sommaruga, 2003). The surface microlayer (SML) represents a unique microbial niche in which the bacterial community (bacterioneuston) is exposed to high doses of solar UVR (Agogué et al., 2005). The higher abundances of microorganisms at the SML in comparison to underlying waters (UW) (Agogué et al., 2004) could indicate that bacterioneuston may have adapted to this “extreme environment”, making it an interesting model system for the assessment of UV effects on aquatic organisms by testing the hypothesis that bacterioneuston and bacterioplankton respond differently (in terms of abundance, activity, and structural and functional diversity) to UVB radiation.

Sampling and experimental setup

Samples from the SML and UW were collected in triplicate (n = 9) from an estuarine system (Ria de Aveiro, Portugal, latitude 40º38'N, longitude 08º46'N) on three consecutive days in June 2008. Samples were collected around noon, with clear sky and minimum wind (< 2 m s^{-1}) and solar radiation levels ranged 30-35 kJ m^{-2} (climetua.fis.ua.pt/legacy/main/current_monitor/cesamet.htm). Water properties of the original samples are presented as supplementary material (Appendix). Bacterioneuston was sampled with glass plates (Harvey and Burzell, 1972). Samples from underlying water were taken at the depth of 20 cm. A total of three irradiation experiments (one in each day), with triplicate sub-samples, was conducted using unfiltered water samples since preliminary experiments did not show a significant effect of grazers on the photobiological responses in terms of abundance, activity or diversity of the bacterial communities (data not shown). For the experiments, sub-samples were transferred to uncovered Petri dishes forming a 1.5 mm layer. Irradiation was conducted with UVB lamps (Philips, UVB TL 100 W/01; maximum emission peak at 302 nm, pre-burned for 1 h to ensure stability of light emission) during 4 hours, at room temperature (25 ºC ± 0.5) with magnetic stirring. The cumulative UVB dose (60 kJ m^{-2}, determined using a spectro-radiometer DM 300, Bentham Instruments, Reading, UK) was equivalent to ambient surface UVR levels at 40 to 44º N latitude on clear summer solstice days (Seckmeyer et al., 2008). Aliquots were collected at pre-determined UVB doses (0, 12, 24, 36, 48, 60 kJ m^{-2}) for analyses. Dark controls were included in all experiments.

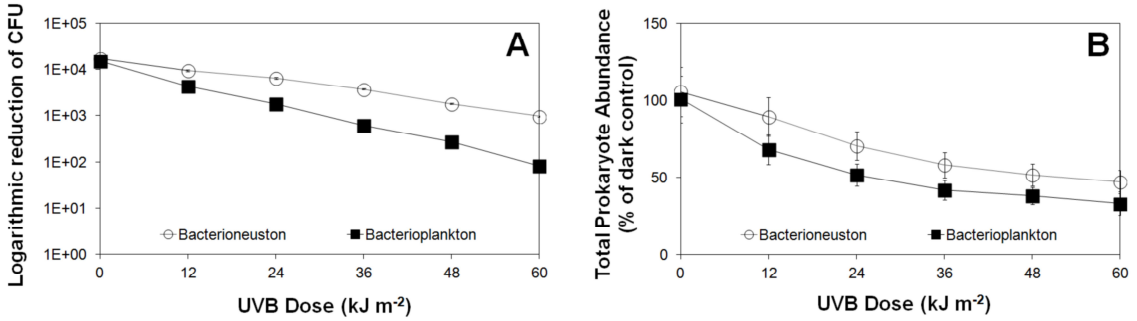

Fig. 2.1. UVB dose-dependent variation of (A) the abundance of culturable bacteria and (B) total prokaryote abundance. Results are expressed as % of the dark controls. Mean values of triplicate determinations in three sub-samples of three independent experiments (n = 27) were plotted. Error bars represent standard deviations. Absence of error bars indicates that standard deviations are too small to see on the scale used.

Effects of UVB on abundance and community composition

Bacterial abundance, determined from colony counts and epifluorescence microscopy (Pernthaler et al., 2001), was less reduced (1-way ANOVA, $p < 0.05$) in bacterioneuston than in bacterioplankton (Fig. 2.1 A, B), indicating enhanced UV tolerance of bacterioneuston, as previously observed in experiments with bacterial isolates (Santos et al., 2011b). DGGE profiling (Santos et al., 2011a) of 16S rDNA sequences showed a reduction in structural diversity (assessed from Shannon diversity index) (Shannon and Weaver, 1963) of 14 and 25 % in bacterioneuston and bacterioplankton, respectively (Fig. 2.2) thus demonstrating the relevance of UVB radiation as driver of the structure of bacterial communities.

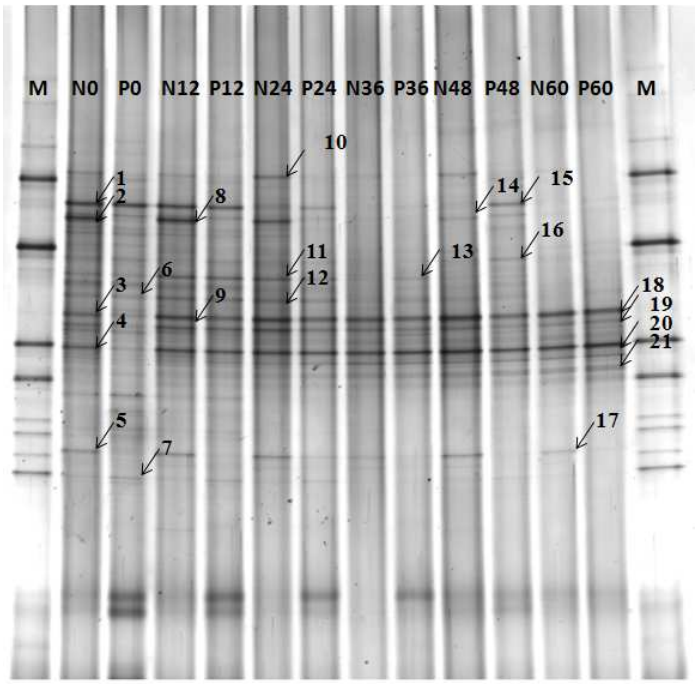

Fig. 2.2. Representative DGGE gel of bacterioneuston and bacterioplankton exposed to different UVB doses (0, 12, 24, 36, 48, 60 kJ m^{-2}), in which sequenced bands are indicated by an arrow. M: marker; N: bacterioneuston; P: bacterioplankton.

Sequencing of selected cloned DGGE bands (supplementary material in Appendix) revealed the predominance of ribotypes affiliated to *Bacteroidetes-Chlorobi* (band 1), *Firmicutes* (band 2) and *Gammaproteobacteria* (bands 3 and 4) in the original bacterioneuston and bacterioplankton samples. After irradiation, *Gammaproteobacteria*-affiliated ribotypes dominated both communities. Two strong bands (identified in Fig. 2.2 as bands 3 = 9 = 18 and 4 = 20) affiliated to *Gammaproteobacteria*, persisted throughout the irradiation period in bacterioneuston and bacterioplankton, suggesting

the selection of resistant strains by UVR in both communities. These bands were already prominent in the original bacterioneuston sample and occurred with equal predominance in bacterioneuston and bacterioplankton after irradiation. *Gammaproteobacteria* have already been reported as resistant to UVR (Alonso-Sáez et al., 2006).

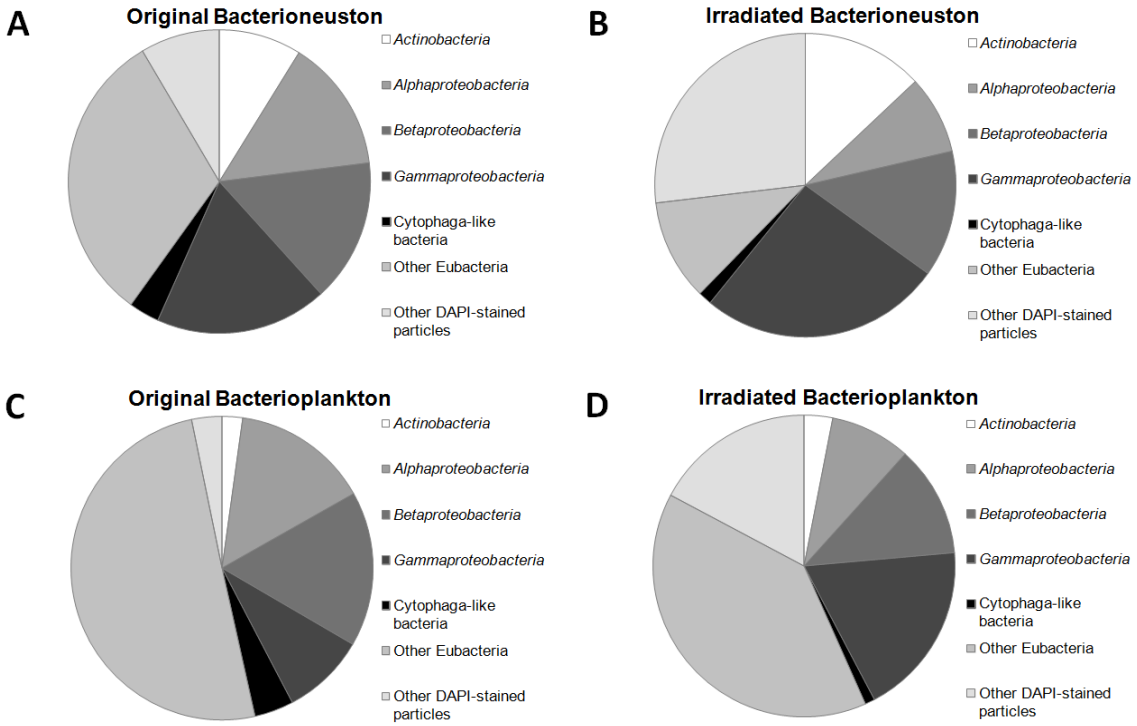

Fig. 2.3. Mean relative abundance (expressed as the percentage of total DAPI counts) of specific bacterial groups detected by FISH before and after exposure of bacterioneuston and bacterioplankton communities to a total dose of 60 kJ m^{-2} of UVB radiation. Mean values (n = 27) were plotted.

The effects of UV exposure on community composition were also studied by Fluorescence *in situ* hybridization (FISH) using Cy3-labeled oligonucleotide probes for the domain Bacteria (Amann et al., 1990; Daims et al., 1999) and classes *Alphaproteobacteria* (Glöckner et al., 1999), *Betaproteobacteria* (Manz et al., 1996), *Gammaproteobacteria* (Manz et al., 1996), *Cytophaga*-like bacteria (Manz et al., 1996) and *Actinobacteria* (Manz et al., 1996). The appropriate controls were included. FISH results confirmed the dominance of *Gammaproteobacteria* in bacterioneuston and an increase of up to 10 % (1-way ANOVA, $p < 0.05$) in the relative abundance of *Gammaproteobacteria* after irradiation of bacterioneuston and bacterioplankton (Fig. 2.3). In general, the different bacterial groups quantified by FISH followed a similar trend of variation in bacterioneuston and bacterioplankton (supplementary material in

Appendix), with the exception of *Actinobacteria*, which increased in abundance by 32.2 % in bacterioneuston during irradiation, remaining un-affected in bacterioplankton. *Actinobacteria* have been proposed to be genetically adapted to high UV levels (Warnecke et al., 2005). The results suggest that bacterioneuston may contain a pool of UV-resistant bacteria that are selected for upon UV exposure.

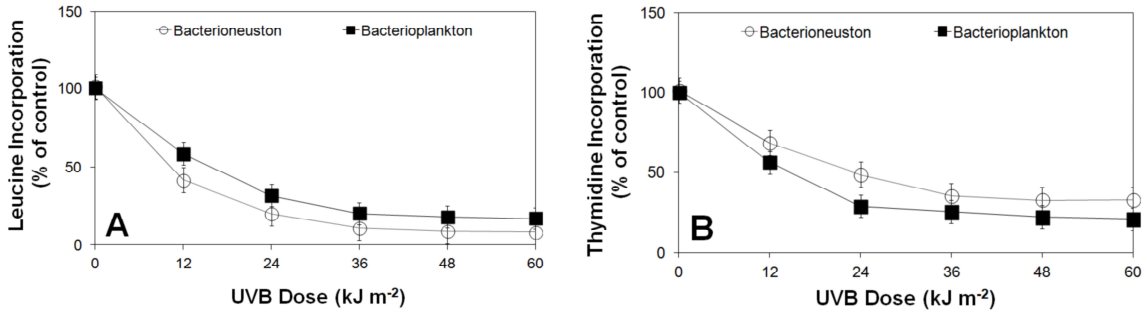

Fig. 2.4. UVB dose-dependent variation of (A) leucine incorporation (protein synthesis) and (B) thymidine incorporation (DNA synthesis). Results are expressed as % of the dark controls. Mean values were plotted. Error bars represent standard deviations. Absence of error bars indicates that standard deviations are too small to see on the scale used.

Effects of UVB on activity

The rates of leucine and thymidine incorporation were used as proxies for protein and DNA synthesis, respectively (Moriarty, 1986; Simon and Azam, 1989). Leucine incorporation was more affected by UVB in bacterioneuston (Fig. 2.4 A), while thymidine incorporation was more inhibited in bacterioplankton (Fig. 2.4 B) (1-way ANOVA, $p < 0.05$). Reducing protein synthesis upon UVB exposure could be a metabolic strategy to enhance survival, as actively growing bacteria are more susceptible to stress (Fischer and Sauer, 2005) and this could underlie the lower impact of UVB on bacterioneuston abundance.

The effect of UVR on the physiological profiles of bacterioneuston and bacterioplankton assessed with Biolog EcoPlates^{TM} (Sala et al., 2010) revealed a shift in the spectrum of carbon sources used, as well as substantial differences in the metabolic profiles of bacterioneuston and bacterioplankton before and after UV exposure (Fig. 2.5). In bacterioneuston, UV exposure resulted in a 31.2 %, 14.4 % and 6.3 % decrease in the use of amino acids, amines and carboxylic acids and an increase in consumption of carbohydrates and phenolic compounds by 42.3 % and 11.6 %, respectively. In bacterioplankton, irradiation caused a decrease in the utilization of carbohydrates and

phenolic compounds by 21.7 and 42.9 %, respectively, and an increase in consumption of amino acids and carboxylic acids by 42.2 and 22.5 %, respectively.

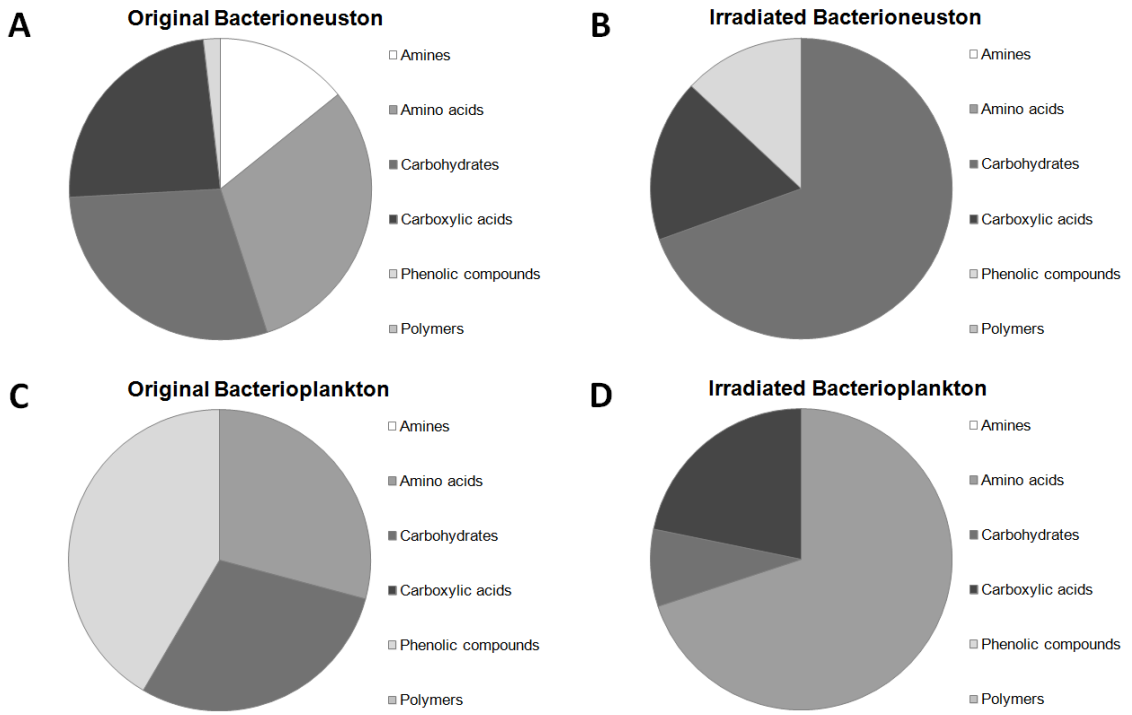

Fig. 2.5. Mean relative consumptions of different substrate categories present in Biolog EcoPlates^{TM} before and after exposure of bacterioneuston and bacterioplankton communities to a total dose of 60 kJ m^{-2} of UVB radiation. Mean values (n=9) were plotted.

In conclusion, the present work demonstrates that UV radiation has clear effects on the structure and function of estuarine bacterial communities and that the SML environment may select for a bacterial community metabolically adapted to high UV exposure.

Acknowledgments

This work was supported by CESAM (Centre for Environmental and Marine Studies, University of Aveiro) and the Portuguese Foundation for Science and Technology (FCT) in the form of a PhD grant to A.L.S. (SFRH/BD/40160/2007) and a post-Doctoral grant to I.H. (SFRH/BPD/63487/2009).

CHAPTER 3

Diversity in UV-Sensitivity and Recovery Potential among Bacterioneuston and Bacterioplankton Isolates

Santos A. L., Lopes S., Baptista I., Henriques I., Gomes N. C. M., Almeida A., Correia A., Cunha A.

Letters in Applied Microbiology (2011) **52**: 360-366

Abstract

Aims: To assess the variability in the UVB (280-320 nm) sensitivity of bacterial isolates from the surface microlayer (SML) and underlying water (UW) of the Ria de Aveiro (Portugal) estuary and their ability to recover from previous UV-induced stress.

Methods and Results: Bacterial cell suspensions were exposed to UVB radiation (3.3 W m^{-2}). Effects on culturability were assessed from colony counts and effects on activity determined from [^{3}H]leucine incorporation rates. Among the nine isolates tested a wide variability in terms of UVB-induced inhibition of culturability (37.4-99.3 %) and activity (36.0-98.0 %) was observed. Incubation of UVB-irradiated cell suspensions under reactivating regimes (UVA, 3.65 W m^{-2}; PAR, 40 W m^{-2}; dark) also revealed diversity in the extent of recovery from UVB stress. Trends of enhanced resistance of culturability (up to 15 %) and enhanced recovery in activity (up to 52 %) were observed in bacterioneuston isolates.

Conclusions: Bacterioneuston isolates were less sensitive and recovered more rapidly from UVB stress than bacterioplankton isolates, showing enhanced reduction of their metabolism during the irradiation period and decreased culturability during the recovery process compared to bacterioplankton.

Significance and Impact of the Study: UV exposure can affect the diversity and activity of microbial communities by selecting UV-resistant strains and alter their metabolic activity towards protective strategies.

Introduction

Since the discovery of the stratospheric ozone hole, concerns regarding the ecological consequences of UV radiation have extensively increased (Häder et al., 2007). In the face of a changing global environment, the assessment of the toxic nature

of UV radiation, most notably in the UVB wavelength (280-320 nm) that is expected to increase as a result of the interaction of changes in UVB fluxes resulting from ozone depletion and other climate changes (Andrady et al., 2010), has gained pertinence.

Bacteria play a key role in nutrient cycling in aquatic ecosystems (Azam and Malfatti, 2007), but their small size, short generation times and the fact that their genome comprehends a large portion of the cell volume, might make them more susceptible to the effects of UV radiation than higher organisms (Garcia-Pichel, 1994).

The main biological effect of UVB results from UV-induced formation of covalent links between adjacent pyrimidine residues, known as cyclobutane pyrimidine dimers. These dimers cannot be replicated and are lethal to the cell, unless damage is repaired (Mitchell and Karentz, 1993). In response to UV-induced damage, bacteria have evolved several repair mechanisms that can basically be divided in dark repair and photoreactivation, a light-dependent repair mechanism that uses the photolyase enzyme, activated by UVA (320-400 nm) and photosynthetically active radiation (PAR, 400 to 700 nm) (Walker, 1984).

Located at the air-water interface, the surface microlayer (SML) represents a stressful environment for microorganisms, where pollutants and heavy metals accumulate due to its lipophilic nature, and the intensity of solar UV radiation is at its highest (Maki, 1993). Adding to their individual effects, pollutants and UV radiation can also act additively or synergistically on aquatic microbes (Pelletier et al., 2006), through the generation of photo-oxidative products that might impose an additional stress on bacterioneuston, *i.e.*, bacteria inhabiting the surface microlayer. Reports of higher bacterial abundance and activities at the SML (Kuznetsova and Lee, 2002) have suggested enhanced resistance of bacterioneuston to stress, most notably, UV-related. However, such a trend has not yet been demonstrated, and recent work has indicated similar UV resistance in bacterial isolates from the SML and underlying water (UW) (Agogué et al., 2005), though the authors only monitored the optical density of the cultures after the irradiation period. To our knowledge, information on the variability of the responses of bacterioneuston isolates in terms of culturability and activity, as well as their repair potential under different reactivating regimes following UV exposure, is virtually inexistent.

The aim of this work was the characterization and comparative analysis of the sensitivity of bacterial isolates from the SML and UW of the estuarine system Ria de Aveiro (Portugal) and the assessment of their repair potential under different light

regimes after UVB exposure. The variability in the extent of UV-induced inactivation and the influence of different light regimes on the recovery of selected bacterial isolates following UVB stress were determined in laboratory experiments using artificial radiation.

Materials and methods

Sampling and isolation of marine bacterial strains

Bacterial strains were isolated from the SML and UW of the estuarine system Ria de Aveiro, located in the western coast of Portugal. Samples from the SML were collected using a glass plate sampler (Harvey and Burzell, 1972). Samples from underlying waters were collected by submerging a polycarbonate bottle and opening it at a depth of 0.5 m. For the isolation of UV-resistant bacteria from the SML and UW, samples from both water layers were exposed to UVB doses between 0 and 2200 J m^{-2} (Philips UVB TL 100 W/01 lamp, maximum emission peak at 302 nm; intensity of 3.3 W m^{-2}), with agitation (50 rpm) and at ~20 ºC, as described by Zenoff, *et al.* (2006). Sample aliquots (100 µL) were removed at pre-determined intervals and plated in marine agar 2216 plates (MA 2216; Difco, Detroit, Mich.). After incubation in the dark at 20°C for 7 to 14 days, isolates were selected from the plates according to morphological differences and purified. Molecular typing of the isolates was performed by BOX-PCR, according to the procedure described by Rademaker, *et al.* (2004) and isolates displaying distinct BOX profiles were identified by sequencing the 16S rRNA gene using the primer 27F and an ABI PRISM BigDye Terminator Cycle Sequencing Ready Reaction Kit (PE Applied Biosystems, Foster City, CA, USA). Sequences were compared with sequences available in the GenBank database by using the BLAST (Basic Local Alignment Search Tool) service to determine their approximate phylogenetic affiliations (Altschul et al., 1990). The sequences obtained were deposited in the GenBank database (see Table 3.1 for accession numbers).

Preparation of cell suspensions and irradiation conditions

Bacterial isolates growing in marine broth were harvested during the exponential phase by centrifugation (3,200 x *g*, 15 min) and the pellet was washed three times with filtered-sterilized autoclaved seawater to remove all traces of the culture medium. Cells were resuspended in filtered-sterilized autoclaved seawater and bacterial abundance was

adjusted to 10^6 cells mL^{-1}, as determined by epifluorescent microscopy counts. Bacterial suspensions were transferred to sterile plates (Corning Science Products, Corning, NY) without the lid and irradiated under the UVB source used for the initial isolation for 20 min (corresponding to a final UVB dose of 3.931 kJ m^{-2}). During irradiation, samples were kept at ~20 ºC and incubated under slow shaking (50 rpm). All experiments were conducted in the absence of ambient light to minimize photoreactivation. After irradiation, appropriate dilutions were plated on marine agar (MA 2216, Difco, Detroit, Mich.). Each experiment was conducted with triplicate replicates in four independent times.

Table 3.1. Origin, phylogenetic affiliation, sequence similarity to the closest relative and NCBI accession number of the UV-resistant bacterial isolates used in this study. SML - Surface microlayer. UW - Underlying waters.

Origin	Strain	Bacterial group	Closest relative in the 16S rRNA gene sequence database (accession no.)	% Sequence similarity	Accession no.[1]
SML	*Pseudomonas* sp. strain NT5I1.2B	*Gammaproteobacteria*	*Pseudomonas* sp. DSM 8628 (FM208263.1)	97	GU084169
	Paracoccus sp. strain NT25I3.1A	*Alphaproteobacteria*	*Paracoccus* sp. JAM-AL07 (AB526330.1)	99	GQ365195
	Staphylococcus sp.strain NT25I2.1	Firmicutes	*Staphylococcus saprophyticus* strain ATCC 15305 (D83371.2)	99	GQ365197
	Micrococcus sp. strain NT25I3.2AA	*Actinobacteria*	*Micrococcus* sp. TA014 (EU308453.1)	98	GQ365196
	Sphingomonas sp. NT15I1.2B	*Alphaproteobacteria*	*Sphingomonas* sp. PA225 (AM900788.1)	100	GU084171
UW	*Brevibacterium* sp. strain PT5I3.3L	*Actinobacteria*	*Brevibacterium casei* strain TSWCW1 (GQ284451.1)	99	GQ365205
	Bacillus sp. strain PT15I3.2CB	Firmicutes	*Bacillus cereus* strain 5YW6 (GU991861.1)	99	GQ365209
	Acinetobacter sp. strain PT5I1.2G	*Gammaproteobacteria*	*Acinetobacter* sp. BS8Y (EU545154.1)	97	GQ365202
	Psychrobacter sp. strain PT15I3.2CA	*Gammaproteobacteria*	*Psychrobacter piscidermidis* strain P4-4(EU127295.1)	99	GQ365208

[1]Accession numbers based on 16S rRNA partial gene sequence.

Repair potential

To determine the repair properties of the bacteria, UVB-irradiated cell suspensions were subjected to three different treatments: (i) photoreactivation with PAR, provided by white cool lamps (13.44 W m^{-2}; Philips TLD 58 W/84), (ii) UVA provided by Philips TL 100W/10R lamps (wavelength range 350 to 400 nm; intensity 3.65 W m^{-2}), and (iii) darkness, by incubating the suspensions in the dark. Aliquots of samples were collected before and after incubation of the cells for 60 and 180 min under the different recovery regimes for culturable counts and bacterial activity assessment. Each experiment was conducted with triplicate replicates in four independent times.

Culturable counts

The UV-inactivation kinetics was followed by collecting triplicate 100 µL aliquots at pre-determined intervals. Aliquots were serially diluted in aged 0.2 µm filtered autoclaved sea-water and plated in Marine agar 2216 plates (Difco). Colonies were counted after 2-7 days of incubation in the dark at 20 ºC. The fraction of surviving cells was calculated by dividing the number of CFU in the treated sample by the number of CFU in the unirradiated sample at time zero. The dilution and plating procedures were carried out under low-luminosity conditions to avoid photoreactivation.

Bacterial activity

The bacterial activity of cell suspensions before irradiation, after irradiation and after reactivation was assessed from the rates of protein synthesis estimated by the incorporation of [^{3}H]leucine (Amersham, specific activity 63.0 Ci mmol^{-1}) into bacterial protein at 480 nM final concentration in triplicate aliquots (1.5 mL) and one trichloroacetic acid (TCA, Sigma, St. Louis, Mo) fixed blank (2 % final concentration). After 1 hour of incubation in the dark, proteins were precipitated by addition of 20 % TCA and samples were centrifuged. TCA-washed pellets were resuspended in 1.5 mL of Universol liquid scintillation cocktail (ICN Biomedicals, USA). The radioactivity incorporated into bacterial cells was counted in a Packard Tri-Carb 2000 Liquid Scintillation Counter using the external standard ratio technique (Simon and Azam, 1989).

Results

In this study, UV-resistant strains isolated after irradiation of samples from the SML and UW were used to assess the variability of UVB sensitivity and recovery potential in bacterioneuston and bacterioplankton isolates. UVB-induced inhibition of culturability ranged from 37.4 % in *Micrococcus* sp. (NT25I3.2AA) (Fig. 3.1 A) to 99.3 % in *Staphylococcus* sp. (NT25I2.1) (Fig. 3.1 E).

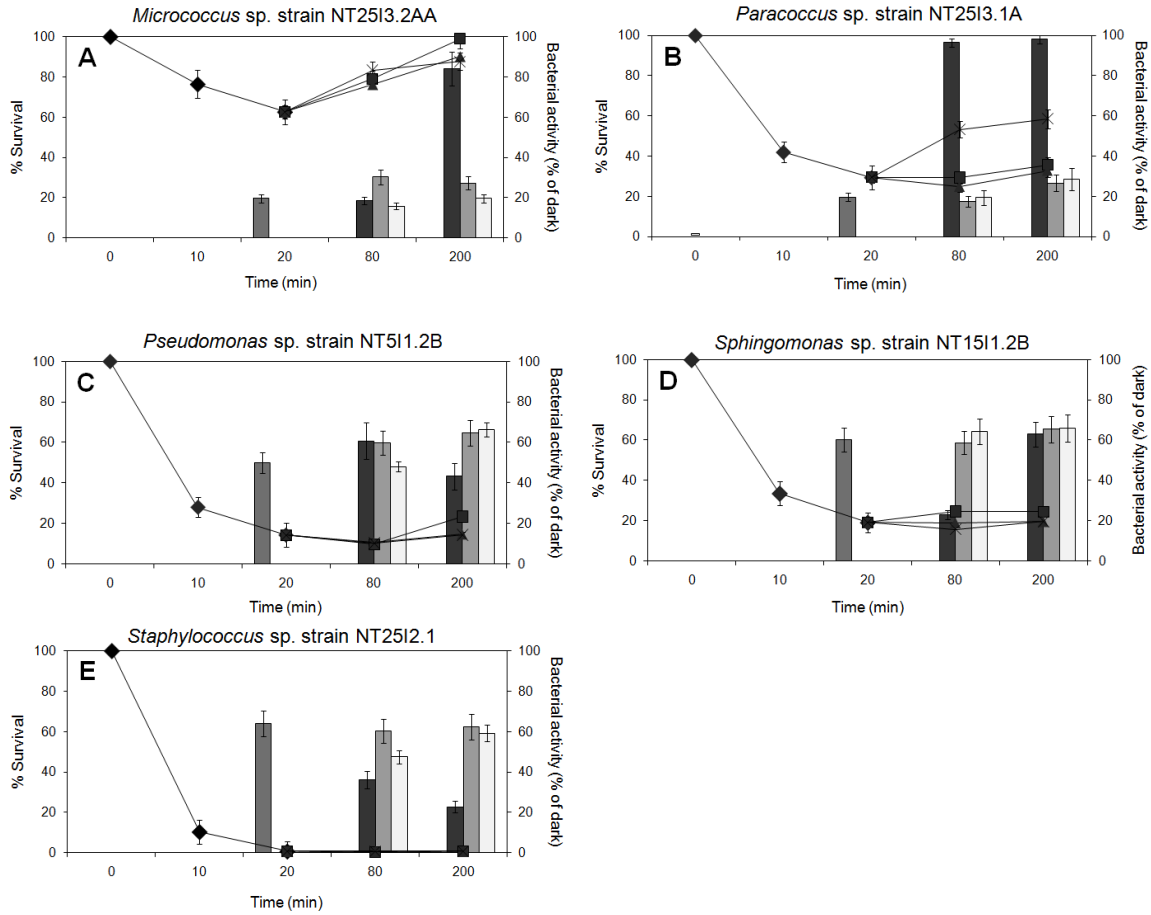

Fig. 3.1. Effects of UVB radiation and reactivation under different light regimes on the culturability and activity (protein synthesis) of UV-resistant bacterioneuston isolates. Cells were exposed to UVB radiation for 20 min. During the following 180 min cells were allowed to recover under photoreactivation light (UVA and PAR) and in the dark. Aliquots of cells suspensions were collected after 60 min and after 120 min of incubation under the different recovery regimes for the assessment of colony counts and activity. Curves and bars in the figures correspond to the variation in survival and activity rates, respectively. Error bars represent standard deviations of triplicate replicates of 4 independent experiments. Absence of error bars indicates standard deviations are too small to see on the scale used. Results are expressed as % of the unirradiated sample at time zero. Symbols: UV-B UV-A PAR Dark UV-B UV-A PAR Dark

The reduction imposed by UVB exposure on bacterial activity ranged from 36.0 % in *Staphylococcus* sp. (NT25I2.1) (Fig. 3.1 E) to 98.0 % in *Bacillus* sp. (PT15I3.2CB) (Fig. 3.2 B), On average, UVB-induced reduction in bacterial culturability was up to 15.0 % higher in bacterioplankton isolates, while the reduction in the activity was up to 25.0 % higher in bacterioneuston isolates (1-way ANOVA, $p < 0.05$) (Fig. 3.1 and 3.2).

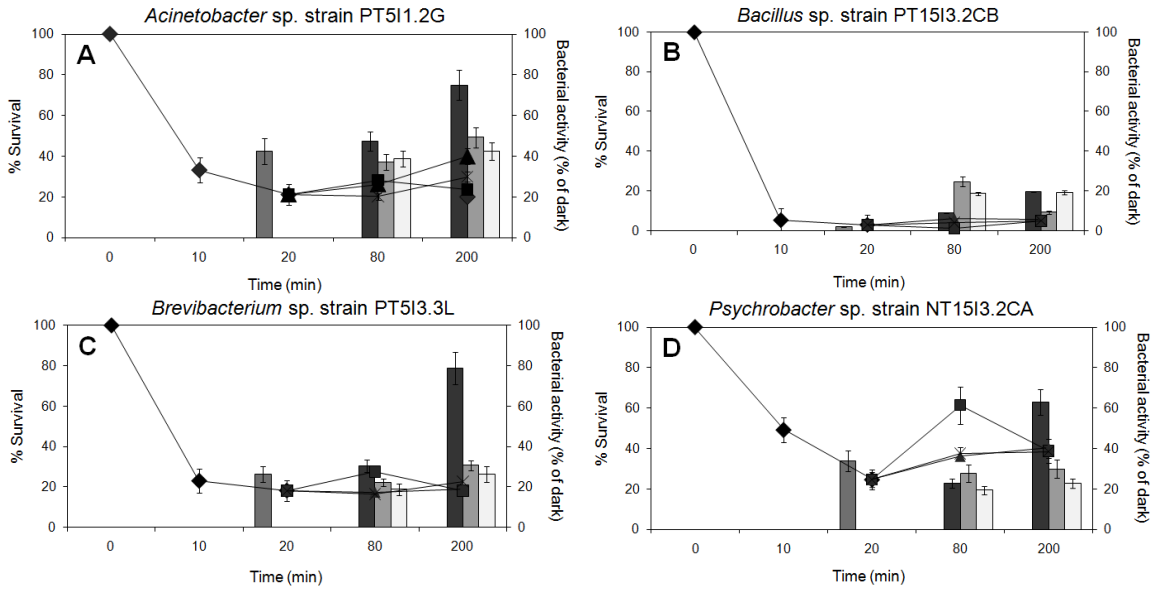

Fig. 3.2. Effects of UVB radiation and reactivation under different light regimes on the culturability and activity (protein synthesis) of UV-resistant bacterioplankton isolates. Cells were exposed to UVB radiation for 20 min. During the following 180 min cells were allowed to recover under photoreactivation light (UVA and PAR) and in the dark. Aliquots of cells suspensions were collected after 60 min and after 120 min of incubation under the different recovery regimes for the assessment of colony counts and activity. Curves and bars in the figures correspond to the variation in survival and activity rates, respectively. Error bars represent standard deviations of triplicate replicates of 4 independent experiments. Absence of error bars indicates standard deviations are too small to see on the scale used. Results are expressed as % of the unirradiated sample at time zero.

Symbols: UV-B UV-A PAR Dark UV-B UV-A PAR Dark

Under the UVA and PAR regimes, recovery of culturability (up to 90.0 % of the initial value) was observed for 8 out of 9 of the isolates tested (Fig. 3.1 and 3.2). Recovery in bacterial culturability (up to 98.0 % of the initial value) was also observed under the dark regime for 6 out of the 9 isolates tested (Fig. 3.1 and 3.2). The bacterioneuston isolates *Micrococcus* sp. strain NT25I3.2AA (73.5 %) (Fig. 3.1 A) and *Paracoccus* sp. strain NT25I3.1A (99.0 %) (Fig. 3.1 B) showed the highest efficiencies in the recovery of bacterial culturability under the UVA and dark regimes, respectively, while the bacterioplankton isolate *Bacillus* sp. strain NT25I3.2AA (90.0 %) (Fig. 3.2 B) recovered the most under the PAR regime. In general, significant differences between the patterns of recovery under the different light regimes were not detected. However, when considering the SML and UW in separate, differences emerged. For SML isolates, the most favourable light regime for the recovery of bacterial culturability was UVA (average recovery of 11.4 %), while PAR induced the lowest recovery rate (6.4 %). For bacterioplankton isolates, PAR led to the highest recovery rates (9.5 %), while the lowest recovery was observed under UVA irradiation (4.6 %).

Bacterial activity also recovered, at variable extensions (0 to 78.4 %), under the different light regimes (Fig. 3.1 and 3.2). In general, UVA radiation was the most favourable light regime (up to 78.4 %) in the recovery of bacterial activity, while significant differences between recovery under PAR (up to 14.6 %) and in the dark (up to 17.2 %) were not found (1-way ANOVA, $p > 0.05$). Bacterioneuston isolates *Paracoccus* sp. strain NT25I3.1A (78.4 %) (Fig. 3.1 B) and *Pseudomonas* sp. strain NT5I1.2B (14.6 %) (Fig. 3.1 C) showed the highest recovery rates in bacterial activity under the UVA and PAR regime, while the planktonic isolate *Bacillus* sp. strain PT15I3.2CB (17.2 %) (Fig. 3.2 B) recovered the most under the dark regime. When considering the compartment from which the bacterial isolates were retrieved, the patterns observed for bacterial culturability were maintained, though for bacterioplankton isolates, significant differences were observed in the extent of the recovery in the dark and under UVA radiation (twice as high than under the dark regime).

Discussion

Several studies on UV sensitivity and recovery potential in bacteria present in diverse aquatic environments have been carried out (Joux et al., 1999; Arrieta et al., 2000; Agogué et al., 2005). However, to our knowledge, no information exists on the diversity of the UV responses of bacterioneuston isolates in terms of culturability, activity and recovery from previous UV-induced stress. Therefore, in this study the variability in the UV-sensitivity and recovery potential of selected UV-resistant bacterioneuston and bacterioplankton isolates was assessed under standardized experimental conditions using a number of isolates similar to previous studies (Joux et al., 1999; Arrieta et al., 2000; Fernández Zenoff et al., 2006b).

Exposure to UVB radiation revealed considerable variability in sensitivity to UV stress among the tested isolates, in agreement with previous reports in different aquatic environments (Arrieta et al., 2000; Ordoñez et al., 2009). *Micrococcus* sp. (NT25I3.2AA) showed the smallest reduction in culturability upon UVB exposure. High UV resistance of several *Micrococcus* strains isolated from other UV-exposed environments is well documented (Fernández Zenoff et al., 2006b; Ordoñez et al., 2009). The characteristically high G+C content of *Actinobacteria* has been proposed to confer a protective effect against UV radiation, by protecting DNA against damage by thymidine dimerization (Singer and Ames, 1970). However, recent work by Matallana-

Surget, *et al.* (2008) has suggested that microorganisms with high G+C content could, in fact, be more prone to UV-induced mutations, since cytosine containing photoproducts are highly mutagenic. The determinants of UV-resistance in *Micrococcus* sp. remain, therefore, unknown.

Considerable differences were also observed in the extent of UV-induced inhibition of bacterial activity probably as a result of differences in the extent of the damage inflicted to bacterial membranes. The observation that *Staphylococcus* sp. (NT25I2.1) was the strain most inhibited in terms of culturability but less inhibited in terms of activity is intriguing, since one would expect the two biological parameters to be correlated. A similar trend was also observed in *Micrococcus* sp. (NT25I3.2AA) that was least affected in terms of culturability but was the second most affected strain in terms of activity (80.4 % inhibition), as assessed from the rates of leucine incorporation. A possible explanation would be the induction of a metabolic shift from growth (protein synthesis) to survival upon UVB exposure, recently proposed to occur in *Bacillus cereus* in response to acid stress (Mols et al., 2010). However, further studies are needed to reveal if such a response also occurs upon UVB stress.

The most important biological effects of UVB radiation are probably a consequence of the stalling of replication fork complexes by UVB-induced DNA lesions that block replisome movement or the synthesis by the polymerase subunits. Therefore, the ability of bacteria to survive UVB radiation is closely related to their ability to either bypass or correct such damaged DNA segments (Friedberg, 1985).

Following UVB exposure, the recovery potential of the bacterial isolates was assessed under different light regimes. UVA and PAR were the most effective regimes in the recovery of culturability, but recovery under the dark regime was also observed for most isolates. Such observation demonstrates the importance of photoreactivation, and particularly the enzyme photolyase, in the recovery from UVB stress, in accordance to previous studies (Kaiser and Herndl, 1997). The importance of photoreactivation for bacterial communities to cope with UV-induced damage might be related to its extreme efficiency, splitting approximately one dimer for every blue-light photon absorbed. Furthermore, unlike dark repair, photoreactivation does not require energy mobilization and may be particularly important in nutrient-limited aquatic microbial populations (Joux et al., 1999). Recovery in terms of bacterial activity was also observed under the different light regimes, demonstrating that UV-induced impairment of biological

functions was not irreversible being, in general, UVA the most effective light regime for activity recovery.

Though the number of isolates used in this study is too small to attempt the establishment of a correlation between the origin of the isolates and their UV sensitivity, some trends were in fact identified. For example, UV-induced reductions in bacterial culturability were up to 15 % lower in bacterioneuston, which might indicate the presence of bacteria displaying enhanced resistance to UV radiation at the SML. The average recovery in terms of culturability was generally higher in bacterioplankton isolates (up to 76 %) than in bacterioneuston for all light regimes. On the other hand, in terms of activity, the recovery was higher in bacterioneuston (up to 52 %) under all the reactivating conditions tested. The observation of enhanced recovery in activity accompanied by reduced recovery in culturability in bacterioneuston isolates could indicate the engagement in a viable but non culturable condition as a stress response and/or defence mechanism that allows for the rapid re-establishment of bacterial activity when UV exposure is terminated. This hypothesis is supported by the observation that, in some cases, the UV-induced decrease in total cell numbers, determined by epifluorescence microscopy counts of acridine orange-stained preparations, was much lower than the one of CFU numbers (data not shown). Such a strategy has been reported, for example, in species of the genus *Vibrio* sp. upon exposure to thermal, saline and acidic stress (Wong and Wang, 2004).

While addressing the resistance of bacterioneuston and bacterioplankton strains to solar UV radiation, by directly isolating culturable bacteria from the SML and underlying waters and monitoring the optical density of the irradiated cells, Agogué, *et al.* (2005) concluded that UV resistance was similarly distributed in bacterioneuston and bacterioplankton. In fact, several studies have indicated that the bacterial community structure of both compartments itself is similar and that the neustonic community might arise from the passive accumulation of members of the planktonic populations at the air-water interface (Joux et al., 2006). In this study, an alternative approach was used, in which samples from the SML and UW were exposed to UVB radiation and the UV-resistant species were isolated (Fernández Zenoff et al., 2006a). While the ecological information retrieved from studies with culturable bacteria is considered limited, this alternative approach is likely to provide a new, ecologically relevant perspective on UV-sensitivity and resistance among culturable bacteria, since these strains are likely the most relevant members of the culturable community upon exposure to UVB-induced

stress, and their metabolic strategies may drive the functioning of the communities under UVB stress conditions.

By the selective elimination of sensitive phenotypes and the enrichment in resistant strains, differences in the UV-sensitivity of bacteria inhabiting the SML and underlying waters seem to emerge, that can indicate the presence of UV-resistant members in the bacterioneuston population.

Acknowledgments

Acknowledgments are due to the anonymous reviewers that greatly improved the earlier version of this manuscript. Financial support for this work was provided by CESAM (Centre for Environmental and Marine Studies, University of Aveiro) and by the Portuguese Foundation for Science and Technology (FCT) in the form of a PhD grant to A.L. Santos (SFR/BD/40160/2007) and a post-Doctoral grant to I. Henriques (SFRH/BPD/63487/2009).

PÁGINA INTENCIONALMENTE DEIXADA EM BRANCO

CHAPTER 4

The UV Responses of Bacterioneuston and Bacterioplankton Isolates Depend on the Physiological Condition and Involve a Metabolic Shift

Santos A. L., Baptista I., Lopes S., Henriques I., Gomes N. C. M., Almeida A., Correia A., Cunha A.

FEMS Microbiology Ecology (2012) **80**: 646-658

Abstract

Bacteria from the surface microlayer (SML) and underlying waters (UW) were isolated upon exposure to UVB radiation and their individual UV sensitivity in terms of CFU numbers, activity (leucine and thymidine incorporation), sole-carbon source use profiles, repair potential (light-dependent and independent), and photoadaptation potential, under different physiological conditions, was compared.

Colony counts were 11.5-16.2 % more reduced by UVB exposure in bacterioplankton isolates (1-way ANOVA, $p < 0.05$). Inhibition of leucine incorporation in bacterioneuston isolates was 10.9-11.5 % higher than in bacterioplankton (1-way ANOVA, $p < 0.05$). These effects were accompanied by a shift in sole-carbon source use profiles, assessed with Biolog EcoPlates^{TM}, with a reduction in consumption of amines and amino acids and increased use of polymers, particularly in bacterioneuston isolates. Recovery under starvation was generally enhanced compared to nourished conditions, especially in bacterioneuston isolates. Overall, only insignificant increases in the induction of antibiotic resistant mutant phenotypes (Rif^R and Nal^R) were observed. In general, a potential for photoadaptation could not be detected among the tested isolates.

These results indicate that UV effects on bacteria are influenced by their physiological condition and are accompanied by a shift in metabolic profiles, more significant in bacterioneuston isolates, suggesting the presence of bacterial strains adapted to high UV levels in the SML.

Introduction

Among the different factors that affect bacteria, solar UV radiation (UVR) (280-400 nm) could be particularly deleterious because of their simple haploid genomes with little or no functional redundancy and their small size which precludes the accumulation of protective pigments (Garcia-Pichel, 1994). The importance of microorganisms in

global biogeochemical cycles and the expected increases in the exposure of aquatic organisms to damaging UV wavelengths over the course of the next decades (Andrady et al., 2010) makes the study of the interaction between UV radiation and microorganisms a timely subject.

Studies of photobiological responses of marine bacterial isolates have shown large variability in their sensitivity to UVR (Joux et al., 1999; Arrieta et al., 2000; Agogué et al., 2005; Santos et al., 2011b). UV-induced changes in bacterial production, growth, survival and species composition, through the selection of phototolerant strains or by inducing photoadaptation, can, in turn, cause changes in the trophodynamics of microbial communities (Arrieta et al., 2000; Winter et al., 2001).

The toxic effects of UVB radiation are considered to be, for the most part, the result of the absorption of photons by DNA, resulting in DNA photoproducts that block DNA replication and RNA transcription and, left unrepaired, can lead to cell death (Walker, 1984). Additionally, absorption of UV radiation by endogenous (*e.g.*, porphyrins, nicotinamide coenzymes) and exogenous (*e.g.*, humic substances and photosynthetic pigments) photosensitizers can lead to the formation of reactive oxygen species and cause oxidative damage, potentially impairing bacterial activity and viability (Baxter and Carey, 1983; Cooper et al., 1988; Glaeser et al., 2010).

In response to UV-induced damage, bacteria have evolved several DNA repair mechanisms that can basically be divided in dark repair and light-dependent repair. At least three dark repair mechanisms can be found in bacteria: (1) nucleotide excision repair (NER), (2) post-replication recombinational repair and (3) error-prone or mutagenic DNA repair (MDR) (Walker, 1984). The latter involves the activation of low fidelity repair polymerases, which are able to perform translesion DNA synthesis across damaged regions, at the expenses of an increased mutation rate (Goodman, 2002; Rattray and Strathern, 2003) and seems to confer an ecological advantage for microorganisms inhabiting UV-exposed habitats (Sundin and Murillo, 1999). Light-dependent repair, also known as photoenzymatic repair (PER) (Walker, 1984), uses a photolyase enzyme that can be activated by UVA (320-400 nm) and photosynthetic active radiation (PAR) (400-700 nm) (Sancar, 1994).

Variability in UV sensitivity among bacterial strains is mainly determined by differences in intrinsic susceptibility and/or defence and repair strategies in response to damage. However, several intrinsic factors such as the nutritional state (Nyström et al., 1992) and growth phase (Berney et al., 2006c; Bucheli-Witschel et al., 2010), or

external factors like temperature (Matallana-Surget et al., 2010) can also influence UV sensitivity.

The bacterioneuston inhabits the surface microlayer (SML), *i.e.* the top millimetre of the water column, being naturally exposed to high levels of solar radiation, including in the UV spectrum. Reports of enhanced prokaryote abundance at the SML in comparison to underlying waters (UW) (Agogué et al., 2004; Aller et al., 2005; Obernosterer et al., 2005; Joux et al., 2006; Santos et al., 2009) have raised the possibility of the presence of bacterial strains adapted to multi-stress conditions, including UV radiation, at the air-water interface. However, experimental testing of the individual sensitivity of strains isolated from the SML and UW did not confirm the different resistance to solar radiation of bacterioneuston and bacterioplankton isolates (Agogué et al., 2005). A more ecologically relevant approach to address UV resistance in natural bacterial communities can be the preliminary selection and isolation of UVB-resistant strains, likely to be relevant in the functioning of the communities under increased UVB stress conditions (Fernández Zenoff et al., 2006b).

The hypotheses of this work are: (1) UV-resistant bacterioneuston and bacterioplankton isolates respond differently to UV radiation, in terms of damage, repair and potential for photoadaptation; (2) physiological/nutritional conditioning (starvation versus nourishment) affects the photobiological responses of bacterioneuston and bacterioplankton isolates; and (3) the pattern of photobiological responses is related to the environment of origin of the isolates.

Materials and methods

Sampling

Samples from the SML and UW were collected at Ria de Aveiro (Portugal), a tidal estuary in the western coast of Portugal. Sampling was conducted on three sequential days in 2008, shortly after the summer solstice, when UVB levels are the highest (Seckmeyer et al., 2008). Daily solar radiation doses on the period of sampling in the South of Europe range 30-35 kJ m^{-2} (Abboudi et al., 2008). At the time of sampling the sky was clear and minimum wind conditions (< 2 m s^{-1}) were observed. Triplicate samples with three sub-samples (n = 9) were collected in each sampling moment. Bacterioneuston samples were collected using a 0.25 m wide x 0.35 m Plexiglas plate, which removes the upper 60-100 µm water layer (Harvey and Burzell, 1972). Samples from underlying water were taken directly by submerging sterile glass

bottles at the depth of approximately 20 cm. Water samples, kept at 4 ºC and in the shade, were processed within 3 h of collection.

Kinetics of community photoinactivation and isolation of UV-resistant bacteria

Samples (30 mL) from the SML (n = 9) and from UW (n = 9) were transferred to uncovered 150 mm-diameter Petri dishes and irradiated with UVB (Philips, UVB TL 100 W/01; maximum emission peak at 302 nm, pre-burned for 1 h to ensure stability of light emission), with magnetic stirring, at 25 ± 0.5 ºC. UV intensities were measured with a monochromator spectro-radiometer placed at the sample level (DM 300, Bentham Instruments, Reading, UK). The inactivation kinetics of whole bacterioneuston and bacterioplankton communities was assessed until an accumulated UVB dose of 120 kJ m^{-2}. Aliquots were taken at pre-determined intervals to monitor the dose-dependent variation of culturable counts during irradiation, as described below. After incubation in the dark at 25 °C for up to 7 days, colonies were counted and the log of survival was plotted as a function of the energy dose. UVB-resistant isolates were selected from the best dilution of plates corresponding to a cumulative dose of 60 kJ m^{-2}, which is equivalent to ambient surface UVR levels at 40 to 44º N latitude on sunny days near the summer solstice (Seckmeyer et al., 2008). Colonies were selected according to colour and shape and streak-plated at least three times for purification. The purity of the strains was verified by microscopic observation after Gram-staining. Pure isolates were transferred to marine broth 2216 (MA 2216; Difco, Detroit, Mich.) and the cultures were used for subsequent molecular characterization.

Molecular characterization of the strains

Bacterial isolates were grown in marine broth on a laboratory shaker at 25°C. Cells from stationary phase cultures in marine broth were collected by centrifugation (3,200 x *g* for 15 min) and the pellet was used for total genomic DNA extraction, as previously described (Henriques et al., 2006b). BOX-PCR fingerprinting was used for molecular typing of the isolates using the BOX A1R primer (5'-CTACGGCAAGGCGACGCTGACG-3') (Versalovic et al., 1994) as previously described (Rademaker et al., 2004).

For isolates displaying distinct BOX-PCR profiles, the 16S rRNA gene was amplified by PCR using primers 27F (59-AGAGTTTGATCCTGGCTCAG-39) and 1492R (59-GG TTACCTTGTTACGACTT-39) as previously described (Lane, 1991).

The PCR products were purified (Jetquick PCR Purification Kit, GENOMED Gmbh, Löhne, Germany) and used as templates in the sequencing reactions, carried out using the primer 27F at an external laboratory (StabVida, Oeiras, Portugal). All PCR reactions were performed in an iCycler thermal cycler (Bio-Rad Laboratories, Richmond, CA, USA) using Taq polymerase, nucleotides and buffers purchased from MBI Fermentas (Vilnius, Lithuania). Sequences were compared with sequences available in the GenBank database by using the BLAST (Basic Local Alignment Search Tool) service to determine their approximate phylogenetic affiliations (Altschul et al., 1990). The 16S rRNA gene sequences obtained (> 430 nucleotides) along with those of related bacteria deposited in GenBank were used to construct a phylogenetic tree. The analysis was performed by the neighbour-joining method (Kimura two-parameter distance optimized criteria) using MEGA version 5.0 (Tamura et al., 2011). The robustness of the tree was confirmed by bootstrap analysis based on 1000 resamplings. Nucleotide sequences generated in this study have been deposited in the GenBank database under the accession numbers GQ365194-GQ365211 and GU084169-GU084170.

Preparation of the isolates for the irradiation experiments

To establish nourished conditions, bacterial isolates were grown in marine broth on an orbital shaker (100 rpm) at 25 °C until late-exponential phase. For starvation experiments, cells were grown in minimal nine-salt solution glucose medium (MNSS) containing 4.0 g L^{-1} of glucose, 2.2 g L^{-1} of $(NH_4)_2SO_4$, and 0.54 g L^{-1} of K_2HPO_4, as previously described (Nyström et al., 1992). The starvation regime was imposed by harvesting 5 mL of an exponentially growing culture by rapid filtration through a Millipore filter (pore size, 0.45 µm), washing the cells twice and ressuspending in 0.2-µm-pore-size-filtered autoclaved seawater, followed by a 40 h incubation on an orbital shaker (100 rpm) at 25°C (Nyström et al., 1992).

Cells grown under the different nutritional conditions were harvested by centrifugation (3,200 x *g* for 15 min, 20 ºC) and the pellet was washed three times in 0.2-µm-pore-size-filtered, autoclaved aged seawater. Cells were resuspended in 0.2-µm-pore-size-filtered, autoclaved seawater. Bacterial abundance was determined by epifluorescence microscopy (Hobbie et al., 1977) and adjusted with 0.2-µm-pore-size-filtered autoclaved seawater to 10^6 cells mL^{-1}.

Experimental testing of isolated strains

Irradiation experiments

A convenient volume of cell suspension for each isolate was transferred to 150 mm-diameter Petri dishes so that the depth of the liquid was < 2 mm. The lid was removed from the culture plate and the bacterial suspension was irradiated as previously described for whole SML and UW samples with a total dose of 60 kJ m^{-2}. Dark controls were covered with aluminium foil and included in all experiments. Each experiment was conducted with triplicate replicates and repeated in three independent moments. Culturable counts and activity (leucine and thymidine incorporation rates and sole-carbon source use profiles) were assessed as described below.

Recovery experiments

To assess cell recovery, UVB-irradiated cell suspensions were subjected to three different treatments: (i) exposure to PAR provided by white cold lamps (Philips TLD 58 W/84, total dose of 193.6 kJ m^{-2}), (ii) exposure to UVA provided by Philips TL 100W/10R lamps (wavelength range 350 to 400 nm, total dose of 52.6 kJ m^{-2}), (iii) incubation in the dark for 4 hours. Aliquots of the cell suspensions were collected before and after incubation under the different recovery regimes for culturable counts and leucine and thymidine incorporation assessments.

For mutagenic DNA repair (MDR) assays, 1-mL aliquots of UVB-irradiated cell suspensions were added to 1 mL of 2 x LB medium (Difco BD, Franklin Lakes, USA) and grown for 12 h in total darkness with shaking. Appropriate dilutions were then plated on LB agar, and on LB agar containing either nalidixic acid (100 µg mL^{-1}) or rifampin (75 µg mL^{-1}) (Sigma-Aldrich, St. Louis, MO). The salinity of LB medium was adjusted to 36 PSU to correspond to that of marine broth routinely used for the maintenance of the cultures. The frequency of mutation to nalidixic acid resistance (Nal^R) and rifampin resistance (Rif^R) was calculated as the number of Nal^R or Rif^R mutants per 10^8 cells as previously described (Zhang and Sundin, 2004).

Photoadaptation experiments

In order to identify UVB photoadaptive responses, the procedure described by Joux et al. (1999) was adopted. Briefly, cell suspensions were irradiated under UVB (Philips, UVB TL 100 W/01; maximum emission peak at 302 nm) for a total dose of 60 kJ m^{-2}. Cell suspensions were subsequently exposed to UVA for a total dose of 52.6 kJ

m^{-2}, which was followed by a 10 hour period of incubation in the dark. Cell suspensions were then subjected to a second round of UVB radiation for a total dose of 60 kJ m^{-2}. At every point in the procedure, aliquots of cell suspensions were removed for the determination of culturable counts.

Biological parameters

Culturable counts

Triplicate 100 µL aliquots were collected before and after irradiation, serially diluted in 0.2-µm-pore-size-filtered autoclaved seawater and pour-plated in marine agar 2216 (Difco, Detroit, Mich.). Colonies were counted after 7 days of incubation in the dark at 25 ºC. The dilution and plating procedures were carried out under low-luminosity conditions to avoid photoreactivation.

Leucine and thymidine incorporation

The effects of UV irradiation on bacterial activity were estimated by the incorporation of [^{3}H]leucine (Simon and Azam, 1989)and [^{3}H]thymidine (Moriarty, 1986). Triplicate 1.5 mL samples and one blank (TCA-fixed sample) were incubated with a mixture of [^{3}H]leucine or [^{3}H]thymidine (Amersham, Specific Activity 64 Ci $mmol^{-1}$) and the equivalent nonradioactive substrate at final saturating concentrations of 485 and 456 nM, respectively. Samples were incubated in the dark at 25 ± 0.5 ºC for 1 h. Incubations were stopped by the addition of trichloroacetic acid (TCA) to a final concentration of 5 %, after which samples were centrifuged at 16,000 x *g* for 10 min. After discarding the supernatant, 1.5 mL of 5 % TCA were added and the samples were subsequently shaken vigorously on a vortex and centrifuged again. The supernatant was discarded and 1.5 mL of UniverSol liquid scintillation cocktail (ICN Biomedicals, USA) were added. The radioactivity incorporated in bacterial cells was measured after 3 days in a Beckman LS 6000 IC liquid scintillation counter using the external standard ratio technique (Fuhrman and Azam, 1982; Simon and Azam, 1989).

Sole-carbon source use profiles

Customized Biolog EcoPlates™ containing 31 ecologically relevant C sources (6 amino acids, 2 amines, 10 carbohydrates, 7 carboxylic acids, 2 phenolic acids and 4 polymers) were used to assess changes in bacterial metabolic profiles during UVB exposure. For operational constraints, the effect of UV exposure on sole-carbon source

use profiles was only assayed under nourished conditions in representative strains of each genus retrieved (*Acinetobacter* sp. strain PT5I1.2G, *Bacillus* sp. strain PT15I3.2CB, *Brevibacterium* sp. strain PT5I3.3L, *Micrococcus* sp. strain NT25I3.2AA, *Paracoccus* sp. strain NT25I3.1A, *Pseudomonas* sp. strain NT5I1.2B, *Psychrobacter* sp. strain PT15I3.2CA, *Sphingomonas* sp. NT15I1.2B, *Staphylococcus* sp. strain NT25I2.1).

Biolog EcoPlates™ were inoculated with 150 µL of cell suspension (unirradiated and irradiated) per well (OD_{600} = 0.2) and incubated for 72 hours at 25 ºC. After incubation, the optical density (OD) of the Biolog EcoPlate™ wells was measured using the microplate reader FL 600 (Bio-Tek, VE). The OD of the control well was subtracted from the OD of all the other wells to correct for background activity. Data were exported into Microsoft Excel and treated using standard software (Garland and Mills, 1991).

Statistical analysis

All experiments were repeated in three independent assays and parameters were always determined in triplicate. Differences between treatments were assessed by 1-way ANOVA using the statistical software SPSS v.17. Levene test was used to assess homogeneity of variances. If variances were not homogeneous, the non-parametric Mann-Whitney test was used to assess the overall effect of treatment. Differences with p values < 0.05 were considered statistically significant.

Results

Kinetics of community photoinactivation and isolation of UV-resistant strains

In bacterioplankton, irradiation with a 72 kJ m^{-2} dose resulted in the reduction of CFU concentration to the detection limit. Complete inactivation of bacterioneuston occurred with a dose of 120 kJ m^{-2}. Exposure to 60 kJ m^{-2} of UVB radiation resulted in a 1 log and 2 log reduction in CFU counts in bacterioneuston and bacterioplankton, respectively (Fig. 4.1).

A total of 21 distinct isolates resistant to up to 60 kJ m^{-2} (10 from the SML and 11 from the UW) were retrieved and identified. Isolates were affiliated with the genera *Acinetobacter, Bacillus, Brevibacterium, Micrococcus, Paracoccus, Pseudomonas, Psychrobacter, Sphingomonas* and *Staphylococcus* (Table 4.1). The 16S rRNA gene

sequence-based phylogeny indicating the relationship of the strains isolated to previously described strains and environmental sequences is presented in Fig. 4.2.

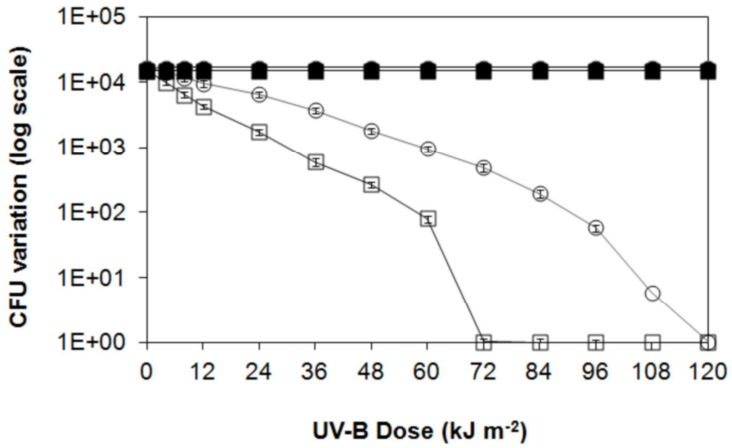

Fig. 4.1. Variation in CFU counts during exposure of bacterioneuston and bacterioplankton to UVB radiation. Error bars represent standard deviation of three independent experiments with three subsamples each and triplicate plates (n = 27). Error bars represent the standard deviation and are sometimes overlapped by the symbols. ○ - Bacterioneuston, ● - Bacterioneuston dark control, □ - Bacterioplankton, ■ - Bacterioplankton dark control.

Irradiation experiments with isolated strains

Culturable counts

In the set of isolates tested, the average reduction of CFU counts (Fig. 4.3 A) by UVB irradiation was significantly (1-way ANOVA, $p < 0.05$) higher in bacterioplankton (63.9 ± 12.5 %) than in bacterioneuston (52.4 ± 13.0 %). Under starvation, the average reduction of colony counts was significantly (1-way ANOVA, $p < 0.05$) higher in both bacterioplankton (76.0 ± 11.1 %) and bacterioneuston (59.8 ± 13.2 %), compared to nourished conditions, and also significantly higher in bacterioplankton than in bacterioneuston (1-way ANOVA, $p < 0.05$).

Leucine and thymidine incorporation

The reduction of leucine incorporation was stronger (1-way ANOVA, $p < 0.05$) in bacterioneuston (38.5 ± 15.8 %) than in bacterioplankton (27.6 ± 10.0 %) isolates. Starvation did not significantly alter (1-way ANOVA, $p > 0.05$) the effect of irradiation on leucine incorporation neither in bacterioneuston (39.3 ± 16.6 %) nor in bacterioplankton (28.7 ± 13.5 %) isolates (Fig. 4.3 B). The average inhibition of thymidine incorporation was similar in the sets of bacterioneuston (15.3 ± 9.6 %) and bacterioplankton isolates (16.3 ± 4.6 %) (1-way ANOVA, $p > 0.05$) (Fig. 4.3 C). Under

starvation, inhibition of thymidine incorporation was significantly enhanced compared to nourished conditions and was higher in bacterioneuston isolates (30.2 ± 15.0 %) than in bacterioplankton (22.1 ± 10.9 %) (1-way ANOVA, $p < 0.05$) (Fig. 4.3 C). In the set of bacterioneuston isolates, the incorporation of leucine was more inhibited than the incorporation of thymidine (1-way ANOVA, $p < 0.05$). In bacterioplankton, the effect of irradiation was similar for the two monomers.

Table 4.1. Phylogenetic affiliation, accession numbers, similarity with database and microbial classification of isolated strains.

Strain	Phylogenetic affiliation (accession no.)	Closest relative in database (accession no.)	% 16S rDNA similarity	Microbial classification
SML				
NT5I1.2B	*Pseudomonas* (GU084169)	*Pseudomonas* sp. (JF749828.1)	99	*Gammaproteobacteria*
NT10I3.2AB	*Bacillus (*GQ365198)	*Bacillus pseudofirmus* (CP001878.2)	100	Firmicutes
NT15I1.2B	*Sphingomonas (*GU084171)	*Sphingomonas* sp. (AM900788.1)	100	*Alphaproteobacteria*
NT25I3.1A	*Paracoccus (*GQ365195)	*Paracoccus* sp. (AB681547.1)	99	*Alphaproteobacteria*
NT15I3.2B	*Staphylococcus (*GQ365194)	*Staphylococcus* capitis (AB626127.1)	99	Firmicutes
NT15I1.1AA	*Paracoccus (*GQ365200)	*Paracoccus* sp. (AB681547.1)	99	*Alphaproteobacteria*
NT25I3.2AA	*Micrococcus (*GQ365196)	*Micrococcus* sp. (HM352362.1)	98	*Actinobacteria*
NT25I2.1	*Staphylococcus (*GQ365197)	*Staphylococcus saprophyticus* (HQ407261.1)	99	Firmicutes
NT10I3.3AC	*Staphylococcus (*GQ365199)	*Staphylococcus* sp. (AY864655.1)	99	Firmicutes
NT15I1.2D	*Staphylococcus (*GU084170)	*Staphylococcus warneri* (JN644590.1)	99	Firmicutes
UW				
PT5I3.3L	*Brevibacterium (*GQ365205)	*Brevibacterium* sp. (JF905605.1)	99	*Actinobacteria*
PT5I1.2G	*Acinetobacter (*GQ365202)	*Acinetobacter* sp. (EU545154.1)	99	*Gammaproteobacteria*
PT5I1.2FA	*Acinetobacter (*GQ365207)	*Acinetobacter* sp. (HM755596.1)	97	*Gammaproteobacteria*
PT5I3.3HA	*Pseudomonas (*GQ365203)	*Pseudomonas oryzihabitans* (AB681726.1)	99	*Gammaproteobacteria*
PT5I3.3J	*Staphylococcus (*GQ365204)	*Staphylococcus equorum* (FR691468.1)	99	Firmicutes
PT15I3.2CA	*Psychrobacter (*GQ365208)	*Psychrobacter piscidermidis* (EU127295.1)	99	*Gammaproteobacteria*
PT15I3.2CB	*Bacillus (*GQ365209)	*Bacillus thuringiensis* (JN084031.1)	99	Firmicutes
PT5I3.3C	*Staphylococcus (*GQ365211)	*Staphylococcus warneri* (JN644590.1)	97	Firmicutes
PT5I1.2AA	*Brevibacterium (*GQ365201)	*Brevibacterium* sp. (JF905605.1)	99	*Actinobacteria*
PT5I3.3HC	*Acinetobacter (*GQ365210)	*Acinetobacter* sp. (HM629404.1)	99	*Gammaproteobacteria*
PT5I1.2D	*Staphylococcus (*GQ365206)	*Staphylococcus* sp. (AB680133.1)	99	Firmicutes

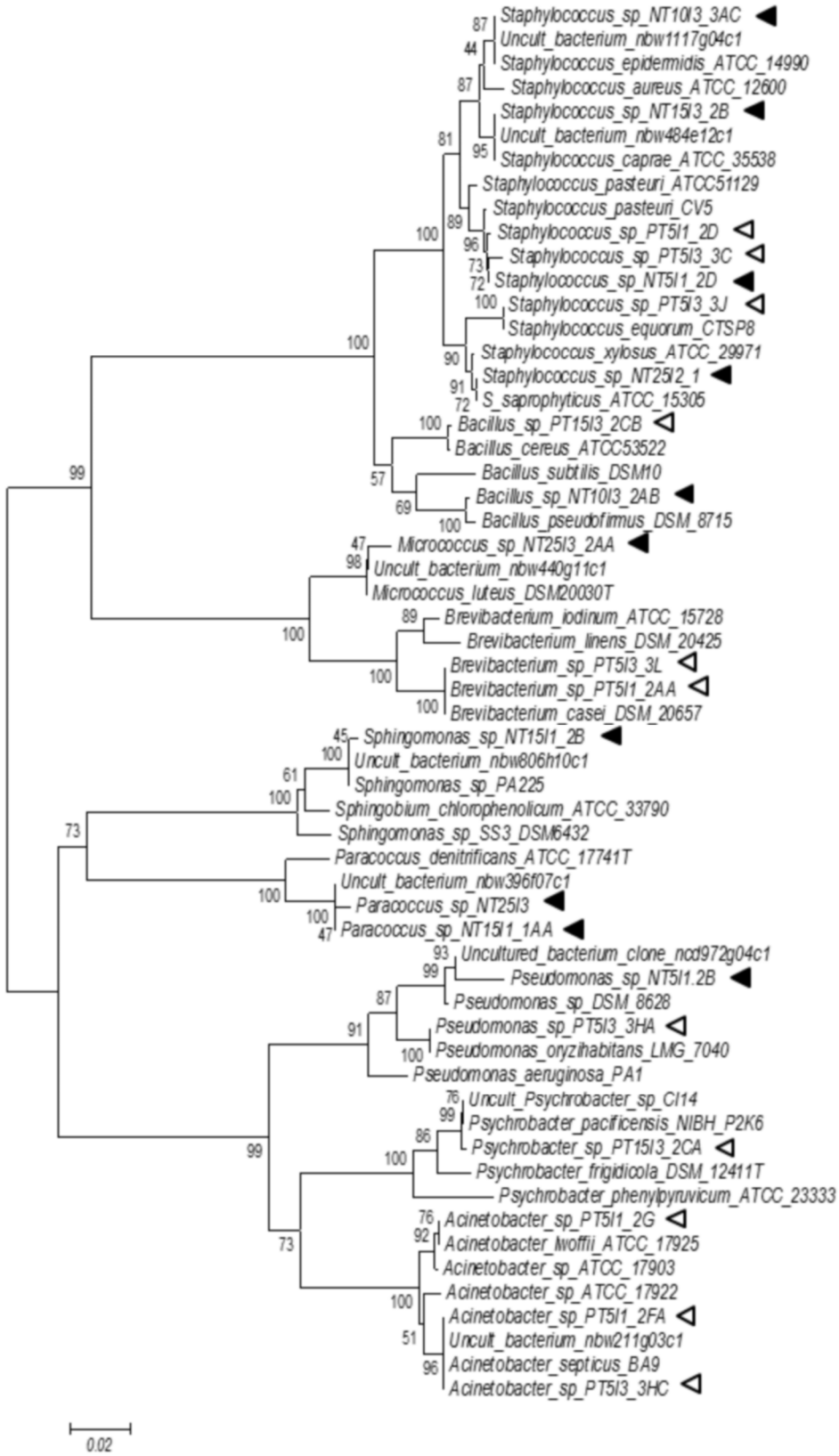

Fig. 4.2. Phylogenetic tree based on 16S rRNA gene sequences showing the phylogenetic position of isolated strains (indicated by arrows). Filled and open arrows denote bacterioneuston and bacterioplankton isolates, respectively. Bootstrap values are shown at the branching points (percentage of 1,000 replicates).

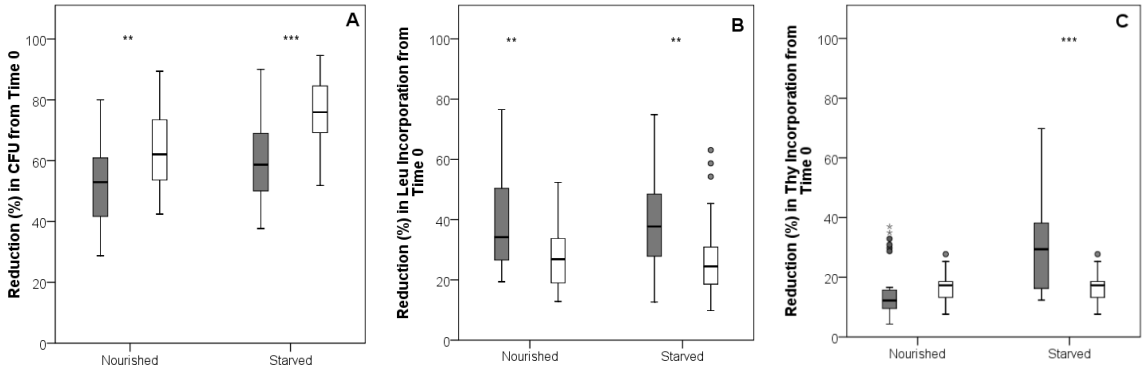

Fig. 4.3. Effects of UV radiation on CFU counts (A), rate of leucine incorporation (B) and rate of thymidine incorporation (C) averaged for the sets of bacterioneuston (■) and bacterioplankton (□) isolates, evaluated under nourished or starvation conditions. Boxes correspond to the averaged response of all the isolates in each community. Bars represent the range of values observed within each set. Points outside boxes represent maximum and minimum outliers. Asterisks denote significance level: *** - $p < 0.005$, ** - $p < 0.01$, * - $p < 0.05$.

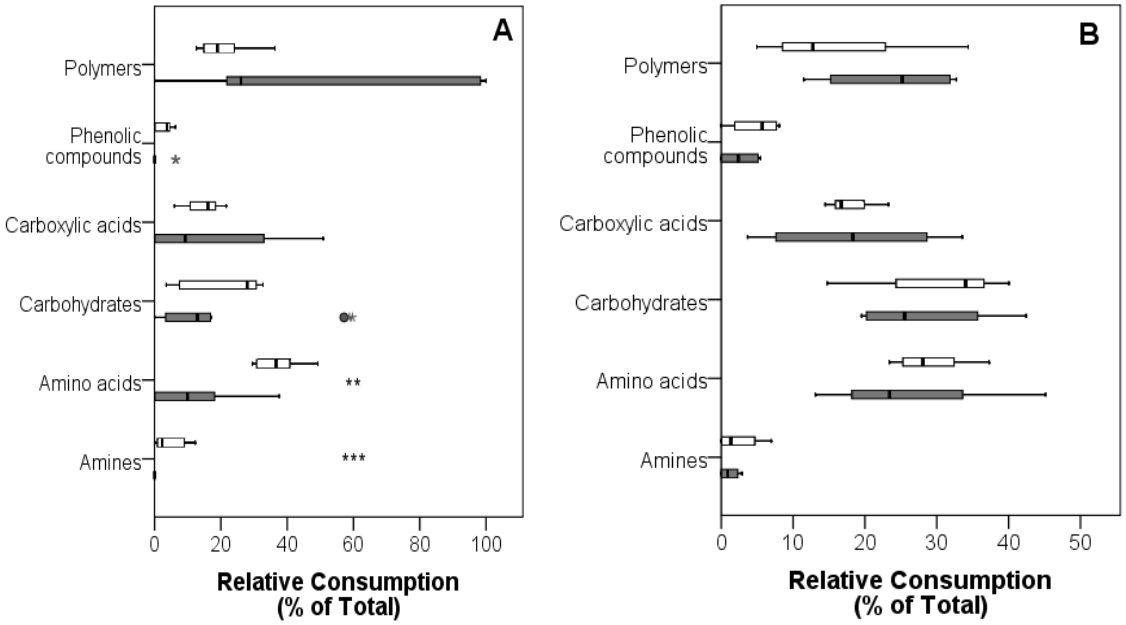

Fig. 4.4. Relative consumption rates of substrates in Biolog EcoPlates™ before (□) and after (■) UV exposure, averaged for the sets of bacterioneuston (A) and bacterioplankton (B) isolates. Boxes correspond to the averaged response of all the isolates in each community. Bars represent the range of values observed within each set. Points outside boxes represent maximum and minimum outliers. Asterisks denote significance level: *** - $p < 0.005$, ** - $p < 0.01$, * - $p < 0.05$.

Sole-carbon source use profiles

UVB exposure of representative bacterial strains was also accompanied by a shift in sole-carbon source use profiles. On average, amino acids (30.3-46.9 %) and polymers (12.8-34.6 %) were the substrates preferred by bacterioneuston before UV exposure. After UV exposure, a significant decrease in the relative consumption rate of amino acids and amines was observed (1-way ANOVA, $p < 0.05$), and the metabolism of bacterioneuston isolates became more dependent on polymers (up to 100 %) (Fig. 4.4

A). On average, before UV exposure bacterioplankton consumed mostly carbohydrates (15.0-38.1 %) and amino acids (24.0-35.5 %). UVB exposure did not significantly change this pattern (Fig. 4.4 B).

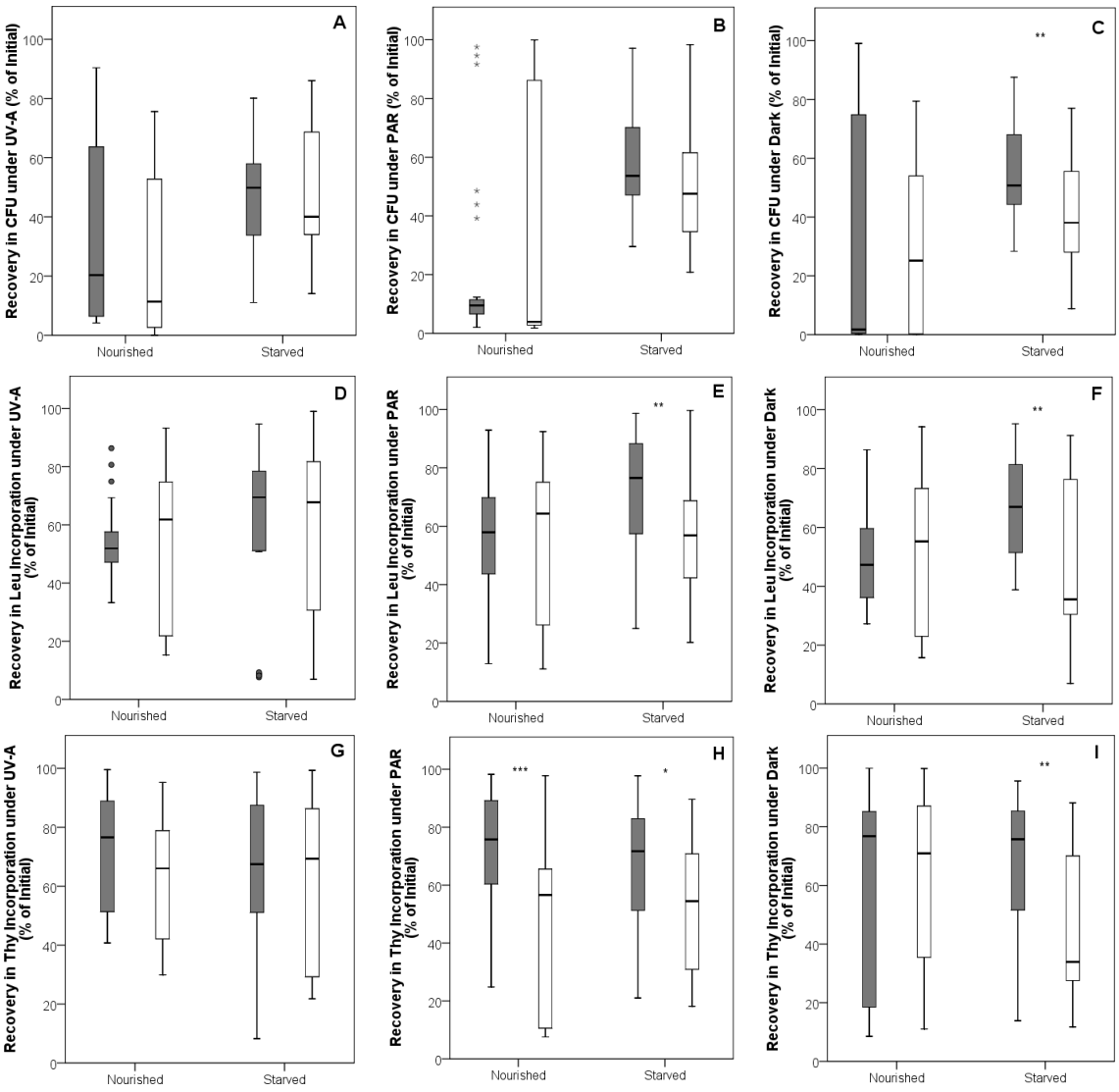

Fig. 4.5. Recovery of CFU counts under UVA (A), PAR (B), dark (C), leucine incorporation under UVA (D), PAR (E), dark (F), and thymidine incorporation under UVA (G), PAR (H), dark (I) averaged for the sets of bacterioneuston (■) and bacterioplankton (□) isolates, evaluated under nourished or starvation conditions. Boxes correspond to the averaged response of all the isolates in each community. Bars represent the range of values observed within each set. Points outside boxes represent maximum and minimum outliers. Asterisks denote significance level: *** - $p < 0.005$, ** - $p < 0.01$, * - $p < 0.05$.

Post-irradiation recovery

Recovery under nourished conditions during post-irradiation incubations, as described by CFU counts, was similar (1-way ANOVA, $p > 0.05$) in bacterioneuston and bacterioplankton isolates with all recovery regimes. Under starvation, recovery in CFU counts in the dark regime was significantly higher in bacterioneuston (55.0 ± 16.0

%) than in bacterioplankton (41.4 ± 19.3 %) (1-way ANOVA, $p < 0.05$). Compared to nourished conditions, recovery under starvation conditions was enhanced by up to 27.0 % with UVA for bacterioplankton isolates and with all recovery regimes (up to 37.9 %) for the bacterioneuston isolate set (1-way ANOVA, $p < 0.05$) (Fig. 4.5 A-C).

The extent of recovery in leucine incorporation rate did not differ significantly (1-way ANOVA, $p > 0.05$) between illumination regimes or isolate sets, under nourished conditions. Under starvation, bacterioneuston recovered 14.4 % and 18.6 % better (1-way ANOVA, $p < 0.05$) than bacterioplankton, during the PAR and dark incubations, respectively. Compared to nourished conditions, bacterioneuston isolates recovered better under starvation conditions (up to 16.9 %) (1-way ANOVA, $p < 0.05$) in all recovery regimes tested (Fig. 4.5 D-F).

In nourished cell suspensions, significant differences in the extent of recovery of thymidine incorporation rates between bacterioneuston and bacterioplankton isolates were only observed for the PAR regime, for which recovery was on average 24.2 % higher in bacterioneuston isolates (1-way ANOVA, $p < 0.05$). Under starvation conditions, the extent of recovery of thymidine incorporation was significantly higher in bacterioneuston than in bacterioplankton under the PAR (by 14.8 %) and dark (by 21.9 %) regimes (1-way ANOVA, $p < 0.05$). In bacterioplankton, the extent of recovery of thymidine incorporation in the dark regime was 17.1 % higher in nourished conditions than under starvation (1-way ANOVA, $p < 0.05$) (Fig. 4.5 G-I).

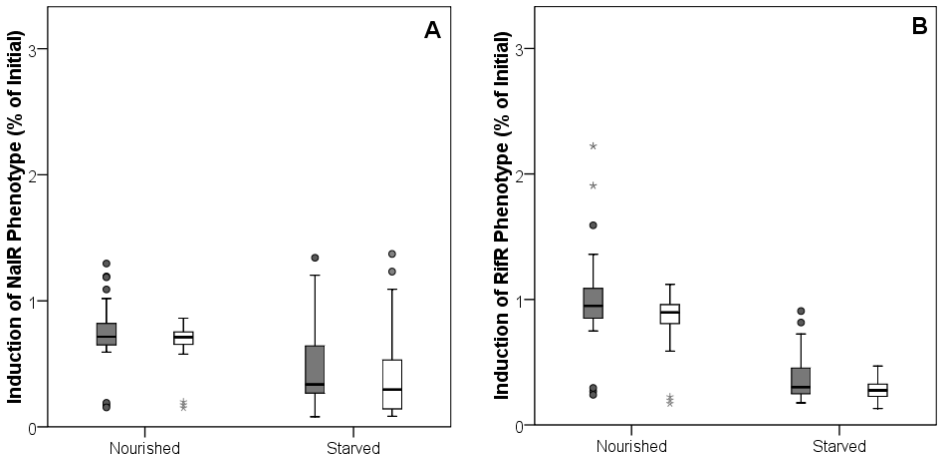

Fig. 4.6. Induction of Nal^R (A) and Rif^R (B) mutant phenotypes averaged for the sets of bacterioneuston (■) and bacterioplankton (□) isolates, evaluated under nourished or starvation conditions. Boxes correspond to the averaged response of all the isolates in each community. Bars represent the range of values observed within each set. Points outside boxes represent maximum and minimum outliers.

In general, exposure to UVB did not result in a significant average increase in the frequency of the Rif^R or Nal^R phenotypes (1-way ANOVA, $p > 0.05$) (Fig. 4.6 A, B). Statistically significant differences between averaged Nal^R or Rif^R frequencies of mutation in bacterioneuston and bacterioplankton isolates and between nourished and starved conditions were not found (1-way ANOVA, $p > 0.05$).

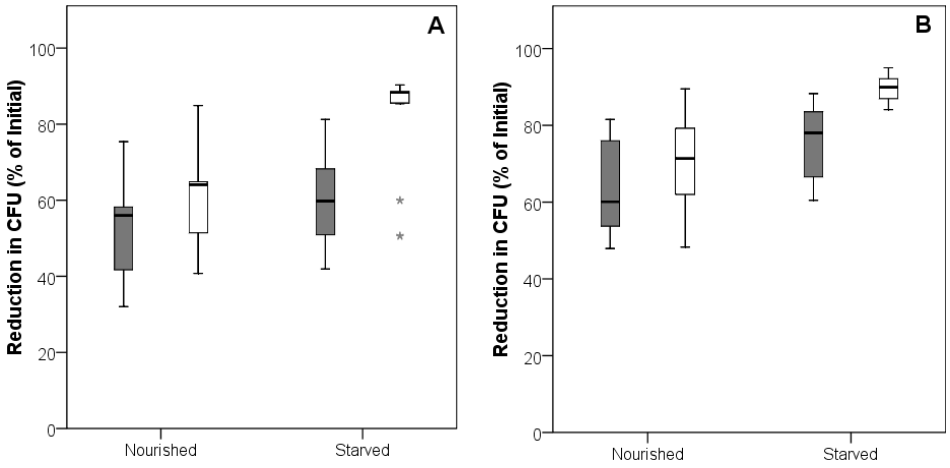

Fig. 4.7. Effects of UV radiation on CFU counts during two periods of UV exposure, used to assess the potential for photoadaptation, averaged for the sets of bacterioneuston (A) and bacterioplankton (B) isolates, evaluated under nourished or starvation conditions. Boxes correspond to the averaged response of all the isolates in each community. Bars represent the range of values observed within each set. Points outside boxes represent maximum and minimum outliers. ■- First irradiation period. □ - Second irradiation period

Photoadaptation potential

On average, the reduction in CFU counts during the second UVB treatment was higher (7.1-22.0 %) (1-way ANOVA, $p < 0.05$) than during the first treatment, for both bacterioneuston and bacterioplankton sets of isolates, regardless of the nutritional condition (Fig. 4.7 A, B).

Discussion

Despite the importance of estuaries in providing crucial ecosystem functions (Mitsch and Gosselink, 2000), studies on the effects of UV radiation on estuarine bacterial assemblages are still scarce in the literature. In the present work, UV-resistant bacteria were isolated from the surface microlayer and underlying waters of an estuarine system and their individual UV sensitivity was assessed in terms of CFU numbers, activity (leucine and thymidine incorporation), sole-carbon source use profiles, repair potential (light-dependent and independent), and photoadaptation potential under different physiological conditions. The fact that only a relatively small number of

bacterial isolates was tested limits the ability to make generalizations for the entire natural bacterioneuston or bacterioplankton communities. However, since these were the only isolates retrieved upon irradiation of samples from the SML and UW, they probably represent the dominant culturable members of the bacterial assemblages inhabiting these compartments. Studying their UV sensitivity responses can, therefore, provide important clues to understand how the corresponding communities might respond to enhanced UV levels.

UV resistance in bacterioneuston and bacterioplankton

Irradiation of samples from the SML and UW resulted in a steady decrease in the abundance of total culturable bacteria. Culturable survivals in bacterioneuston were still detected after an accumulated radiation dose of 108 kJ m^{-2}, while bacterioplankton was inhibited below the detection limit with 72 kJ m^{-2}. This could indicate the presence of bacteria with enhanced tolerance to UVB at the sunlit SML, already reported in other light-exposed habitats, such as the plant phyllosphere (Sundin and Jacobs, 1999) and high altitude wetland waters (Fernández Zenoff et al., 2006b). The bacterial isolates retrieved at different UVB doses were affiliated to four microbial groups: the Gram-negative *Gammaproteobacteria* and *Alphaproteobacteria* and the Gram-positive Firmicutes and *Actinobacteria*.

The average results of the individual testing of the isolated strains revealed a lower (1-way ANOVA, $p < 0.05$) UV-induced reduction in CFU in the bacterioneuston set, compared to bacterioplankton. The reduction in colony counts during irradiation was accompanied by a decrease in bacterial metabolic activity, assessed from the rates of leucine (protein synthesis) and thymidine (DNA synthesis) incorporation. On average, leucine incorporation was more inhibited in bacterioneuston isolates (1-way ANOVA, $p < 0.05$), while thymidine incorporation was equally inhibited in both sets of isolates. Furthermore, in bacterioneuston isolates leucine incorporation was significantly more inhibited than thymidine incorporation, suggesting uncoupling of DNA and protein synthesis rates upon UVB exposure, already reported in other bacterial strains (Arrieta et al., 2000).

UV exposure was accompanied by a shift in the profile of sole-carbon sources used by bacteria. This shift was particularly significant in bacterioneuston isolates, for which a statistically significant decrease in the utilization of amines and amino acids was observed, which could indicate a metabolic restructuring to compensate for UV-

induced damage to the protein synthesis apparatus (Sommaruga et al., 1997). Furthermore, in 7 out of the 9 isolates tested, a tendency towards the use of the polymers Tween 40 and Tween 80 as a preferable carbon source was observed upon irradiation. The observed changes in metabolic profiles could result from an active transcriptional reaction of the cells to UV stress, involving a shift in metabolic strategies from growth to defence/repair, and/or could be a metabolic restructuring to compensate for UV-induced damage to sensitive enzymes. For example, in *Escherichia coli* exposure to stressful conditions (temperature shift, oxidative stress and carbon starvation) induces a reduction in metabolites of the central metabolism (TCA cycle and glycolysis), as well as an increase in free amino acids, as a result of protein degradation and stalling of translation (Jozefczuk et al., 2010). Further characterization of the metabolites induced by UV radiation in bacteria could help to clarify the significance of the observed metabolic shift during UVB exposure.

Recovery from UVB-induced damage and photoadaptation potential

Variability in the extent of the repair of UV-induced damage was also observed among the tested isolates. Only small, non significant increases, if any, in the frequencies of Nal^R and Rif^R mutant phenotypes, used to assay the occurrence of mutagenic DNA repair (MDR), were observed. Since the expression of MDR is differentially induced depending on the amount of DNA damage experienced by the cell (Walker, 1984; Smith and Walker, 1998), the reduced induction of the mutagenic repair pathway observed in the present study could indicate that bacteria are probably able to effectively repair UVB-induced DNA damage by error-free mechanisms (*e.g.*, light dependent repair and NER).

Whether bacterial photoadaptation occurs in aquatic environments has not been clearly established (Pakulski et al., 1998). In the present work, occurrence of photoadaptation to a second round of UV exposure was not observed and the reduction of CFU numbers during the second UV exposure was, in fact, higher than in the first. Unlike DNA photoproducts, which can be effectively reversed by photoreactivation, the overproduction of ROS caused by exposure of organisms to UVB can have far wider ranging consequences, causing oxidative lesions to biomolecules that are energetically expensive to repair (Halliwell and Gutteridge, 1999). Therefore, it is possible that after the first UV exposure, the surviving cells accumulated lesions that made them more vulnerable to the second round of irradiation, which is in accordance with our

observations of accumulation of oxidative products in bacteria after UV exposure is terminated (unpublished results).

Effects of nutritional conditioning on UV-sensitivity responses

Starvation significantly enhanced UV-induced reduction in CFU counts in relation to nourished conditions. This observation suggests that starvation could enhance the sensitivity of bacteria to UV-induced damage, probably as a result of the synergistic action of energy deprivation and accumulation of reactive oxygen species during starvation (Hengge-Aronis, 2002), which is accentuated by UV exposure.

Starvation enhanced the inhibition of thymidine incorporation but had no significant effect on the response of leucine incorporation to irradiation. This indicates that UVB inhibition of DNA synthesis, but not protein synthesis, is modulated by the nutritional status of the cell, probably due to enhanced affinity of the protein synthesis system for ATP and GTP under starvation (Jewett et al., 2009).

Nutritional conditions also affected recovery from UV-induced damage. The extent of recovery was generally higher in starved cells, particularly for bacterioneuston isolates. Since starvation also induces oxidative damage (Hengge-Aronis, 2002), defence mechanisms activated in response to starvation might allow for a more efficient recovery once UV exposure is terminated. Enhanced resistance to UV radiation under oligotrophic conditions has been reported for *Vibrio* sp. strain S14 (Nyström et al., 1992) and *Enterococcus faecalis* (Hartke et al., 1998).

Despite the fact that dissolved organic compounds (*e.g.*, free amino acids) accumulate at the SML, bacterioneuston seems to display lower bacterial growth efficiencies than bacterioplankton, suggesting differences in the physiological state of bacterioneuston and bacterioplankton (Kuznetsova and Lee, 2002; Reinthaler et al., 2008). Rapidly growing cells are often more susceptible to inactivation than slower growing ones, because of the shorter time for excision repair between rounds of replication (Harm, 1980; Jagger, 1985). Whether the natural differences in physiological state of the bacterioneuston and bacterioplankton could influence their UV sensitivity and account for the enhanced UV resistance of bacterioneuston is unknown.

Conclusion

The photobiological responses (UV-induced damage, repair and potential for photoadaptation) of bacterial isolates retrieved from the SML and UW upon exposure to enhanced UVB levels were studied under different nutritional conditions. Regardless of the nutritional condition, CFU counts were more affected in bacterioplankton than in bacterioneuston, while protein synthesis was more inhibited in bacterioneuston. UVB exposure was accompanied by a metabolic shift, most notably in bacterioneuston. Recovery from UV-induced damage was enhanced under starvation conditions, particularly in bacterioneuston isolates. These observations suggest that the SML may contain a pool of bacteria adapted to cope with UV-induced stress.

Acknowledgments

This work was supported by CESAM (Centre for Environmental and Marine Studies, University of Aveiro) and the Portuguese Foundation for Science and Technology (FCT) in the form of a PhD grant to A.L. Santos (SFRH/BD/40160/2007) and a post-Doctoral grant to I. Henriques (SFRH/BPD/63487/2009). Acknowledgments are due to the two anonymous reviewers, whose insightful comments greatly improved the original manuscript.

PÁGINA INTENCIONALMENTE DEIXADA EM BRANCO

CHAPTER 5

Wavelength Dependence of Biological Damage Induced by UV Radiation on Bacteria

Santos A. L., Oliveira V., Baptista I., Henriques I., Gomes N. C. M., Almeida A., Correia A., Cunha A.
Archives of Microbiology **195**: 63-74

Abstract

The biological effects of UV radiation of different wavelengths (UVA, UVB and UVC) were assessed in nine bacterial isolates displaying different UV sensitivities. Biological effects (survival and activity) and molecular markers of oxidative stress (DNA strand breakage/DSB, generation of reactive oxygen species/ROS, oxidative damage to proteins and lipids, and the activity of antioxidant enzymes catalase and superoxide dismutase) were quantified and statistically analyzed in order to identify the major determinants of cell inactivation under the different spectral regions. Survival and activity followed a clear wavelength dependence, being highest under UVA and lowest under UVC. The generation of ROS, as well as protein and lipid oxidation followed the same pattern. DNA damage (DSB) showed the inverse trend. Multiple stepwise regression analysis revealed that survival under UVA, UVB and UVC wavelengths was best explained by DSB, oxidative damage to lipids, and intracellular ROS levels, respectively.

Introduction

Bacteria are very susceptible to the effects of UV radiation, due to their small size, short generation time and absence of effective UV-protective pigmentation (Garcia-Pichel, 1994). Bacterial isolates have different susceptibilities to UV radiation (Joux et al., 1999; Arrieta et al., 2000; Berney et al., 2006d; Chun et al., 2009; Santos et al., 2011b; Santos et al., 2012a), and UV sensitivity is dependent on the wavelength (Sundin and Jacobs, 1999; Qiu et al., 2004; Bauermeister et al., 2009). Since different biomolecules (*e.g.*, DNA, proteins and lipids) absorb UV radiation at different wavelengths, a portion of this variability is likely due to differences in the preferable cellular targets of the various wavelengths. DNA is considered the major target of UV radiation. However, comparable levels of DNA photoproduct accumulation are

observed in bacteria displaying different sensitivities to UV radiation (Joux et al., 1999; Matallana-Surget et al., 2008). In addition, DNA damage alone cannot account for the inhibition of bacterial activity in surface waters (Visser et al., 2002). Accordingly, it is likely that damage to other biomolecules contributes to the inhibitory effects of UV radiation and the variation in UV sensitivity among bacterial isolates.

UV radiation can be divided into three regions: UVA (320-400 nm), UVB (280-320 nm) and UVC (100-280 nm). UVC is filtered by the ozone (O_3) layer and does not reach the Earth's surface. Terrestrial radiation, often called sunlight, contains about 8 % UVA and less than 1 % UVB (Coohill and Sagripanti, 2009). The biological effects of UVA are usually attributed to enhanced production of reactive oxygen species (ROS), which results in oxidative damage to lipids, proteins and DNA (Chamberlain and Moss, 1987; Moan and Peak, 1989; Girotti, 1998; Pattison and Davies, 2006; Zeeshan and Prasad, 2009). UVB and UVC photons cause direct DNA damage by inducing the formation of DNA lesions (photoproducts), most notably pyrimidine dimers, which block DNA replication and RNA transcription (Pfeifer, 1997). Exposure to UVB also causes oxidative stress, as evidenced by the expression of antioxidant defences following UVB irradiation (Qiu et al., 2005a; Matallana-Surget et al., 2009a). Although the UVC region is not environmentally relevant, it is useful for assessing the UV sensitivity of bacteria that are highly tolerant or insensitive to high doses of UVB (Sundin and Jacobs, 1999). UVC radiation is also well known for its bactericidal potential (Jagger, 1985; Coohill and Sagripanti, 2008; King et al., 2011).

Most studies addressing the cellular effects of UV radiation on bacteria conducted to date have focused on one target (either proteins, lipids or DNA) in one bacterial strain (Abboudi et al., 2008; Matallana-Surget et al., 2008; Matallana-Surget et al., 2009a; Bosshard et al., 2010b), which has prevented a full understanding of the molecular basis for the variability in UV sensitivity. Such information is crucial to understand the role of UV radiation as a driver of microbial diversity and function in ecosystems, as well as to the development of efficient and ecologically-friendly UV-based disinfection strategies targeting a broad range of bacteria.

The objective of this study was to identify the major determinants of cell inactivation under different UV wavelengths in a set of bacterial isolates displaying distinct UV sensitivity.

Materials and methods

Experimental layout

The bacterial isolates used in this study were previously isolated from the surface waters of the estuarine system of Ria de Aveiro (Portugal) and characterized in terms of UV sensitivity (Santos et al., 2011b) (Table 5.1). In all irradiation experiments, only vegetative cells were used.

Table 5.1. Bacterial strains used in the experiments, their accession number, phylogenetic affiliation, closest relatives, similarity with database, as well as bacterial group and growth rates. LD_{50} values for each strain under the different UV spectral regions are also shown. Note that UVA and UVB doses are expressed in kJ m^{-2} while UVC doses are expressed in J m^{-2}.

Strain	Accession no.	Phylogenetic affiliation	Closest relative (accession no.)	% 16S rDNA similarity	Growth rate, μ (h^{-1})	LD_{50} UVA (kJ m^{-2})	LD_{50} UVB (kJ m^{-2})	LD_{50} UVC (J m^{-2})
PT5I1.2G	GQ365202	*Acinetobacter* sp.	*Acinetobacter sp.* (EU545154.1)	99	0.3	159.3	34.1	18.0
PT15I3.2CB	GQ365209	*Bacillus* sp.	*Bacillus thuringiensis* (JN084031.1)	99	0.7	152.7	34.1	31.2
PT5I3.3L	GQ365205	*Brevibacterium* sp.	*Brevibacterium sp.* (JF905605.1)	99	0.3	51.9	38.1	16.4
NT25I3.2AA	GQ365196	*Micrococcus* sp.	*Micrococcus* sp. (HM352362.1)	98	0.4	297.5	50.1	45.0
NT25I3.1A	GQ365195	*Paracoccus* sp.	*Paracoccus* sp. (AB681547.1)	99	0.4	285.3	40.3	13.7
NT5I1.2B	GU084169	*Pseudomonas* sp.	*Pseudomonas* sp. (JF749828.1)	99	0.7	221.3	49.3	40.6
PT15I3.2CA	GQ365208	*Psychrobacter* sp.	*Psychrobacter piscidermidis* (EU127295.1)	99	0.1	228.2	29.6	16.7
NT15I1.2B	GU084171	*Sphingomonas* sp.	*Sphingomonas* sp. (AM900788.1)	100	0.3	290.9	39.2	40.6
NT25I2.1	GQ365197	*Staphylococcus* sp.	*Staphylococcus saprophyticus* (HQ407261.1)	99	0.3	138.1	37.0	17.4

Fresh bacterial cultures were prepared in Marine Broth 2216 (Difco, Detroit, MI) and grown with agitation (120 rpm) at 25 ºC. Cells were harvested by centrifugation (3,200 x *g* for 15 min) in the late-exponential phase (defined as the inflection point of the growth curve, at the transition between the exponential and stationary phase, which was usually achieved in 8-14 h). The growth rates (μ) of the isolates were determined as previously described (Berney et al., 2006c) as $\mu = \Delta \ln OD_{546}/\Delta t$. The pellet was washed three times in 0.2-μm-pore-size-filtered autoclaved 0.9 % NaCl solution and cells were resuspended in filter-sterilized autoclaved 0.9 % NaCl. Bacterial abundance was determined by epifluorescence microscopy after acridine orange staining (Hobbie et al., 1977), adjusted with filtered autoclaved 0.9 % NaCl to 10^6 cells mL^{-1} and homogenized by gentle vortexing.

For each isolate, 30 mL of bacterial cell suspension (corresponding, on average, to a biomass of approximately 1 mg mL^{-1} of protein) was transferred to sterile 150 x 25 mm plastic tissue culture dishes (Corning Science Products, Corning, NY, USA) so that

the depth of the liquid was < 2 mm. For irradiation, the lid was removed and cell suspensions were exposed to UVA (Philips TL 100 W/10R lamps, Philips, Eindhoven, The Netherlands, main emission line at 365 nm, intensity of 50 W m^{-2}), UVB (Philips TL 100 W/01 lamps, Philips, Eindhoven, The Netherlands, main emission line at 302 nm, intensity of 2.3 W m^{-2}) and UVC (low pressure mercury lamp NN 8/15, Heraeus, Berlin, Germany, main emission line at 254 nm, intensity of 0.66 W m^{-2}). UV sources were placed at 20 cm from the sample. UV intensities were measured with a monochromator spectro-radiometer placed at the sample level (DM 300, Bentham Instruments, Reading, UK) and the UV dose (in J m^{-2}) was calculated by multiplying the intensity by the irradiation time (in seconds). The total cumulative doses applied were 300 kJ m^{-2}, 90 kJ m^{-2} and 180 J m^{-2}, for UVA, UVB and UVC, respectively. During irradiation, samples were stirred by magnetic agitation and temperature was kept at ± 25 ºC. A dark control (covered in aluminum foil) treated in the same way as the irradiated samples was included in every experiment. Survival curves for each isolate were generated separately for UVA, UVB and UVC for the determination of the LD_{50} (UV dose resulting in 50 % inactivation). Aliquots of cell suspensions were collected before irradiation and at LD_{50} for assessment of activity, indicators of oxidative damage and activity of antioxidant enzymes. Samples were immediately placed at 4 ºC in order to avoid repair until further processing, which was generally conducted in less than 1 hour. All experiments were repeated in three independent assays. Parameters were always determined in a minimum of three analytical replicates. Positive (50 mM H_2O_2-treated) and negative (untreated) controls were always included and processed along experimental samples in order to ensure proper functioning of the procedures on all strains. All determinations were carried out in a red-dark room to minimize photoreactivation.

Colony forming units (CFU)

Sample aliquots of irradiated samples and non-irradiated controls were serially-diluted in filter-sterilized, autoclaved 0.9 % NaCl and 100 µL aliquots were spread-plated in agar plates (Difco). Colonies were counted after 3 days of incubation in the dark at 25 ºC.

Bacterial activity

Bacterial activity was estimated from the rates of [^{3}H]leucine incorporation (Smith and Azam, 1992) in cell suspensions before and after UV exposure. Triplicate 1.5 mL aliquots and a TCA (5 %) fixed control were incubated with a mixture of [^{3}H]leucine (Amersham Biosciences, specific activity 160 Ci mmol^{-1}) and nonradioactive leucine at a previously determined saturating concentration of 480 nM. Samples were incubated in the dark at *in situ* temperatures for 1 h. Incubations were stopped by the addition of trichloroacetic acid (TCA) (5 % final concentration), after which samples were centrifuged at 16,000 x *g* for 10 min. The supernatant was discarded and 1.5 mL of 5 % TCA were added. The samples were then vortexed, centrifuged and the supernatant was discarded. The pellet was washed with 90 % ethanol, dried overnight at room temperature and resuspended in 1.0 mL of Universol liquid scintillation cocktail (ICN Biomedicals). The radioactivity incorporated in bacterial cells was measured after 3 days in a Beckman LS 6000 IC Liquid Scintillation Counter.

Intracellular ROS generation

Intracellular production of ROS was detected using the probe 2',7'-dichlorodihydrofluorescein diacetate (DCFH-DA) (Pérez et al., 2007). Control and irradiated samples were centrifuged and washed with 10 mM potassium phosphate buffer (pH 7.0), amended with the probe (final concentration 10 µM), and incubated for 30 min in the dark. Cells were subsequently washed, sonicated and 100 µL of the cell extracts were mixed with 1 mL of potassium phosphate buffer. The fluorescence of the samples was measured with a Jasco FP-777 Fluorometer at room temperature, with an excitation wavelength of 490 nm and emission wavelength of 519 nm. The fluorescence intensity at 519 nm was corrected against blank controls without cells and then normalized to the protein content (see below for procedure) in comparison with control samples.

DNA strand breakage

UV-induced DNA damage was assessed using the quantification of DNA strand breaks (DSB) as a proxy, due to the inability to detect the more routinely used CPDs in some of the strains even after exposure to 180 J m^{-2} of UVC, potentially due to experimental constraints. On the other hand, DSB accumulation, as well as the variation

of the other parameters assessed, generally followed a dose-dependent trend (data not shown).

DSB were determined following a modified version of the FADU (Fluorimetric Analysis of DNA Unwinding) method (He and Häder, 2002). In addition to the test samples (so-called P-samples), the method requires two sets of untreated control samples: samples not subjected to alkaline unwinding (T-samples) and samples subjected to complete alkaline unwinding (B-samples). Cells were collected by centrifugation (3,000 x *g*, 15 min) and digested with lysozyme (4 mg mL^{-1} final concentration) in EDTA solution, followed by proteinase K (0.25 mg mL^{-1} final concentration). A volume of 300 µL of 0.1 M NaOH was added to the three sets of samples: (1) T-samples were neutralized with 300 µL of 0.1 M HCl and sonicated for 15 s, following a 30 min incubation at room temperature; (2) B-samples were sonicated for 2 min, neutralized with 300 µL of 0.1 M HCl after a 30 min incubation and sonicated again for 15 s; and (3) P-samples were incubated for 30 min, neutralized with 300 µL of 0.1 M HCl and sonicated for 15 s.

A final concentration of 5 µM of Hoechst 33258 was added to all samples and, after centrifugation, a 1 mL volume of supernatant was used for fluorescence measurements (λ_{ex}. 350 nm; λ_{em}. 450 nm) in a Jasco FP-777 Fluorometer. The fraction of double stranded DNA (dsDNA) was calculated as dsDNA = (P−B)/(T−B)×100, where T, P and B were fluorescence intensities of T-, P- and B-samples normalized to the protein content, respectively.

Thiobarbituric acid reactive substances

Lipid peroxidation was determined as the amount of thiobarbituric acid reactive substances (TBARS) as previously described (Pérez et al., 2007). Control and irradiated cells were centrifuged, washed, and resuspended in 1 mL of 50 mM potassium phosphate buffer (pH 7.4) added of 0.1 mM butylated hydroxytoluene and 1 mM PMSF (phenylmethanesulfonyl fluoride). After sonication and centrifugation to remove cellular debris, the soluble fraction was mixed with 1 mL of 20 % trichloroacetic acid and centrifuged (10,000 x *g* for 5 min). Supernatants were removed, mixed with 1 mL of 0.5 % (w/v) thiobarbituric acid in 0.1 M HCl and 10 mM butylated hydroxytoluene. Samples were heated at 100 ºC for 1 h, after which 1 mL aliquots were removed, cooled and then mixed with 1.5 mL of butanol. After centrifugation (4,000 x *g*, 10 min), the organic fraction was removed and the absorbance at 535 nm was determined using a

Thermo Spectronic Genesys 10 UV spectrophotometer. TBARS content was determined using an extinction coefficient of 156 mM^{-1} cm^{-1} and values were normalized to the protein content.

Protein oxidation

Protein oxidation was assessed from carbonyl levels as previously described (Semchyshyn et al., 2005). Aliquots of cell homogenates were incubated for 1 h at room temperature with 10 mM dinitrophenylhydrazine (DNPH) in 2 M HCl. DNPH was omitted in the blanks. Proteins were precipitated with 500 µL of 20 % trichloroacetic acid, centrifuged (14,000 x *g*, 5 min) and the pellet was washed three times with 1 mL of 1:1 (v/v) ethanol-ethyl acetate. The final precipitate was dissolved in 1 mL of 6 M guanidine hydrochloride. Samples were spectrophotometrically analyzed against a blank of 1 mL of guanidine solution (6 M guanidine hydrochloride with 2 mM potassium phosphate). The absorbance at 360 nm was determined and the molar absorption coefficient of 22 mM^{-1} cm^{-1} was used to quantify the levels of protein carbonyls. Values were normalized to the protein content.

Antioxidant enzymatic activity

Irradiated and non-irradiated cells were resuspended in cold 50 mM potassium phosphate buffer (pH 7.8) containing 1 mM EDTA and sonicated in ice. The extracts were centrifuged (10,000 x *g*, 15 min) and the supernatant frozen at -80 °C until analysis.

Catalase (CAT) activity was measured spectrophotometrically by monitoring the rate of decomposition of H_2O_2 (Beers and Sizer, 1952). One unit of CAT activity was defined as the amount of activity required to decompose 1 µmol of H_2O_2 per minute under the assay conditions. The strain *Enterococcus faecalis* was used as a negative control. An additional negative control consisting of a mixture of 18 mM hydrogen peroxide with sterile potassium phosphate buffer (1:5) was also included in every experiment (Anderl et al., 2003). Superoxide dismutase (SOD) activity was determined according to McCord and Fridovich (1969) in which a xanthine-xanthine oxidase system is used to generate O_2^- and nitroblue tetrazolium is used as an indicator. One unit of SOD activity was defined as the amount of SOD that resulted in 50 % inhibition of the reduction of nitroblue tetrazolium. Potassium phosphate buffer was used as a blank. Protein concentration in cell suspensions was determined by the method of Bradford

(1976). The specific activity of antioxidant enzymes was expressed as units per milligram of cellular proteins.

Statistical analysis

Differences between treatments were assessed by 1-way ANOVA using the statistical software SPSS v.17. Levene test was used to assess homogeneity of variances. If variances were not homogeneous, the non-parametric Mann-Whitney test was used to assess the overall effect of the treatment. Differences with p values < 0.05 were considered statistically significant. Principal component analysis (PCA), used to reduce the variability of the data sets and identify the main parameters contributing to the discrimination between UV treatments, was performed using software Primer 5. Stepwise multiple regression, used to identify groups of independent variables that would predict the dependent variable (LD_{50}) with optimal efficiency, was conducted on SPSS v. 17.

Results

UV-effects on survival and activity

UV sensitivity curves of the isolates under the different spectral regions are shown in Fig. 5.1 and were used to determine LD_{50} values (Table 5.1).

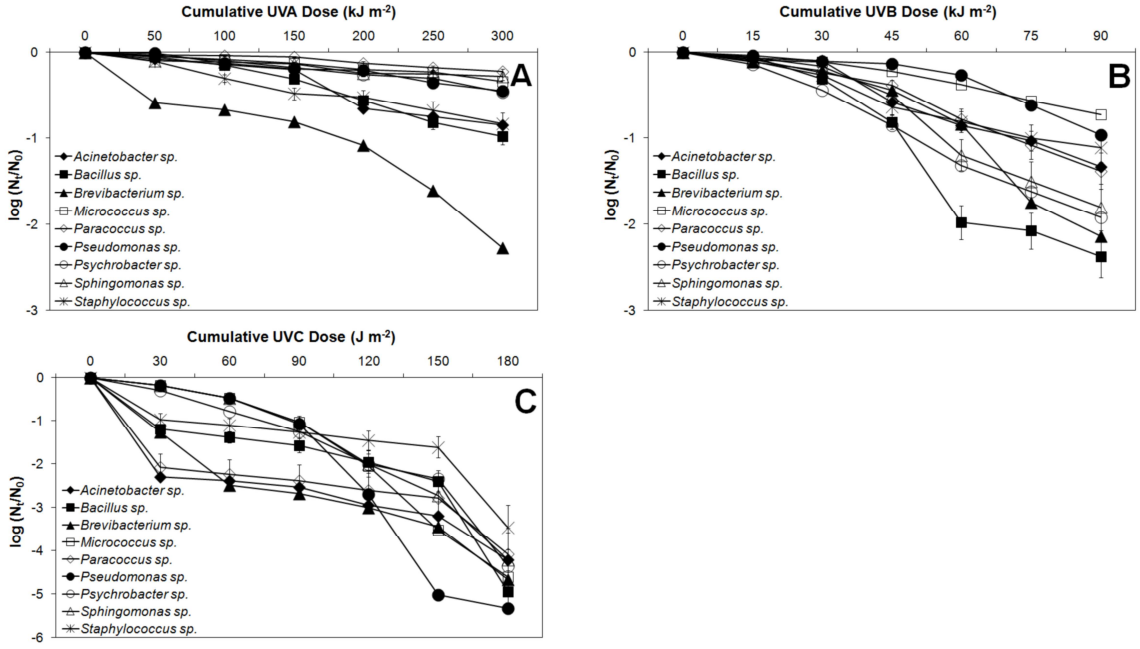

Fig. 5.1. UV sensitivity curves for the bacterial isolates under the different UV spectral regions. Error bars are standard deviation of the mean of three experiments. Where error bars are not displayed, they are smaller than the graph symbol. N_t – number of CFU at the dose t. N_0 – number of CFU at time 0.

LD_{50} values showed expected wavelength dependence, being highest under UVA and lowest under UVC. LD_{50} values for UVA ranged from 51.9 ± 3.7 kJ m^{-2} in *Staphylococcus* sp. to 297.5 ± 16.3 kJ m^{-2} in *Micrococcus* sp. Under UVB, LD_{50} values ranged between 29.6 ± 1.5 kJ m^{-2} in *Psychrobacter* sp. and 50.1 ± 3.8 kJ m^{-2} in *Micrococcus* sp. and for UVC LD_{50} values varied between 13.7 ± 0.3 J m^{-2} in *Acinetobacter* sp. and 45.0 ± 2.4 J m^{-2} in *Micrococcus* sp.

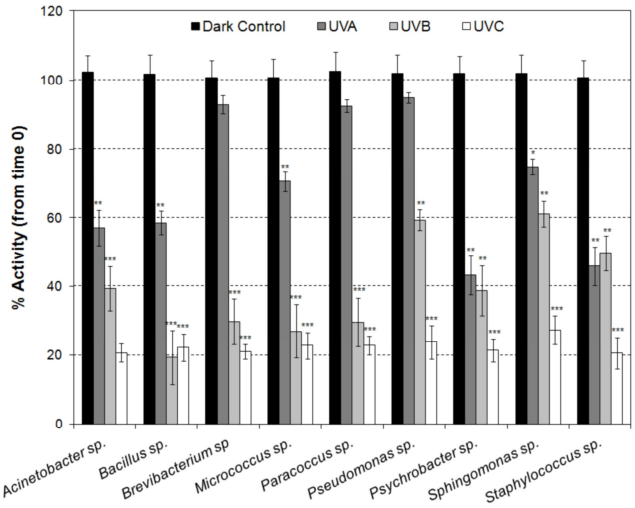

Fig. 5.2. Effects of exposure to the LD_{50} of different UV spectral regions on bacterial activity. LD_{50} values are shown in Table 5.1. Data are presented as group means ± standard deviations of the mean of three experiments. Absence of error bars indicates that standard deviations are too small to see on the scale used.

Inhibition of activity also showed a clear wavelength dependence, with UVC wavelengths causing the highest average inhibition (77.5 ± 2.1 %) and UVA the lowest (30.0 ± 20.2 %). For UVA, at LD_{50} inhibition of activity ranged from 5.1 ± 0.1 % in *Pseudomonas* sp. to 56.8 ± 7.2 % in *Psychrobacter* sp. Exposure to LD_{50} of UVB resulted in an inhibition of activity ranging between 38.9 ± 3.4 % in *Sphingomonas* sp. and 80.6 ± 7.6 % in *Bacillus* sp. Under UVC, exposure to LD_{50} resulted in an inhibition of activity ranging between 72.7 ± 6.5 % in *Sphingomonas* sp. and 79.4 ± 7.0 % in *Staphylococcus* sp. (Fig. 5.2).

ROS generation and oxidation of biomolecules

ROS generation also followed a wavelength-dependent trend of variation, being highest under UVA (42.1 ± 9.4 %) and lowest under UVC (8.2 ± 4.1 %). The enhancement of ROS generation was more marked in *Staphylococcus* sp. with UVA

(56.4 ± 5.9 %) and UVB (39.1 ± 3.9 %) and *Micrococcus* sp. (15.2 ± 1.8 %) with UVC (Fig. 5.3 A).

The increase in DNA strand breaks (DSB) showed a wavelength dependence as well, being highest under UVC (23.2 ± 8.4 %) and lowest under UVA (7.9 ± 5.7 %). DSB generation ranged from 1.4 ± 0.1 % (*Bacillus* sp.) to 19.0 ± 2.0 % (*Staphylococcus* sp.) under UVA, from 5.3 ± 0.6 % (*Micrococcus* sp.) to 31.3 ± 3.1 % (*Staphylococcus* sp.) under UVB and from 10.7 ± 0.9 % (*Acinetobacter* sp.) to 35.7 ± 4.2 % (*Psychrobacter* sp.) under UVC (Fig. 5.3 B).

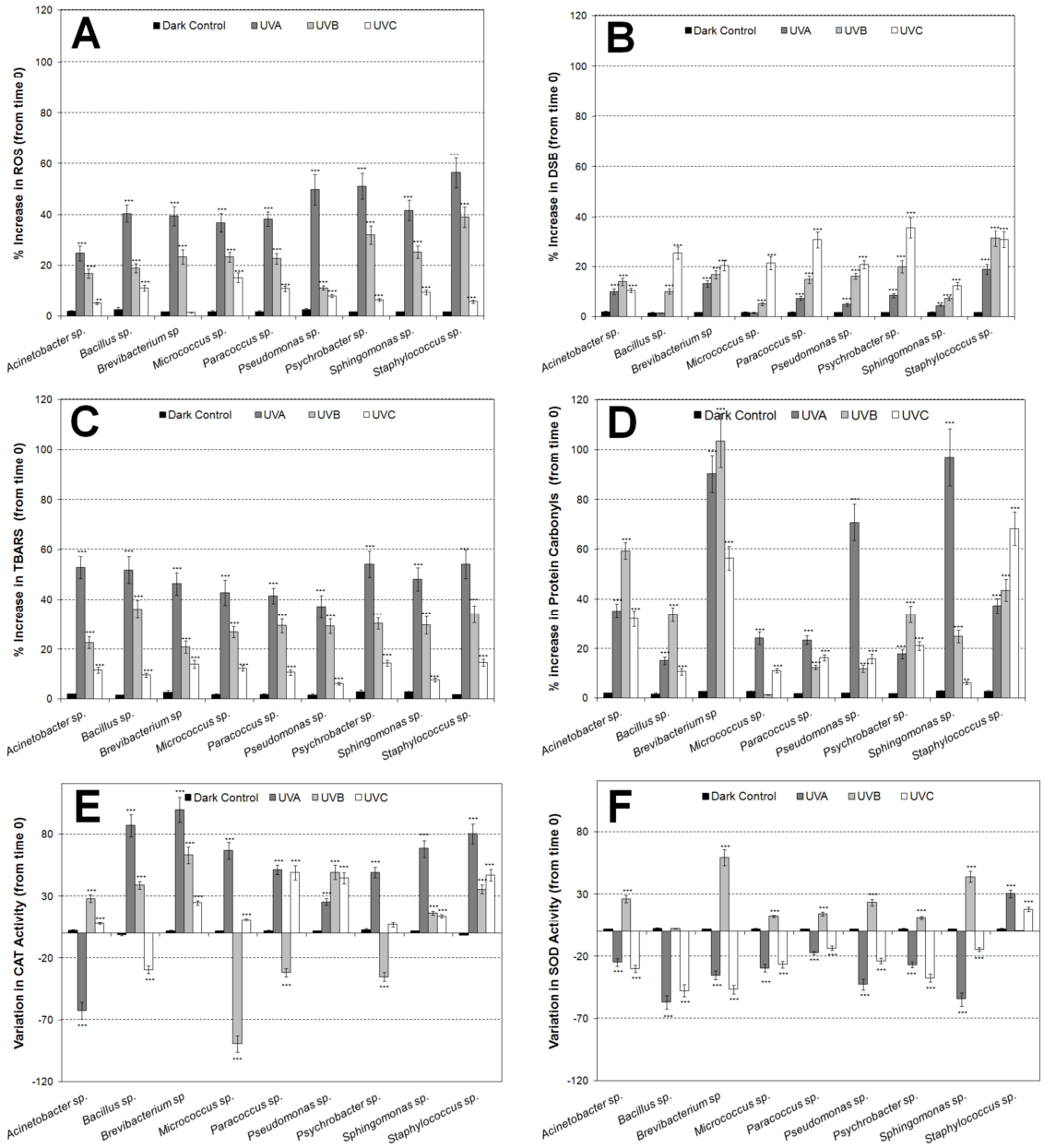

Fig. 5.3. Effects of exposure to the LD_{50} of different UV spectral regions on (A) intracellular ROS generation, (B) DSB, (C) TBARS levels, (D) protein carbonyl levels, (E) CAT and (F) SOD activity. LD_{50} values are shown in Table 5.1. Data are presented as group means ± standard deviations of the mean of three experiments. Absence of error bars indicates that standard deviations are too small to see on the scale used.

The increase in TBARS, used as proxies for the extent of oxidative stress damage to the membrane lipids, varied from 37.1 ± 4.4 % (*Pseudomonas* sp.) to 54.2 ± 5.3 % (*Psychrobacter* sp.) with UVA, from 22.0 ± 2.5 % (*Brevibacterium* sp.) to 36.2 ± 3.5 % (*Bacillus* sp.) with UVB and from 6.3 ± 0.5 % (*Pseudomonas* sp.) to 14.7 ± 1.5 % (*Staphylococcus* sp.) with UVC (Fig. 5.3 C). A wavelength trend of variation was also observed for TBARS, which showed the strongest generation under UVA (47.7 ± 6.2 %) and the lowest under UVC (11.4 ± 3.5 %).

The increase in protein carbonyl levels ranged from 15.2 ± 1.6 % (*Bacillus* sp.) to 97.0 ± 11.5 % (*Sphingomonas* sp.) under UVA (45.7 ± 31.8 %), from 1.2 ± 0.1 % (*Micrococcus* sp.) to 103.6 ± 10.8 % (*Brevibacterium* sp.) under UVB (36.1 ± 30.9 %), and from 6.3 ± 0.7 % (*Sphingomonas* sp.) to 68.4 ± 6.8 % (*Staphylococcus* sp.) under UVC (26.5 ± 21.8 %) (Fig. 5.3 D).

Antioxidant enzyme activity

The effects of UVA on CAT activity (51.6 ± 48.3 %) (Fig. 5.3 E) ranged from a 62.8 ± 6.9 % inhibition (*Acinetobacter* sp.) to a 99.5 ± 9.8 % stimulation (*Brevibacterium* sp.). The effects of UVB (8.3 ± 49.7 %) varied between a 89.1 ± 6.5 % reduction (*Micrococcus* sp.) and a 62.9 ± 6.6 % increase (*Brevibacterium* sp.) and UVC effects (19.4 ± 25.1 %) ranged from an inhibition of 29.3 ± 3.1 % (*Bacillus* sp.) to a 48.8 ± 5.8 % increase (*Paracoccus* sp.) in CAT activity.

Irradiation with UVA and UVC caused an overall decrease in SOD activity (by an average of 28.5 ± 25.8 % and 24.5 ± 20.1 %, respectively), while UVB caused an average increase of 21.5 ± 19.3 %. The effects of UVA ranged from a 53.0 ± 5.7 % inhibition (*Bacillus* sp.) to a 30.4 ± 3.0 % stimulation (*Staphylococcus* sp.) of SOD activity. UVB either had no significant effect (*Staphylococcus* sp.) or enhanced SOD activity by as much as 59.1 ± 6.2 % (*Brevibacterium* sp.) and UVC effects ranged from an inhibition of 47.3 ± 4.9 % (*Bacillus* sp.) to a 18.0 ± 1.7 % increase (*Staphylococcus* sp.) (Fig. 5.3 F).

Differences between wavelengths and determinants of inactivation

PCA was applied to the data set to identify the main determinants of the differences between the effects of the three UV spectral regions tested (Fig. 5.4). The different radiation regimes were clearly separated along PC1, with UVA-treated samples displaying the lowest PC1 scores, mostly related to ROS (-0.495), TBARS (-

0.496) and carbonyl levels (-0.231). UVC-treated samples displayed the highest PC1 scores, related to activity (0.484) and DSB (0.363), while UVB-treated samples were located in between UVA and UVC-treated samples.

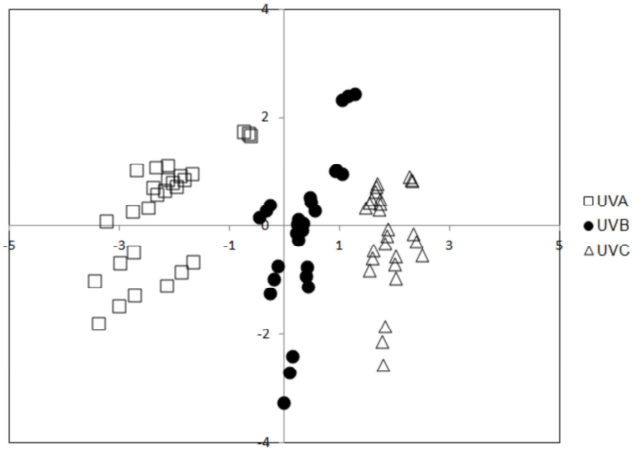

Fig. 5.4. Principal component analysis (PCA) score plot of data (activity, ROS levels, lipid oxidation, protein oxidation, DNA lesions, CAT and SOD activity) used to determine the parameters contributing the most for the separation of UVA, UVB and UVC treatments. A total of 27 data points (9 bacterial isolates x 3 replicates) was used for PCA analysis.

Multiple linear stepwise regression analysis was used to assess the main determinants of bacterial inactivation, expressed as LD_{50}, following exposure to UV radiation of different spectral regions. Results are presented in Table 5.2. Under UVA, 34.2 % of the variability in LD_{50} could be accounted for by DSB and SOD activity. Under UVB, 57.7 % of the variability in LD_{50} could be explained by the combination of TBARS, DSB and activity. Under UVC, ROS and DSB levels accounted with statistical significance for 55.8 % of the variation in LD_{50} values.

Table 5.2. Multiple stepwise regression analysis used to determine the parameters that explained bacterial inactivation under the different UV spectral regions. DSB: DNA strand breaks. SOD: superoxide dismutase. ROS: reactive oxygen species. TBARS: thiobarbituric acid reactive substances. β - standardized coefficient. p – probability. R^2 – coefficient of correlation.

	Adjusted R^2 of the model (p)	**Predictor variable**	**β**	**p**
UVA	0.342 (0.038)	DSB	-0.953	0.001
		SOD	0.557	0.038
UVB	0.577 (0.017)	TBARS	0.753	0.000
		DSB	-0.497	0.001
		Activity	-0.337	0.017
UVC	0.558 (0.003)	ROS	0.684	0.000
		DSB	-0.433	0.003

Discussion

In this study, the cellular and biological effects of UVA, UVB and UVC were assessed for a set of isolates characterized by different UV sensitivities using biological and biochemical methods. Additionally, multivariate analyses (principal component analysis and regression analysis) were conducted to identify the determinants of cell inactivation under different UV spectral regions.

Interspecific variation in UV sensitivity

Responses of the different isolates tested to each UV spectral region varied greatly. Several factors can account for this variability. Specifically, the preferential molecular target (*e.g.*, nucleic acids, proteins, lipids) of UV radiation may differ among strains. For example, it has been suggested that the extent of UV-induced DNA damage in Gram-positive bacteria is lower than that in Gram-negative bacteria because of a shielding effect by the cell wall (Jagger, 1985). Another factor is that the relative contribution of different reactive oxygen species involved in eliciting UV-induced damage may differ among strains, which may then affect the extent of the damage. For instance, the presence of high concentrations of intracellular iron in *Shewanella oneidensis* MR-1 promotes ROS proliferation and the production of the highly toxic hydroxyl radicals via Fenton-type chemistry; accordingly, this strain is extremely susceptible to UV radiation (Qiu et al., 2005a). Finally, the efficiency of the defence and repair strategies to cope with damage may also differ among bacteria (Arrieta et al., 2000; Matallana-Surget et al., 2009b; Santos et al., 2011b).

In the present study, the set of isolates tested showed in general a much higher resistance to UVA radiation than that reported in similar studies using *Shewanella oneidensis* MR1 (Qiu et al., 2004) and *Escherichia coli* (Ubomba-Jaswa et al., 2009). UVB LD_{50} values were, on average, up to 10 times higher than those observed in Antarctic marine bacteria (Hernandez et al., 2006) as well as in a set of marine bacterial isolates and the enteric bacteria *Salmonella typhimurium* CIP 60.62^{T} (Joux et al., 1999). On the other hand, the average UVC LD_{50} (26.6 J m^{-2}) determined in the present study was lower than that detected in *Clavibacter michiganensis* (UVC LD_{50} of approximately 75 J m^{-2}) (Jacobs and Sundin, 2001) and even lower than the average minimal inhibitory UVC dose observed in a set of isolates retrieved from the peanut phyllosphere (Sundin and Jacobs, 1999).

In this study, the Gram-positive, high G+C content *Actinobacteria Micrococcus* sp. showed the highest resistance to each UV spectral region. Highly UV-resistant *Micrococcus* strains have previously been isolated (Ordoñez et al., 2009). It has been suggested that Gram-positive bacteria are better adapted to UV stress because their cell walls screen out a considerable fraction of UV radiation (Jagger, 1985). The genomic composition of microorganisms, particularly the G+C content and bipyrimidine nucleotide frequency, also affects the frequency and spectrum of DNA lesions formed during exposure to UV radiation (Matallana-Surget et al., 2008; Moeller et al., 2010). The high G+C content of *Actinobacteria* has been proposed to confer protective adaptation against UV radiation by minimizing the formation of cyclobutane dimers (Warnecke et al., 2005). However, the other *Actinobacteria* tested in this study (*Brevibacterium* sp.) was quite sensitive to UV radiation, which is in agreement with observations by Ordoñez et al. (2009), demonstrating that cell wall characteristics and G+C content are not the sole determinants of UV resistance. The presence of protective pigmentation (Shick and Dunlap, 2002) and specialized DNA repair systems (Dodson et al., 1994) in *Micrococcus* sp., but not *Brevibacterium* sp., could contribute to the discrepancy in UV sensitivity of these *Actinobacteria*.

Gammaproteobacteria have been reported as the most UV-resistant group in several aquatic environments (Alonso-Sáez et al., 2006; Ordoñez et al., 2009; Santos et al., 2012b). In the present study, *Pseudomonas* sp. showed high levels of resistance to the different UV spectral regions, in agreement with previous studies (Ordoñez et al., 2009). UV-resistant *Acinetobacter* strains have also been isolated and their resistance associated with efficient DNA repair mechanisms (Fernández Zenoff et al., 2006b; Hörtnagl et al., 2011) and high catalase activity (Di Capua et al., 2011). However, in this study, *Acinetobacter* sp. was found to be UV-sensitive. UV-sensitive and UV-resistant *Acinetobacter* strains have been isolated even from the same environment (Ordoñez et al., 2009), suggesting that UV resistance is not a phylogenetic characteristic.

The alphaproteobacterium *Sphingomonas* sp. also showed high resistance to UV radiation, which is in accordance with previous reports of reduced accumulation of DNA lesions in *Sphingomonas* strains following UV exposure (Joux et al., 1999).

General trends in the effects of UV radiation

Despite the interspecies variability observed, some wavelength-dependent trends in the variation of biological and biochemical parameters studied were identified. Specifically, shorter UV wavelengths caused the greatest bacterial inactivation (denoted by lower UV doses being required to reduce bacterial numbers) and reduction in activity, while longer UVA wavelengths had more subtle effects in accordance with their indirect, ROS-mediated mode of action (Eisenstark, 1998). Intracellular ROS generation, lipid oxidation (TBARS) and protein carbonylation, which are indicative of indirect UV effects, showed the strongest response to UVA irradiation. DSB formation resulting from direct interaction of UV with DNA was highest under UVC. The magnitude of UVB effects was generally between those of UVA and UVC, supporting the suggestion that UVB-induced damage comprises elements from both the direct and indirect pathways of damage (Qiu et al., 2005a). No wavelength-dependent variation was detected for CAT or SOD, suggesting that the type of ROS involved in eliciting the damage and the degree to which the interconnected mechanisms of ROS generation and removal by antioxidant enzymes act in each particular strain are extremely variable and ultimately shape the individual patterns of response of CAT and SOD to irradiation.

Principal component analysis applied to the entire data set clearly separated the effects of different irradiation treatments. The extent of the oxidative damage to lipids and proteins, as well as ROS levels, were found to be involved in differentiating UVA effects from the other UV regimes, suggesting that membrane lipids and proteins are major targets of UVA-induced oxidative modifications, in accordance with previous studies (Pizarro and Orce, 1988; Bosshard et al., 2010b). The effects of UVC were more related to the extent of damage to DNA (assessed using DSB as a proxy), which is in agreement with the mutagenic nature of UVC wavelengths (Friedberg et al., 1995), as well as their inhibitory effects on activity. The PCA bidimensional plot showed that UVB-treated samples were positioned between UVA and UVC treatments, supporting the intermediate nature of the effects of UVB when compared with those of UVA and UVC (Qiu et al., 2005a).

Determinants of bacterial inactivation

Multiple linear stepwise regression analysis was used to assess the main determinants of bacterial inactivation following exposure to different UV spectral regions. The amount of DSB emerged as the major determinant of inactivation upon

exposure to UVA. UVA-induced damage has traditionally been attributed to photodynamic reactions mediated by cellular chromophores since DNA does not strongly absorb light in the UVA range (Cadet et al., 2005a). More recently, investigations conducted on eukaryotes have highlighted the high mutagenic potential of UVA (Rünger et al., 2012) and the role of cyclobutane pyrimidine dimers, rather than oxidative lesions, in UVA-induced damage (Ikehata et al., 2008). The finding that UVA induced the lowest reduction in CFU among the investigated spectral regions demonstrates that bacteria are able to minimize UVA-induced DNA lesions. This may involve light-dependent repair mechanisms mediated by photolyase activated by UVA radiation itself, as well as light-independent repair (Mitchell and Karentz, 1993). Additionally, most UVA sensitive strains displayed significantly higher levels of DSB and TBARS (1-way ANOVA, $p < 0.05$). Taken together, these results suggest that the extent of oxidative damage to biomolecules and counteracting protective mechanisms underlie the variability in UVA susceptibility among different bacteria, but that the accumulation of DNA damage ultimately leads to cell death.

Under UVB, oxidative damage to lipids (TBARS), accumulation of DNA damage, and loss of metabolic activity were the main determinants of inactivation. These results indicate that, in addition to DNA damage, changes in the integrity of membrane structure and functionality during UVB exposure play an important role in bacterial inactivation. Such changes may compromise the ability of the cell to generate energy necessary to sustain its activity and elicit repair strategies following irradiation (Bosshard et al., 2010a). Most UVB-sensitive strains displayed significantly higher levels of protein carbonyls than resistant ones (1-way ANOVA, $p < 0.05$), which also identifies protein oxidation as an important determinant of bacterial susceptibility to UVB radiation. UVB was the only irradiation regime to enhance SOD activity levels in all bacteria when compared with non-irradiated controls, indicating that SOD may play an important protective role against UVB. The superoxide radical is able to directly cause oxidative damage to the bases of DNA (Misiaszek et al., 2004). Additionally, superoxide can attack Fe-S clusters of enzymes, rendering them inactive. The released ferrous iron can, in turn, react with H_2O_2, resulting in the formation of the highly toxic hydroxyl radical which is able to attack virtually any biomolecule (Imlay, 2006).

Regression analysis revealed that ROS levels together with DNA damage were the best predictors of cell inactivation under UVC. However, the extent of DNA damage did not differ significantly between resistant and sensitive strains, which is in

accordance with previous observations (De La Vega et al., 2005). On the other hand, most UVC sensitive strains displayed significantly higher TBARS and carbonyls levels than resistant ones (1-way ANOVA, $p < 0.05$), which suggests that the extent of oxidative damage to lipids and proteins interferes with vital biological functions and is therefore an important component of UVC-induced inactivation (Krisko and Radman, 2010; Schenk et al., 2011). Unexpectedly, ROS levels were significantly higher in resistant strains (1-way ANOVA, $p < 0.05$); however, it is unclear if these findings have any biological significance. Accordingly, additional studies to investigate whether ROS generation is involved in eliciting specific defence strategies in response to UVC exposure, as in cyanobacteria (Dillon et al., 2002) and plants (Murphy and Huerta, 1990), are warranted.

New insights into the mechanisms of UV-induced damage in bacteria

The present work aimed to dissect the wavelength dependence of the damage induced by UV radiation. In order to do so, a combination of a multitude of UV-sensitivity tests and their statistical analysis was applied. Using this combined innovative approach new clues regarding the targets of UV radiation of different spectral regions across a range of bacteria with different UV susceptibilities emerged. In particular, the involvement of DNA damage in eliciting bacterial inactivation upon UVA exposure was observed, which is in accordance with work reporting the induction of the SOS response in UVA-irradiated bacteria (Qiu et al., 2005a; Berney et al., 2006a). Oxidative damage to lipids was found to be determinant for bacterial inactivation during UVB exposure. Such observation is in agreement with recent reports of enhanced expression of the glyoxalase protein and alkyl hydroperoxide reductase AhpC, involved in the detoxification of lipid peroxidation by-products, following UVB exposure of *Photobacterium angustum* S14 (Matallana-Surget et al., 2012). Finally, oxidative stress was also found to be crucial for cell inactivation under UVC, supporting evidence accumulating in recent years (Gomes et al., 2005; Krisko and Radman, 2010; Schenk et al., 2011).

Most investigations on the effects of UV radiation on bacteria have been conducted on a small number of genetically-well characterized microorganisms that are not always representative of natural environmental communities. By using bacterial strains originating from a photo-stressed microbial community (Santos et al., 2011b), the information gained from the isolates used in the present work could provide clues to

understand how natural microbial assemblages might react to global changes, particularly changes in environmentally relevant UV radiation.

Acknowledgments

The authors would like to thank the anonymous reviewers and editors who provided helpful criticism and suggestions which greatly contributed to improve the original manuscript. Acknowledgments are due to Francisco Coelho and Abel Ferreira for assistance in UV intensity measurements and to Prof. Rosário Correia (Physics Department, Universiy of Aveiro) for reviewing the manuscript. Financial support for this work was provided by CESAM (Centre for Environmental and Marine Studies, University of Aveiro) and the Portuguese Foundation for Science and Technology (FCT) in the form of a PhD grant to A. L. Santos (SFRH/BD/40160/2007) and a post-Doctoral grant to I. Henriques (SFRH/BPD/63487/2009).

CHAPTER 6

Effects of UV Radiation on the Lipids and Proteins of Bacteria Studied by Mid-Infrared Spectroscopy

Santos A. L., Moreirinha C., Henriques I., Almeida A., Delgadillo I., Correia A., Cunha A.

Submitted for publication

Abstract

The knowledge of the mechanisms of bacterial inactivation by UV radiation of different wavelengths can contribute for a better understanding of the environmental effects of enhanced UV levels associated with global environmental changes, as well as the optimization of UV-based disinfection strategies.

In the present work, the effect of exposure to UV radiation of different spectral regions (UVC, 100-280 nm; UVB, 280-320 nm; UVA, 320-400 nm) on the lipids and proteins of two bacterial strains with distinct UV sensitivities was studied by mid-infrared spectroscopy. Exposure to UV radiation caused a general increase in lipid methylation, accompanied by lipid oxidation and potentially altered lipid composition, which could reflect UV-induced damage to enzymes involved in lipid metabolism and/or a metabolic strategy to preserve the resources of the cell for defence/repair strategies. Mid-infrared spectroscopy also revealed effects of UV radiation on protein conformation and/or composition, oxidative damage to amino acid side chain residues and potentially changes in the propionylation, glycosylation and/or phosphorylation status of proteins. These results highlight the array of modifications induced by UV radiation on the lipids and proteins of bacteria, giving further support to the role of modifications induced in these biomolecules in the UV-based inactivation process.

Introduction

UV radiation is an important stress factor for aquatic bacterial communities (Herndl et al., 1997; Moran and Zepp, 2000; Häder, 2001; Buma et al., 2003). UV radiation can be divided in three categories: UVC (100-280 nm), UVB (280-320 nm) and UVA (320-400 nm). Most environmental photobiology studies have focused on UVB effects on bacteria (Wängberg et al., 1998; Joux et al., 1999; Arrieta et al., 2000; Gustavson et al., 2000; Buma et al., 2001; Chatila et al., 2001; Fernández Zenoff et al.,

2006a; Fernández Zenoff et al., 2006b; Wängberg et al., 2008; Martin et al., 2009; Santos et al., 2011a; Santos et al., 2012b). Though on a photon basis UVA radiation contains less energy than UVB radiation, the fraction of solar radiation in the UVA (95 %) spectrum is greater than that in the UVB spectrum (5 %) and can potentially cause substantial biological damage (Frederick and Lubin, 1988; Nunez et al., 1994; Moan et al., 1999), which is explored in the process of solar disinfection (Wegelin et al., 1994). UVC radiation does not penetrate the Earth's atmosphere, but it is a convenient experimental tool to assess UV sensitivity in bacteria that are highly tolerant or insensitive to high doses of UVB (Sundin and Jacobs, 1999). Furthermore, its ability to inactivate bacteria is widely recognized (Jagger, 1985; Coohill and Sagripanti, 2008; King et al., 2011).

The biological effects of the different UV wavelengths are distinguished in their preferential cellular targets and mechanisms by which they induce damage. The effects of UVA are considered to be mostly indirect, that is, mediated by reactive oxygen species (ROS) formed by photodynamic reactions involving intracellular or extracellular photosensitizers (Chamberlain and Moss, 1987; Moan and Peak, 1989; Girotti, 1998; Pattison and Davies, 2006; Zeeshan and Prasad, 2009). These ROS can react with cellular constituents, most notably proteins and lipids, leading to altered membrane permeability and/or disruption of transmembrane ion gradients that eventually can result in cell death (Bose and Chatterjee, 1995; Futsaether et al., 1995). UVC radiation is the most detrimental to living cells, because it is directly absorbed by DNA, causing the formation of cyclobutane dimers and single-strand breaks in the sugar-phosphate backbone of DNA (Pfeifer, 1997). UVB radiation produces both direct and indirect damage (Moran and Zepp, 2000).

Iron is a key mediator of the processes of ROS generation, due to its involvement in the Fenton reaction which generates the highly reactive hydroxyl radical (Wardman and Candeias, 1996). Fenton reactions are accelerated by light (photo-Fenton reactions) (Chamberlain and Moss, 1987). Accordingly, Fenton-mediated oxidative damage is enhanced upon UV exposure (Moss and Smith, 1981). The presence of high amounts of iron sequestered in membranes, particularly associated with respiratory proteins, makes bacterial cell membranes potentially important targets of oxidative reactions (Kohen et al., 1995).

While there are several studies of the effects of UV radiation on DNA (Moeller et al., 2007a; Matallana-Surget et al., 2008; Matallana-Surget et al., 2010; Moeller et al.,

2010), the observation of comparable levels of DNA photoproduct accumulation in bacteria displaying different sensitivities to UV radiation (Joux et al., 1999; Matallana-Surget et al., 2008) and the fact that DNA damage alone cannot account for the inhibition of bacterial activity in surface waters (Visser et al., 2002) seems to imply that damage to other biomolecules contributes to the inhibitory effects of UV radiation. Oxidative damage to lipids and proteins may play a role in the process (Chamberlain and Moss, 1987; Hoerter et al., 2005a; Bosshard et al., 2010b).

The knowledge of the targets of UVA and UVB on bacterial cells is crucial to understand their roles as drivers of bacterial community structure and function and fully comprehend how enhanced UV fluxes resulting from global changes (Andrady et al., 2010) can impact biogeochemical cycles. Additionally, integrated information of the effects of UV radiation of different wavelengths may contribute for the design of more efficient and ecologically-friendly UV-based disinfection strategies applicable either in the industrial setting or in a solar disinfection context.

The objective of this work was to study the modifications induced by exposure to UV radiation of different spectral regions on the lipids and proteins of two bacterial strains displaying different UV sensitivities using mid-infrared spectroscopy.

Materials and methods

Bacterial strains and irradiation conditions

The bacterial strains used in this study (*Acinetobacter* sp. strain PT5I1.2G, NCBI accession number GQ365202 and *Pseudomonas* sp. strain NT5I1.2B, NCBI accession number GU084169) were isolated from the surface waters of the estuarine system of Ria de Aveiro (Portugal) (Santos et al., 2011b) (Table 6.1). Two *Gammaproteobacteria* strains were selected because this group is dominant in the UV-exposed surface layers of water bodies and several of their members have been proposed to be UV-resistant (Franklin et al., 2005; Alonso-Sáez et al., 2006; Santos et al., 2012b). The *Pseudomonas* strain used in the present study is UVB-resistant (LD_{50} for UVA, UVB and UVC of 221.3 kJ m^{-2}, 49.3 kJ m^{-2} and 40.6 J m^{-2}, respectively), recovering efficiently from UVB-induced damage, while the *Acinetobacter* strain is more sensitive to UVB radiation (LD_{50} for UVA, UVB and UVC of 159.3 kJ m^{-2}, 34.1 kJ m^{-2} and 18.0 J m^{-2}, respectively) and less able to recover from UVB-induced damage (Santos et al., 2011b).

Table 6.1. Bacterial strains used in the experiments, their accession number, phylogenetic affiliation, closest relatives, similarity with database, as well as bacterial group. LD_{50} values for each strain under the different wavelengths are also shown.

Strain	Accession no.	Phylogenetic affiliation	Closest relative (accession no.)	% 16S rDNA similarity	LD_{50} UVA (kJ m^{-2})	LD_{50} UVB (kJ m^{-2})	LD_{50} UVC (J m^{-2})
PT5I1.2G	GQ365202	*Acinetobacter* sp.	*Acinetobacter sp.* (EU545154.1)	99	159.3	34.1	18.0
NT5I1.2B	GU084169	*Pseudomonas* sp.	*Pseudomonas* sp. (JF749828.1)	99	221.3	49.3	40.6

Bacterial isolates were grown in Marine Broth 2216 on an orbital shaker (100 rpm) at 25°C until late-exponential phase (defined as the inflection point of the growth curve, at the transition between the exponential and stationary phase, which was usually achieved in approximately 10 h). Cells were harvested by centrifugation (3,200 x *g* for 15 min, 20 ºC, Eppendorf centrifuge 5415R, Hamburg, Germany) and the pellet was washed three times in 0.9 % NaCl, in order to remove all traces of nutrients originating from the culture medium. Bacterial cells were then resuspended in 0.9 % NaCl and bacterial abundance was adjusted with 0.9 % NaCl to 10^6 cells mL^{-1}, as determined by epifluorescence microscopy (Hobbie et al., 1977).

Cell suspensions were placed in sterile Petri dishes (150 x 25 mm; Corning) and irradiated (without the lid) with UVA (Philips TL 100 W/10R lamps, Philips, Eindhoven, The Netherlands, main emission line at 365 nm, intensity of 50 W m^{-2}), UVB (Philips TL 100 W/01 lamps, Philips, Eindhoven, The Netherlands, main emission line at 302 nm, intensity of 2.3 W m^{-2}) and UVC (low pressure mercury lamp NN 8/15, Heraeus, Berlin, Germany, main emission line at 254 nm, intensity of 0.66 W m^{-2}). For each spectral region tested, the samples were irradiated to their LD_{50} (UV dose resulting in 50 % inactivation). UV sources were placed at 20 cm from the sample. UV intensities were measured with a monochromator spectro-radiometer placed at the sample level (DM 300, Bentham Instruments, Reading, UK) and the UV dose (in J m^{-2}) was calculated by multiplying the intensity by the irradiation time (in seconds).

During irradiation, samples were stirred by magnetic agitation and temperature was kept at approximately 25 ºC. A dark control (covered in aluminum foil) treated in the same way as the irradiated samples was included in every experiment. Aliquots of cell suspensions were collected before and after irradiation, washed with ultrapure water and immediately used for lipid and protein extraction. For every irradiation treatment, experiments were repeated in three independent assays with three biological replicates.

Dark controls (covered in aluminium foil), treated in the same way as the irradiated samples, were included in every experiment.

Lipid extraction

Total lipid extracts were obtained according to standard protocols (Bligh and Dyer, 1959). Briefly, irradiated and unirradiated cell suspensions were centrifuged and the pellet was washed with pure desalted water. The suspensions were centrifuged again and the supernatant discarded. A volume of 125 µL of chloroform and 250 µL of methanol was added to the pellet and the mixture was vortexed vigorously. Then, 8.4 µL of hydrochloric acid (6 M) and 125 µL of chloroform were added and the mixture vortexed again. Finally, 125 µL of pure desalted water were added, the solution was vortexed again, and centrifuged for 20 min at 300 x *g*. Total lipid extract was collected in the lower phase and immediately used for spectra acquisition.

Protein extraction

Proteins were extracted according to previously described procedures (Ojanen et al., 1993). Briefly, irradiated and unirradiated cell suspensions were centrifuged and the pellets were resuspended in 10 mM Tris-HCl (pH 8.0). The suspension was sonicated in an ice bath four times for 5 s using a sonifier (Branson 450, Danbury, CT, USA), followed by a centrifugation step at 15,000 x *g* for 1 h at 4 °C. The pellet was resuspended with 10 mL of 10 mM Tris-HCl (pH 8.0), and sarcosyl (Sigma, St. Louis, MO, USA) was added to a final concentration of 1.5 % (v/v). After incubation at room temperature for 20 min, the protein extract was collected by centrifugation at 15,000 x *g* for 90 min at 4 °C and suspended in ultrapure water.

Spectra acquisition and analysis

Mid-infrared spectra were obtained using a GoldenGate single reflection diamond ATR system in an infrared (IR) spectrometer (Perkin-Elmer Spectrum BX System 2000) equipped with a DTGS detector. Measurements were recorded over the wavelength range of 4000 to 700 cm^{-1} with a spectral resolution of 8 cm^{-1}. The final spectra of the samples were achieved averaging 32 scans. A total of 6 spectra were used for chemometric analysis. Spectra were normalized and baseline-corrected and then used to obtain difference spectra (irradiated minus control) using OPUS version 6.5 software (Bruker, Germany). Additionally, the original spectra were transferred via

JCAMP.DX format into the data analysis software package described in Barros (1999) for Principal Component Analysis (PCA).

Results and discussion

Fig. 6.1 (A to D) shows the original mid-infrared spectra of the extracted lipids and proteins of *Acinetobacter* sp. PT5I1.2G and *Pseudomonas* sp. NT5I1.2B. In order to gain further insights into the modifications induced by the different UV treatments in lipids and proteins, difference spectra were calculated by subtracting the controls to the irradiated spectra. Difference spectra are shown in Fig. 6.2 and Fig. 6.4. In the resultant irradiated-minus-control difference spectra, upward-moving bands correspond to mid-infrared bands that appear (or increase in intensity) after irradiation, while downward-moving bands correspond to mid-infrared bands that disappear (or decrease in intensity) upon irradiation.

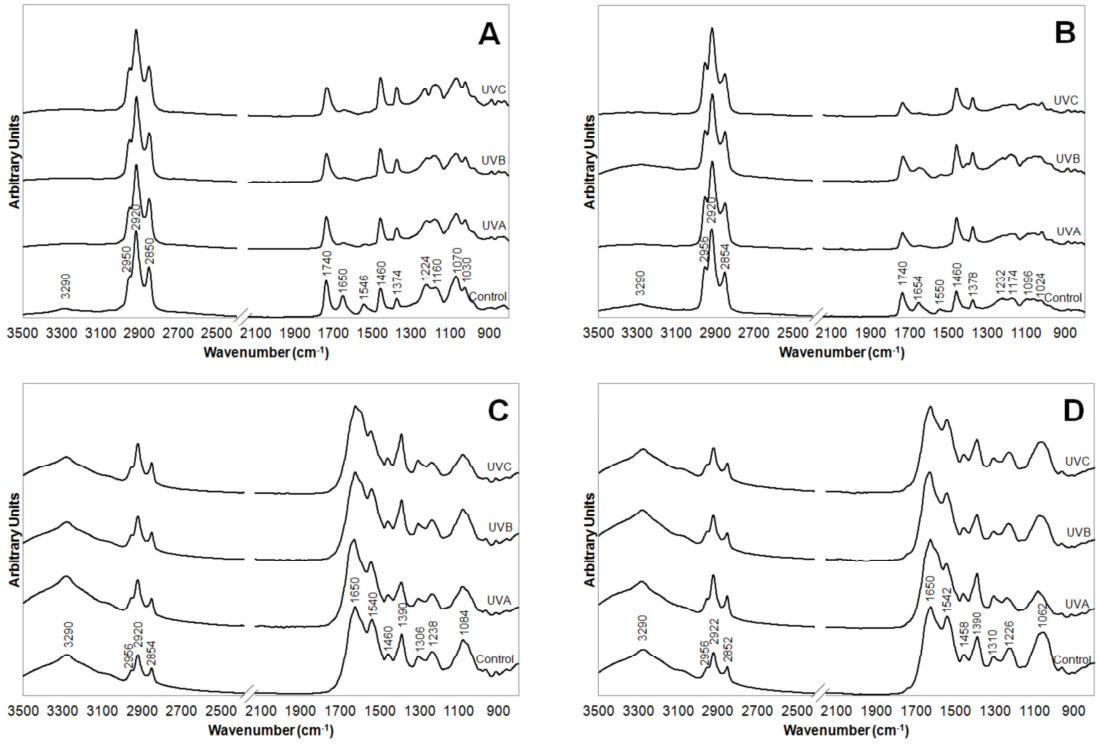

Fig. 6.1. Original spectra of lipid extracts of (A) *Acinetobacter* sp. PT5I1.2G, (B) *Pseudomonas* sp. NT5I1.2B, and protein extracts of (C) *Acinetobacter* sp. PT5I1.2G, (D) *Pseudomonas* sp. NT5I1.2B. The main bands detected in the original spectra are identified. The spectra were normalized, baseline-corrected and a 13-point smooth was applied. The presented spectra correspond to the average of 6 replicate spectra. Spectra are shown offset to facilitate visualization. The region between 2400-2200 cm^{-1} corresponding to the CO_2 region was removed from the spectra.

UV effects on lipids

In general, exposure to the different UV spectral regions resulted in similar overall effects on the lipids of the two strains tested. These effects included a drastic decrease in intensity of bands assigned to lipoproteins and/or nitrogen-containing lipids (≈ 3290 cm^{-1}, ≈ 1650 cm^{-1} and ≈ 1540 cm^{-1}) (Fig. 6.2). Lipoproteins are known to be susceptible to oxidative damage, due to the presence of aromatic side chains residues (such as tryptophan or tyrosine) that act as chromophores during photosensitized reactions (Esterbauer et al., 1987; Salmon et al., 1990). Therefore, reducing the amount of lipoproteins in the cell could be a mechanism to minimize oxidative damage.

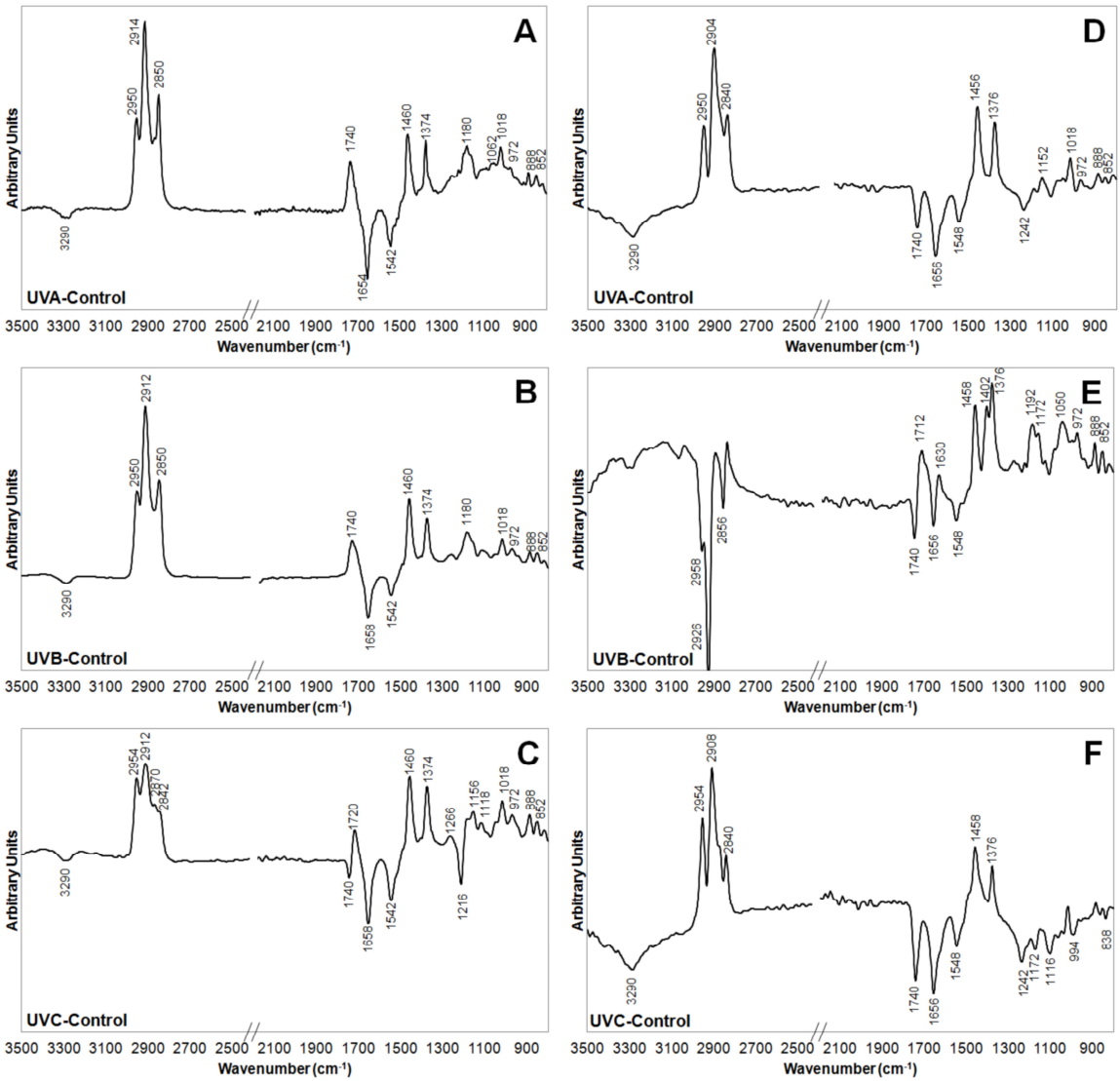

Fig. 6.2. Difference spectra (irradiated-minus-control) for the lipid extracts of *Acinetobacter* sp. PT5I1.2G under UVA (A), UVB (B) and UVC (C) and *Pseudomonas* sp. NT5I1.2B under UVA (D), UVB (E) and UVC (F). A 13-point smooth was applied to the difference spectra. The region between 2400-2200 cm^{-1}, corresponding to the CO_2 region, was removed from the spectra.

On the other hand, it is also possible that photosensitized reactions occurring in the protein fraction of the molecule could have interfered with lipid-protein interactions, resulting in the dissociation of the lipid and protein moieties of the molecules (Salmon et al., 1990). As a result, during the process of lipid extraction, proteins previously associated with lipids could have been lost.

Exposure to UV radiation of different wavelengths also resulted in an increase in intensity of methyl bands (≈ 2950 cm^{-1}, ≈ 2870 cm^{-1}, ≈ 1460 cm^{-1}, ≈ 1380 cm^{-1}) (Fig. 6.2). This effect was particularly accentuated in UVC-treated *Acinetobacter* sp. PT5I1.2G (Fig. 6.2 C). Increasing methyl groups disrupts the packing of acyl chains and reduces the number of interactions in the membrane, leading to enhanced membrane fluidity (Zhang and Rock, 2008). Changes in membrane fluidity can also be inferred by the change in frequency of methylene bands at ≈ 2920 cm^{-1} and ≈ 2850 cm^{-1} that can be observed in the original spectra. Altered membrane fluidity, mediated by the expression of specific membrane proteins, have been shown to have a positive effect on cellular adaptation of *Oenococcus oeni* to stress (Delmas et al., 2001). Changes in membrane fluidity have also been associated with signal transduction involved in the activation of intracellular mechanisms of protection, following exposure to stress factors. For example, in plants, membrane fluidization is implicated in the activation of the heat-shock response (Sangwan et al., 2002). Whether such a mechanism could be involved in the response of bacteria to UV radiation is unknown. Additionally, changes in phospholipid composition of the cell, consistent with the observed changes in the band at 1740 cm^{-1} assigned to esters of fatty acids (Rothschild et al., 1980), could also explain the increase in methyl bands verified in irradiated samples.

In most cases, UV exposure also resulted in oxidative damage to lipids, denoted by the increased intensity of bands at 1018 cm^{-1} assigned to O-O bonds of hydroperoxides (Merle et al., 2010), 972 cm^{-1} assigned to *trans* C = C bonds (Le Dréau et al., 2009), as well as 1402 cm^{-1} assigned to carboxyl groups formed during the oxidation process (Nadtochenko et al., 2005) and 888 cm^{-1} assigned to CH_2 and CH_3 rocking modes of oxidized lipids (Nadtochenko et al., 2005). In the case of UVC-treated *Acinetobacter* sp. PT5I1.2G there was also an increase in intensity of a band at 1720 cm^{-1} (Fig. 6.2 C), reflecting the possible formation of aldehydes due to lipid peroxidation (Le Dréau et al., 2009). In *Acinetobacter* sp. PT5I1.2G (Fig. 6.2 A-C) effects on oxidative damage marker bands were noted mostly under UVC, while in

Pseudomonas sp. NT5I1.2B oxidation seemed to occur under every spectral region (Fig. 6.2 D-F).

In the case of *Pseudomonas* sp. NT5I1.2B exposed to UVB, a marked increase in the area between 1200-900 cm^{-1} and a general increase in the area between 3000 and 3500 cm^{-1}, dominated by OH bands particularly associated with polysaccharides (Gonzaga et al., 2005), as well as a decrease in all the CH region (3000 to 2800 cm^{-1}) and the ester carbonyl band (1740 cm^{-1}), were observed. Together, these observations suggest an alteration in the lipid composition of the cell, with an increase in the relative abundance of glycolipids in detriment of fatty acids. A relative increase in glycolipids could contribute to enhance the stability of the cell membrane when confronted with environmental changes due to the ability of these compounds to undergo interlipid hydrogen bonding via glycosyl headgroups (Curatolo, 1987) and has been reported in the response of bacteria to acid stress and temperature shifts (Hunter et al., 1981; Fernández Murga et al., 2000; Taranto et al., 2006). On the other hand, *Pseudomonas* species are known to produce extracellular glycophospholipids containing fatty acids with 10 and 12 carbons (Silipo et al., 2002; Andolfi et al., 2008). The production of such kind of compound could also account for the increase in glycolipids and at the same time explain the smaller effects of UVB on the lipoproteins of *Pseudomonas* sp. in the UVB treatment (Fig. 6.2 E), since these molecules contain amide links (Silipo et al., 2002).

PCA scores and loadings plots of the analysis of the spectra of lipids of *Acinetobacter* sp. PT5I1.2G exposed to the different irradiation regimes are presented in Fig. 6.3 A and 6.3 B. The PCA score plot revealed a clear separation between control and irradiated samples along PC1, while the different wavelength treatments were separated along PC2. Among the different irradiation regimes, UVA and UVC were found together in negative PC2, whereas UVB was in positive PC2. Control samples (negative PC1) were separated from irradiated samples (positive PC1) by higher intensity of bands assigned to ester carbonyls from phospholipids and triglycerides (1740 cm^{-1}), amide I and amide II of lipoproteins (1654, 1546 cm^{-1}) as well as bands assigned to phospholipids and/or glycolipids (1230, 1074 cm^{-1}). Irradiated samples displayed enhanced intensity of methyl bands (2954 and 1460 cm^{-1}) as well as bands associated with lipid peroxidation products, including *trans* C = C bonds (970 cm^{-1}) and CH_2 and CH_3 rocking modes of oxidized lipids (888 cm^{-1}). Therefore, PCA confirmed the involvement of changes in lipid composition and/or structure, as well as effects

exerted on lipoproteins and/or nitrogen-containing lipids, in differentiating irradiated and non-irradiated samples, as suggested from the analysis of difference spectra.

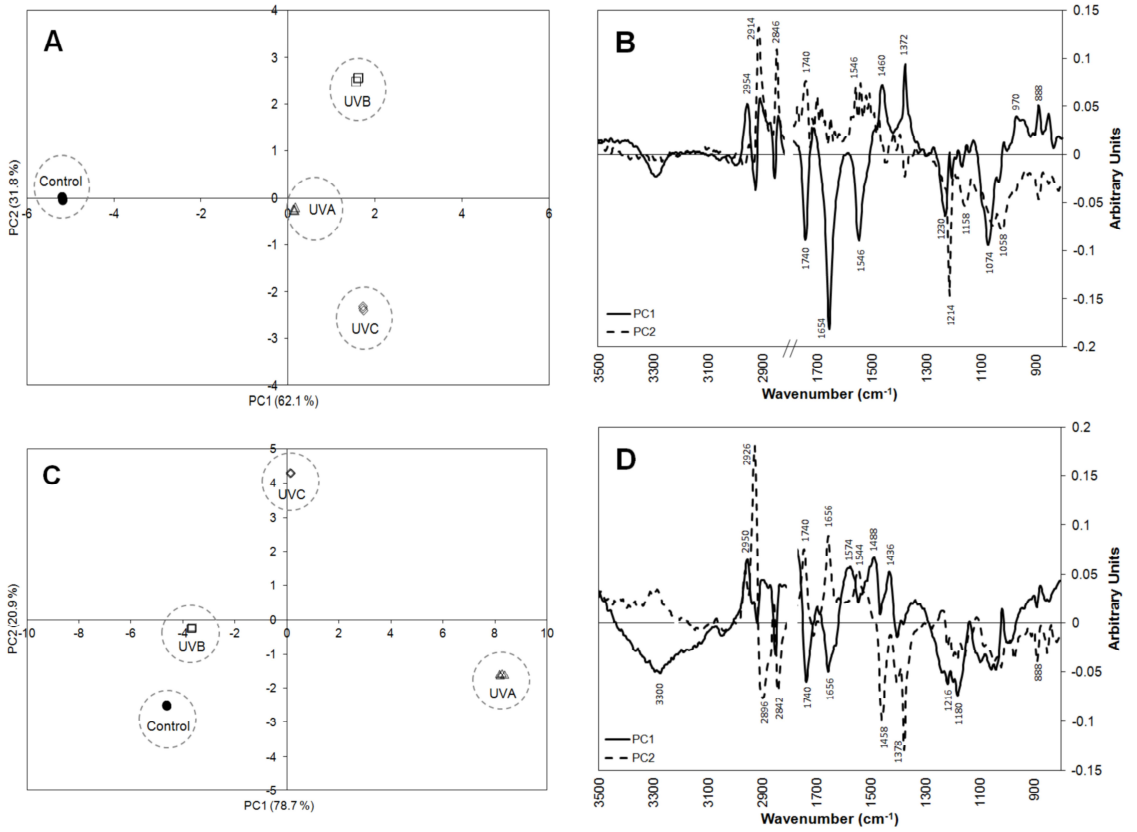

Fig. 6.3. Scores and loading plots for PCA analysis of lipid extracts irradiated with different UV spectral regions of *Acinetobacter* sp. PT5I1.2G (A, B) and *Pseudomonas* sp. NT5I1.2B (C, D).

The different UV treatments were discriminated mostly along PC2 being UVB irradiated samples characterized by higher intensity of bands assigned to methylene groups (2914 cm^{-1}, 2846 cm^{-1}), ester groups of phospholipids and triglycerides (1740 cm^{-1}) and nitrogen-containing lipids and/or lipoproteins (1654, 1546 cm^{-1}), while UVC-treated samples were mostly differentiated by higher intensity of bands assigned to phospholipids and/or glycolipids (1214, 1158 cm^{-1}) and oxidation products (888 cm^{-1}).

PCA scores and loadings plots of the spectra of the lipids of *Pseudomonas* sp. NT5I1.2B are presented in Fig. 6.3 C and 6.3 D. Contrary to what was observed in *Acinetobacter* sp. PT5I1.2G, PCA analysis of the lipids of *Pseudomonas* sp. NT5I1.2B in the different irradiation regimes did not show a clear separation between controls and irradiated samples, with the UVB treatment located together with the control samples in negative PC1, and separated from the remaining UV regimes located in positive PC1. Control and UVB-treated samples were differentiated from UVA-treated samples by enhanced intensity of bands assigned to carbonyl ester groups of phospholipids and

triglycerides (1740 cm^{-1}), N-H stretching vibrations of amide and amine (3300 and 1656 cm^{-1}) and bands assigned to phospholipids and glycolipids (1216, 1180 cm^{-1}), while UVA-treated samples were differentiated by enhanced intensity of CH_3 bands (2940 cm^{-1}) and bands associated with lipid oxidation products (888 cm^{-1}). PC2 basically separated the UVC treatment from UVA-irradiated samples and controls. Separation of these sets of samples was mostly associated with bands assigned to CH bonds (2940, 2926, 2896, 2842, 1458, 1378 cm^{-1}), esters of phospholipids (1740 cm^{-1}) as well as lipoproteins and/or nitrogen-containing lipids (1656 and 1544 cm^{-1}).

Taken together, PCA results identify methyl and/or methylene groups associated with lipids, as well as lipoproteins and/or nitrogen-containing lipids, as targets of UV radiation. Additionally, variations in bands assigned to phospholipids and/or glycolipids were also observed denoting changes on bacterial lipid composition upon exposure to UV radiation. Altered lipid composition can be a result of UV-induced damage to lipid metabolic pathways, for example, damage to enzymes involved in lipid synthesis. On the other hand, changes in lipid composition may also reflect a metabolic strategy of bacteria to cope with UV radiation. For instance, the general decrease in the relative abundance of phospho- and glycolipids in UV-treated samples, revealed in PCA results, could possibly be explained by the high susceptibility of unsaturated fatty acids to oxidative damage (Panagopoulos et al., 1990; Kramer et al., 1991). Decreased phospholipid and glycolipid content was also reported in the marine cyanobacteria *Phormidium tenue* in response to UV radiation and attributed to oxidative damage of the membrane (Bhandari and Sharma, 2011). Alternatively, UV-induced changes in the allocation of elements to biomolecules could also account for the observed changes in the relative proportion of phospho- and glycolipids with irradiation. Bacteria are known to replace their phospholipids with membrane lipids that do not contain any phosphorus in response to phosphorus limitation, so that less phosphorus is consumed for the formation of membranes (López-Lara et al., 2005). A reduction in phosphorus directed to membranes could be a mechanism elicited in order to ensure that enough phosphate supply is present for cellular repair strategies, such as nucleotide excision repair, which requires ATP (Batty and Wood, 2000).

UV effects on proteins

UV irradiated samples were characterized by increased intensity of methyl (≈ 2950 cm^{-1}) and particularly methylene (≈ 2920 cm^{-1}, ≈2850 cm^{-1}) bands associated with proteins and amino acids, especially in *Acinetobacter* sp. PT5I1.2G (Fig. 6.4 A-C). The observed increase in intensity of methylene bands associated with proteins and amino acids with irradiation could be attributed to changes in protein composition, specifically, an increase in the relative proportion of amino acids rich in CH_2 groups, like proline, lysine, isoleucine, glutamine or glutamic acid. The concentration of proline has been shown to increase upon UV exposure in the green algae *Scenedesmus quadricauda* and hypothesized to be a stress-defence response (Kováčik et al., 2010).

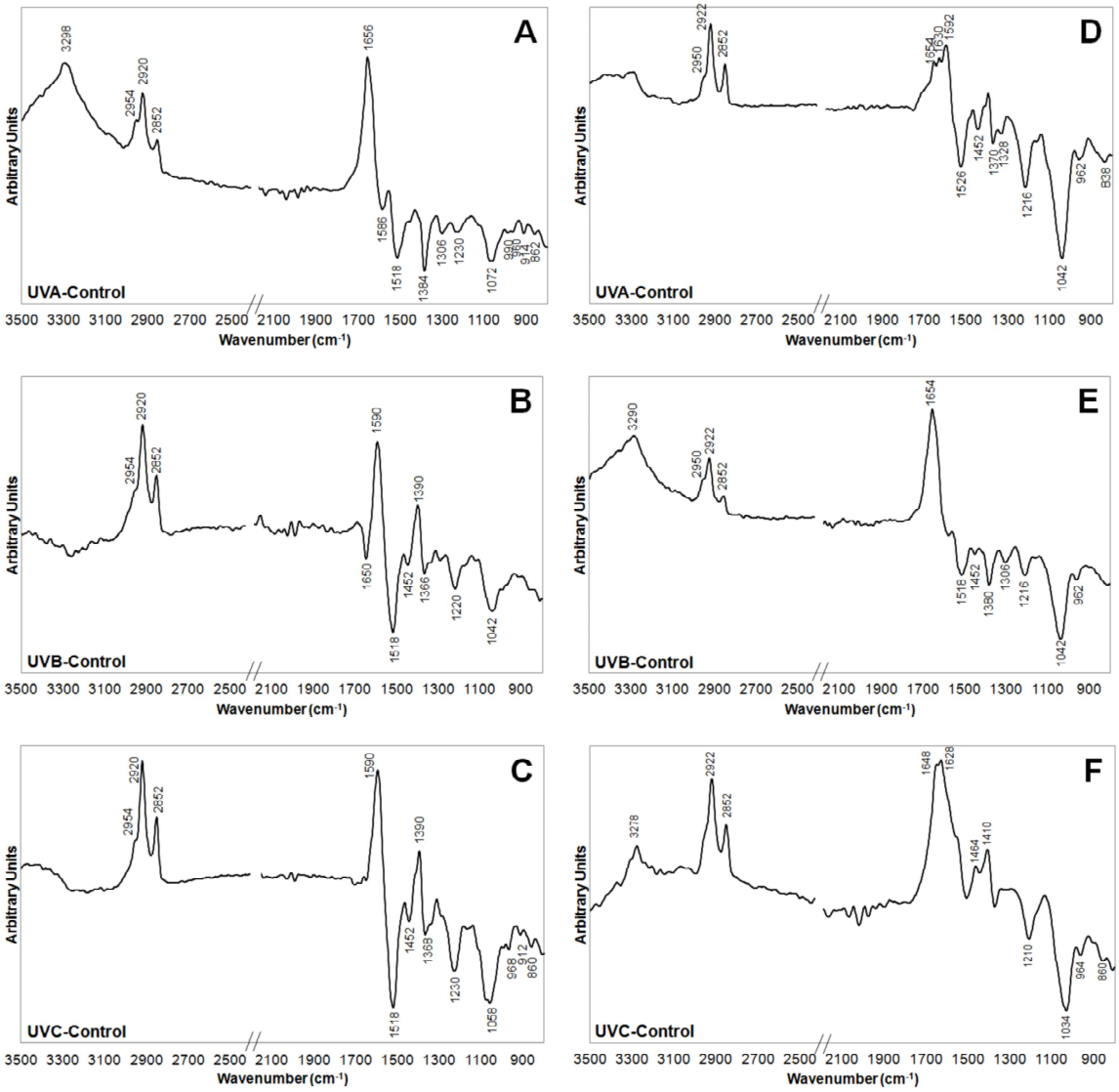

Fig. 6.4. Difference spectra (irradiated-minus-control) for the protein extracts of *Acinetobacter* sp. PT5I1.2G under UVA (A), UVB (B) and UVC (C) and *Pseudomonas* sp. NT5I1.2B under UVA (D), UVB (E) and UVC (F). A 13-point smooth was applied to the difference spectra. The region between 2400-2200 cm^{-1}, corresponding to the CO_2 region, was removed from the spectra.

Additionally, enhanced intensity of bands assigned to methyl and methylene stretching vibrations can arise as a result of the introduction of CH_3 and CH_2 groups during the process of propionylation of lysine residues (Singh et al., 2012). However, the fact that lysine is not an strong infrared absorber and that its two main bands located near 1626 cm^{-1} and 1526 cm^{-1} are hidden by the amide I and amide II bands, respectively (Barth, 2000), limits further analysis. Propionylation is involved in the regulation of the activity of some enzymes in bacteria (Garrity et al., 2007). Whether this process could play a role in the metabolic response of bacteria to UV-induced stress is unknown.

Mid-infrared spectroscopy also revealed a decrease in the intensity of bands assigned to aromatic amino acids, most notably tyrosine (1518 cm^{-1}) and tryptophan (1452 cm^{-1}) in all *Acinetobacter* sp. PT5I1.2G irradiated samples (Fig. 6.4 A-C) and in UVB-irradiated *Pseudomonas* sp. NT5I1.2B (Fig. 6.4 E). This decrease can be attributed to oxidative modifications of amino acid side chains (Lasch et al., 2001), that have also been observed upon exposure of cells to hydrogen peroxide and gamma-irradiation (Gault et al., 2005). Additionally, it is known that, at least in *Escherichia coli*, exposure to severe oxidative stress results in the inability of the cell to synthesize aromatic amino acids (Benov and Fridovich, 1999). Therefore, the observed decrease in intensity of mid-infrared bands associated with tyrosine and tryptophan can also be attributed to decreased synthesis of aromatic amino acids upon exposure to UV radiation.

UV exposure also caused a general decrease in the intensity of the main bands detected in the region between 1200-900 cm^{-1}. This spectral region comprises vibrations of amino acids, as well as sugar and phosphate moieties associated with glycosylated and phosphorylated proteins. Understanding the modifications in this region in response to UV radiation is, therefore, more difficult. Possible explanations for the observed changes in this spectral region include decreased protein phosphorylation levels, which have been found to occur in *Xanthomonas oryzae* upon UVC exposure (Huang et al., 1995) and/or decreased protein glycosylation. Protein glycosylation is known to be involved in the regulation of the activity of specific proteins, including the RecA protein which mediates the SOS response of bacteria (Fischer and Haas, 2004). Whether decreased protein glycosylation levels fulfil a physiological role in the response of bacteria to UV radiation is unknown.

A substantial increase in intensity of the N-H bands around 3300 and 1650 cm^{-1} was observed in *Acinetobacter* sp. PT5I1.2G exposed to UVA (Fig. 6.4 A) and *Pseudomonas* sp. NT5I1.2B exposed to UVB (Fig. 6.4 E), potentially denoting the accumulation of protein oxidation products, such as kynurenine which results from the oxidation of tryptophan. This is also consistent with the observed decrease in intensity of the tryptophan band at 1452 cm^{-1}. Additionally, ROS-mediated conversion of histidine to asparagine (Cabiscol et al., 2000) could also account for the increase in the intensity of N-H bands.

All irradiation treatments resulted in changes in the intensity and/or frequency of the component bands of amide I, which characterize the secondary structure of proteins, thus denoting changes in protein conformation with irradiation. Conformational changes in proteins upon UV exposure may be elicited in order to protect sensitive amino acid residues from direct UV-induced damage. For example, the proteins involved in protecting spore DNA from UV damage undergo a major conformational change upon binding to DNA (Hayes et al., 2000), which protects the protein against methionine oxidation and asparagine deamidation (Hayes and Setlow, 1997; Hayes et al., 1998). Protein conformational changes may also be involved in eliciting stress mechanisms and repair strategies, as observed in the case of the activation of the OxyR regulon which initiates the bacterial response to oxidative stress (Demple, 1991). Changes in bands characteristic of the secondary structure of proteins can also arise as a result of oxidative modifications of amino acid side chains, conformational stability alteration and/or aggregation of proteins (Lasch et al., 2001). Besides altered protein conformation due to UV-induced damage, it is also possible that synthesis of proteins with different conformation, including proteins involved in DNA repair, ROS scavenging, iron homeostasis and chaperones (Matallana-Surget et al., 2009a; Bosshard et al., 2010b), may have occurred in response to UV radiation, and contributed for the observed changes in the amide I band.

UV exposure also resulted in variable changes in the intensity of carboxylate bands. In the case of UVB- and UVC-treated *Acinetobacter* sp. PT5I1.2G, an increase in the intensity of the carboxylate bands (1590 and 1390 cm^{-1}) was observed, which can reflect the occurrence of deamidation of asparagine and glutamine. This process can alter the tertiary structure of the protein and affect its biological properties and has been associated with a number of stress conditions, including UV exposure (D'Angelo et al., 2001). *In vivo* deamidation of proteins can be used as a mechanism to initiate the

production of unique proteins of biological significance (Robinson and Robinson, 2001). Whether such mechanism could be involved in the coordination of the response of bacteria to UV radiation is unknown.

PCA analysis of the protein spectra of *Acinetobacter* sp. PT5I1.2G showed a general separation between control and UVB-treated samples (negative PC1) and UVA- and UVC-treated samples (positive PC1) (Fig. 6.5 A, B). UVA- and UVC-treated samples were characterized by enhanced intensity of the N-H band (3294 cm^{-1}) and amide I band (1652 cm^{-1}), potentially denoting the accumulation of protein oxidation products, while control and UVB-treated samples were characterized by enhanced intensity of bands assigned to the aromatic amino acid tyrosine (1518 cm^{-1}) and CH_3 deformation of amino acids (1380 cm^{-1}), as well as bands assigned to phosphorylated and/or glycosylated proteins (1084, 1064 cm^{-1}). PC2 separated UVC-treated samples from the remaining irradiation regimes and was mostly associated with enhanced intensity of CH_2 bands and carboxylate bands (1594, 1392 cm^{-1}) in UVC-treated samples, while the remaining irradiation regimes were characterized by enhanced intensity of the N-H band (3294 cm^{-1}), tyrosine band (1518 cm^{-1}) and bands assigned to phosphorylated and/or glycosylated proteins (1084, 1064 cm^{-1}).

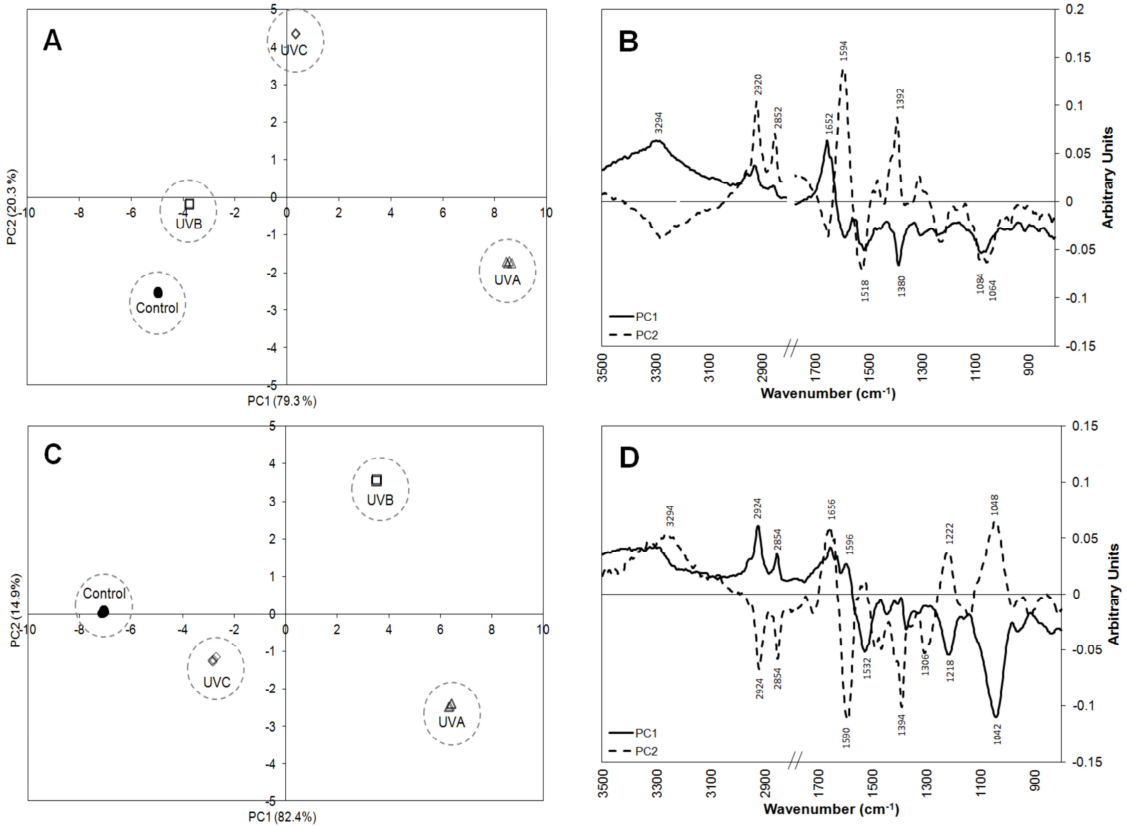

Fig. 6.5. Scores and loading plots for PCA analysis of protein extracts irradiated with different UV spectral regions of *Acinetobacter* sp. PT5I1.2G (A, B) and *Pseudomonas* sp. NT5I1.2B (C, D).

In *Pseudomonas* sp, PCA analysis showed the separation of control and UVC-treated samples (negative PC1) from UVA- and UVB-treated samples (positive PC1) (Fig. 6.5 C, D). Separation along PC1 was mostly due to bands 2924 and 2854 cm^{-1} assigned to CH_2 bands, as well as amide I (1656 cm^{-1}) and the carboxylate band at 1596 cm^{-1} which were enhanced in UVA- and UVB-treated samples. Control and UVC-treated samples showed enhanced intensity of amide II (1532 cm^{-1}), as well as enhanced intensity of bands assigned to phosphorylated and/or glycosylated proteins (1218, 1042 cm^{-1}). PC2 mostly separated UVA- and UVC-treated samples (negative PC2) from UVB-treated samples (positive PC2). Bands contributing the most for the separation along PC2 included 3294 cm^{-1} (N-H band), 1656 cm^{-1} (amide I) and bands assigned to phosphorylated and/or glycosylated proteins (1222, 1048 cm^{-1}), which were enhanced in UVB-treated samples. Bands assigned to CH_2 groups (2924, 2854 cm^{-1}) and carboxylate groups (1590 and 1394 cm^{-1}) were enhanced in UVA- and UVC-treated samples.

Taken together these results highlight the involvement of changes in protein secondary structure, aromatic amino acids, protein phosphorylation, glycosylation and/or propionylation levels, as well as the potential formation of protein oxidation products, in the effects of UV irradiation in the two bacteria.

Interspecific variability in UV effects on lipids and proteins

While, in general, the two strains tested shared common effects upon exposure to each UV spectral region, substantial differences also occurred. For example, while effects of UVA radiation on the lipids of the two strains tested were very similar, effects of UVB differed considerably, particularly in the bands corresponding to lipoproteins and/or nitrogen-containing lipids (3300, 1650, 1540 cm^{-1}) and the CH region (3000-2800 cm^{-1}). UVC effects also showed some differences between strains, particularly in the region between 1300-800 cm^{-1}. Regarding proteins, differences of the effects of each spectral region in the two strains were mostly associated to effects on the N-H band (≈ 3300 cm^{-1}), carboxylate band (≈ 1590 cm^{-1}), amide I component bands and tyrosine band (1518 cm^{-1}).

Differences in the original lipid and protein composition of the two strains can contribute to explain the different effects of each spectral region in each strain. For example, enhanced abundance of unsaturated fatty acids, highly susceptible to oxidative damage, can make bacteria more sensitive to photoreactions elicited by UV exposure (Ferreri and Chatgilialoglu, 2009). On the other hand, high abundance of aromatic

amino acids, which act as chromophores during photosensitized reactions (Pattison and Davies, 2006), might also render bacteria more susceptible to UV radiation. Alternatively, differences in the efficiency of defence mechanisms elicited to counteract the damage induced to proteins and lipids can also contribute to the differences observed in the type of damage produced by the same spectral region in the different strains. Further studies using complementary approaches to mid-infrared spectroscopy, such as mass spectrometry-based lipidomics and proteomics analysis, will help to explore the hypothesis emerging in the present study in order to gain further insights into the mechanisms of UV-based bacterial inactivation.

Conclusions

In the present work, the effects of exposure to UV radiation of different spectral regions on the lipids and proteins of two bacterial strains with distinct UV sensitivities were studied by mid-infrared spectroscopy. Exposure to UV radiation of different spectral regions caused a general increase in lipid methylation, accompanied by oxidative modifications and potentially altered lipid composition. Effects of UV radiation on proteins included changes in protein conformation and/or composition, oxidative damage to amino acid side chain residues and potentially changes in the propionylation, glycosylation and/or phosphorylation status of cellular proteins. Whether such modifications reflect UV-induced damage to biomolecules or could actually be the basis of a UV-stress response mechanism in bacteria is unknown and warrants further research.

Infrared spectroscopy was proven to be an excellent tool to study changes in bacterial components upon UV exposure, providing detailed clues to drive future studies concerning the mechanisms involved in the inactivation of bacteria by UV irradiation.

Acknowledgments

Financial support for this work was provided by Centre for Environmental and Marine Studies (CESAM) (project Pest-C/MAR/LA0017/2011), University of Aveiro and the Portuguese Foundation for Science and Technology (FCT) in the form of a PhD grant to A. L. Santos (SFRH/BD/40160/2007) and a post-Doctoral grant to I. Henriques (SFRH/BPD/63487/2009). Funding to the Organic Chemistry, Natural and Agrofood Products Research Unit (QOPNA) was provided by FCT and FEDER (European Fund for Regional Development) - COMPETE/QREN/EU (PEst UI 62-2011-2012).

PÁGINA INTENCIONALMENTE DEIXADA EM BRANCO

CHAPTER 7

Contribution of Reactive Oxygen Species to UVB-Induced Damage in Bacteria

Santos A. L., Gomes N. C. M., Henriques I., Almeida A., Correia A., Cunha A.

Journal of Photochemistry and Photobiology B: Biology **117**: 40-46

Abstract

The present work aimed to identify the reactive oxygen species (ROS) produced during UVB exposure and their biochemical targets, in a set of bacterial isolates displaying different UV susceptibilities. For that, specific exogenous ROS scavengers (catalase/CAT, superoxide dismutase/SOD, sodium azide and mannitol) were used. Biological effects were assessed from total bacterial number, colony counts and heterotrophic activity (glucose uptake and respiration). DNA strand breakage, ROS generation, oxidative damage to proteins and lipids were used as markers of oxidative stress. Sodium azide conferred a statistically significant protection in terms of lipid oxidation and cell survival, suggesting that singlet oxygen might play an important role in UVB-induced cell inactivation. Mannitol exerted a significant protection against DNA strand breakage and protein carbonylation, assigning hydroxyl radicals to DNA and protein damage. The addition of exogenous CAT and SOD significantly protected the capacity for glucose uptake and respiration, suggesting that superoxide and H_2O_2 are involved in the impairment of activity during UVB exposure. The observation that amendment with ROS scavengers can sometimes also exert a pro-oxidant effect suggests that the intracellular oxidant status of the cell ultimately determines the efficiency of antioxidant defences.

Introduction

UVB radiation represents the most cytotoxic waveband of solar radiation reaching the Earth's surface, causing several structural and physiological effects in aquatic organisms (Moran and Zepp, 2000; Bancroft et al., 2007). UVB-induced damage to biological systems has traditionally been attributed to the direct absorption of UV photons by nucleic acids, resulting in lesions (photoproducts) that block DNA replication and RNA transcription and can ultimately lead to cell death (Mitchell and Karentz, 1993). Additionally, damage can also arise indirectly via photosensitization

processes involving the absorption of UV light by an endogenous or exogenous photosensitizer (Muela et al., 2002; Bolton et al., 2010). The electronically excited sensitizer can harmlessly revert back to its ground state via intramolecular decay processes or can damage other cellular material via reactive oxygen species (ROS) (Pattison and Davies, 2006).

Cellular damage by photosensitization can occur by two major pathways, often called type I and type II mechanisms. In the type I process, the electronically excited sensitizer reacts directly with the cellular component, subtracting one electron or hydrogen atom from the cellular target, resulting in free radical formation (*e.g.*, superoxide ions and hydroxyl radicals) which initiate free radical chain reactions. Type II mechanism involves energy transfer from the sensitizer to molecular oxygen with the consequent formation of an excited state of oxygen, singlet oxygen (Pattison and Davies, 2006). As a consequence of photosensitization, several cytotoxic reactions are triggered in the cells, including disruption of cell membrane, inactivation of different enzymes and damage of DNA that can eventually lead to cell death (Luksiene, 2003; Demidova and Hamblin, 2004; Luksiene, 2005).

Several studies addressing the effects of UV radiation in aquatic bacteria have reported extensive variability in the UV sensitivity of bacteria (Joux et al., 1999; Arrieta et al., 2000; Santos et al., 2011b; Santos et al., 2012a), which can affect the structure and functioning of aquatic bacterial communities faced with changes in environmental UV levels. However, the observed variability does not seem to be supported by differences in the extent of DNA damage among different bacteria (Joux et al., 1999), suggesting that heterogeneity in susceptibility to UVB radiation could be due to differences in: (i) the type and magnitude of oxidative damage, (ii) the ability to cope with oxidative damage, and/or (iii) differences in the ROS involved in eliciting the damage in different bacteria. Furthermore, unlike DNA photoproducts, which can be effectively reversed through the process of photoreactivation, enhanced ROS production during UVB exposure and subsequent oxidative damage can have far wider consequences, since oxidative damage to biomolecules is energetically expensive to prevent and repair (Halliwell and Gutteridge, 1999). However, the identity and role of ROS involved in UVB-induced damage to different bacteria remains mostly unknown.

The objectives of this work were to ascertain the identity and the targets of ROS involved in UVB-induced damage using specific exogenous ROS scavengers and

monitoring their effects on biological and biochemical parameters in a set of phylogenetically distinct bacterial isolates with different UVB sensitivities.

Materials and methods

Bacterial isolates

The bacterial strains used in this study (Table 7.1) are representatives of the four culturable bacterial groups (*Alphaproteobacteria*, *Gammaproteobacteria*, *Actinobacteria* and Firmicutes) retrieved after irradiation of samples from the surface layers of an estuarine system (Ria de Aveiro, Portugal) (Santos et al., 2012a) and thus considered to represent the most relevant culturable members of a UV-stressed community. The isolates were grown in Marine Broth 2216 (Difco, Detroit, MI) at 25 ºC with agitation (120 rpm). In the late-exponential phase (usually achieved in 8-14 h), cells were harvested by centrifugation (3,200 x *g* for 15 min, Thermo Scientific Heraeus Pico 21 Microcentrifuge, Hamburg, Germany). Cells were washed and resuspended in 0.2-µm-pore-size-filtered autoclaved 0.9 % NaCl solution and bacterial abundance was adjusted with filtered autoclaved 0.9 % NaCl to 10^6 cells mL^{-1}. Cell suspensions (30 mL) were transferred to sterile Petri dishes (150 x 25 mm; Corning) and irradiated (without the lid) with UVB (Philips TL 100 W/01 lamps, main emission line of 302 nm). Aliquots of cell suspensions were collected at pre-determined times to construct the inactivation curves, which were used to determine the LD_{50} (UVB dose necessary for the inactivation of 50 % of bacteria). UV intensities were measured with a monochromator spectro-radiometer placed at the sample level (DM 300, Bentham Instruments, Reading, UK).

Table 7.1. Bacterial strains used in the experiments, their closest relatives, 16S rRNA gene accession number bacterial group and UVB LD_{50} values.

Strain	16S rRNA gene accession no.	Affiliation	Group	UVB LD_{50} (kJ m^{-2})
NT25I3.2AA	GQ365196	*Micrococcus* sp.	*Actinobacteria*	50.1
NT25I3.1A	GQ365195	*Paracoccus* sp.	*Alphaproteobacteria*	40.3
NT5I1.2B	GU084169	*Pseudomonas* sp.	*Gammaproteobacteria*	49.3
NT25I2.1	GQ365197	*Staphylococcus* sp.	Firmicutes	37.0

In order to identify the different ROS involved in UVB-induced damage and assess their impact on bacterial survival and activity (glucose uptake and respiration), cell suspensions were amended with the exogenous scavengers sodium azide (specific

singlet oxygen scavenger), mannitol (specific hydroxyl radical scavenger), catalase/CAT (specific hydrogen peroxide scavenger) and superoxide dismutase/SOD (specific superoxide radical scavenger). Stock solutions of antioxidants were prepared in PBS and 0.2-µm-filter-sterilized, stored and used at a final concentration of 10 mM in the cases of sodium azide and mannitol, and at a 50 U mL^{-1} concentration for SOD and 20 U mL^{-1} for CAT. These concentrations were chosen from preliminary experiments, as those that resulted in the highest reduction of intracellular ROS levels and minimal inhibition of the cells (data not shown). The cells were pre-incubated with the antioxidants for 30 min at room temperature in the dark, with agitation (120 rpm), after which cells were washed and resuspended in double distilled water (Joshi et al., 2011). Cell suspensions were irradiated at UVB LD_{50} (50.1 kJ m^{-2} for *Micrococcus* sp., 40.3 kJ m^{-2} for *Paracoccus* sp., 49.3 kJ m^{-2} for *Pseudomonas* sp. and 37.0 kJ m^{-2} for *Staphylococcus* sp.) (Table 7.1). Aliquots for biological and biochemical analysis were collected before and after irradiation. During irradiation, temperature was kept at 25 ºC. Non-irradiated dark controls (cell suspensions unamended and amended with each tested scavenger), otherwise treated in the same way as the irradiated samples, were included in every experiment.

For the determination of protein content and protein carbonyl levels, cell homogenates were prepared by collecting cells by centrifugation immediately after irradiation, resuspending them in cold 50 mM potassium phosphate buffer (pH 7.8) containing 1 mM EDTA, followed by sonication in ice (Branson Instruments Co. Sonifier, Stamford, Conn.; 2 min, 30-s pulses, 1-min cooling). Homogenates were stored at -80 ºC until the measurements. All experiments were repeated in three independent assays. Parameters were always determined in a minimum of three analytical replicates. Positive (H_2O_2-treated) and negative (untreated) controls were always included and processed along experimental samples in order to ensure proper functioning of the procedures.

Colony counts

Before and after each treatment, sample aliquots were serially-diluted in filter-sterilized, autoclaved 0.9 % NaCl and spread-plated in triplicate on marine agar 2216 plates (Difco, Detroit, MI). The number of colony forming units per mL (CFU mL^{-1}) was counted after 3 days of incubation at 25 ºC in the dark. The dilution and plating

procedures were carried out under low-luminosity conditions to minimize photoreactivation.

Total bacterial number (TBN)

For the determination of total bacterial numbers, samples were filtered through 0.2-µm-pore-size black polycarbonate membranes (Poretics, Livermore, CA, USA), and stained with 0.03 % (w/v) acridine orange (Hobbie et al., 1977). Cells were counted by epifluorescence microscopy using a Leitz Laborlux K microscope (Leitz Meβtechnik, Wetzlar, Germany) equipped with a I 2/3 filter for blue light. At least 200 cells or 20 microscope fields were counted in each of three replicate membranes.

Glucose incorporation and respiration

The effects of UV radiation on bacterial activity were estimated from glucose incorporation and respiration. Triplicate 10 mL aliquots of bacterial suspension plus a 2 % (vol/vol) formalin-fixed control were incubated with [^{14}C]glucose (Amersham Biosciences, Buckinghamshire, UK; SA 310 mCi mmol^{-1}). The tracer concentration was 8.1 nM. Samples were incubated in the dark at room temperature for 2 h, after which incubations were stopped by adding 2 % formalin (vol/vol) (Sigma, St. Louis, MO, USA). Samples for glucose incorporation were filtered through nitrocellulose filters (0.2-µm-pore-size; Millipore, Tokyo, Japan) and rinsed three times with chilled 5 % trichloroacetic acid. For the determination of bacterial respiration, samples were transferred to respiration bottles to which 200 µL of 5 N HCl were added to drive out the $^{14}CO_2$. A strip of filter paper saturated with 200 µL of ethanolamine was suspended above the sample in the respiration bottle and used to absorb the emitted $^{14}CO_2$ over a period of 24 h. The efficiency of ^{14}C recovery was determined from a similar volume of water treated with [^{14}C]bicarbonate. Nitrocellulose filters and paper filters from incorporation and respiration experiments, respectively, were then transferred to mini-vials to which a volume of 1.5 mL of Universol liquid scintillation cocktail (ICN Biomedicals, USA) was added. The radioactivity incorporated into bacterial cells was counted in a Beckman LS 6000 IC liquid scintillation counter (Beckman Instruments, Inc., Fullerton, CA) (Gocke, 1977).

Intracellular ROS production

Intracellular ROS production was detected using the probe 2',7'-dichlorodihydrofluorescein diacetate (DCFH-DA, Cayman Chemical Co. Ltd., MI, USA) (Pérez et al., 2007). Control and irradiated cell suspensions were centrifuged and washed with 10 mM potassium phosphate buffer (pH 7.0), amended with the probe diluted in the same buffer (final concentration 10 µM), and incubated for 30 min in the dark. Cells were subsequently washed, sonicated and 100 µL of the cell extracts were mixed with 1 mL of the potassium phosphate buffer. The fluorescence of the samples was measured with a Jasco FP-777 Fluorometer (Japan Spectroscopic Co., Ltd., Tokyo, Japan) at room temperature, with an excitation wavelength of 490 nm and emission wavelength of 519 nm. The fluorescence intensity at 519 nm was corrected against blank controls (cell-free suspensions) and then normalized to protein content (see below for procedure) and compared with the values obtained before irradiation. Unless otherwise specified, all reagents were purchased from Sigma-Aldrich (St Louis, MO). Results were expressed per mg of protein.

DNA strand breakage

UV-induced DNA damage was assessed by the quantification of DNA strand breaks (DSB) using a modified version of the FADU (Fluorimetric Analysis of DNA Unwinding) method, as described by He and Häder (2002). In addition to the test samples (so-called P-samples), the method requires two sets of untreated control samples: samples not subjected to alkaline unwinding (T-samples) and samples subjected to complete alkaline unwinding (B-samples). Cells were collected by centrifugation (3,000 g, 15 min) and digested with lysozyme (4 mg mL^{-1} final concentration) in EDTA solution, followed by proteinase K (0.25 mg mL^{-1} final concentration). A volume of 300 µL of 0.1 M NaOH was added to the three sets of samples: (1) T-samples were neutralized with 300 µL of 0.1 M HCl and sonicated for 15 s, following a 30 min incubation at room temperature; (2) B-samples were sonicated for 2 min, neutralized with 300 µL of 0.1 M HCl after a 30 min incubation and sonicated again for 15 s; and (3) P-samples were incubated for 30 min, neutralized with 300 µL of 0.1 M HCl and sonicated for 15 s.

A final concentration of 5 µM of Hoechst 33258 was added to all samples and after centrifugation, a 1 mL volume of supernatant was used for the fluorescence measurements (λ_{ex}. 350 nm; λ_{em}. 450 nm) in a Jasco FP-777 Fluorometer (Japan

Spectroscopic Co., Ltd., Tokyo, Japan). The fraction of double stranded DNA (dsDNA) was calculated as dsDNA = (P−B)/(T−B)×100, where T, P and B were fluorescence intensities of T-, P- and B-samples normalized to the protein content, respectively (He and Häder, 2002). All reagents were purchased from Sigma-Aldrich (St Louis, MO).

Lipid peroxidation

Lipid peroxidation was determined as the amount of thiobarbituric acid reactive substances (TBARS) as described by Pérez et al. (2007). Control and irradiated cells were centrifuged, washed, and suspended in 1 mL of 50 mM potassium phosphate buffer (pH 7.4) added of 0.1 mM butylated hydroxytoluene and 1 mM PMSF (phenylmethanesulfonyl fluoride). After sonication and centrifugation in order to remove cellular debris, the soluble fraction was mixed with 1 mL of 20 % trichloroacetic acid and centrifuged at 10,000 x *g* for 5 min. The supernatant was transferred to a new microtube and mixed with 1 mL of 0.5 % (w/v) thiobarbituric acid in 0.1 M HCl and 10 mM butylated hydroxytoluene. Samples were heated at 100 ºC for 1 h, after which 1 mL aliquots were removed, cooled and then mixed with 1.5 mL of butanol. After centrifugation (4,000 x *g*, 10 min), the organic fraction was removed and the absorbance at 535 nm was read in a Thermo Spectronic Genesys 10 UV spectrophotometer. TBARS content was determined by the extinction coefficient of 156 $mM^{-1}cm^{-1}$. All reagents were purchased from Sigma-Aldrich (St Louis, MO). Results were expressed per mg of protein.

Protein oxidation

The carbonyl content in oxidized proteins was determined according to Semchyshyn et al. (2005). Aliquots of homogenates were incubated for 1 h at room temperature with 10 mM dinitrophenylhydrazine (DNPH) in 2 M HCl. DNPH was omitted in the blanks. Proteins were precipitated with 500 µL of 20 % trichloroacetic acid, centrifuged (14,000 x *g*, 5 min) and the pellet was washed three times with 1 mL of 1:1 (vol/vol) ethanol-ethyl acetate. The final precipitate was dissolved in 1 mL of 6 M guanidine hydrochloride. Samples were spectrophotometrically analyzed against a blank of 1 mL of guanidine solution (6 M guanidine hydrochloride with 2 mM potassium phosphate). The absorbance at 360 nm was determined and the molar absorption coefficient of 22 $mM^{-1}cm^{-1}$ was used to quantify the levels of protein

carbonyls. All reagents were purchased from Sigma-Aldrich (St Louis, MO). Results were expressed per mg of protein.

Protein concentration

Protein concentration in cell homogenates was determined by the Bradford method using BSA as a standard (Bradford, 1976).

Statistical analysis

All experiments were repeated in three independent assays and biochemical and microbiological analysis were always conducted in triplicate. Differences between the treatments with and without scavengers were assessed by 1-way ANOVA using the statistical software SPSS v.17. Levene test was used to assess homogeneity of variances. If variances were not homogeneous, the natural logarithm transformation was applied. If variances were still not homogenous, the non-parametric Mann-Whitney test was used to assess the overall effect of treatment (Sokal and Rolf, 1995).

Results

Sodium azide significantly attenuated the reduction in colony counts upon irradiation in all strains tested (1-way ANOVA, $p < 0.05$), from 16.2 % to 45.8 %. Pre-treatment of bacterial cell suspensions with CAT, SOD, or mannitol did not significantly affect survival during UVB exposure in any of the strains tested (Fig. 7.1 A). Sodium azide was also the only scavenger to mitigate the UVB reduction in total bacterial number, by up to 32.2 %, in all of the strains tested (Fig. 7.1 B).

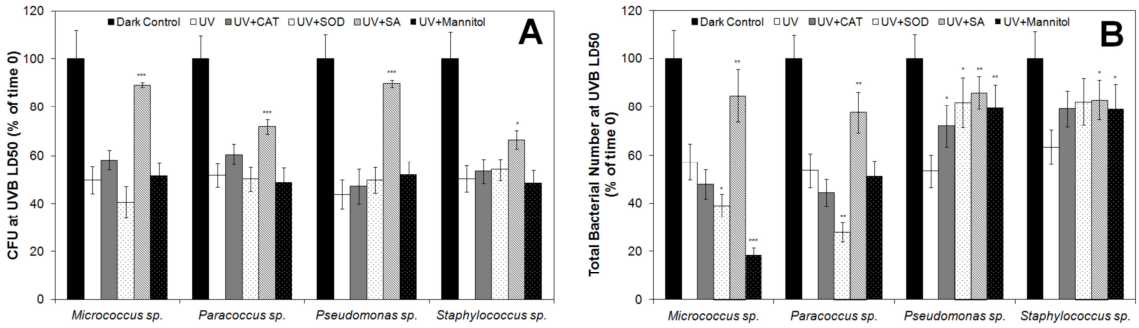

Fig. 7.1. Effects of UVB exposure in (A) colony forming units (CFU) and (B) total bacterial number, in the presence and absence of different ROS scavengers. Results are expressed as % of the initial values. Mean values (n = 9) were plotted. Error bars represent standard deviations. Absence of error bars indicates that standard deviations are too small to see on the scale used. Asterisks denote the significance of the differences between scavenger-amended and unamended samples. *** - $p < 0.005$, ** - $p < 0.01$, * - $p < 0.05$. CAT – catalase. SOD – superoxide dismutase. SA – sodium azide.

Amendment with CAT significantly (1-way ANOVA, $p < 0.05$) attenuated the inhibition of bacterial activity by UVB in all the strains tested, from 14.1 % to 49.6 %. SOD also exerted a significant protective effect against UVB-induced inhibition of bacterial activity in all strains tested ranging from 14.6 % to 55.4 %. Mannitol exerted a similar protective effect against UVB inhibition of bacterial activity ranging from 17.1 % to 52.4 %. Effects of sodium azide ranged from a 31.4 % exacerbation to a 53.2 % attenuation of the detrimental effects of UVB on activity (Fig. 7.2 A). CAT and SOD also significantly attenuated the inhibition of glucose respiration in all the strains tested, by up to 48.6 % and 50.3 %, respectively (Fig. 7.2 B).

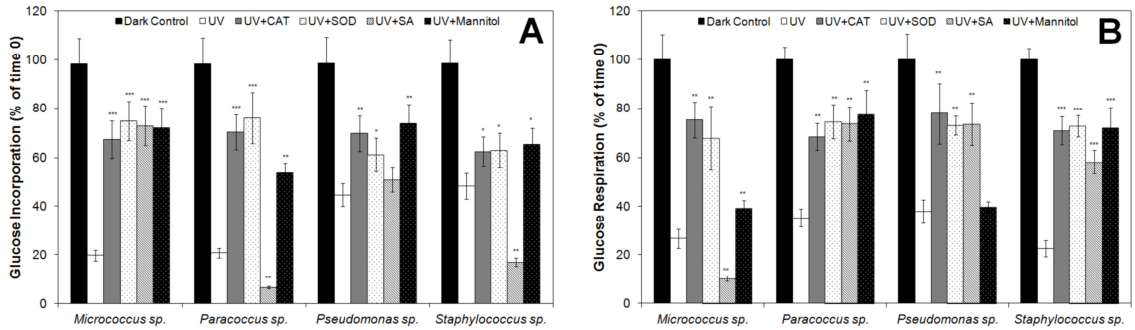

Fig. 7.2. Effects of UVB exposure in (A) glucose incorporation and (B) respiration in the presence and absence of different ROS scavengers. Results are expressed as % of the initial values. Mean values (n = 9) were plotted. Error bars represent standard deviations. Absence of error bars indicates that standard deviations are too small to see on the scale used. Asterisks denote the significance of the differences between scavenger-amended and unamended samples. *** - $p < 0.005$, ** - $p < 0.01$, * - $p < 0.05$. CAT – catalase. SOD – superoxide dismutase. SA – sodium azide.

Sodium azide significantly (1-way ANOVA, $p < 0.05$) attenuated ROS generation during UVB exposure in all strains ranging from 6.3 % to 20.8 %. A similar effect was observed in mannitol-amended cells, which displayed a 5.3 % to 40.2 % reduction in ROS generation during UVB exposure, compared to unamended cells. Effects of amendment with CAT ranged from a 13.7 % attenuation to a 4.9 % increase in ROS generation during irradiation, while amendment with SOD either did not significantly affect ROS generation or resulted in a 17.6 % increase in ROS levels under UVB (Fig. 7.3).

Amendment of cell suspensions with mannitol significantly (1-way ANOVA, $p < 0.05$) attenuated the formation of DSB during UVB exposure in all strains tested, from 2.2 % to 10.0 %. Amendment with CAT increased DSB from 6.3 to 15.7 % (1-way ANOVA, $p < 0.05$). Pre-treatment of cells with SOD also increased DNA damage during UVB exposure from 6.4 to 13.8 % (1-way ANOVA, $p < 0.05$). Sodium azide

either had no significant effect or increased DSB during irradiation by up to 9.2 % (Fig. 7.4).

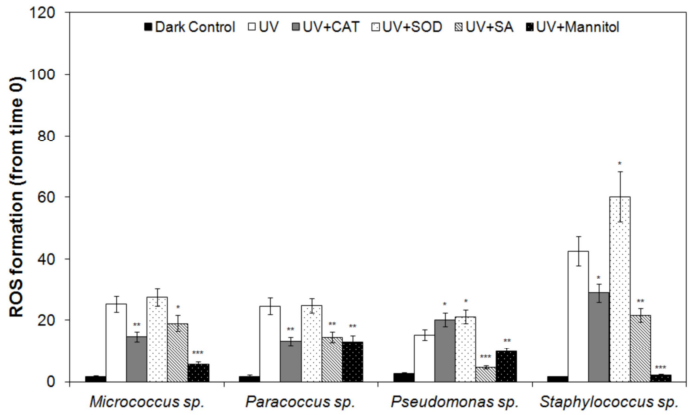

Fig. 7.3. Effects of UVB exposure in ROS generation in the presence and absence of different ROS scavengers. Results are expressed as % of the initial values. Mean values (n = 9) were plotted. Error bars represent standard deviations. Absence of error bars indicates that standard deviations are too small to see on the scale used. Asterisks denote the significance of the differences between scavenger-amended and unamended samples. *** - $p < 0.005$, ** - $p < 0.01$, * - $p < 0.05$. CAT – catalase. SOD – superoxide dismutase. SA – sodium azide.

Sodium azide significantly (1-way ANOVA, $p < 0.05$) decreased TBARS generation upon UVB exposure from 8.5 % to 21.7 %. Effects of amendment with CAT ranged from a 26.7 % attenuation to a 18.8 % increase of TBARS levels during irradiation. Pre-treatment of cells with SOD also resulted in variable effects on lipid peroxidation during UVB irradiation, ranging from a 25.1 % attenuation to a 27.2 % increase, while in mannitol-amended cells TBARS levels were either decreased by up to 17.5 % or increased by up to 24.1 % (Fig. 7.5).

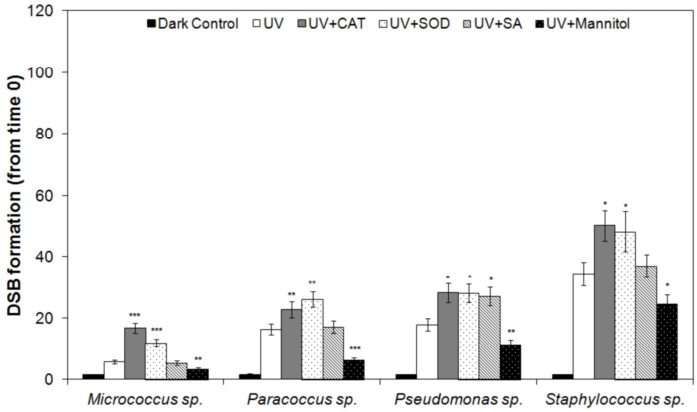

Fig. 7.4. Effects of UVB exposure in DSB levels in the presence and absence of different ROS scavengers. Results are expressed as % of the initial values. Mean values (n = 9) were plotted. Error bars represent standard deviations. Absence of error bars indicates that standard deviations are too small to see on the scale used. Asterisks denote the significance of the differences between scavenger-amended and unamended samples. *** - $p < 0.005$, ** - $p < 0.01$, * - $p < 0.05$. CAT – catalase. SOD – superoxide dismutase. SA – sodium azide.

Mannitol significantly (1-way ANOVA, $p < 0.05$) attenuated protein carbonyl levels during UVB exposure in all strains tested, ranging from 4.4 % to 23.1 %. CAT amendment either had no significant effect or increased carbonyl levels by up to 13.6 %. Effects of amendment with SOD ranged from a 33.3 % attenuation to a 66.7 % increase (Fig. 7.6). In sodium azide-amended cells protein carbonyl levels were either decreased by up to 17.5 % or increased by up to 53.5 % (Fig. 7.6).

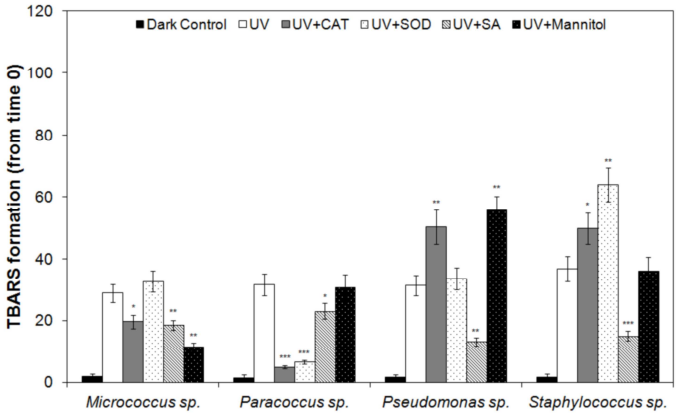

Fig. 7.5. Effects of UVB exposure in TBARS levels in the presence and absence of different ROS scavengers. Results are expressed as % of the initial values. Mean values (n = 9) were plotted. Error bars represent standard deviations. Absence of error bars indicates that standard deviations are too small to see on the scale used. Asterisks denote the significance of the differences between scavenger-amended and unamended samples. *** - $p < 0.005$, ** - $p < 0.01$, * - $p < 0.05$. CAT – catalase. SOD – superoxide dismutase. SA – sodium azide.

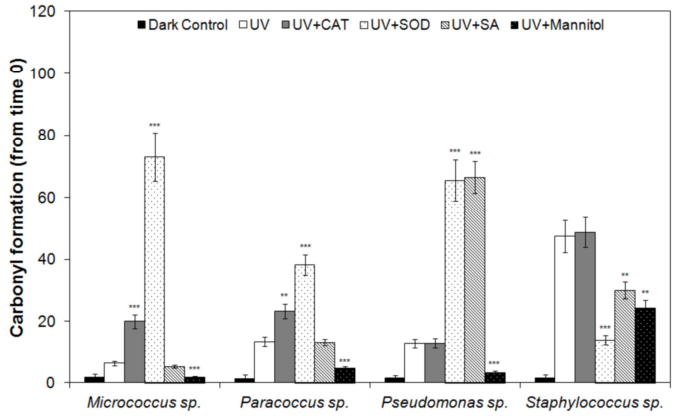

Fig. 7.6. Effects of UVB exposure in protein carbonyls levels in the presence and absence of different ROS scavengers. Results are expressed as % of the initial values. Mean values (n = 9) were plotted. Error bars represent standard deviations. Absence of error bars indicates that standard deviations are too small to see on the scale used. Asterisks denote the significance of the differences between scavenger-amended and unamended samples. *** - $p < 0.005$, ** - $p < 0.01$, * - $p < 0.05$. CAT – catalase. SOD – superoxide dismutase. SA – sodium azide.

Discussion

Solar radiation elicits a complex chain of cellular events in microorganisms, which are not yet fully understood. Oxidative damage induced by increased ROS

generation is an important outcome of the exposure of bacteria to UVB radiation and can actually be a more prominent threat to microorganisms than direct DNA damage (Halliwell and Gutteridge, 1999). Yet, information on the role of UVB-induced ROS in biological and biochemical damage to bacteria is rather scarce and mostly obtained indirectly from transcriptomic and proteomic studies reporting the induction of antioxidant defences upon exposure of bacteria to UVB radiation (Qiu et al., 2005a; Matallana-Surget et al., 2009a).

In the present work, the involvement and targets of ROS in UVB-induced damage was investigated in a direct experimental approach using specific scavengers for different ROS (hydroxyl radical, hydrogen peroxide, singlet oxygen and superoxide radical) and assessing the effects on biological and biochemical parameters. A set of isolates with distinct UV sensitivities, isolated after irradiation of estuarine surface water samples, were used as tentative representatives of the culturable fraction of a UV-stressed community. Therefore, their responses can provide insights into the mechanisms by which global changes, such as changes in UVB levels, are affecting the functions of bacterial mixed communities and may impact biogeochemical cycles.

The effects of ROS scavengers on biological and biochemical parameters were variable among the different isolates tested. In the present work, two Gram-positive (*Micrococcus* sp. and *Staphylococcus* sp.) and two Gram-negative (*Paracoccus* sp. and *Pseudomonas* sp.) phylogenetically distinct bacterial isolates were used. Due to their cell wall characteristics, Gram-positive bacteria have been proposed to be more resistant to UV radiation than Gram-negative strains (Jagger, 1985). However, significant fundamental differences in neither UVB sensitivity, nor in the responses to amendment with different scavengers, between Gram-positive and Gram-negative bacteria were observed, in accordance with previous works (Agogué et al., 2005).

Singlet oxygen

Sodium azide exerted a significant protective effect on culturable and total bacterial abundance (1-way ANOVA, $p < 0.05$) during UVB exposure. Singlet oxygen also protected against lipid peroxidation (1-way ANOVA, $p < 0.05$) during irradiation. These results suggest that singlet oxygen ($^1O_2$) is an important mediator of UVB-induced cell inactivation, in which lipid oxidation probably plays an important role. Previous studies had already demonstrated the ability of $^1O_2$ to react with the double

bond of unsaturated fatty acids leading to the formation of lipid hydroperoxides (Vile and Tyrrell, 1995).

Hydroxyl radical

The observation that mannitol was the only scavenger that significantly reduced the amount of DSB during UVB exposure confirms the involvement of hydroxyl radical ($^{\bullet}OH$) in DNA damage, in accordance with previous observations (Peak and Peak, 1990). Mannitol was also able to significantly attenuate protein carbonylation during UVB exposure, suggesting the importance of the hydroxyl radical in protein oxidative damage during UVB exposure.

In the cell, the hydroxyl radical can be formed via the Fenton reaction in which the divalent metal ions Fe^{2+} or Cu^{+} catalyze the degradation of hydrogen peroxide (Bast et al., 1991; Koppenol, 2001), according to the reaction:

$$H_2O_2 + Fe^{2+} \rightarrow OH^- + Fe^{3+} + {}^{\bullet}OH$$

To a lesser extent, the hydroxyl radical can also be formed via the Haber-Weiss reaction in which superoxide reduces Fe^{2+} or Cu^{+}, which can subsequently combine with hydrogen peroxide to form the hydroxyl radical (Kehrer, 2000)

$$O_2^{\bullet -} + H_2O_2 \rightarrow {}^{\bullet}OH + OH^- + O_2$$

Additionally, the hydroxyl radical can also be formed by metal-independent processes, as a result of the decomposition of peroxynitrite, an oxidant formed by combination between nitric oxide and the superoxide radical (Hogg et al., 1992).

The extremely short half-life of the hydroxyl radical limits its reactivity to the immediate vicinity from where it is formed. Therefore, Fe-S clusters of proteins and enzymes using iron as prosthetic metal are major targets of oxidative damage by the hydroxyl radical (Imlay, 2006). Iron bound to DNA can also catalyze the formation of the hydroxyl radical which then attacks DNA bases or the deoxyribosyl backbone of DNA to produce damaged bases or strand breaks (Imlay et al., 1988).

Superoxide and hydrogen peroxide

Glucose incorporation and respiration were effectively protected from UVB by amendment with exogenous CAT and SOD, suggesting that superoxide and/or hydrogen peroxide are involved in the impairment of bacterial activity. Glucose incorporation was also protected by amendment with mannitol, suggesting a role of the hydroxyl radical in the impairment of membrane processes. The auto-oxidation of flavoenzymes is

probably the predominant endogenous source of both $O_2^{\bullet-}$ and H_2O_2 (Imlay, 2003), but the activity of SOD itself is also an important source of H_2O_2 (Buettner et al., 2006). Detrimental effects of H_2O_2 could be related to its ability to directly oxidize and thus alter the activity of proteins containing deprotonated cysteine residues (Pattison and Davies, 2006). Superoxide oxidizes and inactivates proteins containing Fe-S clusters, such as respiratory chain proteins of the membrane, releasing Fe^{2+} ions and hydrogen peroxide that can further produce the highly toxic hydroxyl radical by the Fenton reaction. The resulting hydroxyl radical is very reactive and therefore preferentially affects the neighbourhood in which it is generated, compromising membrane integrity and the function of membrane transport proteins (Girotti and Giacomoni, 2007).

Role of antioxidant defences in UVB-induced damage

The antioxidant status is an important determinant of the magnitude of UVB-induced oxidative injuries, with SOD and CAT usually considered as the first line of defence of cells against ROS (Apel and Hirt, 2004). However, in some cases amendment with ROS scavengers exacerbated the detrimental effect of UVB radiation on biological parameters. Such effect was not attributed to toxicity of the scavenger, since significant differences between dark controls without scavenger and dark controls amended with every scavenger tested were not found for any of the biological and biochemical parameters tested (1-way ANOVA, $p > 0.05$). In particular, a statistically significant increase in the amount of DSB was observed in SOD- and CAT-amended samples, suggesting that the activity of these enzymes can contribute to oxidative damage to biomolecules during exposure to UVB. It is well established that CAT is involved in the degradation of hydrogen peroxide and a potentially protective role of CAT in UV resistance among *Acinetobacter* sp. isolates was recently proposed (Di Capua et al., 2011). However, when intracellular antioxidant moieties are limited, CAT activity can generate ROS during UVB exposure (Heck et al., 2003; Heck et al., 2010). SOD can also increase the oxidative burden of the cell since hydrogen peroxide generated from its activity is a more oxidant species than superoxide (Scott et al., 1989). Ultimately, depending of the intracellular oxidation status, the activity of these antioxidant enzymes in response to UVB light can be either protective or cytotoxic.

Conclusions

The present work identifies an important role of singlet oxygen in UVB-induced cell inactivation, potentially by mediating oxidative damage to lipids, as suggested by attenuation of the reduction in cell abundance (culturable and total) and TBARS levels in sodium azide-amended samples. DNA strand breakage and protein carbonylation during UVB exposure were attenuated in samples amended with mannitol, suggesting the involvement of the hydroxyl radical in DNA and protein damage. Superoxide and hydrogen peroxide could play important roles in impairment of membrane transport and respiration during UVB exposure.

Acknowledgments

Acknowledgments are due to the two anonymous reviewers whose insightful comments and suggestions contributed to improve the original manuscript. We also acknowledge Attila Köfalvi and Caroline Veloso at the Center for Neurosciences and Cell Biology of the University of Coimbra for providing access to the scintillation counter. Financial support for this work was provided by CESAM (Centre for Environmental and Marine Studies, University of Aveiro) and the Portuguese Foundation for Science and Technology (FCT) in the form of a PhD grant to A.L. Santos (SFRH/BD/40160/2007) and a post-Doctoral grant to I. Henriques (SFRH/BPD/63487/2009).

PÁGINA INTENCIONALMENTE DEIXADA EM BRANCO

CHAPTER 8

Role of Transition Metals in UVB-Induced Damage to Bacteria

Santos A. L., Gomes N. C. M., Henriques I., Almeida A., Correia A., Cunha A.

Photochemistry and Photobiology (accepted)

Abstract

The purpose of this study was to explore the possible link between metals and UVB-induced damage in bacteria. The effect of growth in the presence of enhanced concentrations of different transition metals (Co, Cu, Fe, Mn and Zn) on UVB sensitivity of a set of bacterial isolates was explored in terms of survival, activity and oxidative stress biomarkers (ROS generation, damage to DNA, lipid and proteins, and activity of antioxidant enzymes). Metal amendment, particularly Fe, Cu and Mn, enhanced bacterial inactivation during irradiation by up to 35.8 %. Amendment with Fe increased ROS generation during irradiation by 1.2 %-13.3 %, DNA damage by 10.8 %-37.4 % and lipid oxidative damage by 9.6 %-68.7 %. Lipid damage during irradiation also increased after incubation with Cu and Co by up to 66.8 % and 56.5 %, respectively. Mn amendment decreased protein carbonylation during irradiation by up to 44.2 %. These results reveal a role of Fe, Co, Cu and Mn in UVB-induced bacterial inactivation and the importance of metal homeostasis to limit the detrimental effects of ROS generated during irradiation.

Introduction

UVB radiation (280-320 nm) is the most detrimental wavelength of the solar radiation spectrum. The severest biological consequence of UVB radiation has been traditionally considered to be DNA damage, most notably the formation of DNA photoproducts (Häder and Sinha, 2005). However, UVB induced cell damage can also arise as the result of increased production of reactive oxygen species (ROS) during irradiation and subsequent oxidative damage to biomolecules (Halliwell and Gutteridge, 1999). Studies reporting the induction of antioxidant defences during UVB exposure of bacteria support the hypothesis of the contribution of oxidative stress to UVB-induced damage (Qiu et al., 2005a; Matallana-Surget et al., 2009a). The cellular and biological consequences of ROS are strongly influenced by metal ion homeostasis (Halliwell and

Gutteridge, 1999). Metal ions, most notably iron (Fe^{2+}) and copper (Cu^{+}), play a catalytic role in the generation of ROS through participation in Fenton and Haber-Weiss reactions that generate toxic hydroxyl radicals that can damage biomolecules and cause cell death (Wardman and Candeias, 1996). Since many of the respiratory chain proteins use iron as a cofactor, they are among the first targets of oxidative damage through the Fenton reaction (Choksi et al., 2008). The hydroxyl radicals generated in the process can in turn attack membrane lipids and other membrane proteins (Bourdon and Blache, 2001; Niki et al., 2005). On the other hand, cobalt (Co^{2+}) can compete directly with iron, thereby affecting the synthesis of Fe-S clusters (Ranquet et al., 2007; Thorgersen and Downs, 2007), leading to decreased iron bioavailability and eventually oxidative stress (Fantino et al., 2010).

Recently, a possible protective role of transition metal ions against ionizing radiation has been discussed. A high capacity for intracellular copper ion sequestration was detected in *Kineococcus radiotolerans* (Domain Bacteria, Phylum Actinobacteria) that provided protection against the damaging effects of ionizing radiation (Bagwell et al., 2008). Manganese (Mn^{2+}) ions also seem to play a role in the prevention of oxidative damage during exposure to different types of stress including UVC radiation, gamma-irradiation, wet and dry heat and H_2O_2 (Daly et al., 2007; Barnese et al., 2008; McEwan, 2009; Daly et al., 2010; McNaughton et al., 2010; Slade and Radman, 2011). Zinc (Zn^{2+}) uptake is also a key component of the adaptive response to peroxide stress (Gaballa and Helmann, 2002), protecting copper-treated *Escherichia coli* against superoxide killing (Korbashi et al., 1989) and countering the effects of oxidative stress in *Lactococcus lactis* (Scott et al., 2000).

Increased levels of proteins involved in iron homeostasis, induction of iron-sequestering protein-encoding genes and repression of genes involved in iron uptake have been observed in bacteria irradiated with UVB (Qiu et al., 2005a; Matallana-Surget et al., 2009a), suggesting the importance of regulation of the intracellular iron ion pool following UVB exposure. However, whether certain transition metal ions play a physiological role in bacterial resistance to environmentally relevant UV radiation, most notably UVB radiation, remains uncertain. This information is critical to understanding the effects of UV radiation on the ecological context of natural communities, where these metals can be particularly enriched when industries and agriculture facilities are located nearby (Zhou et al., 2008). Furthermore, understanding the role that metals play during UV-induced bacterial inactivation can help develop

more efficient photocatalytic disinfection strategies (Sciacca et al., 2010). Accordingly, the objectives of this study were to investigate the potential synergistic effects of transition metals and exposure to UVB radiation in bacterial cells and evaluate their potential protective role against structural and functional cellular damage elicited during UVB exposure in a set of bacterial isolates.

Materials and methods

Culture conditions and experimental layout

The bacterial strains used in the present study were previously isolated from the surface waters of an estuarine system. The isolates are affiliated to different phylogenetic groups: *Alphaproteobacteria* (*Paracoccus* sp.), *Gammaproteobacteria* (*Pseudomonas* sp.), *Bacilli* (*Staphylococcus* sp.) and *Actinobacteria* (*Micrococcus* sp.) and display different UVB sensitivities (Santos et al., 2011), which are presented in Table 8.1 as LD_{50} values (UVB dose necessary for the inactivation of 50 % of bacteria).

Stock solutions (10 mM) of various transition metals (Co, Cu, Fe, Mn and Zn) were prepared in deionized, filter-sterilized water from the corresponding metallic salts: ferrous ammonium sulfate, manganese chloride, zinc sulfate, cupric sulfate and cobalt sulfate. In order to select the metal concentration that affected the least the growth curve of the different bacterial strains, and that was subsequently used for UV exposure assays, preliminary experiments were conducted with different metal concentrations (1 µM, 10 µM, 100 µM) in TGY medium (1.0 % tryptone, 0.1 % glucose, 0.5 % yeast extract) (Bagwell et al., 2008). Growth curves obtained in these conditions were compared with those obtained in the absence of added metals. Cultures were incubated for up to 72 h at 25 ºC with agitation (120 rpm). At pre-determined intervals, triplicate aliquots were collected and the optical density (OD) at 600 nm was determined.

Table 8.1. Bacterial strains used in the experiments, their closest relatives, accession number and bacterial group and UVB LD_{50} values. Non-significant differences in LD_{50} values of metal-amended treatments compared to unamended samples are indicated by n.s.

Strain	Closest relative	Accession no.	Group	LD_{50}(kJ m^{-2})					
				UVB	+Co	+Cu	+ Fe	+Mn	+Zn
NT25I3.2AA	*Micrococcus* sp.	GQ365196	*Actinobacteria*	50.1	48.9$^{n.s.}$	42.0	43.1	40.1	42.5
NT25I3.1A	*Paracoccus* sp.	GQ365195	*Alphaproteobacteria*	40.3	35.6	29.8	35.4	29.1	39.9$^{n.s.}$
NT5I1.2B	*Pseudomonas* sp.	GU084169	*Gammaproteobacteria*	49.3	42.0	27.9	30.1	29.0	40.5
NT25I2.1	*Staphylococcus* sp.	GQ365197	*Bacilli*	37.0	38.7$^{n.s.}$	32.5	30.7	33.8	39.0$^{n.s.}$

From the results of the preliminary experiments, 1 µM was found to be the maximum non-inhibitory concentration for all metals (see results sections) and used in the UV irradiation assays. Liquid cultures of each isolate were grown to mid-exponential phase (OD_{600} of 0.2-0.3) in TGY or TGY amended with 1 µM of Co, Cu, Fe, Mn or Zn. Cells were harvested by centrifugation (3,200 x *g* for 15 min, Eppendorf Centrifuge 5415R, Hamburg, Germany) and the pellet was washed three times with 50 mM EDTA/ 10 mM Phosphate Buffered Saline (PBS; pH 7.5) to remove cell surface-adsorbed transition metals (Bagwell et al., 2008). Cells were then resuspended in 10 mM PBS for determination of bacterial abundance by epifluorescence microscopy (Hobbie et al., 1977), and adjusted to 10^6 cells mL^{-1} with 10 mM PBS. A convenient volume of cell suspension was transferred to sterile 150 x 25 mm plastic tissue culture dishes (Corning Science Products, Corning, NY, USA) so that the depth of the liquid was < 2 mm. The lid was removed from the culture during UVB irradiation (Philips TL 100 W/01 lamps, main emission wavelength line of 302 nm). Metal-amended and unamended dark controls (covered in aluminum foil) treated in the same way as the irradiated samples were included in every experiment. Inactivation curves of bacterial strains under the different metal-amended and unamended regimes were determined by irradiating bacterial suspensions under UVB for a total light dose of 60 kJ m^{-2} and collecting aliquots at pre-determined light doses for CFU determination, as described below. UV intensities were measured with a monochromator spectro-radiometer placed at the sample level (DM 300, Bentham Instruments, Reading, UK). Inactivation curves were used to determine the LD_{50} in metal-amended and unamended conditions. Additionally, aliquots of cell suspensions were collected before and after irradiation at the LD_{50} of unamended samples (50.1 kJ m^{-2} for *Micrococcus* sp., 40.3 kJ m^{-2} for *Paracoccus* sp., 49.3 kJ m^{-2} for *Pseudomonas* sp. and 37.0 kJ m^{-2} for *Staphylococcus* sp.) (Table 8.1) for biological and biochemical analysis. For protein carbonyls and antioxidant activity (catalase/CAT and superoxide dismutase/SOD) determinations, cells were immediately resuspended in cold 50 mM PBS (pH 7.8) containing 1 mM EDTA and sonicated in ice (Branson Instruments Co. Sonifier, Stamford, Conn.; 2 min, 30-s pulses, 1 min cooling). The extracts were centrifuged (10,000 x *g*, 15 min) and the supernatant frozen at -80 °C until analysis. All experiments were repeated in three independent assays. Parameters were always determined in a minimum of three analytical replicates. Positive (50 mM H_2O_2-treated) and negative (untreated) controls

were always included and processed along experimental samples in order to ensure proper functioning of the procedures on all strains.

Colony forming units (CFU)

Before and after irradiation, sample aliquots were serially-diluted in 1 x PBS and spread-plated in triplicate in agar plates (Difco, Detroit, MI). Colonies were counted after up to 7 days of incubation in the dark, at 25 ºC. The dilution and plating procedures were carried out under low-luminosity conditions to minimize photoreactivation.

Glucose uptake

The effects of UV radiation combined with the exposure to metals on bacterial energy metabolism were assessed from glucose uptake activity, using a protocol adapted from Harada et al. (2010). Triplicate 1.5 mL aliquots of bacterial suspension and a 5 % (wt/vol) trichloroacetic acid-fixed control were incubated with [^{14}C]glucose (Amersham Biosciences, Buckinghamshire, UK; SA 310 mCi mmol^{-1}) at a saturating concentration of 150 µM. Samples were incubated in the dark at *in situ* temperatures for 1 h. Incubations were stopped by the addition of chilled 5 % (wt/vol) trichloroacetic acid (Sigma, St. Louis, MO, USA) and samples were filtered through nitrocellulose filters (0.2-µm-pore-size; Millipore, Tokyo, Japan). Filters were then rinsed three times with chilled 5 % trichloroacetic acid and transferred to eppendorfs. A volume of 1.5 mL of Universol liquid scintillation cocktail (ICN Biomedicals, USA) was added. The amount of radioactivity incorporated into bacterial cells was determined in a Beckman LS 6000 IC liquid scintillation counter (Beckman Instruments, Inc., Fullerton, CA).

In vivo *production of ROS*

In vivo production of ROS was detected using the probe 2',7'-dichlorodihydrofluorescein diacetate (DCFH-DA, Cayman Chemical Co. Ltd., MI, USA) (Pérez et al., 2007). Control and irradiated samples were centrifuged and washed with 10 mM PBS (pH 7.0). After amendment with the probe (final concentration 10 µM), the mixture was incubated in the dark for 30 min. Afterwards, cells were washed, sonicated and the cell extracts were mixed with potassium phosphate buffer. The fluorescence of the samples was measured with a Jasco FP-777 Fluorometer (Japan Spectroscopic Co., Ltd., Tokyo, Japan) at room temperature ($\lambda_{ex.}$ 490 nm; $\lambda_{em.}$ 519 nm).

The fluorescence intensity at 519 nm was corrected against the blank control (without cells) and then normalized to the biomass, determined as the amount of cellular protein according to the method of Bradford (Bradford, 1972). Unless otherwise specified, all reagents used for this and subsequent protocols were purchased from Sigma-Aldrich (St Louis, MO).

DNA strand breakage

UV-induced DNA damage was assessed using the quantification of DNA strand breaks (DSB) as a proxy, following a previously described procedure (He and Häder, 2002). The method requires three sets of samples: test samples (so-called P-samples), samples not subjected to alkaline unwinding (T-samples) and samples subjected to complete alkaline unwinding (B-samples). Cells were collected by centrifugation (3,000 x *g*, 15 min) and digested with lysozyme (4 mg mL^{-1} final concentration) and proteinase K (0.25 mg mL^{-1} final concentration). A volume of 300 µL of 0.1 M NaOH was added to the three sets of samples: (1) T-samples were immediately neutralized with 300 µL of 0.1 M HCl, incubated at room temperature for 30 min and sonicated for 15 s; (2) B-samples were sonicated for 2 min, incubated for 30 min at room temperature, neutralized with 300 µL of 0.1 M HCl and sonicated again for 15 s; and (3) P-samples were incubated for 30 min, neutralized with 300 µL of 0.1 M HCl and sonicated for 15 s.

A final concentration of 5 µM of Hoechst 33258 was added to all samples. After centrifugation, the supernatant was used for fluorescence measurements ($\lambda_{ex.}$ 350 nm; $\lambda_{em.}$ 450 nm) in a Jasco FP-777 Fluorometer (Japan Spectroscopic Co., Ltd., Tokyo, Japan). The fraction of double stranded DNA (dsDNA) was calculated as dsDNA = (P−B)/(T−B)×100, where T, P and B were fluorescence intensities of T-, P- and B-samples normalized to the biomass, respectively.

Lipid peroxidation

Lipid peroxidation was determined as the amount of thiobarbituric acid reactive substances (TBARS) as previously described (Pérez et al., 2007). Control and irradiated cells were centrifuged, washed, and suspended in 50 mM PBS (pH 7.4) containing 0.1 mM butylated hydroxytoluene and 1 mM of the protease inhibitor PMSF (phenylmethanesulfonyl fluoride). Afterwards, cell suspensions were sonicated and centrifuged, and the soluble fraction was mixed with an equal volume of 20 %

trichloroacetic acid. Following another centrifugation step at 10,000 x *g* for 5 min, supernatants were removed and mixed with 1 volume of 0.5 % (w/v) thiobarbituric acid in 0.1 M HCl and 10 mM butylated hydroxytoluene. After incubation at 100 ºC for 1 h, aliquots were removed, cooled and mixed with 1.5 volumes of butanol. The mixture was centrifuged (4,000 x *g*, 10 min) and the organic fraction was removed. The absorbance at 535 nm was read using a Thermo Spectronic Genesys 10 UV spectrophotometer and TBARS content was determined using an extinction coefficient of 156 $mM^{-1}cm^{-1}$. Results were normalized to the cell biomass.

Protein oxidation

The carbonyl content in oxidized proteins was determined as previously reported (Semchyshyn et al., 2005). Aliquots of sonicated cells were incubated with 10 mM dinitrophenylhydrazine (DNPH) in 2 M HCl for 1 hour at room temperature. In blanks, DNPH was omitted. In order to precipitate proteins, 20 % trichloroacetic acid was added, after which suspensions were centrifuged (14,000 x *g*, 5 min), and the pellet washed three times with 1:1 (vol/vol) ethanol-ethyl acetate. The final precipitate was dissolved in 6 M guanidine hydrochloride. The absorbance at 360 nm was determined against a blank of guanidine solution (6 M guanidine hydrochloride with 2 mM potassium phosphate), and a molar absorption coefficient of 22 mM^{-1} cm^{-1} was used to quantify the levels of protein carbonyls. Results were normalized to the biomass.

Antioxidant enzymatic activity

Catalase (CAT) activity was measured spectrophotometrically by monitoring the rate of decomposition of H_2O_2 (Beers and Sizer, 1952). One unit of CAT activity was defined as the amount of activity required to decompose 1 µmol of H_2O_2 per minute under the assay conditions. The strain *Enterococcus faecalis* was used as a negative control. A mixture of 18 mM hydrogen peroxide and sterile potassium phosphate buffer (1:5) was used as an additional negative control (Anderl et al., 2003). Superoxide dismutase (SOD) activity was determined according to McCord and Fridovich (McCord and Fridovich, 1969), in which a xanthine-xanthine oxidase system is used to generate superoxide and nitroblue tetrazolium is used as an indicator. One unit of SOD activity was defined as the amount of SOD that resulted in 50 % inhibition of the reduction of nitroblue tetrazolium. Potassium phosphate buffer was used as a blank. Results were normalized to the biomass.

Bacterial biomass

Bacterial biomass was determined from the protein concentration in cell homogenates according to the Bradford method, using bovine serum albumin (BSA) as a standard (Bradford, 1976).

Statistical analysis

All experiments were repeated in three independent assays and biochemical and microbiological analysis were always conducted in triplicate. Differences between treatments were assessed by 1-way ANOVA using the statistical software SPSS v.17. Levene test was used to assess homogeneity of variances. If variances were not homogeneous, the natural logarithm transformation was applied. If variances were still not homogenous, the non-parametric Mann-Whitney test was used to assess the overall effect of treatment. Stepwise multiple regression, used to identify groups of independent variables (ROS, DSB, TBARS and carbonyls levels, as well as SOD and CAT activity) with the most significant contribution to the variability of the dependent variable (bacterial inactivation expressed as LD_{50}), was conducted with SPSS v. 17.

Results

Effects of UV-Irradiation on Biological and Biochemical Parameters

To select metal concentrations that would not significantly affect neither the growth curve of bacterial isolates nor the level of oxidative stress markers on unirradiated cells, thereby minimizing any potential toxic effect of the metals during irradiation experiments, different metal concentrations were tested. A concentration of 1 μM affected the least the growth curve and did not significantly alter the levels of oxidative stress markers of cells (Table 8.2) and was therefore chosen for subsequent UV-assays.

UVB inactivation curves of bacterial isolates grown with and without added concentrations of metals are represented in Fig. 8.1. Dark controls for every metal treatment were also performed but not included in the figure for simplicity, since significant differences between dark controls of unamended and metal-amended samples were not observed (1-way ANOVA, $p > 0.05$).

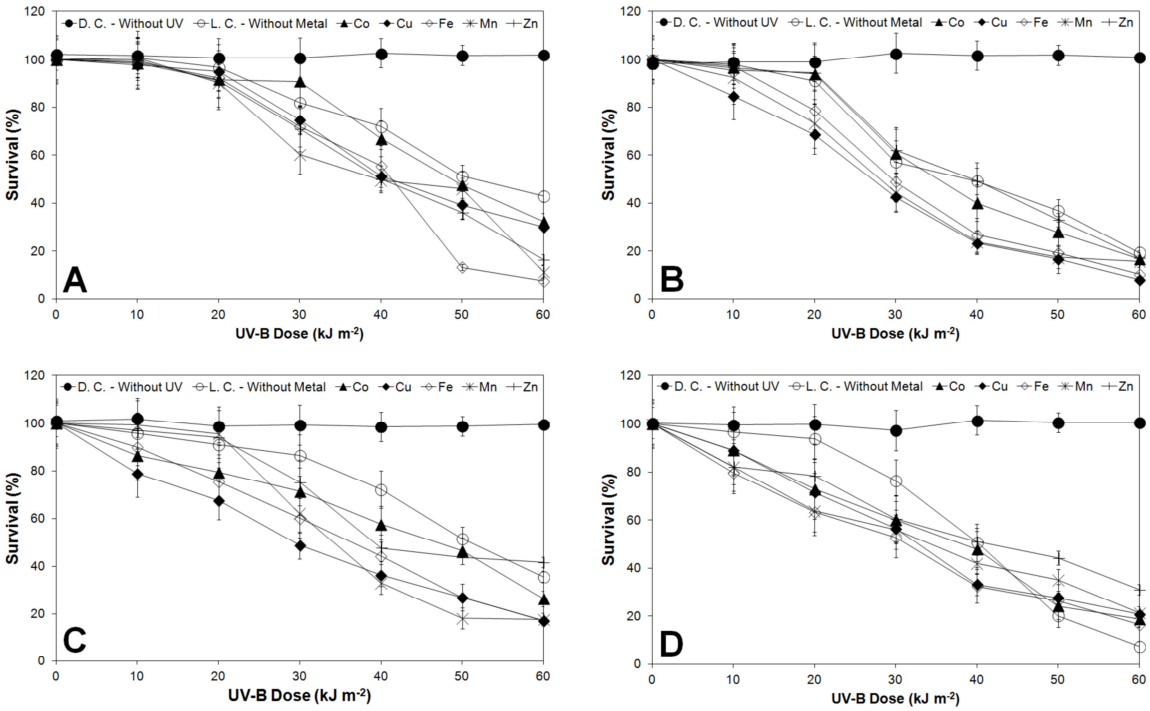

Fig. 8.1. Influence of transition metals on UVB inactivation curves of (A) *Micrococcus* sp., (B) *Paracoccus* sp., (C) *Pseudomonas* sp. and (D) *Staphylococcus* sp. Each point corresponds to the average of three independent experiments, conducted with triplicate replicas (n = 9). Error bars are standard deviation of the mean. Where error bars are not visible, they are smaller than the graph symbol. D.C. – dark control. L.C. – light control (without metal).

Compared to unamended samples, metal amendment generally reduced the LD_{50} by up to 21.4 kJ m^{-2}. This effect was particularly significant for the Cu, Fe and Mn treatments and variable depending on the bacterial isolate (Table 8.1). The effects of different transition metals on survival and activity during UVB exposure are represented in Fig. 8.2. Amendment with Cu, Fe and Mn significantly (1-way ANOVA, $p < 0.05$) decreased survival following exposure to UVB by 10.8 %-27.7 %, 16.5 %-35.8 % and 13.1 %-31.0 %, respectively, in all isolates tested (Fig. 8.2 A). Depending on the strain, the effects of metal treatment were not significant, protective or detrimental to glucose incorporation during irradiation (Fig. 8.2 B).

Treatment with Co and Zn resulted in either an increase or attenuation of ROS generation, depending on the strains. Cu and Fe treatments were responsible for a net increase in ROS generation during UVB exposure by up to 9.8 and 13.3 %, respectively. Amendment with Mn significantly attenuated ROS generation during irradiation (up to 20.5 %; 1-way ANOVA, $p < 0.05$) in all strains (Fig. 8.3 A).

Table 8.2. Absolute values of the different stress markers in unirradiated metal-amended and unamended cell suspensions. A.U. – arbitrary units. Non-significant differences (1-way ANOVA, $p > 0.05$) in the values of the different stress markers in metal-amended treatments compared to unamended samples are indicated by n.s.

Strain	Treatment	ROS (DCF fluorescence, A. U.)	DSB (Hoechst 33258 fluorescence, A.U.)	TBARS (pmol/mg protein)	Carbonyls (µmol/mg protein)	CAT (µmol/min/mg protein)	SOD (U/mg protein)
***Micrococcus* sp. NT25I3.2AA**	No metal	8432.7±846.4	171.7±16.4	23.3±2.9	6.7±0.6	41.8±4.7	266.7±25.7
	Co	9023.0±954.6 n.s.	189.2±18.1 n.s.	26.1±2.9 n.s.	7.3±0.6 n.s.	44.8±4.7 n.s.	289.3±29.7 n.s.
	Cu	7715.9±853.6 n.s.	157.1±17.7 n.s.	20.3±2.8 n.s.	6.1±0.9 n.s.	37.5±5.3 n.s.	248.0±26.4 n.s.
	Fe	8390.5±831.5 n.s.	172.6±18.7 n.s.	23.3±2.7 n.s.	6.7±0.7 n.s.	41.4±4.2 n.s.	268.0±28.8 n.s.
	Mn	8977.8±851.3 n.s.	188.5±20.2 n.s.	25.8±2.6 n.s.	7.9±0.7 n.s.	47.9±5.1 n.s.	290.8±29.0 n.s.
	Zn	7677.3±850.5 n.s.	173.1±18.2 n.s.	20.5±3.0 n.s.	6.6±0.6 n.s.	40.1±3.9 n.s.	249.2±23.5 n.s.
***Paracoccus* sp. NT25I3.1A**	No metal	12870.0±1115.3	110.9±10.2	17.2±2.0	6.7±0.8	34.8±4.1	172.0±21.5
	Co	14414.4±1609.2 n.s.	122.3±11.7 n.s.	18.7±2.3 n.s.	7.7±0.8 n.s.	39.7±4.1 n.s.	194.4±21.5 n.s.
	Cu	11196.9±1608.8 n.s.	103.1±10.6 n.s.	16.2±2.3 n.s.	6.0±1.4 n.s.	31.5±4.1 n.s.	151.4±21.8 n.s.
	Fe	12827.1±1584.9 n.s.	112.1±13.0 n.s.	17.4±2.1 n.s.	6.8±1.1 n.s.	35.3±4.6 n.s.	172.6±21.6 n.s.
	Mn	14366.4±1603.8 n.s.	114.9±13.8 n.s.	18.4±1.3 n.s.	7.7±1.1 n.s.	35.2±5.7 n.s.	195.0±21.6 n.s.
	Zn	11159.6±862.3 n.s.	113.8±11.9 n.s.	15.7±1.8 n.s.	6.8±1.0 n.s.	35.9±4.7 n.s.	151.9±24.7 n.s.
***Pseudomonas* sp. NT5I1.2B**	No metal	12020.0±1365.9	121.5±12.7	14.3±1.2	6.8±0.8	50.3±5.0	143.3±17.9
	Co	13582.6±1502.9 n.s.	130.0±12.7 n.s.	15.3±1.1 n.s.	7.5±0.8 n.s.	55.9±5.0 n.s.	160.5±17.9 n.s.
	Cu	10577.6±1502.5 n.s.	108.7±11.4 n.s.	13.1±1.1 n.s.	6.0±1.2 n.s.	45.8±8.3 n.s.	124.7±17.7 n.s.
	Fe	12060.1±1525.3 n.s.	120.1±13.6 n.s.	14.3±1.5 n.s.	6.8±1.0 n.s.	50.7±6.5 n.s.	142.9±17.9 n.s.
	Mn	13627.9±1507.9 n.s.	139.1±14.6 n.s.	16.1±1.8 n.s.	7.4±1.0 n.s.	52.0±6.6 n.s.	160.0±17.9 n.s.
	Zn	10612.9±1034.4 n.s.	116.3±12.2 n.s.	12.5±1.1 n.s.	6.6±0.9 n.s.	50.8±5.6 n.s.	124.3±17.8 n.s.
***Staphylococcus* sp. NT25I2.1**	No metal	15193.3±1384.0	157.9±16.6	37.0±3.2	5.3±0.4	34.8±3.7	240.0±22.2
	Co	16560.7±1705.6 n.s.	171.3±16.0 n.s.	42.1±5.0 n.s.	5.7±0.4 n.s.	37.2±3.7 n.s.	262.8±22.2 n.s.
	Cu	13750.0±1405.4 n.s.	141.3±16.3 n.s.	32.2±4.0 n.s.	4.9±0.7 n.s.	31.8±4.1 n.s.	218.4±22.4 n.s.
	Fe	15168.0±1491.7 n.s.	156.8±17.4 n.s.	37.1±4.8 n.s.	5.3±0.5 n.s.	34.6±4.2 n.s.	240.4±22.1 n.s.
	Mn	16533.1±1603.2 n.s.	155.9±18.9 n.s.	41.8±4.6 n.s.	5.2±0.5 n.s.	39.8±4.1 n.s.	263.2±22.0 n.s.
	Zn	13727.1±1294.8 n.s.	153.3±16.6 n.s.	32.5±4.6 n.s.	5.3±0.4 n.s.	34.1±3.9 n.s.	218.8±22.3 n.s.

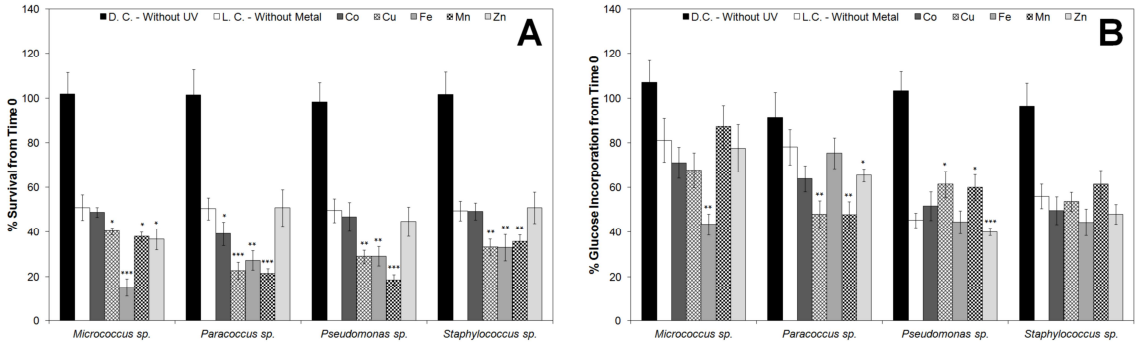

Fig. 8.2. Variation of (A) cell survival and (B) glucose incorporation upon UVB exposure in cell suspensions unamended and amended with 1 µM of the different transition metals. Each bar corresponds to the average of three independent experiments, conducted with triplicate replicas (n = 9). Error bars are standard deviation of the mean. Some error bars are hidden behind the graph symbol. The significance of the differences between metal amended and non-amended samples is presented: *- $p < 0.05$. ** - $p < 0.01$. *** - $p < 0.005$. D.C. – dark control. L.C. – light control (without metal).

Treatment with Co, Cu, Mn and Zn had variable effects on DNA damage (assessed as DSB) during UVB exposure, depending on the strain, while amendment with Fe significantly increased DNA damage by up to 37.4 % in all strains (Fig. 8.3 B).

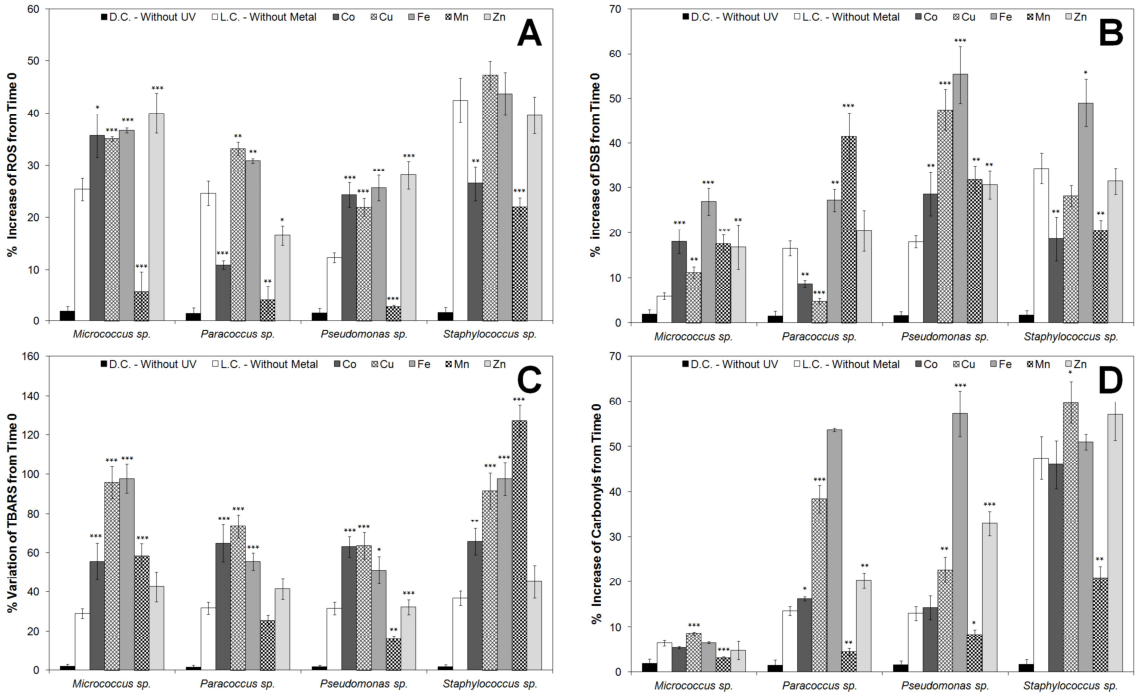

Fig. 8.3. Variation of (A) ROS, (B) DSB, (C) TBARS and (D) carbonyl levels upon UVB exposure in cell suspensions unamended and amended with 1 µM of the different transition metals. Each bar corresponds to the average of three independent experiments, conducted with triplicate replicas (n = 9). Error bars are standard deviation of the mean. Some error bars are hidden behind the graph symbol. The significance of the differences between metal amended and non-amended samples is presented: *- $p < 0.05$. ** - $p < 0.01$. *** - $p < 0.005$. D.C. – dark control. L.C. – light control (without metal).

Cultures grown with additional concentrations of Co, Cu and Fe displayed increased TBARS formation during irradiation by 56.5 %, 66.8 % and 68.7 %, respectively. Treatment with Zn either had no effect or increased TBARS generation during irradiation by up to 53.5 %, while Mn either attenuated or increased UV-induced TBARS formation depending on the strain (Fig. 8.3 C). Amendment with Co, Cu, Fe and Zn either attenuated or increased the formation of protein carbonyls during UVB irradiation, depending on the strain, while modification with Mn attenuated carbonyl formation in all strains by up to 44.2 % (Fig. 8.3 D).

Effects of metal treatment on CAT and SOD activity were more variable depending on the strain (Figs. 8.4 A, B). In *Micrococcus* sp., metal-amended suspensions showed greater CAT activity compared to unamended controls by up to 61.6 %, while in *Paracoccus* sp. and *Pseudomonas* sp., irradiation in the presence of added metal decreased CAT activity compared to metal-free cell suspensions by up to 50.2 % and 70.1 %, respectively. In *Staphylococcus* sp., the presence of different metals either increased or decreased CAT activity compared to unamended samples. SOD activity was decreased in metal-amended suspensions of *Micrococcus* sp. by up to 70.4 % and enhanced in *Pseudomonas* sp. by up to 40.3 %, compared to unamended samples. In *Paracoccus* sp. and *Staphylococcus* sp., effects of metal amendment on SOD activity during irradiation depended on the metal added.

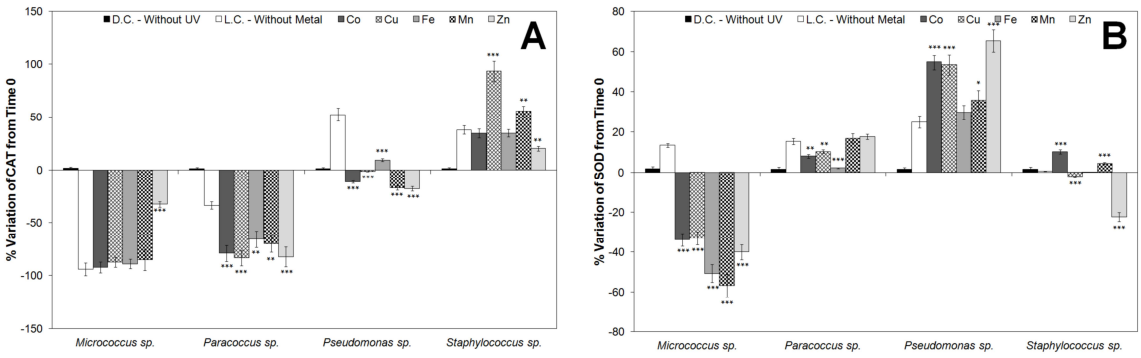

Fig. 8.4. Variation of (A) CAT activity and (B) SOD activity upon UVB exposure in cell suspensions unamended and amended with 1 µM of the different transition metals. Each bar corresponds to the average of three independent experiments, conducted with triplicate replicas (n = 9). Error bars are standard deviation of the mean. Some error bars are hidden behind the graph symbol. The significance of the differences between metal amended and non-amended samples is presented: *- $p < 0.05$. ** - $p < 0.01$. *** - $p < 0.005$. D.C. – dark control. L.C. – light control (without metal).

Multiple Stepwise Linear Regression

To obtain further insights on the influence of metals on UV-induced inactivation, a multiple stepwise linear regression analysis was applied to the dataset using LD_{50} as a dependent variable and oxidative stress markers (ROS levels, DSB, TBARS, protein carbonyls, CAT and SOD activity) as predictor variables (Table 8.3).

Table 8.3. Multiple stepwise regression analysis used to infer the parameters contributing to bacterial inactivation (expressed as LD_{50}) under the different treatments. DSB: DNA strand breaks. CAT: catalase. ROS: reactive oxygen species. TBARS: thiobarbituric acid reactive substances. β - standardized coefficient. p – probability. R^2 – coefficient of correlation.

	Adjusted R^2 of the model (p)	Predictor variable	β	p
UV	0.994 (0.001)	DSB	0.604	0.000
		TBARS	0.285	0.023
		CAT	0.186	0.001
UV+Co	0.965 (0.005)	SOD	-0.801	0.000
		Carbonyls	2.115	0.000
		CAT	-1.422	0.005
UV+Cu	-	-	-	-
UV+Fe	0.993 (0.000)	ROS	0.854	0.000
		TBARS	0.397	0.000
		DSB	0.296	0.000
UV+Mn	0.327 (0.030)	TBARS	0.623	0.030
UV+Zn	0.998 (0.020)	CAT	-0.204	0.004
		Carbonyls	1.054	0.000
		ROS	0.628	0.000

In controls not treated with metals, 99.4 % of the variability of LD_{50} was accounted for by DSB levels, TBARS and CAT activity. In cultures supplemented with Co, 96.5 % of the variation in LD_{50} was predicted by the contributions of SOD, carbonyls and CAT. In Cu-treated samples, variations in LD_{50} were not significantly explained by any of the independent variables used. In the Fe treatment, 99.3 % of the variability in LD_{50} was explained by ROS, TBARS and DSB, while in Mn treatments, 32.7 % of the variation in LD_{50} was explained by TBARS. In the Zn treatment, 99.8 % of the variations in LC_{50} was explained by CAT, carbonyls and ROS.

Discussion

Research conducted with several biological systems has highlighted the role of transition metal ions in protecting against the detrimental effects of gamma-radiation, UVC radiation, wet and dry heat and H_2O_2 (Daly et al., 2004; Bagwell et al., 2008; Ghosh et al., 2011; Granger et al., 2011). However, the role of transition metals on the susceptibility of bacteria to environmentally relevant UV radiation remains unknown. This lack of information impairs the realistic understanding of UV effects in bacterial

communities in natural environments where metals are frequently present, seasonally variable and can represent additional stress factors (Zhou et al., 2008).

In the present work, the effect of five transition metals on the UV sensitivity and UV-induced cellular damage on a set of bacterial isolates was studied. The concentrations of metals used were generally in agreement with reported environmental concentrations in aquatic systems, particularly in the runoff of urban areas (Mudhoo et al., 2012). The importance of metals to UVB-induced damage was evident from the shift in the descriptors that contributed the most to explain bacterial inactivation (expressed as LD_{50}) following treatment with different metals, as revealed by linear regression.

Role of Co, Cu and Fe

Despite the observed variability in the effects of UV-induced damage in the different strains tested, amendment with metals generally decreased the dose necessary for inactivation by UVB (LD_{50}), thereby suggesting a synergistic effect of metals and UVB radiation in bacterial cell damage.

The Fenton reactive metals Fe and Cu had a significant detrimental effect on bacterial survival during irradiation, potentially associated to enhanced ROS and TBARS generation following irradiation in metal-treated bacterial suspensions. In the case of Fe, an increase in DNA damage compared to untreated controls was also observed, and together with ROS generation and TBARS, accounted for 99.3 % of the variation in LD_{50}, as shown by linear regression. Such effects are in line with the role of the divalent Fe ion (Fe^{2+}) in promoting the generation of the powerful oxidant hydroxyl radical according to the following reaction:

$$Fe^{2+} + H_2O_2 \rightarrow Fe^{3+} + OH^- + OH^{\bullet}$$

The hydroxyl radical can in turn cause damage to any biomolecule. The current study confirms the involvement of Fe in UVB-induced oxidative damage and the importance of Fe homeostasis through the regulation of genes involved in Fe influx, storage and expression of Fe-containing enzymes (Qiu et al., 2005a; Matallana-Surget et al., 2009a) in limiting the detrimental effects of exposure to UVB.

Under aerobic conditions, Cu (similarly to Fe) can participate in Haber-Weiss reactions to mediate the generation of the hydroxyl radical (Santo et al., 2011). In accordance to what was observed with Fe, treatment with Cu increased TBARS and ROS generation. However, as opposed to Fe, it did not significantly increase DNA

damage during irradiation. This observation can be explained, at least in Gram-negative bacteria, by the compartmentalization of hydroxyl radicals generated by Cu in the periplasm of the cell, which limited its damage to the membrane and cell wall (Macomber et al., 2007), thus accounting for the observed increase in TBARS in Cu-amended samples.

Irradiation of cell suspensions after treatment with Co also caused a significant increase in TBARS levels which, in Gram-negative bacteria, can be attributed to the ability of Co to react with H_2O_2 generated inside the cell by a Fenton-type reaction within the periplasmic space (Barras and Fontecave, 2011). The resulting hydroxyl radicals are able to subsequently attack membrane and cell wall components (Moorhouse et al., 1985; Barras and Fontecave, 2011).

Together, these results suggest that the toxicity of ROS generated during UV exposure is mediated by intracellular metals, particularly by the more biologically relevant Fe and Cu, whose homeostasis plays a crucial role in limiting the detrimental effects of oxidative damage during UVB irradiation.

Role of Mn

Mn was the only metal that reduced protein carbonyl levels during UV exposure in all strains tested. High levels of intracellular Mn have also been shown to contribute to resistance of bacteria to UVC radiation and ionizing radiation by mitigating protein oxidation (Daly et al., 2004; Ghosh et al., 2011; Granger et al., 2011). The protective effect of Mn against protein carbonylation seems to stem from its ability to metallate mononuclear enzymes containing Fe-S clusters, thereby replacing Fe ions and preventing the formation of damaging hydroxyl radicals (Anjem et al., 2009). Additionally, Mn is also able to form complexes with metabolites that can scavenge superoxide, H_2O_2 and hydroxyl radicals (Daly et al., 2010). Accordingly, cell suspensions added of Mn showed significantly lower (1-way ANOVA, $p < 0.05$) ROS generation, compared to the unamended counterparts. Surprisingly, the protective effect of Mn against protein carbonylation and ROS generation was accompanied by a statistically significant reduction in survival during exposure to UVB, compared to non-amended controls, and in three of the strains tested, a significant increase in DNA damage was observed. The reason for such effects is still unclear, in face of current knowledge. Recently, a transcriptomic study surveying UVC effects on *Deinococcus gobiensis* reported an over twofold reduction in the levels of the Mn transporter *mntA*,

thus suggesting reduced Mn influx during irradiation (Yuan et al., 2012). It has been suggested that, by replacing Fe ions in the Fe-S clusters of proteins, Mn can selectively protect the function of metabolic pathways (*e.g.*, pentose phosphate pathway), which may or may not be favourable for survival depending on the stressful condition (Berlett et al., 1990; Sobota and Imlay, 2011). Such replacement could have also compromised the correct functioning of the biochemical pathways on which these proteins participate, resulting in a detrimental effect on survival during UV exposure.

The intracellular Mn/Fe concentration ratio is also crucial in determining the protective effect of manganese against ionizing radiation (Daly et al., 2004; Daly et al., 2007). For example, *Neisseria gonorrhoeae* accumulates Mn^{2+}, but is sensitive to ionizing radiation due to its high requirement for Fe^{2+} (Archibald and Duong, 1986). It should be noted that the concentrations of Mn used in this study were chosen so that no significant effects on bacterial survival, activity and markers of oxidative stress were observed in the respective dark controls, in order to minimize the possible confounding effects of metal toxicity in the UV response. As a result, concentrations used were up to 25 times lower than those reported in similar studies (Daly et al., 2004; Ghosh et al., 2011; Granger et al., 2011), which could have hindered the detection of a potential protective role of Mn in UVB-induced damage that might require higher concentrations of manganese. Further studies are required to elucidate the role of Mn in photooxidative stress in bacteria.

Experimental limitations on the determination of metal oxidation status

The oxidation status of transition metals is important in determining their biological effects. The cycling between oxidation states is involved in oxidative stress, as in the case of Cu and Fe. When Cu^{2+} enters the cell it is readily reduced to the toxic Cu^{+} form which establishes complexes with thiol groups and certain amino acid residues, such as cysteine or ascorbic acid (Silver and Phung, 2005). In *Escherichia coli* the CueO protein in the periplasm converts Cu^{+} into the less permeable and thus less toxic Cu^{2+} (Singh et al., 2004). Metal iron, on the other hand, can be readily acquired by bacteria through the reduction of insoluble Fe^{3+} to soluble and potentially more toxic Fe^{2+}, followed by transport of Fe^{2+} to the cytoplasm (Kammler et al., 1993; Braun et al., 1998).

Cycling between oxidation states is also involved in the protective effect of Mn against oxidative stress. Quenching of the superoxide radical and peroxyl radical species

by Mn^{2+} results in the formation of Mn^{3+} species, which are stabilized by coordination ligands such as pyrophosphate or carboxylic acids, thus lowering the redox potential of the Mn^{2+}-Mn^{3+} couple (Stadtman et al., 1990).

However, the ability of metal ions to undergo redox cyclying poses some complications in terms of experimental work. For example, while free Cu^{2+} ions are stable in air-exposed neutral aqueous solutions, free Cu^{+} can only be maintained at very acidic pH or in complexed forms (Magnani and Solioz, 2007). In the case of iron, in the presence of oxygen at a pH of $\geq$7, Fe^{2+} is readily converted into the almost completely insoluble Fe^{3+} (Crossley et al., 2007).

Another difficulty in the study of the interaction between cells and metals is the ability of metals to form complexes with biological molecules, which compromises the determination of the actual concentration of free, bioavailable metal in a biological system (Magnani and Solioz, 2007). Accordingly, by using a complex growth medium like TGY it is likely that some of the metal added to the bacterial cultures could have complexed with the components of the medium and it is therefore virtually impossible to predict the metallic species present in the system. However, it is unlikely that in natural aquatic systems these metals are freely available in solution in their cationic form, which makes our experimental conditions more similar to what probably occurs in the environment, than using, for instance, solution buffers with low metal-binding properties.

Conclusions

Metal amendment generally acted synergistically with UVB exposure to promote bacterial inactivation. Fe and Cu amendment exacerbated oxidative damage during UVB exposure, highlighting the importance of regulating the availability of these metals in the cell in response to irradiation. Mn attenuated the UV-induced formation of protein carbonyls but had a negative impact on survival, suggesting that displaced Fe ions might promote oxidative damage in other targets of the cell. Furthermore, the observation of some differences in the responses of Gram-negative and Gram-positive bacteria to the synergistic effects of metal amendment and irradiation (data not shown) might suggest that the presence of metals in the environment could influence the effects of UV exposure on bacterial community composition.

Acknowledgments

Acknowledgments are due to Prof. Dr. Amparo Faustino (Chemistry Department, University of Aveiro) for carefully reviewing the preliminary version of the manuscript and providing access to the spectrofluorimeter. We also thank the anonymous reviewers for their helpful criticism. Financial support for this work was provided by CESAM (Centre for Environmental and Marine Studies, University of Aveiro) and the Portuguese Foundation for Science and Technology (FCT) in the form of a PhD grant to A.L. Santos (SFRH/BD/40160/2007) and a post-Doctoral grant to I. Henriques (SFRH/BPD/63487/2009).

CHAPTER 9

Influence of Water Properties on UVB Effects in Estuarine Bacteria

Santos A. L., Baptista I., Gomes N. C. M., Henriques I., Almeida A., Correia A., Cunha A.

Submitted for publication

Abstract

The influence of nutrient (nitrogen and phosphorus) availability and the properties of the suspension medium on the UV sensitivity responses of two distinct bacterial assemblages (bacterioneuston and bacterioplankton) was assessed in laboratory experiments in which marine and brackish water communities were inoculated in (i) water of different nutrient contents (unamended and amended with high and low nutrient concentrations) and (ii) water of different origins (surface and subsurface). The effects on bacterial abundance and activity (leucine incorporation) were determined. Additionally, the influence of the suspension media on UV sensitivity responses was also studied in a set of bacterial isolates.

Inoculation of bacterial communities in high nutrient medium attenuated UV-induced inhibition (by up to 34.2 % for abundance and 54.4 % for activity) compared to unamended conditions. Under nutrient depleted conditions, marine bacterioneuston was less affected by UV radiation than marine bacterioplankton (by up to 17.8 % for abundance and 21.4 % for activity). In brackish water, nutrient conditions did not affect inactivation but high nutrient concentrations attenuated the UV-induced inhibition of activity (up to 53.2 %). Suspension in natural water resulted in less pronounced inhibitory effects of UV exposure compared to suspensions prepared in a mineral solution (by up to 11.8 % for abundance and 13.2 % for activity). The effects of the different suspension media were more variable on isolated strains than in mixed assemblages.

These results demonstrate that the nutrient content and quality of the suspension medium affect bacterial photobiological responses and that the abiotic environment of bacterial communities influences their UV sensitivity.

Introduction

In aquatic ecosystems, UV radiation (UVR) can reach considerable depths (> 20 m) in the water column (Smith, 1989). Climate changes, namely, warming, acidification and modifications of ocean stratification patterns, are expected to increase the penetration of UVB wavelengths (280-320 nm) in the water column and enhance the exposure of aquatic organisms to UVB in forthcoming years (Andrady et al., 2010). These concerns make the study of the effects of UVB radiation on the structure and function of aquatic microbial communities a critical and timely subject.

Field and laboratory studies indicate that exposure to UVR results in a general decrease in total bacterial abundance (Müller-Niklas et al., 1995; Pakulski et al., 1998), monomer incorporation (Bailey et al., 1983; Santos et al., 2011a), exoenzymatic activities (Müller-Niklas et al., 1995; Santos et al., 2011a), oxygen consumption (Pakulski et al., 1998; Joux et al., 2009), protein and DNA synthesis (Herndl et al., 1993; Sommaruga et al., 1997; Hernández et al., 2007; Joux et al., 2009; Santos et al., 2012b) and single-cell activity (Alonso-Sáez et al., 2006).

UVB radiation has both direct and indirect effects on cells. The direct effects of UVB result from the absorption of UV photons by DNA and proteins (Cadet et al., 2005b; Pattison and Davies, 2006). Additionally, damage can arise as a result of photosensitized reactions whereby a photosensitizer (endogenous or exogenous) absorbs light, enters an excited state and initiates damaging photodynamic reactions that can affect lipids, proteins and DNA (Chamberlain and Moss, 1987; Moan and Peak, 1989; Girotti, 2001; Pattison and Davies, 2006). Endogenous photosensitizers include porphyrin derivatives and flavins present inside the cell, while exogenous photosensitizers include humic substances and photosynthetic pigments (Curtis et al., 1992).

The impact of solar UVR on marine microorganisms is complex and depends on both the radiation levels received and on several environmental (temperature, salinity, and nutrients) (Ogbebo and Ochs, 2008; Joux et al., 2009; Bullock and Jeffrey, 2010; Matallana-Surget et al., 2010) and biological (specific sensitivity, repair mechanisms, nutritional state, and growth phase) (Berney et al., 2006c; Bucheli-Witschel et al., 2010) factors. Nutrients, in particular, can influence susceptibility to UVR by affecting the penetration of radiation in the water body (Joux et al., 2009) or altering bacterial physiology (Chrzanowski and Kyle, 1996; Bowden and Li, 1997; Ferenci, 1999; Klančnik et al., 2009).

The light history of a bacterial assemblage can also affect the response of bacterial communities to UVR. For example, exposure to solar radiation inhibits bacterial productivity in surface waters (0.5 m) but stimulates activity in deep waters (80 m) (Hernández et al., 2007). The reduced sensitivity of bacterioneuston inhabiting the top millimetre of the water column (or surface microlayer, SML) compared to bacterioplankton inhabiting underlying waters (UW) is also considered indicative of the influence of light history on the effects exerted by UVR on bacterial communities (Santos et al., 2011a). Accumulation of exopolysaccharides and chromophoric dissolved and particulate organic matter at the air-water interface has also been suggested to account for the enhanced resistance of bacterioneuston to solar radiation (Elasri and Miller, 1999; Whitehead and Vernet, 2000; Obernosterer et al., 2005). However, exogenous photosensitizers, such as humic substances and phenolic compounds, which can affect bacterial photobiological responses (Muela et al., 2000), concentrate at the SML (Liss, 1975; Carlson, 1982) and may influence the UV sensitivity responses of microorganisms at the air-water interface.

The objectives of this work were to study the role of nutrients and suspension medium on the UV sensitivity of bacterioplankton and bacterioneuston. Additionally, the variability of the effects of different suspension media on UV-induced damage was also addressed in a set of bacterial isolates.

Materials and methods

Sampling

Samples were collected from an outer oligotrophic marine section (CN, 40º 38' N, 08º 46' W) and an inner mesotrophic brackish water section (I6, 40º 35' N, 08º 41' W) of Ria de Aveiro (Portugal). Sampling was conducted on three consecutive days in June 2010, around the time of the summer solstice when UVB levels are the highest (Seckmeyer et al., 2008). Daily solar radiation levels on the period of sampling ranged from 30 to 35 kJ m^{-2} (climetua.fis.ua.pt/legacy/main/current_monitor/cesamet.htm). At the moment of sampling, the sky was clear with minimum wind conditions (< 2 m s^{-1}). Samples were collected approximately at noon at high tide. This time was previously determined as the moment during the tide that best corresponded to minimum differences in chromophoric dissolved organic matter (cDOM) concentrations (an indicator of the optical properties of water samples) between water from the SML and

UW (data not shown) to minimize the interference of optical properties in UV sensitivity responses of bacterioneuston and bacterioplankton.

Two 0.25-m x 0.35-m glass plates that roughly collect the upper 60-100 µm of the water column were used for bacterioneuston sampling (Harvey and Burzell, 1972). SML water was transferred to acid-rinsed sterilized glass bottles. Samples from underlying water were taken directly by submerging acid-rinsed sterilized glass bottles to a depth of approximately 20 cm. The samples were maintained in the shade at 4 ºC during the transport to the laboratory and were processed within 3 h of collection.

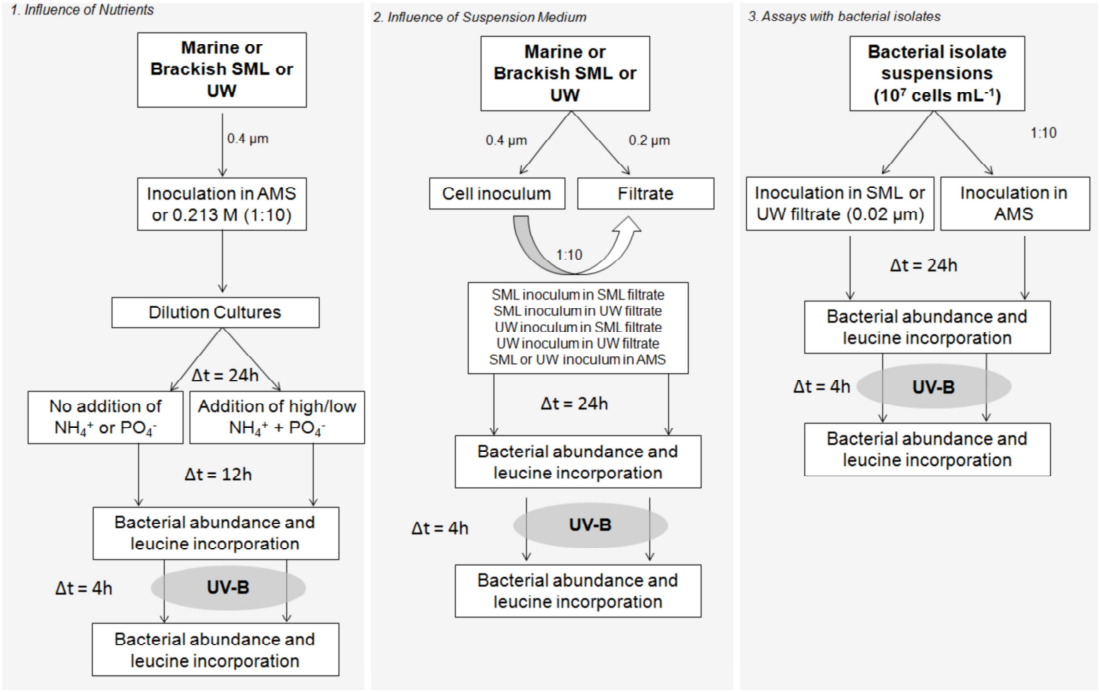

Fig. 9.1. Schematic representation of the experimental setup used to test the influence of nutrients and suspension media on the UV sensitivity responses of bacterioneuston, bacterioplankton and bacterial isolates. SML – surface microlayer, UW – underlying water, AMS – artificial mineral solution.

Physical and chemical properties of the original samples

Temperature and conductivity were measured in the field using a WTW LF 196 Conductivity Meter (WTW, Weilheim, Germany). Chlorophyll *a* was estimated fluorometrically (Yentsch and Menzel, 1963) after filtration of 100 mL triplicate samples through Whatman GF/C glass filters (Brandel, Gaithersburg, MD, USA) and overnight cold extraction in 90 % (v/v) acetone. Samples for nutrient analysis were filtered through 0.45-µm-pore-size cellulose acetate membrane filters (GE Osmonics Labstore, Minnetonka, MN). Nutrient concentrations (dissolved inorganic nitrogen, phosphate, silicate and ammonia) were determined using standard procedures

(Grasshoff et al., 1983). A spectrophotometer (Thermo, Spectronic Genesys 10UV, USA) and Merck reagents were used in all determinations. The determination of the concentration of suspended solids (seston) was performed after filtration of 500 mL triplicate samples through Whatman GF/C (47 mm diam.) pre-weighted, pre-combusted filters. The filters were dried at 60 °C for 24 h, and the seston content was calculated as the difference in weight. Particulate organic matter (POM) was determined by the difference in the weight of the dry seston filters after 4 h incineration at 525 °C (Parsons et al., 1984). Particulate organic carbon (POC) was calculated as 50 % of the POM (Rodier, 1996).

Preparation of dilution cultures

An overview of the experimental layout, identifying the conditions that were experimentally manipulated, is presented in Fig. 9.1.

Influence of nutrient concentration

Dilution cultures were prepared as previously described (Pausz and Herndl, 2002). Water samples from the SML and UW were pre-filtered and filtered through 0.8- and 0.4-µm-pore-size polycarbonate filters (Millipore), respectively, to remove particles and most phytoplankton and zooplankton cells. The filtrate containing the < 0.4 µm fraction was taken as the inoculum and used in a 1:10 (v/v) proportion to obtain cell dilution cultures in artificial mineral solution (AMS, 0.009 M KCl, 0.009 M $CaCl_2 \cdot 2H_2O$, 0.026 M $MgSO_4 \cdot 7H_2O$, 0.023 M $MgCl_2 \cdot 6H_2O$, and 0.002 M $NaHCO_3$) containing 0.425 M NaCl for marine samples or 0.213 M NaCl for brackish water samples. Suspensions were then amended with a mixture of amino acids (L-arginine, L-histidine, L-isoleucine, L-leucine, L-lysine, L-methionine, L-phenylalanine, L-threonine, L-tryptophan, and L-valine) (0.4 µM), glucose (100 or 20 µM), NH_4^+ (10 or 2 µM) and PO_4^{3-} (1 or 0.2 µM) at different concentrations to simulate high- and low-nutrient availability, as previously described (Pausz and Herndl, 2002). Cultures were incubated at 25 ºC in the dark for 24 h. Subsequently, the dilution cultures were split in aliquots to which PO_4^{3-} (40 or 8 µM) and NH_4^+ (4 or 0.8 µM) were added at different concentrations to establish high nutrient and low nutrient conditions. Nutrient-unamended samples were prepared as described for nutrient amendments, except that no PO_4^{3-} or NH_4^+ was added to the dilution cultures. After 12 h, cultures were irradiated as

described below. Bacterial activity and abundance were determined immediately before and after irradiation.

Influence of dissolved components of the suspension medium

Marine and brackish bacterioneuston (SML) and bacterioplankton (UW) inocula (< 0.4 µm filtrates) prepared as described above were diluted (1:10) in 0.2-µm-pore-size filtered water from the SML and UW of the corresponding estuarine site (marine or brackish) and incubated at 25 ºC in the dark for 24 h before irradiation. The following experimental conditions were tested: (i) bacterioneuston inoculum in SML water, (ii) bacterioneuston inoculum in UW water, (iii) bacterioplankton inoculum in SML water, and (iv) bacterioplankton inoculum in UW water. Bacterial suspensions were irradiated as described below. Bacterial activity and abundance were determined immediately before and after irradiation.

Bioassays with bacterial isolates

To evaluate the interspecies variability of the influence of the suspension medium during UVB irradiation, bioassays were conducted with environmental bacterial isolates (*Micrococcus* sp., *Paracoccus* sp., *Pseudomonas* sp., and *Staphylococcus* sp.) selected by their differences in terms of UVB sensitivity (Santos et al., 2011b). Fresh cultures were prepared in Marine Broth 2216 (Difco, Detroit, MI), and cells were harvested by centrifugation (3,200 ×*g* for 15 min; Thermo Scientific Heraeus Pico 21 Microcentrifuge, Hamburg, Germany) in late-exponential phase. The pellets were washed three times with filter-sterilized autoclaved 0.9 % NaCl and resuspended in the same solution, and the bacterial abundance was adjusted to 10^7 cells mL^{-1}. Bacterial suspensions were then diluted (1:10) in AMS or in 0.2-µm-pore-size filtered samples of SML and UW from the marine or brackish water sites.

Irradiation conditions

Dilution cultures or cell suspensions were transferred to sterile 150 x 25 mm plastic tissue culture dishes (Corning Science Products, Corning, NY, USA) so that the depth of the liquid was < 2 mm. For irradiation, the lid was removed, and cell suspensions were exposed to UVB (Philips TL 100 W/01 lamps, main emission wavelength line of 302 nm) for a total dose of 37 kJ m^{-2}, approximately corresponding to UV levels detected in the field at the sampling period. UV intensities were measured

with a monochromator spectro-radiometer placed at the sample level (DM 300, Bentham Instruments, Reading, UK). During irradiation, the temperature was maintained at 25 ºC. Dark controls (covered in aluminum foil) for every experimental condition, treated in the same way as the irradiated samples, were always included. Aliquots of cell suspensions were collected before and after irradiation to assess bacterial abundance and activity. All experiments were conducted in three independent assays.

Bacterial abundance

Bacterial abundance was determined by epifluorescence microscopy (Hobbie et al., 1977) after fixing triplicate samples from each condition tested with 2 % formaldehyde (final concentration). Samples were then filtered through 0.2-µm-pore-size black polycarbonate membranes (Poretics Products, Livermore, USA) and stained with 0.03 % acridine orange (Difco Laboratories, Detroit, Michigan, USA). Cells were counted by epifluorescence microscopy using a Leitz Laborlux K microscope equipped with a BP 450-490 exciter filter and an LP 515 barrier filter (Leitz Meßtechnik, Wetzlar, Germany). At least 200 cells or 20 microscopic fields were counted for each of the three replicate measurements for each condition tested.

Bacterial activity

Bacterial activity was estimated from the rates of [^{3}H]leucine incorporation (Smith and Azam, 1992). Triplicate 1.5-mL sample aliquots and a 5 % TCA-fixed control were incubated with a mixture of [^{3}H]leucine (Amersham Biosciences, Buckinghamshire, UK; specific activity 160 Ci mmoL^{-1}) and nonradioactive leucine at a previously determined saturating concentration of 83 nM and 483 nM for environmental samples and suspensions of bacterial isolates, respectively. Samples were incubated in the dark at *in situ* temperatures for 1 h. Incubations were stopped by the addition of TCA (Sigma, St. Louis, MO, USA) to a final concentration of 5 %; then, the samples were centrifuged at 16,000 ×*g* for 10 min (Thermo Scientific Heraeus Pico 21 Microcentrifuge, Hamburg, Germany). The supernatant was discarded, and 1.5 mL of 5 % TCA was added. The mixture was vortexed, centrifuged and the supernatant was discarded. The pellet was washed with 90 % ethanol, dried overnight at room temperature and resuspended in 1.0 mL Universol liquid scintillation cocktail (ICN Biomedicals, USA). The radioactivity incorporated into bacterial cells was measured

after 3 days in a Beckman LS 6000 IC Liquid Scintillation Counter (Beckman Coulter, Inc., USA).

Statistical analysis

All experiments were repeated in three independent assays, and parameters were always determined in triplicate. Differences between treatments were assessed by a one-way ANOVA using the statistical software SPSS version 17.0 (SPSS Inc, Chicago IL). The Levene test was used to assess homogeneity of variances. If variances were not homogeneous, the natural logarithm transformation was applied. If variances were still not homogenous, a non-parametric Mann-Whitney test was used to assess the overall effect of treatment.

Results

Water properties

The physical, chemical and biological properties of the original samples of bacterioneuston and bacterioplankton are summarized in Table 9.1.

Table 9.1. Physical and chemical properties of original samples collected from the marine (CN) and brackish water (I6) stations. Results are expressed as the average ± standard deviation (n = 9). DIN – dissolved inorganic nitrogen. POC – particulate organic carbon. n.s. – non-significant.

	Marine-water (CN)			**Brackish-water (I6)**		
	SML	UW	p (n = 9)	SML	UW	p (n = 9)
Secchi depth (m)	-	2.5 ± 0.5	-	-	0.7 ± 0.1	-
Salinity (PSU)	28.5 ± 3.2	28.2 ± 3.9	n.s.	16.5 ± 1.9	16.0 ± 1.3	n.s.
pH	6.9 ± 0.7	7.0 ± 0.8	n.s.	7.2 ± 0.8	7.1 ± 0.8	n.s.
Temperature (ºC)	17.9 ± 1.9	18.0 ± 2.0	n.s.	13.9 ± 1.4	13.4 ± 1.7	n.s.
DIN (µM)	30.1 ± 3.4	28.7 ± 3.0	n.s.	128.8 ± 6.8	103.7 ± 7.8	0.014
Phosphate (µM)	14.8 ± 1.5	10.2 ± 0.9	0.010	17.2 ± 1.6	17.7 ± 1.9	n.s.
Silicates (µM)	13.9 ± 1.5	17.5 ± 2.2	n.s.	17.2 ± 2.1	23.7 ± 2.6	0.029
Ammonia (µM)	0.7 ± 0.1	0.6 ± 0.0	0.031	3.2 ± 0.1	2.6 ± 0.2	0.005
POC (mg L^{-1})	12.7 ± 1.3	6.7 ± 0.7	0.002	13.6 ± 1.6	9.2 ± 0.9	0.015
Chlorophyll a (µg L^{-1})	3.5 ± 0.3	2.8 ± 0.2	0.025	6.4 ± 0.4	5.5 ± 0.3	0.04
Seston (mg L^{-1})	37.5 ± 2.6	30.0 ± 2.9	0.029	66.5 ± 2.4	57.7 ± 4.5	0.04

At the marine station CN, the concentrations of phosphate (44.4 %), ammonia (22.6 %), POC (89.6 %), chlorophyll *a* (25.6 %) and seston (25.2 %) were significantly higher (1-way ANOVA, $p < 0.05$) in SML water. At the brackish water station I6, dissolved inorganic nitrogen (DIN) (24.1 %), ammonia (25.5 %), POC (47.8 %), chlorophyll *a* (15.1 %) and seston (15.3 %) were also significantly (1-way ANOVA, p <

0.05) enriched at the SML, while silicates were 27.4 % more concentrated in the UW (1-way ANOVA, $p < 0.05$). Enrichment factors are indicated in parenthesis.

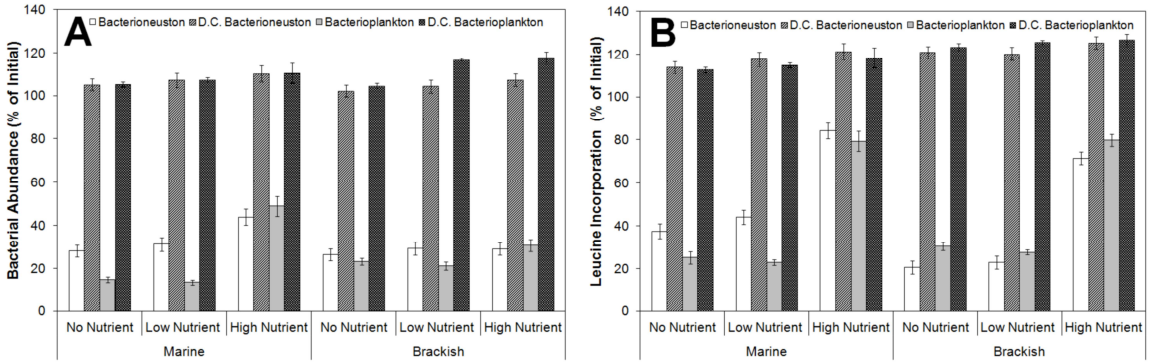

Fig. 9.2. Effects of different nutrient concentrations on (A) abundance and (B) activity (expressed as leucine incorporation) of bacterioneuston and bacterioplankton of marine and brackish origin. Data are presented as the group means ± standard deviations of the mean of three experiments. The absence of error bars indicates that standard deviations are too small to see on the scale used. D.C. – Dark control.

Table 9.2. One-way ANOVA results (p value, n = 9) for the comparisons between different nutrient treatments and suspension media in each community from the two estuarine sites. AMS – Artificial Mineral Solution. LNC – low nutrient concentration. HNC – high nutrient concentration. SML – surface microlayer. UW – underlying water. n.s. – non-significant.

			Marine		**Brackish**	
			Bacterioneuston	*Bacterioplankton*	*Bacterioneuston*	*Bacterioplankton*
Experiment 1: Influence of nutrients	*Abundance*	AMS x LNC	n.s.	n.s.	n.s.	n.s.
		AMS x HNC	0.009	0.000	n.s.	0.041
		LNC x HNC	0.017	0.000	n.s.	0.013
	Activity	AMS x LNC	n.s.	n.s.	n.s.	n.s.
		AMS x HNC	0.001	0.000	0.000	0.001
		LNC x HNC	0.002	0.000	0.000	0.000
Experiment 2: Influence of the type of suspension medium	*Abundance*	AMS x SML	0.030	0.010	n.s.	0.004
		AMS x UW	n.s.	0.026	n.s.	n.s.
		SML x UW	n.s.	n.s.	n.s.	0.004
	Activity	AMS x SML	0.007	0.001	0.045	0.045
		AMS x UW	0.040	0.006	n.s.	n.s.
		SML x UW	n.s.	0.030	0.044	0.031

Influence of nutrient amendments on UVB effects on bacterioneuston and bacterioplankton

For marine bacterioneuston, the effects of UV exposure on bacterial abundance and activity after amendment with a low nutrient concentration were not significantly different from those observed in AMS (1-way ANOVA, $p > 0.05$). The amendment with a high nutrient concentration attenuated the UV-induced reduction in abundance and activity by 15.6 and 46.7 % (1-way ANOVA, $p < 0.05$), respectively, compared to the effects in AMS (Fig. 9.2 A, B, Table 9.2). For marine bacterioplankton, the effects of UV exposure on bacterial abundance and activity after amendment with a low nutrient

concentration were also not significantly different from those observed in AMS. The amendment with a high nutrient concentration attenuated the UV-induced reduction in bacterial abundance and activity by 34.2 and 54.4 % (1-way ANOVA, $p < 0.05$), respectively, compared to the effects on AMS (Fig. 9.2 A, B, Table 9.2).

Marine bacterioplankton in AMS suspensions and in low nutrient concentration dilution cultures was significantly more affected by irradiation than marine bacterioneuston, in terms of both cell abundance (up to 17.8 %) and leucine incorporation (up to 21.4 %) (1-way ANOVA, $p < 0.05$) (Fig. 9.2 A, B, Table 9.3).

Table 9.3. One-way ANOVA results (p value, n = 9) for the comparisons between the responses of bacterioneuston and bacterioplankton to the different treatments. AMS – Artificial Mineral Solution. LNC – low nutrient concentration. HNC – high nutrient concentration. SML – surface microlayer. UW – underlying water. n.s. – non-significant.

		Experiment 1: Influence of nutrients					
		Marine			**Brackish**		
		AMS	*LNC*	*HNC*	*AMS*	*LNC*	*HNC*
Bacterioneuston x Bacterioplankton	Abundance	0.003	0.001	n.s.	n.s.	0.017	n.s.
	Activity	0.013	0.002	n.s.	0.013	n.s.	n.s.
		Experiment 2: Influence of the type of suspension medium					
		Marine			**Brackish**		
		AMS	*SML*	*UW*	*AMS*	*SML*	*UW*
	Abundance	0.006	0.015	0.019	0.001	0.008	0.001
	Activity	0.001	0.003	0.002	0.049	n.s.	0.035

For brackish water bacterioneuston, the effects of the different nutrient treatments on the variation of bacterial abundance upon UV irradiation were not significantly different from those observed in AMS (1-way ANOVA, $p > 0.05$). The amendment with a low nutrient concentration also did not significantly affect the inhibition of bacterial activity during irradiation (1-way ANOVA, $p > 0.05$) compared to the AMS treatment, while the amendment with a high nutrient concentration attenuated the inhibition of bacterial activity by 51.8 % (Fig. 9.2 A, B, Table 9.2). For brackish bacterioplankton, the amendment with a low nutrient condition did not significantly affect the reduction in bacterial abundance and activity during irradiation (1-way ANOVA, $p > 0.05$) compared to AMS dilution cultures, while the high nutrient treatment attenuated UV effects on bacterial abundance and activity by 7.3 and 50.1 %, respectively, compared to the AMS treatment (Fig. 9.2 A, B, Table 9.2).

In AMS suspensions, the effects of irradiation in terms of abundance were similar in brackish bacterioneuston and bacterioplankton (1-way ANOVA, $p > 0.05$), but bacterial activity was 7.1 % less inhibited in bacterioplankton than in

bacterioneuston (1-way ANOVA, $p < 0.05$). Under the low nutrient regime, bacterial abundance was 8.2 % less inhibited by UV exposure in bacterioneuston than in bacterioplankton (1-way ANOVA, $p < 0.05$), while the effects on activity were not significantly different between the two communities. In the high nutrient treatment, the effects of UV exposure on bacterioneuston and bacterioplankton were similar (1-way ANOVA, $p > 0.05$) (Fig. 9.2 A, B, Table 9.3).

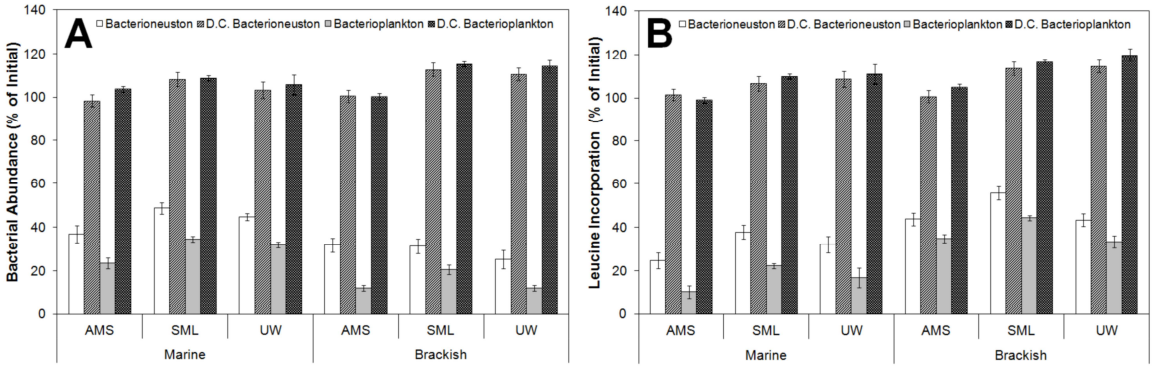

Fig. 9.3. Effects of irradiation on different media (AMS – artificial mineral solution, SML – surface microlayer, and UW – underlying water) on (A) abundance and (B) activity (expressed as leucine incorporation) of bacterioneuston and bacterioplankton of marine and brackish origin. Data are presented as the group means ± standard deviations of the mean of three experiments. The absence of error bars indicates that standard deviations are too small to see on the scale used. D.C. – Dark control.

Influence of dissolved components of the suspension medium

To test the influence of the suspension medium on UV-induced damage, samples of marine and brackish bacterioneuston and bacterioplankton were diluted in water from the SML and UW of the corresponding origin sites, and their UV sensitivity responses were compared to those observed in AMS suspensions.

For marine bacterioneuston, inoculation in SML water attenuated the UV-induced reduction in bacterial abundance and activity by 11.8 and 13.2 % (1-way ANOVA, $p < 0.05$), respectively, compared to samples in AMS. Inoculation in UW did not affect bacterial inactivation but attenuated the reduction of activity during irradiation by 7.4 % compared to the AMS treatment. The variation of abundance and activity was similar in SML and UW cell suspensions (Fig. 9.3 A, B, Table 9.2). For marine bacterioplankton, significant (1-way ANOVA, $p < 0.05$) attenuations in the reduction in bacterial abundance (up to 11.1 %) and activity (up to 12.0 %) during irradiation were observed upon inoculation in SML and UW compared to AMS (Fig. 9.3 A, B, Table 9.2).

For brackish bacterioneuston, significant differences in terms of inactivation between the different suspension media were not observed. Inoculation in SML attenuated the UV-induced reduction in activity by 12.0 % (1-way ANOVA, $p < 0.05$) compared to AMS dilution cultures, whereas the reduction in activity in samples inoculated in UW and AMS was not significantly different (Fig. 9.3 A, B, Table 9.2). For brackish bacterioplankton, inoculation in SML attenuated the UV-induced reduction in abundance and activity by 8.4 and 9.6 %, respectively, compared to the AMS treatment, whereas inoculation in UW did not significantly affect the reduction in abundance and activity compared to the dilutions in AMS (Fig. 9.3 A, B, Table 9.2).

In marine and brackish water samples, the inhibition of bacterial abundance and activity by UV radiation was generally higher in bacterioplankton than in bacterioneuston by up to 19.9 and 15.7 %, respectively (Fig. 9.3 A, B, Table 9.3).

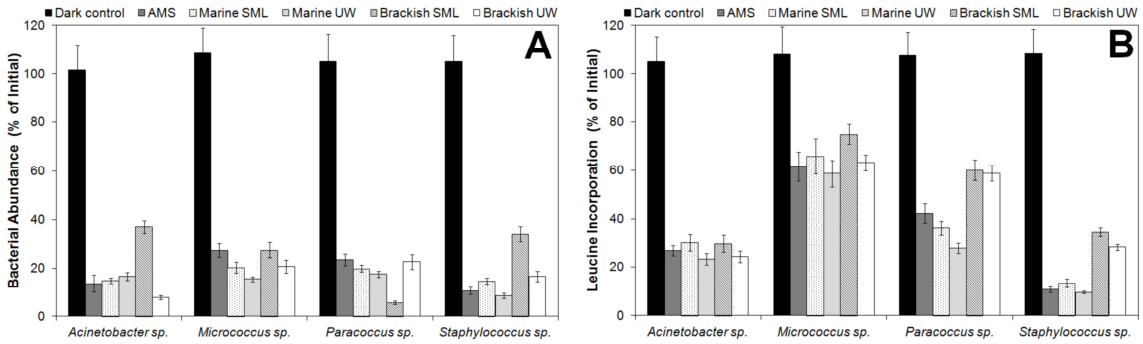

Fig. 9.4. Effects of irradiation on different media (AMS – artificial mineral solution, SML – surface microlayer, and UW – underlying water) on (A) abundance and (B) activity (expressed as leucine incorporation) in bacterial isolates. Data are presented as the group means ± standard deviations of the mean of three experiments. The absence of error bars indicates that standard deviations are too small to see on the scale used.

Bioassays with bacterial isolates

To address the interspecies variability of the effects of the suspension medium on UV sensitivity, four bacterial isolates were tested for their photobiological responses upon inoculation in AMS and in marine or brackish water of the SML or UW. Dark controls were included for all treatments but are not shown in the figures for simplicity because these controls were not significantly different (1-way ANOVA, $p > 0.05$) from the dark controls performed in AMS.

Depending on the isolate, inactivation compared to that observed in AMS ranged from 4.0 % less to 7.0 % more in marine SML water, from 3.0 % less to 11.7 % more in marine UW, from 23.1 % less to 17.8 % more in brackish SML water and from 5.9 %

less to 6.7 % more in brackish UW (Fig. 9.4 A, see Table 9.4 for statistical significance).

Similar results were observed for leucine incorporation. Compared to the AMS treatment, the effects of irradiation in different media on UV-induced inhibition of leucine incorporation ranged from a 4.3 % attenuation to a 6.2 % enhancement for marine SML, from a 1.2-14.6 % enhancement for marine UW, from a 3.0-23.6 % attenuation for brackish SML and from a 2.4 % enhancement to a 17.5 % attenuation for brackish UW (Fig. 9.4 B, see Table 9.4 for statistical significances).

Table 9.4. One-way ANOVA results (p value, n = 9) for the comparisons between the responses of the different treatments in each bacterial strain tested. AMS – Artificial Mineral Solution. M_{SML} – Marine surface microlayer. M_{UW} – Marine underlying water. B_{SML} – Brackish surface microlayer. B_{UW} – Brackish underlying water. n.s. – non-significant.

		AMS x M_{SML}	**AMS x M_{UW}**	**AMS x B_{SML}**	**AMS x B_{UW}**
Abundance	*Acinetobacter* sp.	n.s.	n.s.	0.001	0.003
	Micrococcus sp.	0.023	0.003	n.s.	0.029
	Paracoccus sp.	n.s.	0.027	0.000	n.s.
	Staphylococcus sp.	0.020	n.s.	0.000	0.007
Activity	*Acinetobacter* sp.	n.s.	n.s.	n.s.	n.s.
	Micrococcus sp.	n.s.	n.s.	n.s.	n.s.
	Paracoccus sp.	n.s.	0.008	0.014	0.018
	Staphylococcus sp.	n.s.	n.s.	0.000	0.001

Discussion

The effects of UV exposure on marine microorganisms are influenced by several environmental and biological factors. In the present work, we compared the influence of the availability of inorganic nutrients and the type of the suspension medium on the UV responses of estuarine bacterial communities that are naturally exposed to different nutrient and light regimes (bacterioneuston and bacterioplankton) and that originate from different sites within an estuary (marine and brackish water). The variability of the effects of the suspension medium on different bacterial isolates was also assessed.

Effects of nutrient concentration

Inhibition by UV radiation, in terms of abundance and activity, was generally attenuated when the suspension medium was amended with high nutrient concentrations (40 µM NH_4^+ and 4 µM PO_4^{3-}). Repair processes elicited in response to UVR require nitrogen for synthesis of proteins involved in DNA repair and ROS scavenging and thus can potentially be inhibited by a limitation in nitrogen supply (Beardall et al., 2009). These repair processes are also energy dependent, requiring ATP, and are consequently

susceptible to limitation in the supply of organic matter and inorganic phosphorus (Beardall et al., 2009). Our results indicate that the high nutrient amendments may have provided sufficient amounts of the elements required for nucleic acid and protein synthesis, including those involved in repair of UV-induced damage, which were likely not fulfilled with the low nutrient regime. Such observations are in accordance with previous reports of the ability of nutrient inputs to promote recovery from UV-induced damage (Joux et al., 2009).

In general, under the unamended (AMS) and low nutrient conditions, bacterioneuston was more resistant to UV inactivation than bacterioplankton. The differences in UV sensitivity of the two communities, particularly of those originating from the brackish water site, were attenuated upon amendment with high nutrient concentrations. Rapidly growing cells are considered to be more sensitive to inactivation than slow growing cells due to the shorter time interval required for excision repair between subsequent rounds of replication (Harm, 1980; Jagger, 1985). In the original samples, bacterioplankton growth rates, estimated from bacterial secondary production and bacterial biomass (Hernández et al., 2006), were up to 25 % higher than those of bacterioneuston (data not shown). Leucine incorporation is also enhanced at the UW, though bacterial abundance is higher in the SML (Lindroos et al., 2011; Santos et al., 2012b). The higher growth rates of bacterioplankton could be a contributing factor for its higher susceptibility to UVR observed in the present work and previous reports (Santos et al., 2011a; Santos et al., 2012b). Low bacterial growth rates at the SML have been reported by other authors and attributed to the low lability of dissolved organic compounds (*e.g.*, free amino acids) accumulating in this layer (Reinthaler et al., 2008). Taken together, these observations may suggest that bacterial cells at the SML are intrinsically adapted to nutritional stress and thus are less affected in their UV sensitivity by variations in nutrient concentrations. This finding is in agreement with our previous observations of the enhanced ability of starved bacterioneuston isolates to recover from UV-induced damage compared to bacterioplankton isolates in the same nutritional conditions (Santos et al., 2012a).

Differences in the community composition of bacterial assemblages from the SML and UW at the oligotrophic and mesotrophic estuarine sites may also account for the differences in the observed responses. Marine and brackish water bacterial communities from Ria de Aveiro (Portugal) are physiologically (Almeida et al., 2001) and structurally (Henriques et al., 2006a) distinct. Bacterioneuston and bacterioplankton

community structure in this estuary also seems to differ, as suggested by the occurrence of SML-specific bacterial members affiliated with *Actinobacteria*, Cyanobacteria, *Gammaproteobacteria* and Bacteroidetes (Azevedo et al., 2012), as well as the dominance of the UV-resistant *Gammaproteobacteria* in bacterioneuston (Santos et al., 2012b).

Influence of dissolved components of the suspension medium

The influence of dissolved components of the suspension media on the UV-induced effects on bacterial communities was tested by inoculating bacterial assemblages in cell-free water from the SML or UW. The effects of irradiation on bacterial numbers and activity were monitored and compared to those observed in an artificial medium (AMS). For marine communities of bacterioneuston and bacterioplankton, suspension in SML and UW attenuated the inhibitory effects of UV radiation. In brackish water bacterial communities, the UV-induced effects on abundance and activity were generally attenuated upon suspension in SML water.

Attenuation of the inhibitory effects of UV exposure in bacterial communities irradiated in SML and/or UW compared to the AMS treatment may be due to stimulation of bacterial metabolism by low molecular weight compounds resulting from the photolytic cleavage of DOM present in environmental samples (Amador et al., 1989; Bushaw et al., 1996; Moran and Zepp, 1997; Bertilsson and Tranvik, 1998; Obernosterer et al., 1999), thus compensating for the direct negative effects of irradiation. Furthermore, natural environmental samples could have provided the cells with nutrients necessary for the synthesis of repair proteins (Beardall et al., 2009), allowing them to cope with the effects of irradiation better than those maintained in AMS. Finally, a shield and quenching effect of DOC and humic materials present in the environmental samples (Muela et al., 2000; Bracchini et al., 2005) may have also mitigated the inhibitory effects of irradiation in samples diluted in SML and/or UW, compared to samples in AMS. Together, these results demonstrate that the medium in which bacteria are suspended influences the effects of UV radiation and also suggest the importance of the SML and UW abiotic environments in determining the UV responses of the corresponding bacterial communities.

Additionally, to gain further insights into the influence of the irradiating medium on UVR sensitivity, bioassays were also conducted with individual isolated strains. Bacterial isolates were inoculated in different suspension media, and variations of

abundance and activity with irradiation were determined. The responses of the different isolates to the tested treatments were widely variable, either protecting or accentuating the inhibitory effects of UVB, depending on the suspension medium and the isolate. However, in general, brackish SML water attenuated the inhibitory effects of UVR on cell activity. The protective effect of inoculation in brackish water may have resulted from a shield effect of organic matter and humic compounds concentrated in these samples and/or from the enhanced production of low molecular weight compounds from the phototransformation of DOM that was used for bacterial growth (Amador et al., 1989; Bushaw et al., 1996; Moran and Zepp, 1997; Bertilsson and Tranvik, 1998; Obernosterer et al., 1999; Muela et al., 2000; Bracchini et al., 2005).

The variability in the effects of the suspension media in UV-induced inactivation and inhibition of activity observed in the different isolates may be attributed to interspecies differences in protection and repair mechanisms (Fernández Zenoff et al., 2006b; Santos et al., 2011b). Alternatively, differences in the ability to use the products of phototransformation of DOM for bacterial growth can also contribute to the variable effects that each suspension medium exerted on the different bacterial isolates. For example, *Gammaproteobacteria* are negatively affected by the photochemical alteration of cDOM or outcompeted by the other bacterial groups during phototransformation experiments (Piccini et al., 2009), and *Actinobacteria* are favoured under those circumstances (Pérez and Sommaruga, 2007).

These results indicate that the suspension medium in which bacteria are irradiated is important for determining the biological consequences of UV exposure, which likely depend on the compromise between the protective effects of organic matter, the stimulatory effects of UV radiation mediated by the photolysis of organic matter and the oxidative stress imposed by ROS generated during the process.

Conclusions

The availability of inorganic nitrogen and phosphorus, as well as the overall composition of the medium in which cell suspensions for irradiation experiments were prepared, influenced the UV effects on bacterial abundance and activity. Nutrient amendment attenuated the inhibitory effects of UV exposure. Attenuation of the inhibitory effects of irradiation was also observed when cells were suspended in water from the SML and/or UW, compared to AMS. This effect likely occurs as a consequence of photoreactions resulting in the formation of low molecular weight

compounds that promote bacterial growth or a shield effect by humic material present in natural samples that compensates for the detrimental effects of UVR. These results demonstrate that the role of UVR as an environmental regulator of the abundance and activity of aquatic bacteria is modulated by interactions with abiotic water properties and can vary significantly in different aquatic niches.

Acknowledgments

Financial support for this work was provided by CESAM (Centre for Environmental and Marine Studies, University of Aveiro) and the Portuguese Foundation for Science and Technology (FCT) in the form of a PhD grant to A.L. Santos (SFRH/BD/40160/2007) and a post-Doctoral grant to I. Henriques (SFRH/BPD/63487/2009).

PÁGINA INTENCIONALMENTE DEIXADA EM BRANCO

CHAPTER 10

Growth Conditions Influence UVB Sensitivity and Oxidative Damage in an Estuarine Bacterial Isolate

Santos A. L., Gomes N. C. M., Henriques I., Almeida A., Correia A., Cunha A.

Photochemical & Photobiological Sciences (accepted)

Abstract

The dose-dependent variation of oxidative cellular damage imposed by UVB exposure in a representative estuarine bacterial strain, *Pseudomonas* sp. NT5I1.2B, was studied at different growth phases (mid-exponential, late-exponential, and stationary), growth temperatures (15 ºC and 25 ºC) and growth media (nutrient-rich Tryptic Soy Broth [TSB] and nutrient-poor M9). Survival and markers of oxidative damage (lipid peroxidation, protein carbonylation, DNA strand breakage, and DNA-protein cross-links) were monitored during exposure to increasing UVB doses (0-60 kJ m^{-2}).

Oxidative damage did not follow a clear linear dose-dependent pattern, particularly at medium-high UVB doses (> 10 kJ m^{-2}), suggesting a dynamic interaction between damage induction and repair during irradiation and/or saturation of oxidative damage. Survival of stationary phase cells generally exceeded that of exponential phase cells by up to 33.5 times; the latter displayed enhanced levels of DNA-protein cross-links (up to 15.6-fold) and protein carbonylation (up to 6.0-fold). Survival of mid-exponential phase cells was generally higher at 15 ºC than at 25 ºC (up to 6.6-fold), which was accompanied by lower levels of DNA strand breaks (up to 4,000-fold), suggesting a temperature effect on reactive oxygen species (ROS) generation and/or ROS interaction with cellular targets. Survival under medium-high UVB doses (> 10 kJ m^{-2}) was generally higher (up to 5.4-fold) in cells grown in TSB than in M9.

These results highlight the importance of growth conditions preceding irradiation on the extent of oxidative damage induced by UVB exposure in bacteria.

Introduction

Bacteria are highly susceptible to solar radiation, particularly in the UV range, due to their small size, short generation time, and the fact that their genetic material comprises a significant portion of their cellular volume (Garcia-Pichel, 1994).

The main biological effects of UVB radiation (280-320 nm) have traditionally been attributed to its ability to induce direct DNA damage (DNA photoproducts), most notably cyclobutane pyrimidine dimers and pyrimidine (6-4) pyrimidone photoproducts (Mitchell and Karentz, 1993). However, the observation of the accumulation of similar levels of DNA photoproducts in bacteria with distinct UV sensitivities (Joux et al., 1999; Matallana-Surget et al., 2008) and the fact that DNA damage alone cannot account for the inhibitory effects of UV radiation on bacteria inhabiting surface waters (Visser et al., 2002) suggest that UV-induced damage to other biomolecules, particularly lipids and proteins, may play a role in the inhibitory effects of UV radiation on bacteria.

The action spectrum for UV effects does not correlate with the absorption spectrum of lipids. Therefore, UV-induced damage to lipids is likely to be a result of indirect oxidative damage mediated by reactive oxygen species (ROS) (Girotti, 2001). Proteins are also key targets of photosensitized damage, which may cause functional changes in structural and enzymatic proteins (Bosshard et al., 2010b). Proteins that contain iron as a prosthetic metal are particularly noteworthy targets of oxidation through the Fenton reaction, being readily oxidizable by hydrogen peroxide (Beyer and Fridovich, 1991; Tamarit et al., 1998; Murakami et al., 2006). Besides direct damage, DNA can also be damaged by ROS generated during photosensitized reactions, resulting in the formation of strand breaks, alkali-labile sites, and DNA-protein cross-links (Mitchell, 1995).

The importance of oxidative damage in UVB-induced bacterial inactivation has recently been highlight in studies directly quantifying oxidative stress markers during irradiation in a set of estuarine bacterial isolates (Santos et al., 2013), as well as studies reporting enhanced levels of transcripts and proteins involved in the response to oxidative stress upon UVB exposure in *Shewanella oneidensis* MR-1 and *Photobacterium angustum* S14 (Qiu et al., 2005a; Matallana-Surget et al., 2012). Contrary to DNA dimers, which can be effectively reversed by photoreactivation, oxidative damage resulting from ROS overproduction upon UVB exposure is more difficult and energetically expensive to repair (Halliwell and Gutteridge, 1999). These

observations make the study of UVB-induced oxidative damage in bacteria, and the factors that influence it, of utmost importance.

It is well known that the biological response of microorganisms to UV radiation is influenced by multiple intrinsic and extrinsic factors. Among extrinsic or environmental factors, temperature, nutrient concentration, and light availability have all been shown to affect the biological responses of microorganisms to UV radiation by affecting light penetration and/or the physiological condition of cells, with variable results (Pausz and Herndl, 2002; Bullock and Jeffrey, 2010; Matallana-Surget et al., 2010). For example, the effects of increased temperature on UV sensitivity have been reported to be non-significant in *Escherichia coli* (Gayán et al., 2011), protective in bacterioplankton (Bullock and Jeffrey, 2010), and detrimental in *Sphingopyxis alaskensis* (Matallana-Surget et al., 2010).

Intrinsic properties of microorganisms also influence the biological consequences of UV exposure. For example, cell size, by affecting the pathway of light penetration, seems to contribute to the vulnerability for DNA damage accumulation in planktonic organisms, with smaller cells displaying higher levels of DNA damage (Karentz et al., 1991; Garcia-Pichel, 1994; Buma et al., 2001). Cell-specific growth rate is also a key determinant of the effects of UVA (Berney et al., 2006c) and UVC exposure in *E. coli* (Bucheli-Witschel et al., 2010). UVA effects have also been found to depend on the growth phase, with stationary phase cells recovering faster and being more resistant to the lethal effects of irradiation than exponential growing cells (Dantur and Pizarro, 2004). Other authors have reported that, at least in *S. alaskensis*, the growth phase does not affect total DNA photoproduct formation during exposure to simulated solar radiation (Matallana-Surget et al., 2010). However, to our knowledge, studies on the influence of intrinsic and extrinsic properties on UVB-induced oxidative damage in bacteria are virtually nonexistent.

The present work aimed to study the influence of the growth conditions of cells (growth phase, growth temperature and growth medium) and light dose on UVB-induced oxidative damage to DNA, lipids, and proteins in bacteria.

Materials and methods

Bacterial strain and growth conditions

The bacterial strain used in this study (*Pseudomonas* sp. strain NT5I1.2B, NCBI accession number GU084169) was isolated from the surface waters of the estuarine

system of Ria de Aveiro (Portugal) (Santos et al., 2011b). This strain shows a 98 % 16S rRNA gene similarity with the hexazinone-degrading *Pseudomonas kuykendallii* strain H2A and a 97 % 16S rRNA gene similarity with *Pseudomonas putida* strain DAPG5. *Pseudomonas* sp. strain NT5I1.2B shows a minimal growth temperature of 9±1 ºC and a maximal growth temperature of 37±1 ºC. The optimal growth temperature of the strain is 27±1 ºC (data not shown). A *Gammaproteobacteria* strain was selected because this lineage seems to dominate UV-exposed surface waters and has been proposed to be UV-resistant (Franklin et al., 2005; Alonso-Sáez et al., 2006; Santos et al., 2012b). Furthermore, *Pseudomonas* strains seem to be particularly enriched in the sunlit surface microlayer of the Ria de Aveiro estuary which could suggest enhanced resistance of the genera to environmental stress factors at the estuarine water surface, particularly enhanced UV levels (Azevedo et al., 2012; Santos et al., 2012b). Finally, the resistance and repair mechanisms of the *Pseudomonas* genus have been well studied (Kokjohn and Miller, 1985; Simonson et al., 1990; Kokjohn and Miller, 1994; Kidambi et al., 1996).

The strain was grown in either nutrient-rich Tryptic Soy Broth (TSB, Difco Laboratories, Detroit, Mich.) or nutrient-poor M9 medium (22 mM KH_2PO_4, 42 mM Na_2HPO_4, 19 mM NH_4Cl, 9 mM NaCl, 1 mM $MgSO_4$ and 0.09 mM $CaCl_2$, pH 6.8, containing 5.5 mM glucose as a carbon source) adjusted to 36 PSU (Practical Salinity Units) at 15 ºC or 25 ºC with agitation (120 rpm). The temperatures 15 ºC or 25 ºC were chosen because they represent the approximate maximum and minimum temperatures detected in the estuarine system of Ria de Aveiro throughout the year (Santos et al., 2011c). Aliquots were collected at pre-determined intervals and the absorbance at 600 nm (OD_{600}) was measured in a Thermo Spectronic Genesys 10 UV spectrophotometer (Thermo Fisher Scientific SL, Alcobendas, Spain) and used to construct the respective growth curves. Cells in the mid-exponential phase, late-exponential phase and stationary phase grown in the different media and at different temperatures were used for subsequent irradiation experiments. These growth phases were chosen because they correspond to the growth phases that have most commonly been used in studies of UV effects on bacteria (Joux et al., 1999; Arrieta et al., 2000; Qiu et al., 2004; Agogué et al., 2005; Fernández Zenoff et al., 2006b; Hörtnagl et al., 2011; Santos et al., 2011b; Santos et al., 2012a).

Total bacterial number (TBN) and cell biovolume

Cells in the different growth conditions were characterized in terms of total bacterial number (TBN) and biovolume. For the determination of TBN, samples were filtered through 0.2-µm-pore-size black polycarbonate membranes (Poretics, Livermore, CA, USA), and stained with 0.03 % (w/v) acridine orange (Hobbie et al., 1977). Cells were counted by epifluorescence microscopy using a Leitz Laborlux K microscope (Leitz Meβtechnik, Wetzlar, Germany) equipped with a I 2/3 filter for blue light. At least 200 cells or 20 microscope fields were counted in each of three replicate membranes per sample.

Cell biovolume was determined on acridine orange-stained preparations by epifluorescence microscopy by using an ocular grid with black and transparent circles. For cell volume calculations, bacteria were assumed to represent cylinders with hemispherical ends (Jürgens and Jeppesen, 2000).

Irradiation conditions

Cells in the different growth conditions were harvested by centrifugation (3,200 x *g* for 15 min, Thermo Scientific Heraeus Pico 21 Microcentrifuge, Hamburg, Germany), washed and resuspended in 0.2-µm-pore-size-filtered autoclaved 0.9 % NaCl solution and bacterial abundance was adjusted with filtered autoclaved 0.9 % NaCl to 10^6 cells mL^{-1}.

Cell suspensions (30 mL, corresponding, on average, to a biomass of approximately 1 mg mL^{-1} of protein) were transferred to sterile Petri dishes (150 x 25 mm; Corning) and irradiated (without the lid) under UVB (Philips TL 100 W/01 lamps, main emission line of 302 nm). Suspensions were stirred during irradiation using a magnetic stirrer. UV sources were placed at 20 cm from the sample. UV intensities were measured with a monochromator spectro-radiometer (DM 300, Bentham Instruments, Reading, UK) placed at the sample level. The UV intensity during irradiations corresponded to 2.3 W m^{-2}. The UV dose (in J m^{-2}) was calculated by multiplying the intensity by the irradiation time (in seconds). A cumulative dose of 60 kJ m^{-2} was applied. Aliquots of cell suspensions were collected at pre-determined doses (0, 2, 4, 6, 8, 10, 20, 30, 40, 50 and 60 kJ m^{-2}) to construct the inactivation curves and for oxidative stress marker analysis and immediately reserved at 4 ºC in order to avoid cell recovery. During irradiation, temperatures were kept at 15 ºC or 25 ºC, depending on the growth temperature of the treatment being considered. Cell homogenates for protein content

and protein carbonyl levels analysis were prepared by collecting cells by centrifugation immediately after irradiation, resuspending them in cold 50 mM potassium phosphate buffer (pH 7.8) containing 1 mM EDTA, followed by sonication in ice (Branson Instruments Co. Sonifier, Stamford, Conn.; 2 min, 30-s pulses, 1-min cooling). Homogenates were stored at -80 ºC until the measurements. Positive (H_2O_2-treated) and negative (untreated) controls were always included and processed along experimental samples in order to ensure proper functioning of the procedures. All experiments were repeated in three independent assays and biochemical and microbiological analysis were always conducted in triplicate. All the procedures were conducted under low-luminosity conditions to minimize photoreactivation. All reagents were purchased from Sigma-Aldrich (St Louis, MO), unless otherwise specified.

Colony formation assay

Control and irradiated sample aliquots collected at different UVB doses were serially-diluted in filter-sterilized, autoclaved 0.9 % NaCl and spread-plated in triplicate in the solid medium corresponding to the one used to prepare cell suspensions (*i.e.*, either Tryptic Soy Agar or agarized M9 medium). After 3 days of incubation in the dark at 15 ºC or 25 ºC, depending on the treatment, colonies were counted. Survival was calculated from the ratio between the number of colony forming units (CFU) after irradiation and at time zero.

DNA strand breakage

DNA strand breaks (DSB) were quantified using a modified version of the FADU (Fluorimetric Analysis of DNA Unwinding) method, as previously described (He and Häder, 2002). The procedure requires two sets of untreated control samples, besides test samples (so-called P-samples): samples not subjected to alkaline unwinding (T-samples) and samples subjected to complete alkaline unwinding (B-samples). Briefly, cells were collected by centrifugation (3,000 x *g*, 15 min) and treated with lysozyme (4 mg mL^{-1} final concentration) and proteinase K (0.25 mg mL^{-1} final concentration). A volume of 300 µL of 0.1 M NaOH was then added to the three sets of samples: (1) T-samples were immediately neutralized with 300 µL of 0.1 M HCl, followed by a 30-min incubation at room temperature and sonication for 15 s; (2) B-samples were sonicated for 2 min, neutralized with 300 µL of 0.1 M HCl after a 30-min

incubation, and sonicated again for 15 s; and (3) P-samples were incubated for 30 min, neutralized with 300 µL of 0.1 M HCl and sonicated for 15 s.

A final concentration of 5 µM of Hoechst 33258 (Sigma-Aldrich, St Louis, MO) was added to all samples. After centrifugation, the supernatant was used for fluorescence measurements ($\lambda_{ex.}$ 350 nm; $\lambda_{em.}$ 450 nm) in a Jasco FP-777 Fluorometer (Japan Spectroscopic Co., Ltd., Tokyo, Japan). Data were expressed as the strand scission factor (SSF), defined as SSF = -ln(Ft/F0), where Ft is the fluorescence of the treated sample at time t and F0 is the fluorescence of the sample at time 0 (Baumstark-Khan and Horneck, 2007).

DNA-protein cross-links

DNA-protein cross-links (DPC) were determined as previously described (Nguyen et al., 2000). Briefly, control and irradiated samples were treated with 1 % SDS (sodium dodecyl sulfate) and 1 M NaCl. After vigorous vortexing, two volumes of chloroform:isopentyl alcohol (24:1) were added and the mixture was vortexed again. After centrifugation at 6,000 x *g* for 15 min, the absorbance at 260 nm of the aqueous phase was read in a Thermo Spectronic Genesys 10 UV spectrophotometer (Thermo Fisher Scientific SL, Alcobendas, Spain). The fraction of DNA-protein cross-linking was determined according to the equation:

$$\text{Fraction cross-linked} = (A_0 - A_t)/A_0$$

where A_0 is the absorbance of sample at time 0 and A_t is the absorbance of the treated samples at time t.

Lipid peroxidation

Lipid peroxidation was determined as the amount of thiobarbituric acid reactive substances (TBARS), as previously described (Pérez et al., 2007). Control and irradiated cells were centrifuged, washed, and suspended in 1 mL of 50 mM potassium phosphate buffer (pH 7.4). A final concentration of 0.1 mM butylated hydroxytoluene and 1 mM PMSF (phenylmethanesulfonyl fluoride) was added to prevent further lipid oxidation. After sonication and centrifugation, the soluble fraction was mixed with 1 mL of 20 % trichloroacetic acid and centrifuged at 10,000 x *g* for 5 min. The supernatant was removed and mixed with 1 mL of 0.5 % (w/v) thiobarbituric acid in 0.1 M HCl and 10 mM butylated hydroxytoluene in a new tube. After heating at 100 ºC for 1 h, 1 mL aliquots were removed, cooled at room temperature and then mixed with 1.5

mL of butanol. After centrifugation (4,000 x *g*, 10 min), the absorbance at 535 nm of the organic fraction was read in a Thermo Spectronic Genesys 10 UV spectrophotometer (Thermo Fisher Scientific SL, Alcobendas, Spain). TBARS content was determined using an extinction coefficient of 156 $mM^{-1}cm^{-1}$. Results were expressed per mg of protein.

Protein oxidation

The carbonyl content in oxidized proteins was determined as previously described (Semchyshyn et al., 2005). Aliquots of homogenates were mixed with 10 mM dinitrophenylhydrazine (DNPH) in 2 M HCl. DNPH was omitted in the blanks. After incubation at room temperature for 1 hour, proteins were precipitated with 500 µL of 20 % trichloroacetic acid. The mixture was centrifuged (14,000 x g, 5 min), and the pellet was washed three times with 1 mL of 1:1 (vol/vol) ethanol-ethyl acetate. The final precipitate was dissolved in 1 mL of 6 M guanidine hydrochloride. The absorbance at 360 nm was determined, using guanidine solution (6 M guanidine hydrochloride with 2 mM potassium phosphate) as a blank. A molar absorption coefficient of 22 $mM^{-1}cm^{-1}$ was used to quantify the levels of protein carbonyls. Results were expressed per mg of protein.

Protein concentration

Protein concentration in cell homogenates was determined by the Bradford method using BSA as a standard (Bradford, 1976).

Statistical analysis

Prior to statistical analysis, data normality was tested by the Kolmogorov-Smirnov test. Differences between treatments were assessed by 1-way ANOVA using the statistical software SPSS v.17. Levene test was used to assess homogeneity of variances. If variances were not homogeneous, the natural logarithm transformation was applied. If variances were still not homogenous, the non-parametric Mann-Whitney test was used to assess the overall effect of the treatment (Sokal and Rolf, 1995).

Results

Initial characterization of cell suspensions

The growth curve of *Pseudomonas* sp. strain NT5I1.2B under different conditions is presented in Fig. 10.1. Table 10.1 summarizes the characteristics of the cell suspensions used in the subsequent irradiation assays. Mid-exponential phase, late-exponential phase and stationary phase were achieved in 4-12 h, 6-14 h and 12-18 h, respectively. Total bacterial abundance, determined by epifluorescence microscopy, ranged between 5.2 x 10^7 and 1.4 x 10^9 cells mL^{-1} in mid-exponential phase, between 6.4 x 10^7 and 1.8 x 10^9 cells mL^{-1} in late-exponential phase and 6.6 x 10^7 and 2.0 x 10^9 cells mL^{-1} in the stationary phase. These results were consistent with CFU determinations (data not shown), suggesting that cells remained culturable under all growth conditions tested. Cell biovolume varied between 0.192-0.360 μm^3 in the mid-exponential phase, 0.390-0.740 μm^3 in the late-exponential phase and 0.529-1.266 μm^3 in the stationary phase.

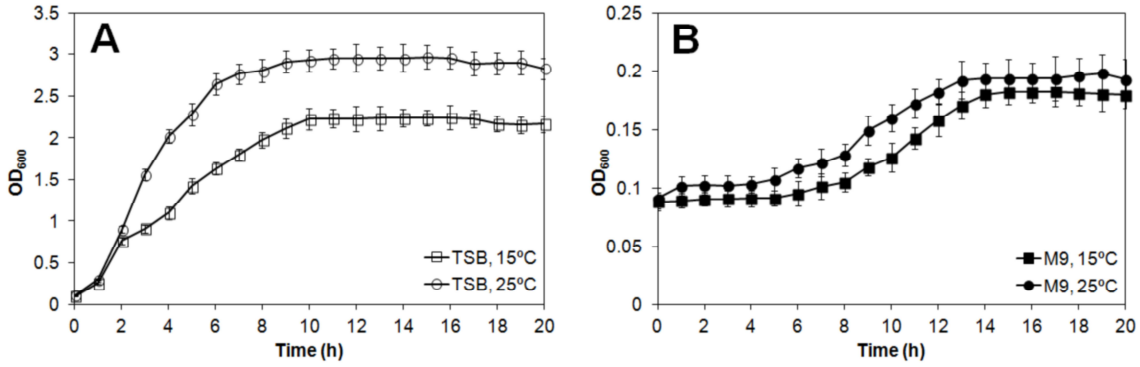

Fig. 10.1. Growth curve of *Pseudomonas* sp. NT5I1.2B cultivated at 15 ºC and 25 ºC in (A) TSB and (B) M9 medium. Results are expressed as means ± standard deviations of the mean of three experiments. Absence of error bars indicates that standard deviations are too small to see on the scale used.

Table 10.1. Initial characteristics (time to achieve a certain growth phase, optical density at 600 nm, total bacterial abundance and biovolume) of *Pseudomonas* sp. NT5I1.2B cultures under the different growth conditions. Results are expressed as average ± standard deviation of three assays.

	Mid-exponential Phase				**Late-exponential Phase**				**Stationary Phase**			
	15 ºC		**25 ºC**		**15 ºC**		**25 ºC**		**15 ºC**		**25 ºC**	
	M9	**TSB**	**M9**	**TSB**	**M9**	**TSB**	**M9**	**TSB**	**M9**	**TSB**	**M9**	**TSB**
Time (h)	12	6	11	4	14	9	13	6	18	14	18	12
OD_{600}	0.158	1.635	0.172	2.024	0.180	2.119	0.191	2.645	0.182	2.238	0.193	2.952
Abundance (x 10^7 cells mL^{-1})	5.2	110.6	6.3	139.6	6.4	145.7	7.1	183.9	6.6	154.4	7.7	203.0
Biovolume (x 10^{-1} μm^3)	1.9	3.1	2.4	3.6	3.9	4.0	4.4	7.4	5.3	10.0	9.7	13.0

Influence of light dose

UVB inactivation curves of *Pseudomonas* sp. strain NT5I1.2B under the different growth conditions are shown in Fig. 10.2. Dark controls were always performed for every growth condition tested and did not vary significantly (1-way ANOVA, $p > 0.05$) throughout the duration of the corresponding irradiation period. Therefore, only a representative dark control is shown in Fig. 10.2. The survival of *Pseudomonas* sp. in the mid-exponential phase grown in different media and at different temperatures followed a general dose-dependent variation. The percentage of cell survival at 60 kJ m^{-2} ranged between 1.8 and 11.7 % (Fig. 10.2 A). Late-exponential phase cells grown in TSB at 15 ºC and in M9 at 25 ºC showed a linear decrease in cell survival up to a cumulative dose of 10 kJ m^{-2}, after which cell survival stabilized. Cells grown in M9 at 15 ºC displayed a linear decrease in survival up to a cumulative dose of 40 kJ m^{-2} and stabilized thereafter. For cells grown in TSB at 25 ºC, survival decreased progressively up to the end of the irradiation period. The percentage of cell survival at 60 kJ m^{-2} varied between 18.4 and 52.2 % (Fig. 10.2 B).

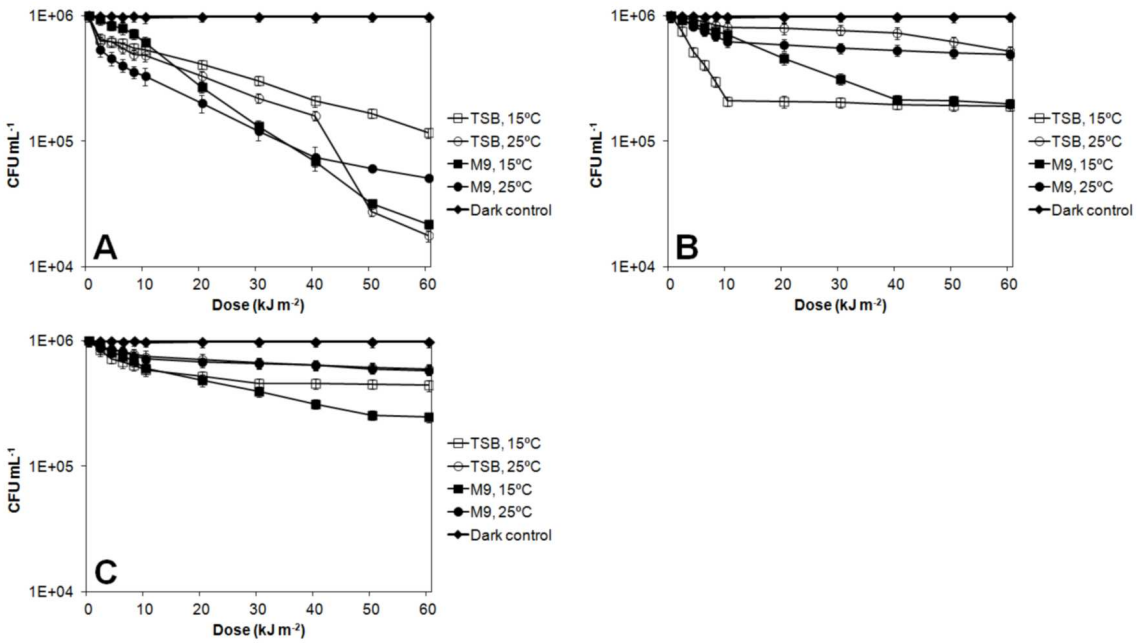

Fig. 10.2. UVB survival curves of *Pseudomonas* sp. NT5I1.2B grown at 15 ºC and 25 ºC in TSB and M9 medium in (A) mid-exponential, (B) late-exponential and (C) stationary phase. Results are expressed in log scale as means ± standard deviations of the mean of three experiments. Absence of error bars indicates that standard deviations are too small to see on the scale used.

Stationary phase cells grown in M9 at 15 ºC showed a progressive decrease in cell survival up to a cumulative dose of 50 kJ m^{-2}. The survival of cells grown in TSB at

15 ºC decreased steadily up to a cumulative dose of 30 kJ m^{-2} and stabilized afterwards. The survival of cells grown at 25 ºC in M9 and TSB varied in a dose-dependent pattern up to a cumulative dose of 60 kJ m^{-2}. Cell survival at 60 kJ m^{-2} ranged between 24.6 and 59.1 % (Fig. 10.2 C).

In late-exponential and stationary phase cells, TBARS levels varied in a dose-dependent pattern up to a cumulative UVB dose of 10 kJ m^{-2}. In general, TBARS levels peaked at 19.4-52.5 pmol/ mg of protein upon exposure to low UVB doses (2-10 kJ m^{-2}), showing different trends of variation in the period thereafter (Fig. 10.3 A-C).

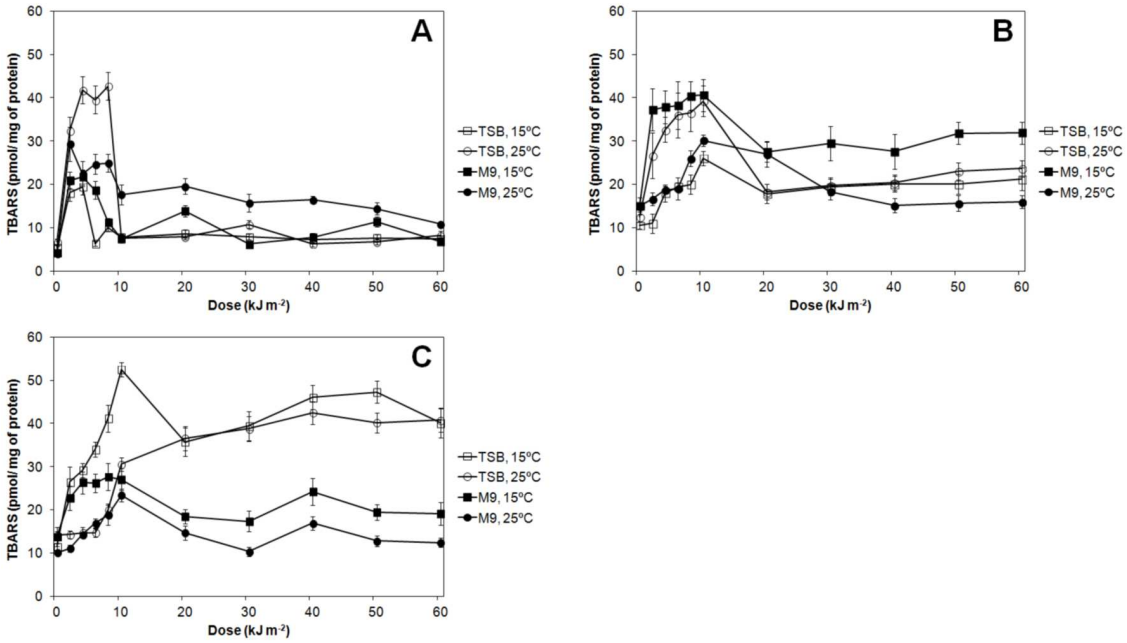

Fig. 10.3. Dose-dependent variation of TBARS levels in *Pseudomonas* sp. NT5I1.2B grown at 15 ºC and 25 ºC in TSB and M9 medium in (A) mid-exponential, (B) late-exponential and (C) stationary phase. Results are expressed as means ± standard deviations of the mean of three experiments. Absence of error bars indicates that standard deviations are too small to see on the scale used.

DNA strand breaks, expressed as SSF (strand scission factor), increased in a general dose-dependent fashion up to 10 kJ m^{-2} in all treatments. In mid-exponential phase cells, SSF peaked at 0.2-0.8 after 40 kJ m^{-2}, varying thereafter (Fig. 10.4 A). SSF in late-exponential and stationary phase cells oscillated strongly at UVB doses over 10 kJ m^{-2}, peaking at 0.3-0.8 between 30-60 kJ m^{-2} (Fig. 10.4 B, 10.4 C).

The levels of DNA-protein cross-links (DPC) also showed a general dose-dependent variation up to 10 kJ m^{-2} of UVB. For mid-exponential phase cells, DPC levels peaked at 0.3 after 10 kJ m^{-2} for cells grown in TSB at 15 ºC, and at 0.3-0.5 after a cumulative dose of 60 kJ m^{-2} for the remaining treatments (Fig. 10.5 A). For late-exponential phase cells, DPC levels peaked at 0.2-0.3 after exposure to 10 kJ m^{-2} and 50

kJ m^{-2} for cells grown in M9 and TSB, respectively (Fig. 10.5 B). Stationary phase cells showed maximum levels of DPC (0.1-0.4) after exposure to 10 kJ m^{-2} of UVB (Fig. 10.5 C).

With the exception of cells grown in TSB at 25 ºC, carbonyl levels in mid-exponential phase cells peaked (22.0-48.5 µmol/mg of protein) after exposure to 8 kJ m^{-2}, strongly decreasing afterwards and tendentially increasing again towards the end of the irradiation period (Fig. 10.6 A). In late-exponential phase and stationary phase cells, carbonyl levels generally peaked at 16.5-67.0 µmol/mg of protein at 50-60 kJ m^{-2} of UVB (Fig. 10.6 B, 10.6 C).

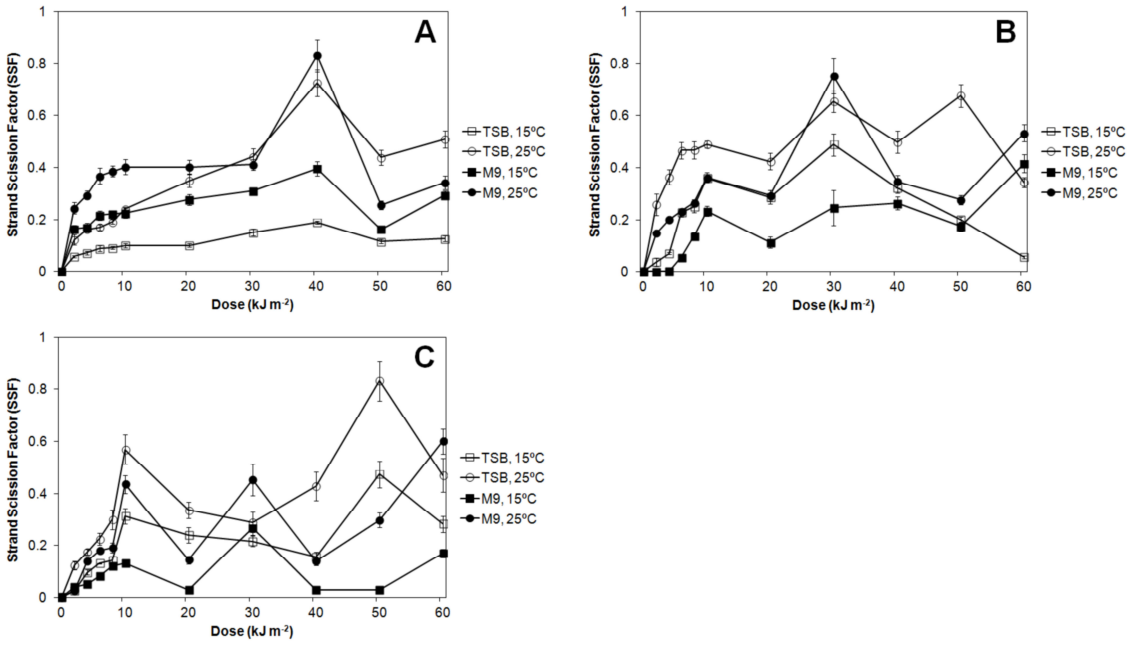

Fig. 10.4. Dose-dependent variation of DNA strand breaks (expressed as strand scission factor, SSF) in *Pseudomonas* sp. NT5I1.2B grown at 15 ºC and 25 ºC in TSB and M9 medium in (A) mid-exponential, (B) late-exponential and (C) stationary phase. Results are expressed as means ± standard deviations of the mean of three experiments. Absence of error bars indicates that standard deviations are too small to see on the scale used.

Influence of growth phase

Survival was generally enhanced in late-exponential and stationary phase cells compared to mid-exponential phase cells, by up to 33.5-fold (1-way ANOVA, $p < 0.05$) (Fig. 10.2). At medium-high UVB doses (≥ 10 kJ m^{-2}), TBARS levels were generally enhanced in late-exponential and stationary phase cells, compared to mid-exponential phase cells, by as much as 6.8-fold (1-way ANOVA, $p < 0.05$) (Fig. 10.3). Regarding DSB levels, consistent significant differences between growth phases could not be detected (Fig. 10.4). DPC levels were generally higher in exponential phase cells than in

stationary phase cells by up to 15.6 times (1-way ANOVA, $p < 0.05$) (Fig. 10.5). Carbonyl levels showed the same trend, being up to 6-fold higher in exponential phase cells than in stationary phase cells (1-way ANOVA, $p < 0.05$) (Fig. 10.6).

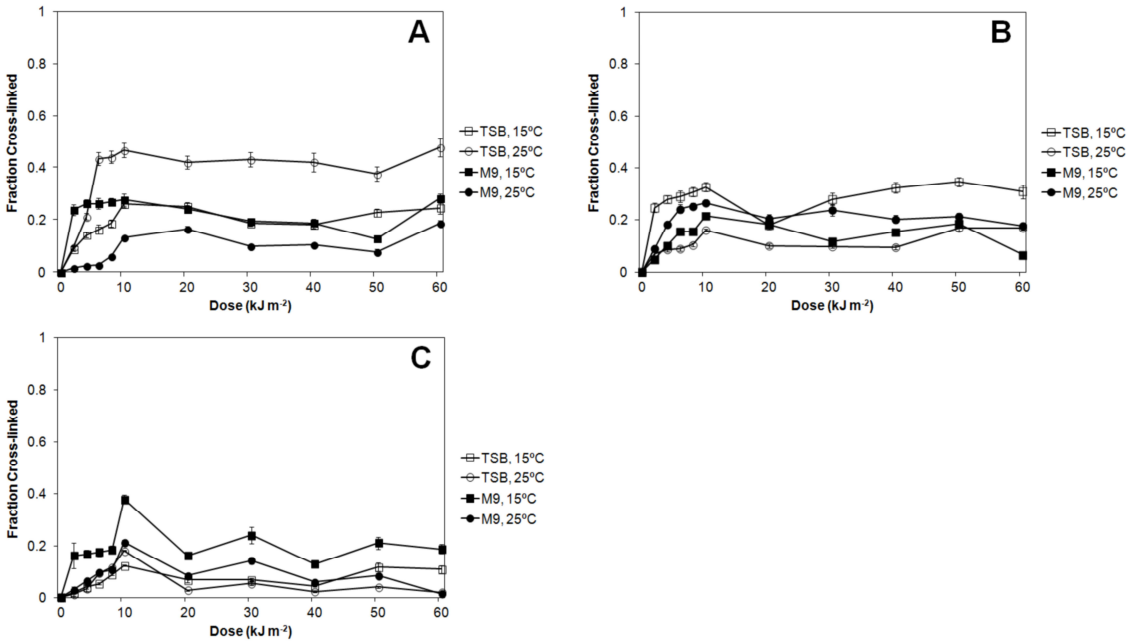

Fig. 10.5. Dose-dependent variation of the levels of DNA-protein cross-links (DPC) in *Pseudomonas* sp. NT5I1.2B grown at 15 ºC and 25 ºC in TSB and M9 medium in (A) mid-exponential, (B) late-exponential and (C) stationary phase. Results are expressed as means ± standard deviations of the mean of three experiments. Absence of error bars indicates that standard deviations are too small to see on the scale used.

Influence of growth temperature

Mid-exponential phase cells grown at 15 ºC generally survived up to 6.6-fold better than cells grown at 25 ºC, particularly at low-medium UVB doses ($\leq$ 30 kJ m^{-2}) (1-way ANOVA, $p < 0.05$) (Fig. 10.2 A). Survival of late-exponential and stationary phase cells grown at 25 ºC in TSB and M9 was generally enhanced compared to cells grown at 15 ºC, by as much as 4.0-fold (1-way ANOVA, $p < 0.05$) (Fig. 10.2 B, 10.2 C).

The levels of TBARS of mid-exponential phase cells grown in TSB and M9 at 25 ºC were up to 6.0 times higher than those of cells grown at 15 ºC (1-way ANOVA, $p < 0.05$) (Fig. 10.3 A). This temperature trend was inverted in stationary phase cells (Fig. 10.3 C). For late-exponential phase cells, TBARS levels were either enhanced at 15 ºC or 25 ºC, depending on the medium (Fig. 10.3 B).

In all growth phases and growth media tested, the DNA strand scission factor (SSF) was enhanced in cells grown at 25 ºC compared to cells grown at 15 ºC, by up to 4,000-fold (1-way ANOVA, $p < 0.05$) (Fig. 10.4 A-C).

The levels of DNA-protein cross-links (DPC) in mid-exponential and stationary phase cells grown in M9 medium were up to 14.0-fold higher in cells grown at 15 ºC than at 25 ºC (1-way ANOVA, $p < 0.05$) (Fig. 10.5 A, 10.5 C). The inverse pattern was observed in late-exponential phase cells (Fig. 10.5 B). Mid-exponential phase cells grown in TSB at 25 ºC showed 2.7 times more DPC levels than cells grown at 15 ºC (Fig. 10.5 A). The opposite trend was observed in late-exponential phase cells (Fig. 10.5 B). For stationary phase cells, DPC levels were 1.8-fold enhanced in cells grown at 25 ºC for low UVB doses ($\leq$ 10 kJ m^{-2}) (1-way ANOVA, $p < 0.05$), being this trend inverted at higher UVB doses (Fig. 10.5 C).

Mid-exponential phase cells grown at 25 ºC showed up to 4.4 times more levels of carbonyls than cells grown at 15 ºC (1-way ANOVA, $p < 0.05$) (Fig. 10.6 A). In late-exponential and stationary phase cells, carbonyls levels were enhanced by up to 2-fold at 15 ºC or 25 ºC, for cells grown in M9 or TSB, respectively (Fig. 10.6 B, 10.6 C).

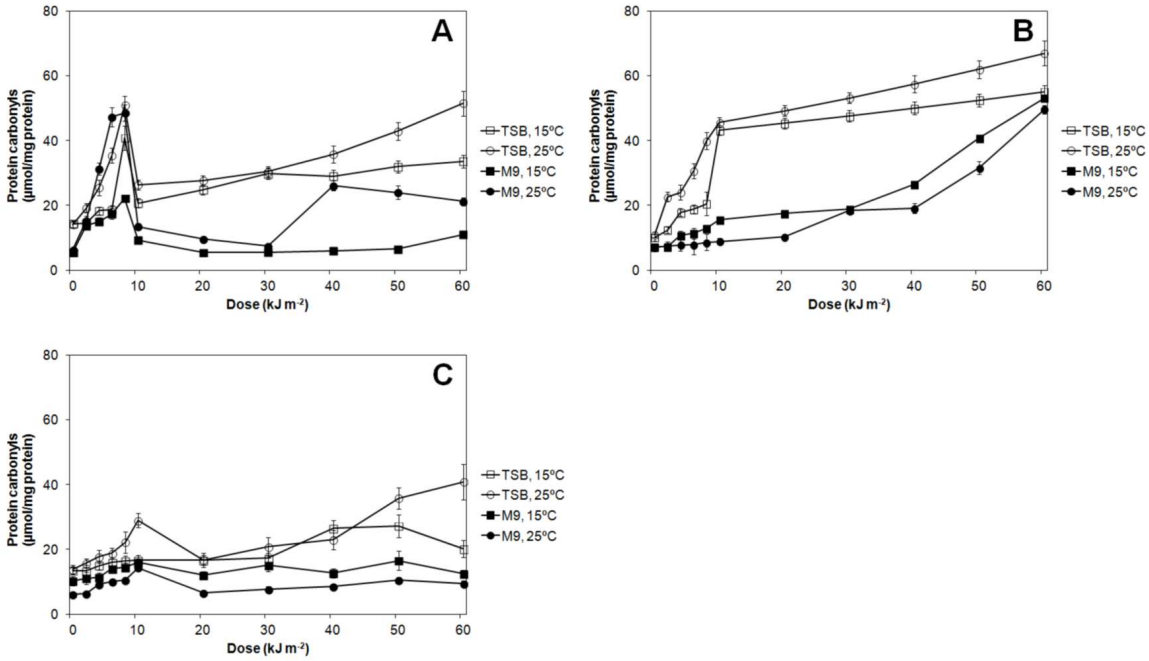

Fig. 10.6. Dose-dependent variation of carbonyl levels in *Pseudomonas* sp. NT5I1.2B grown at 15 ºC and 25 ºC in TSB and M9 medium in (A) mid-exponential, (B) late-exponential and (C) stationary phase. Results are expressed as means ± standard deviations of the mean of three experiments. Absence of error bars indicates that standard deviations are too small to see on the scale used.

Influence of growth medium

For mid- and late-exponential phase cells grown at 15 ºC, survival at low UVB doses (≤ 20 kJ m^{-2}) was generally enhanced when cells were cultivated in M9 than in TSB by as much as 2.5-fold (1-way ANOVA, $p < 0.05$). At higher UVB doses, this trend was inverted, with cells grown in TSB surviving up to 5.4 times better than those grown in M9. For cells grown at 25 ºC, survival was generally higher in TSB than in M9 by as much as 2.2-fold (1-way ANOVA, $p < 0.05$) (Fig. 10.2 A, 10.2 B). In stationary phase cells, survival was either enhanced in TSB (by up to 1.8-fold) or not significantly different between growth media (Fig. 10.2 C).

For cells grown at 15 ºC in the mid-exponential phase, TBARS levels were up to 19.6 times higher in M9 than in TSB (1-way ANOVA, $p < 0.05$) (Fig. 10.3 A). For cells in the late-exponential and stationary phases, TBARS were either enhanced in M9 or TSB depending on the growth temperature (Fig. 10.3 B, 10.3 C).

Mid-exponential phase cells grown at 15 ºC in M9 showed up to 3 times more levels of DSB than when grown in TSB (1-way ANOVA, $p < 0.05$) (Fig. 10.4 A). In the remaining treatments, DSB levels were generally enhanced when cells were grown in TSB, by up to 16.8-fold, particularly for medium-high UVB doses (≥ 10 kJ m^{-2}) (1-way ANOVA, $p < 0.05$) (Fig. 10.4 A-C). DPC levels were either enhanced in M9 or TSB depending on the growth temperature and growth phase (Fig. 10.5).

In mid-exponential phase cells, at low UVB doses (≤ 10 kJ m^{-2}) carbonyl levels were enhanced in M9, by up to 7-fold (1-way ANOVA, $p < 0.05$) (Fig. 10.6 A). In late-exponential and stationary phase cells, carbonyls levels were generally enhanced in TSB, particularly at medium-high UVB doses (> 10 kJ m^{-2}), by as much as 5.3 fold (1-way ANOVA, $p < 0.05$) (Fig. 10.6 B, 10.6 C).

Discussion

Oxidative damage is an important component of the mechanism of action of UVB radiation in bacteria, as denoted by the rapid induction of oxidative stress defences following irradiation (Qiu et al., 2005a; Matallana-Surget et al., 2009a; Matallana-Surget et al., 2012). The present work investigated the influence of the light dose and growth conditions (growth phase, growth temperature, and growth medium) on the oxidative damage elicited by exposure to UVB radiation in a bacterial isolate representative of *Gammaproteobacteria*, which have been found to dominate sunlit surface waters and proposed to be UV-resistant (Franklin et al., 2005; Alonso-Sáez et

al., 2006; Santos et al., 2012b). The *Pseudomonas* strain used in the present study is affiliated with *P. putida*, which accumulates only low levels of DNA damage following UVB exposure and shows low repair capabilities (Fernández Zenoff et al., 2006b). Certain *P. putida* members also contain a plasmid (pWW0), which encodes an error-prone DNA polymerase involved in mutagenic DNA repair, that confers evolutionary fitness to plasmid-carrying strains upon exposure to UV radiation (Tark et al., 2005).

UVB dose-dependence of cellular damage

The markers of cellular damage used in the present study (lipid oxidation, protein carbonylation, and DNA damage) varied in a general dose-dependent manner for low UVB doses ($\leq$ 10 kJ m^{-2}). Frequently, maximum levels of oxidative stress markers were observed in this period, particularly in mid-exponential phase cells. For higher UVB doses, the levels of oxidative stress markers either stabilized or oscillated, suggesting that oxidative damage is eventually compensated by the appropriate repair mechanisms. The alkyl hydroperoxide reductase (AhpC) protein plays an important role in the reduction of organic hydroperoxides and in the defence against sulphur-containing radicals (Poole, 2005), and has been proposed to be involved in the protection against lipid peroxidation (Mishra et al., 2009). Enhanced levels of the AhpC protein have been shown in UVB-irradiated *Photobacterium angustum* S14 (Matallana-Surget et al., 2012). Since protein carbonylation is an irreversible process, variation in the levels of protein carbonyls during the course of irradiation may reflect enhanced activity of proteases involved in the degradation of carbonylated proteins, including DnaK, GroEL, and Clp (Fredriksson et al., 2005). Accordingly, the abundance of these proteins has been shown to increase in response to UV exposure (Matallana-Surget et al., 2009a).

Alternatively, there can be a saturation of oxidative damage in the cell, potentially associated with the formation of multiple lesions as a result of consecutive molecule excitation by high UV doses, resulting in a complex, non-linear dependence of oxidative damage on the irradiation dose (Byeong et al., 2007). Further studies, potentially using more powerful and sensitive techniques (*e.g.*, mass spectrometry-based assessment of quantitative and qualitative changes in proteins and lipids during irradiation) are necessary to elucidate the lack of a dose-dependence in oxidative stress markers at high UVB doses.

Influence of growth phase

In general, survival upon UVB exposure was highest in stationary phase cells. Enhanced survival of stationary phase cells was also associated with lower levels of DNA-protein cross-links and protein carbonyls, compared to exponential phase cells. Several studies have suggested that cells with reduced specific growth rates, such as stationary phase cells, are more resistant than exponential phase cells to multiple stresses, including extremes of temperature and osmolarity, oxidative stress, UV and gamma irradiation, iron and copper toxicity, as well as acid and base shock (Nair and Finkel, 2004). Enhanced survival during the stationary phase has been attributed to the expression of different biosynthetic pathways, gene regulators, and enzyme systems that confer an adaptive advantage to cells in the stationary phase (Rees, 1995; Dodd et al., 1997). The alternative sigma factor RpoS or σ^{38} encoded by the *rpoS* gene, plays a critical role in stress resistance of stationary phase cells by regulating the expression of antioxidant enzymes, particularly catalase (Hengge-Aronis, 1999; Oppezzo et al., 2011).

Mid-exponential phase cells were the least resistant to irradiation, displaying high levels of protein carbonyls, especially at low UVB doses ($\leq$ 10 kJ m^{-2}). An intrinsically weaker oxidative stress defence stock (Eisenstark et al., 1996) coupled with enhanced ROS production associated with high aerobic respiration rates of mid-exponential phase cells (Nyström, 2004) and small size (Garcia-Pichel, 1994), potentially contributed to the high sensitivity of mid-exponential phase cells to UVB radiation.

Influence of growth temperature

Mid-exponential phase cells grown at 15 ºC showed greater survival after UVB exposure than cells grown at 25 ºC, particularly at low UVB doses. The levels of DNA strand breaks were higher in cells grown at 25º C than at 15 ºC in all treatments, which was also accompanied by enhanced levels of lipid peroxidation in mid-exponential phase cells. These results are consistent with previous studies documenting a higher yield of UV-induced DNA damage at higher temperature (24 °C versus 12 °C) in *Sphingopyxis alaskensis* (Matallana-Surget et al., 2010), thus suggesting that the formation of DNA lesions during UV exposure is temperature-dependent. The temperature dependence of DNA damage has been attributed to a possible influence of temperature on the conformational state of DNA (Li et al., 2002) and/or an indirect effect on DNA by affecting DNA-binding proteins (Matallana-Surget et al., 2010).

The reactions involved in the interaction of ROS and their targets might also be temperature-dependent (Li et al., 2002). The electron transport chain is a key source of ROS in the cell (Imlay and Fridovich, 1991; González-Flecha and Demple, 1995). Lower temperatures could have reduced oxygen consumption rates, particularly in the highly active mid-exponential phase cells, which in turn reduced the rates of normal ROS production and the risk of oxidative damage. On the other hand, low temperature can also modify the metabolic status of the cell, increasing the efficiency of damage repair and/or production of antioxidants (Borgeraas and Hessen, 2000).

However, in stationary phase cells, particularly at high UVB doses, the trend observed for mid-exponential phase cells was inverted, with cells grown at 25 ºC surviving better and showing lower levels of oxidative stress markers. One possibility to account for this observation is that in stationary phase cells, in which there is a lower oxidative burden associated with respiration (Nyström, 2004), enhanced temperature might stimulate the enzymatic processes involved in defence against UV-induced lesions (*e.g.*, the activity of antioxidant enzymes) (Bullock and Jeffrey, 2010). Additionally, enhanced cell size, by providing higher internal self-shading (Garcia-Pichel, 1994) could have also contributed for enhanced survival during UVB exposure.

Influence of the growth medium

Cells cultivated in nutrient-rich TSB generally survived better to medium-high UVB doses (> 10 kJ m^{-2}) than those grown in nutrient-poor M9 medium. These results are consistent with the enhanced sensitivity of a set of bacterial isolates exposed to 60 kJ m^{-2} of UVB radiation under nutrient depleted conditions, compared to nourished counterparts (Santos et al., 2012a). Nutrient-rich TSB, but not M9, could possibly have provided sufficient amounts of the chemical elements required for the synthesis of macromolecules necessary to withstand high UVB doses (*e.g.*, enzymes involved in DNA repair and ROS scavenging), thus accounting for the enhanced UVB resistance of cells grown in TSB. Accordingly, supply with high nutrient concentrations (nitrogen and phosphorus) has been found to result in reduced UV-sensitivity and enhanced repair capabilities in bacterioplankton, compared to the amendment with lower nutrient concentrations (Pausz and Herndl, 2002; Joux et al., 2009).

However, it is possible that the higher rates of macromolecule synthesis in cells grown in TSB could carry an increased risk of oxidative damage to the cells, as indicated by the generally enhanced levels of oxidative stress markers during irradiation

in cells grown in nutrient-rich media, compared to cells grown in M9. It is known that the composition of the growth medium affects the lipid composition of the bacterial cell, and this can in turn affect susceptibility to oxidative stress. For instance, supplementing the bacterial growth medium with free polyunsaturated fatty acids (PUFA) is known to result in enhanced incorporation of a given PUFA into bacterial fatty acids (Kankaanpää et al., 2004) which are the main targets of peroxidation (Imlay, 2003). Further studies are necessary to elucidate the role of the growth medium in bacterial cell composition and in the subsequent sensitivity to UVB-induced stress.

Importance of growth conditions for UVB-induced damage

Most studies reporting UVB effects on bacterial isolates have typically considered cells in the mid-exponential and late-exponential phase (Joux et al., 1999; Arrieta et al., 2000; Qiu et al., 2004; Agogué et al., 2005; Fernández Zenoff et al., 2006b; Hörtnagl et al., 2011; Santos et al., 2011b; Santos et al., 2012a). The results obtained in the present study indicate that the growth phase, growth temperature, and growth medium of bacteria influence their levels of oxidative damage during UVB exposure, thus highlighting the importance of the growth conditions of bacteria in determining their responses to UVB exposure. This is in accordance with previous studies conducted with *Escherichia coli* exposed to different UV wavelengths (Berney et al., 2006c; Bucheli-Witschel et al., 2010). These results also highlight the difficulties in understanding UV-bacteria interaction in natural bacterial communities and the limitations of extrapolating results from laboratorial experiments with bacterial isolates to the environment.

The temporal variation in survival and oxidative damage to different biomolecules is illustrated in the representative conceptual graphs shown in Fig. 10.7 for the interval corresponding to 0-10 kJ m^{-2}, in which survival was dose-dependent in all treatments. Growth conditions preceding irradiation might influence bacterial sensitivity to UVB radiation potentially by affecting the temporal progression of biomolecule damage. For instance, cells in the mid-exponential phase displayed a strong increase in TBARS levels with irradiation, which preceded damage to the other molecules (Fig. 10.7). This observation suggests an important role of lipid damage in determining the reduction of cell survival during the very early stages of UVB exposure. There is increasing experimental evidence suggesting that lipid peroxidation is

physiologically important in microorganisms (Semchyshyn et al., 2005; Pérez et al., 2007; Pérez et al., 2008).

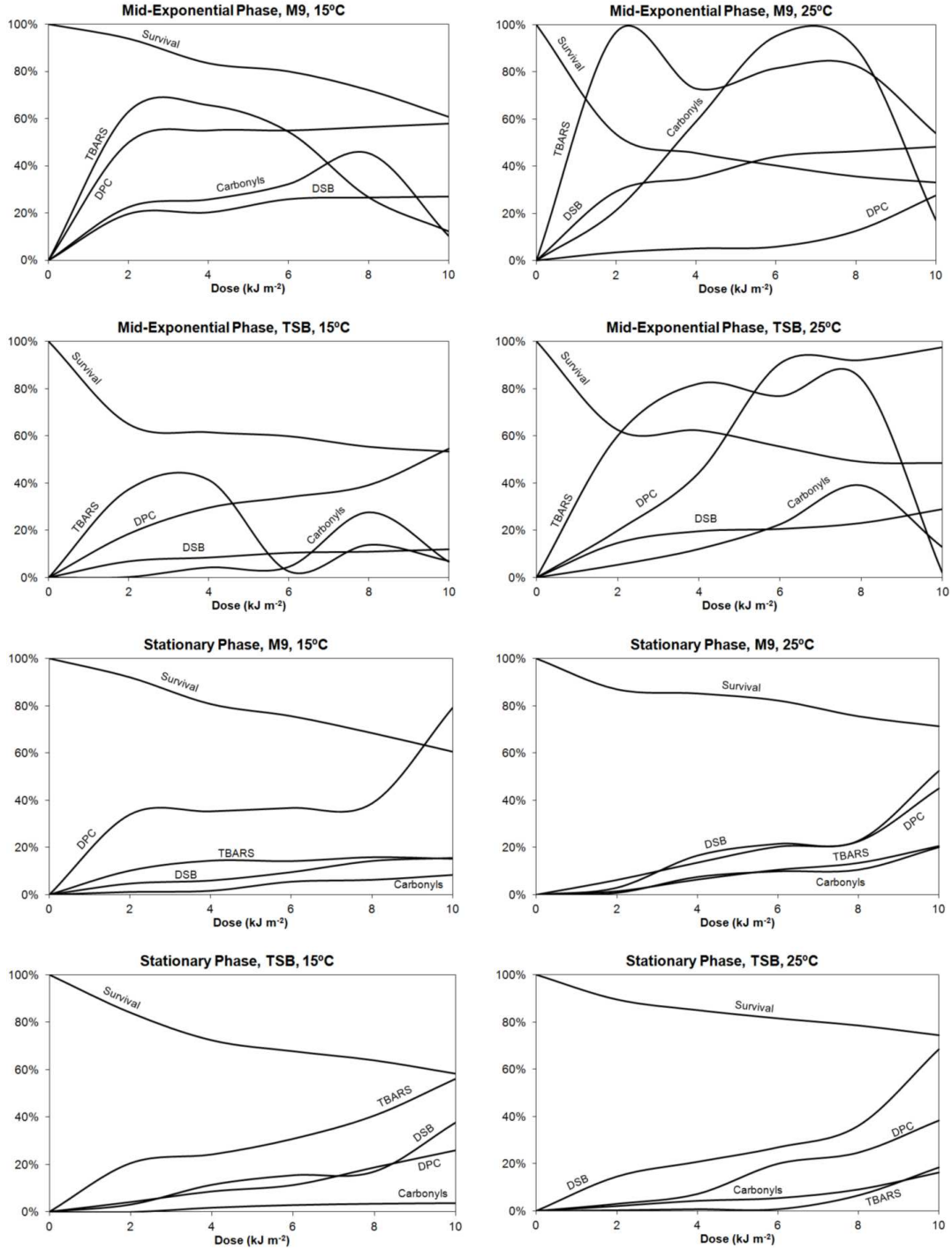

Fig. 10.7. Graphical representation of the temporal variation of survival and markers of oxidative stress in *Pseudomonas* sp. NT5I1.2B upon exposure to low UVB doses (0-10 kJ m^{-2}). Late-exponential and stationary phase cells followed a broad similar pattern of variation. Therefore only the temporal variation of stationary phase cells is shown.

The observed importance of lipid damage in UVB-induced inactivation is consistent with recent results obtained for a set of bacterial isolates (Santos et al., 2013), and the strong induction of the AhpC protein, involved in the defence of the cell against lipid peroxidation, in UVB-irradiated *Photobacterium angustum* S14 (Matallana-Surget et al., 2012).

In late-exponential and stationary phase cells, DNA damage (DNA strand breaks and DNA-protein cross-links) seems to play a more determinant role in the reduction of cell survival, generally preceding damage to lipids and proteins (Fig. 10.7). The growth temperature and medium might affect UVB sensitivity by strongly influencing the magnitude of the damage to particular biomolecules.

These results indicate that the variability of the effects associated with the different growth conditions must be considered for an in-depth understanding of the mechanisms of UVB-induced damage in bacteria. In order to gain environmentally relevant information from laboratorial studies with isolated bacteria, the growth conditions of those bacteria should be as similar as possible to the ones observed in the natural environment.

Conclusions

In general, a linear dose-dependent variation of oxidative damage parameters upon exposure to UVB was observed for low doses (0-10 kJ m^{-2}) only, suggesting the occurrence of a dynamic process between damage induction and repair and/or potential saturation of oxidative damage at high UVB doses. Stationary phase cells were the most resistant to UVB radiation, and mid-exponential phase cells were the least resistant. Differences in UVB sensitivity between growth phases were mostly associated with the extent of protein carbonylation and DNA-protein cross-links. In mid-exponential phase cells, oxidative damage was generally higher at 25 ºC than at 15 ºC, suggesting a temperature dependence of ROS generation and/or ROS interaction with cellular targets at low UVB doses. At high UVB doses, survival was enhanced in cells grown in TSB than in M9. Growth conditions preceding irradiation are important determinants of survival and oxidative damage imposed by UVB exposure, potentially by affecting the temporal progression and the magnitude of the biomolecular damage.

Acknowledgments

Acknowledgments are due to Susana Machado, Inês Baptista and Silvia F. Lopes (Department of Biology, University of Aveiro) for assistance with laboratorial work. Financial support for this work was provided by CESAM (Centre for Environmental and Marine Studies, University of Aveiro) and the Portuguese Foundation for Science and Technology (FCT) in the form of a PhD grant to A.L. Santos (SFRH/BD/40160/2007) and a post-Doctoral grant to I. Henriques (SFRH/BPD/63487/2009).

CHAPTER 11

The *recA* Gene on Bacterial Genomes: When one Chromosomal Gene is not a Universal Rule

Santos A. L., Henriques I., Moura A., Jové T., Cunha A., Correia A.

Manuscript in preparation

Abstract

The RecA protein plays a crucial role in the processes of homologous recombination and in the bacterial SOS response elicited by exposure to DNA damaging agents. Therefore, it can be hypothesized that the importance of recombination and ability to cope with DNA damage during the life history of microorganisms could be reflected in RecA phylogeny and frequency in the genome.

In the present work, the diversity of *recA* genes among completely sequenced bacterial genomes was studied. Additionally, *recA* and 16S rRNA gene trees of *Gammaproteobacteria*, *Deltaproteobacteria* and Firmicutes were constructed and compared. The presence of multiple *recA* copies in sequenced genomes and the frequency of plasmid-encoded *recA* genes were also examined.

RecA was confirmed to be absent only in bacterial endosymbionts. Phylogenetic analysis of the RecA protein was, in general, coherent with the phyla defined by 16S rRNA gene analysis. *recA* gene trees of *Deltaproteobacteria* and Firmicutes were in general agreement with 16S rRNA trees, but were more divergent in *Gammaproteobacteria*. Duplication of the *recA* gene was found to be widespread in myxobacteria, and also frequent among Firmicutes. Putative *recA* paralogs, resulting from a recent duplication event, were identified in some genomes. In other cases, divergent genomic G+C content suggests that this extra copy of *recA* could have arisen through horizontal gene transfer. The presence of *recA* homologs in plasmids and, in some cases, in the vicinity of transposase genes supports the possibility of plasmid or transposon-mediated mobility of the *recA* gene. We suggest that these plasmid-encoded *recA* genes could complement the activity of one or several of the chromosome-encoded *recA* genes in the bacterial SOS response.

Introduction

Exposure to DNA damaging agents can cause halting of bacterial replication forks at sites of DNA lesions. Rescue of stalled DNA replication forks is mediated by homologous recombination, a process which is critical for genomic stability and cellular viability, contributing also for the generation of genetic diversity (Cox, 2007). The multifunctional RecA protein is the central factor in homologous recombination and recombinational DNA repair. In this process, RecA binds stretches of single-stranded DNA, unwinds duplex DNA, finds regions of homology between chromosomes and then promotes strand invasion and exchange between homologous DNA molecules. RecA also has a regulatory role in the induction of the SOS response involved in DNA repair through its co-protease activity, responsible for inducing the autocatalytic cleavage of the LexA repressor which initiates the expression of several DNA repair genes (Radman, 1975). Additionally, the RecA co-protease activity facilitates the activation of UmuD, a component of the error-prone DNA polymerase V that mediates replicative bypass of DNA lesions during the SOS response (Schlacher and Goodman, 2007). Another catalytic activity of RecA is the self-cleavage of bacteriophage repressors, like CI from lambda, inducing the shift from lysogeny to lytic growth (Galkin et al., 2009). Recently, disruption of the *recA* gene in *Acinetobacter* revealed a pleiotropic effect on phenotypes like antibiotic resistance, virulence and heat-shock and oxidative stress responses (Aranda et al., 2011).

The RecA activity is found in virtually all bacteria, with the exception of obligate intracellular symbionts that have undergone dramatic genome size reductions, which adopt alternative strategies for sustainable DNA replication and repair (Sharples, 2009). The wide distribution of bacterial *recA* genes, in phylogenetic groups that took separate evolutionary paths during Precambrian times, including Bacteria, Archaea and Eukarya, indicates that the RecA protein ancestor preceded the separation of the three major biological domains (Roca and Cox, 1990). Based on studies of the RecA of *Escherichia coli*, the protein (352 aa) is generally divided into three domains (Bianco et al., 1998): an N-terminal domain (aa 1-33), involved in filament formation; the central 'core' region (aa 33-240), which contains the residues involved in ATP binding; and the C-terminal domain (aa 241-352) which is involved in the DNA strand exchange reaction (Lusetti et al., 2003). At the amino acid level, the degree of conservation stretches basically across the entire sequence with the exception of the highly acidic C-terminus, less conserved. The near universality and degree of conservation of the *recA* gene has

made it a potentially useful tool for molecular systematic studies of bacteria (Eisen, 1995; Ludwig and Klenk, 2001; Zeigler, 2003) and has been proposed as an alternative phylogenetic marker to 16S rRNA genes in several bacterial groups (Van Waasbergen et al., 2000; Torriani et al., 2001; Thompson et al., 2004; Payne et al., 2005; Scholz et al., 2008; Sepe et al., 2008; Weng et al., 2009; Costechareyre et al., 2010; Landeta et al., 2011).

Evidences suggest that structural or kinetic properties of RecA are related to specific requirements of DNA damage repair systems in some species. For example, although the overall fold of the RecA of the radiation-resistant *Deinococcus radiodurans* is similar to that of *E. coli*, there is a large reorientation of the C-terminal domain involved in binding dsDNA. Additionally, it displays unique amino acid residues around a flexible β-hairpin that is implicated in DNA binding (Rajan and Bell, 2004).

Most known bacterial species possess only one *recA*. The presence of two *recA* genes has been documented in *Bacillus megaterium* (Nahrstedt et al., 2005) and *Myxococcus xanthus* (Norioka et al., 1995). *Acaryochloris marina* MBIC11017 seems to possess seven copies of this gene, four of which located in four out of its nine plasmids (Swingley et al., 2008). A *recA* gene homolog is also present on a 65 kb conjugative lactococcal plasmid (Garvey et al., 1997) and on a 53 kb plasmid from an environmental *Vibrio* strain (Hazen et al., 2007). More recently, the presence of two *recA* (*recA*$_{P1}$ and *recA*$_{P3}$) in two different plasmids in *Deinococcus deserti* in addition to the chromosomal *recA* was also reported (Dulermo et al., 2009). The authors proposed that the extra *recA*$_{P1}$ and *recA*$_{P3}$ genes may provide higher levels of RecA protein for efficient error-free repair of DNA damage.

With the increasing number of bacterial genomes available in public databases, opportunities for more extensive analyses and contextualization of genes and proteins among complete sequenced organisms arise. The aims of this study were: (1) to inspect the presence of *recA* genes in sequenced bacterial genomes, including extrachromosomal replicons; (2) to evaluate the performance of the *recA* gene and deduced amino acid sequence as phylogenetic markers and (3) to search for evidences of events contributing for genome evolution, such as duplication or lateral transfer of *recA* genes.

Materials and methods

Data retrieval

The *recA* nucleotide sequences and deduced amino acid sequences within fully sequenced bacterial genomes were retrieved from GenBank NRAA database (ftp://ftp.ncbi.nih.gov/blast/db/FASTA/nr.gz) and manually inspected for the presence of sequences annotated as "*recA*", "recombination protein A" or "recombinase A". For the genomes where such annotation could not be found, the presence of *recA* homologs was inferred by searching for sequences with high similarity to the *recA* gene of *E. coli* using BLASTN (E value = 0.0). To search for homologs of the *recA* gene in plasmids, all the retrieved sequences were used as queries in BLASTN, TBLASTN, and PSI-BLAST searches. Genes wrongly annotated as *recA* that displayed no similarity with *recA* homologs were excluded from the analysis (supplementary material in Appendix).

G+C contents of genomes and *recA* genes were estimated based on nucleotide sequences retrieved from KEGG database (http://www.genome.jp/kegg/) (Kanehisa, 2002) using locally developed Perl scripts. The genomic context of *recA* genes was manually retrieved from the GenBank database.

Phylogenetic analyses

To study the evolution of the RecA protein, phylogenetic trees using the amino acid sequence of the most conserved core region of RecA (aa 33-240 in *E. coli*) were constructed. DMC1 (*Homo sapiens* and *Danio rerio*), Rad51 (*Drosophila simulans* and *Saccharomyces cerevisiae*) and RadA (*Pyrococcus abyssi*) sequences (homologous of the bacterial RecA) were included in the phylogenetic tree as outgroups. Preliminary multiple sequence alignments were carried out with CLUSTALX 1.8 (Thompson et al., 1997). Preliminary Neighbour-Joining (NJ) trees were then generated using MEGA 3.0. To reduce the complexity of the phylogenetic tree, one representative sequence was chosen for closely related branches (diverging by less than 4 %). Each representative sequence was aligned again separately and then combined by using profile alignment in CLUSTALX. Different tree construction methods (Neighbour-Joining, Minimum Evolution and Maximum Parsimony) were compared and yielded similar results. The final Neighbour-Joining tree was constructed with MEGA 3.0 using the pairwise gap deletion option, Poisson correction as distance measure and 1000 bootstrap replicates.

To address the congruence between the phylogenetic information provided by *recA* and 16S rRNA nucleotide sequences, alignments of the corresponding genes were

produced using MEGA 3.0 with the pairwise gap deletion option. Phylogenies for specific bacterial groups (*Deltaproteobacteria*, *Gammaproteobacteria* and Firmicutes) were reconstructed using the Neighbour-Joining method and distances estimated using the Jukes-Cantor model with 1000 bootstrap replicates.

Results and discussion

Distribution of the recA *gene in sequenced bacterial genomes*

Fig. 11.1 shows the distribution by phylum of the 1076 genomes considered in the present study. Sequences belonging to Proteobacteria (41.7 %), Firmicutes (24.4 %), *Actinobacteria* (12.5 %) and Bacteroidetes (8.9 %) were the most represented in the database. The presence of the *recA* gene was detected in all the analyzed genomes, except those of the endosymbionts Candidatus *Hodgkinia cicadicola* (*Alphaproteobacteria*), Candidatus *Sulcia muelleri* (Bacteroidetes), *Buchnera aphidicola* (*Gammaproteobacteria*), species belonging to the Candidatus *Blochmannia* genus (*Gammaproteobacteria*), Candidatus *Ruthia magnifica* (*Gammaproteobacteria*), Candidatus *Vesicomyosocius okutanii* (*Gammaproteobacteria*) and phytoplasmas (Mollicutes). In these cases, the absence of recombination confers genetic stability to the mutualistic bacteria by precluding the occurrence of genetic rearrangements and lateral gene transfer (Sharples, 2009).

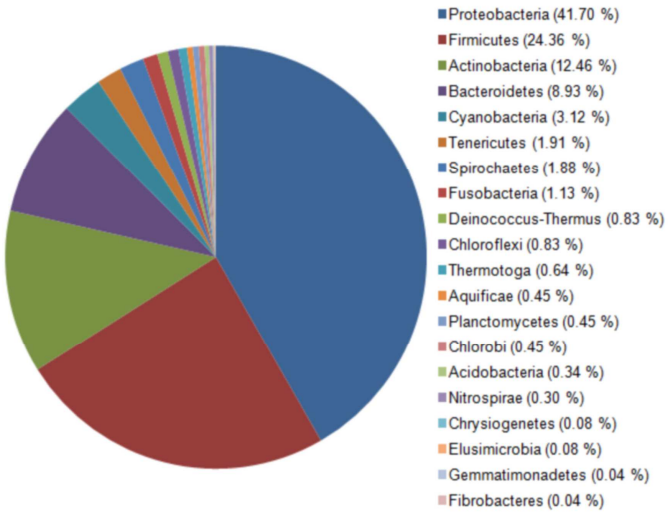

Fig. 11.1. Relative distribution of *recA* sequences considered in this study by phylum. The relative frequency of each bacterial phylum in the total sequenced bacterial genomes is presented in brackets.

In general, the *recA* genes analyzed contained 888 to 1341 nucleotides. On several genomes, smaller or larger sequences annotated as *recA* were also found. These

smaller sequences frequently corresponded to the C- or N- terminal regions of the RecA protein annotated separately and, in some cases, interrupted by introns or intein-coding sequences (Table 11.1). In other cases, longer *recA* gene sequences were also detected, that were subsequently found to contain introns or inteins. Introns are non-coding sequences located within genes that are transcribed but not translated into proteins, being removed by self-splicing whereby the intron catalyzes its own removal from the gene and the joining of coding sequences (exons) (Haugen et al., 2005). Inteins are protein intervening sequences that are able to cleave themselves from a precursor protein while joining the flanking sequences (Boles and Horswill, 2008).

As the result of the presence of intein-coding sequences, longer *recA* genes were identified in a plasmid of *E. coli* (779 aa), several mycobacterium species (up to 790 aa) and in the soil-living actinomycete *Thermobifida fusca* (1172 aa, two inteins) (Table 11.1). The presence of RecA inteins in the obligate intracellular mycobacterial pathogens have led to the hypothesis that these inteins might play a role in mycobacterial functions related to pathogenesis or virulence (Davis et al., 1994). In *M. tuberculosis* and *M. leprae* the RecA intein contains a catalytically active homing endonuclease domain which determines an endonuclease that promotes the spreading of the intein (Haugen et al., 2005). In the present work, the presence of a sequence encoding a homing endonuclease motif associated with an intein was also detected in the *recA* genes of the deep-sea actinomycete *Verrucosispora maris* and the thermophilic actinomycete *Thermomonospora curvata*, suggesting a recent spread of *recA* inteins among *Actinomycetales*.

In several strains of *Bacillus* sp. and *Geobacillus* sp. the *recA* gene was also found to be interrupted by group I or group II introns (Table 11.1), which differ by their splicing mechanism (Haugen et al., 2005). Intein-coding sequences and introns in the *recA* of mycobacteria and *Bacillus* species have been proposed to be evolutionary related (Ko et al., 2002), though an endonuclease activity has not been found in the *recA* introns of *Bacillus* sp. (Nord et al., 2007). In *B. anthracis* the presence of an intron does not affect RecA activity nor the expression, pathogenicity, or the survival of the host organism (Ko et al., 2002). In *Geobacillus kaustophilus* the presence of the *recA* intron does not affect UV sensitivity (Chee and Takami, 2005). These observations suggest that the current function of *recA* intron seems dispensable (Ko et al., 2002), indicating that the spread of *recA* introns could have occurred through neutral evolution.

Table 11.1. *recA* genes containing introns or inteins.

Organism	Accession no.	Group	Type of intervening sequence
***Bacillus anthracis* A0248**	CP001598	Firmicutes	Group I intron
***Bacillus anthracis* Ames**	AE016879	Firmicutes	Group I intron
***Bacillus anthracis* 'Ames Ancestor'**	AE017334	Firmicutes	Group I intron
***Bacillus anthracis* CDC 684**	CP001215	Firmicutes	Group I intron
***Bacillus anthracis* Sterne**	AE017225	Firmicutes	Group I intron
***'Bacillus caldolyticus'* BCRC 11954**	EU484370.1	Firmicutes	Group II intron
***Bacillus cereus* 03BB102**	CP001407	Firmicutes	Group I intron
***Bacillus cereus* AH187**	CP001177	Firmicutes	Group I intron
***Bacillus cereus* AH820**	CP001283	Firmicutes	Group I intron
***Bacillus cereus* ATCC 10987**	AE017194	Firmicutes	Group I intron
***Bacillus cereus* ATCC 14579**	AE016877	Firmicutes	Group I intron
***Bacillus cereus* B4264**	CP001176	Firmicutes	Group I intron
***Bacillus cereus* bv. anthracis CI**	CP001176	Firmicutes	Group I intron
***Bacillus cereus* E33L**	CP000001	Firmicutes	Group I intron
***Bacillus cereus* F837/76**	CP003187	Firmicutes	Group I intron
***Bacillus cereus* G9842**	CP001186	Firmicutes	Group I intron
***Bacillus cereus* NC7401**	AP007209	Firmicutes	Group I intron
***Bacillus cereus* Q1**	CP000227	Firmicutes	Group I intron
***Bacillus* sp. EA1**	EF165030	Firmicutes	Group II intron
***Bacillus thuringiensis* BMB171**	CP001903	Firmicutes	Group I intron
***Bacillus thuringiensis* sv. chinensis CT-43**	CP001907	Firmicutes	Group I intron
***Bacillus thuringiensis* sv. finitimus YBT-020**	CP002508	Firmicutes	Group I intron
***Bacillus thuringiensis* sv. konkukian str. 97-27**	AE017355	Firmicutes	Group I intron
***Bacillus thuringiensis* Al Hakam**	CP000485	Firmicutes	Group I intron
***Bacillus weihenstephanensis* KBAB4**	CP000903	Firmicutes	Group I intron
***Escherichia coli* LF82 plasmid**	CU638872	*Gammaproteobacteria*	Intein
***Geobacillus kaustophilus* HTA426**	BA000043	Firmicutes	Group II intron
***Geobacillus kaustophilus* BCRC 11223**	EU484362	Firmicutes	Group II intron
***Geobacillus* sp. C56-T3**	CP002050	Firmicutes	Group II intron
***Geobacillus* sp. NTU 03**	JF316706	Firmicutes	Group II intron
***Geobacillus* sp.WCH70**	CP001638	Firmicutes	Group II intron
***Geobacillus* sp.Y412MC61**	CP001794	Firmicutes	Group II intron
***Geobacillus thermocatenulatus* BCRC 17466**	EU484360	Firmicutes	Group II intron
***Geobacillus thermoleovorans* CCB_US3_UF5**	CP003125	Firmicutes	Group II intron
***Geobacillus thermoleovorans* BCRC 17253**	EU484359	Firmicutes	Group II intron
***Mycobacterium africanum* GM041182**	FR878060	*Actinobacteria*	Intein
"Mycobacterium canettii" CIPT 140010059	HE572590	*Actinobacteria*	Intein
***Mycobacterium tuberculosis* H37Rv**	AL123456	*Actinobacteria*	Intein
Mycobacterium tuberculosis RGTB423	CP003234	*Actinobacteria*	Intein
Mycobacterium bovis* subsp. *bovis AF2122/97	BX248343	*Actinobacteria*	Intein
Mycobacterium bovis BCG* str. *Mexico	CP002095	*Actinobacteria*	Intein
Mycobacterium bovis BCG* str. *Pasteur 1173P2	AM408590	*Actinobacteria*	Intein
Mycobacterium bovis BCG* str. *Tokyo 172	AP010918	*Actinobacteria*	Intein
Mycobacterium leprae Br4923	FM211192	*Actinobacteria*	Intein
Mycobacterium* sp. *JDM601	CP002329	*Actinobacteria*	Intein
***Thermobifida fusca* YX**	CP000088	*Actinobacteria*	Intein
Isoptericola variabilis 225	CP002810	*Actinobacteria*	Intein
Verrucosispora maris AB-18-032	CP002638	*Actinobacteria*	Intein
Thermomonospora curvata DSM 43183	CP001738	*Actinobacteria*	Intein

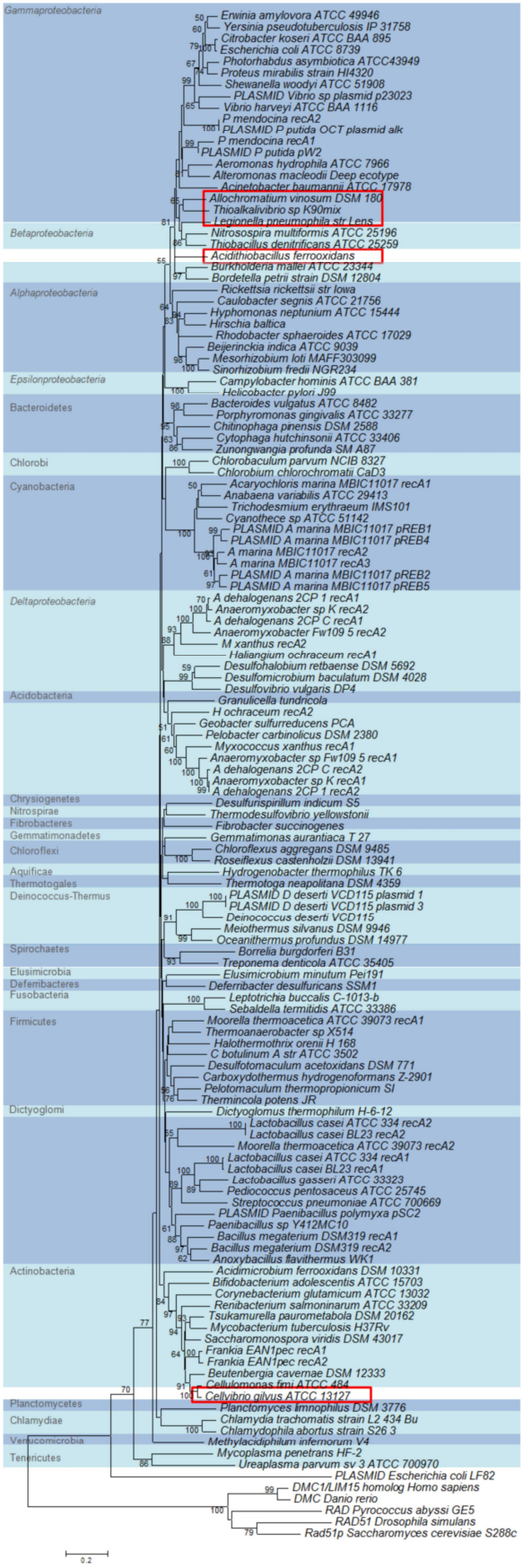

Fig. 11.2. Phylogenetic tree of RecA proteins in Bacteria. Bootstrap values of 50 % or greater are shown at the appropriate nodes. Red boxes denote discrepancies between RecA and 16S rRNA phylogeny. Labels and colour shadings are used to put in evidence commonly used subdivisions.

RecA is a potential phylogenetic marker

To construct the phylogenetic tree of RecA, only sequences within the range between 296 and 447 amino acids were used. Analysis of the phylogenetic tree of RecA protein revealed the early divergence of sequences from Tenericutes from the remaining bacterial phyla (Fig. 11.2). Such observation is in accordance with previous work (Dybvig et al., 1992), and probably results from the rapid evolutionary rate of mycoplasmas compared to other prokaryotes and is consistent with 16S rRNA phylogeny (Woese, 1987).

In general, the phylogenetic tree of RecA was consistent with the bacterial groups defined on the basis of the 16S rRNA gene analysis (Ludwig, 2010), demonstrating the high degree of conservation of RecA which broadly parallels that of 16S rRNA. However, some discrepancies were observed, which are identified in Fig. 11.2 by red boxes. In the case of *Gammaproteobacteria*, the phylogenetic tree of RecA showed a separation of *Acidithiobacillus* and representatives of *Chromatiales* and *Legionellales* from the remaining *Gammaproteobacteria* members, which is in agreement with the polyphyletic nature of *Gammaproteobacteria* previously proposed based on a set of 356 protein families (Williams et al., 2010). The gammaproteobacterium *Cellvibrio gilvus* was found to cluster with *Actinobacteria*, which is in accordance with recent observations leading to the proposal of the reclassification of this species (Christopherson et al., 2012). Sequences from *Deltaproteobacteria* were located distantly from the remaining proteobacterial members, suggesting that the Proteobacteria phylum itself does not have a monophyletic origin, in accordance with conclusions drawn by several authors using molecular markers alternative to rRNA-coding genes (Zouine et al., 2002; Gophna et al., 2005; Dagan et al., 2010). Furthermore, the representative sequence for phylum Acidobacteria used in the present study clustered within the class *Deltaproteobacteria*, in agreement with a previous work that used 31 gene orthologs to reconstruct the tree of life (Ciccarelli et al., 2006). In conclusion, these results suggest that the RecA protein is a useful molecular marker to infer evolutionary relationships among bacteria since, in general, it reflects 16S rRNA phylogeny.

In order to gain further insights into the suitability of the *recA* gene as a phylogenetic marker, as suggested by the RecA protein tree, the phylogenetic information provided by *recA* and the 16S rRNA genes was compared by constructing phylogenetic trees using the two genes for *Deltaproteobacteria* and Firmicutes, which

were found to contain several bacterial members with multiple *recA* copies (see section bellow). Additionally, since the RecA protein tree suggested a polyphyletic nature of *Gammaproteobacteria*, *recA* and 16S rRNA trees were also constructed for this group.

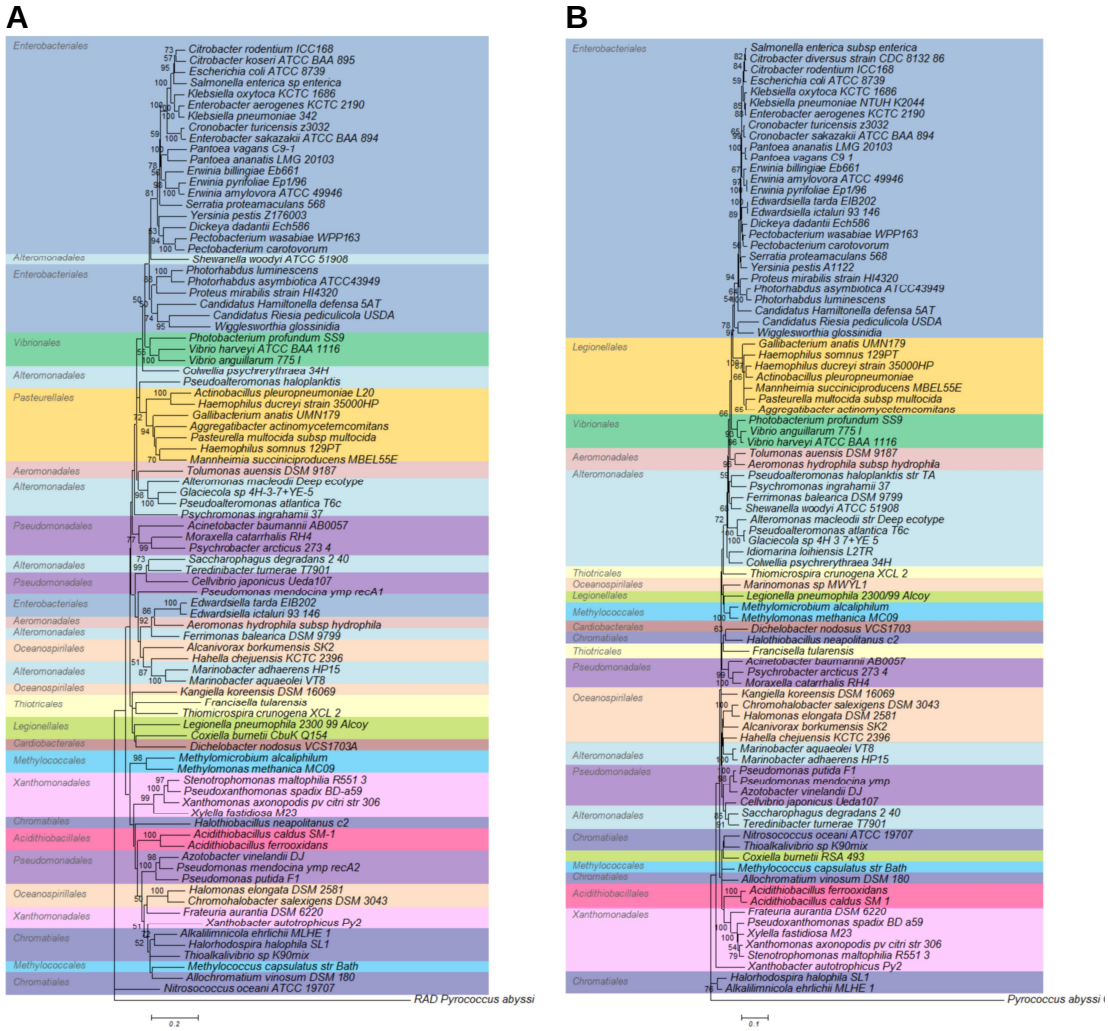

Fig. 11.3. Phylogenetic tree of *recA* (A) and 16S rRNA (B) genes in *Gammaproteobacteria.* Bootstrap values of 50 % or greater are shown at the appropriate nodes. Labels and colour shadings are used to put in evidence commonly used subdivisions.

The phylogeny of *Gammaproteobacteria* based on *recA* and 16S rRNA gene sequences is represented in Fig. 11.3. Both trees indicate that several of the established gammaproteobacterial orders, including *Alteromonadales*, *Oceanospirillales*, *Pseudomonadales* and *Chromatiales*, are not monophyletic, in accordance with the conclusions of Williams *et al.* (2010) based on a set of 356 protein families. Additionally, in the *recA* tree the representative sequences of the *Enterobacteriales* order did not cluster together, being the sequences from *Edwardsiella* species more close to those from members of *Pseudomonadales* than to the remaining

Enterobacteriales. Additionally, sequences from *Shewanella* species, belonging to the *Alteromonadales* order, were found to cluster within *Enterobacteriales*. *Gammaproteobacteria* show particularly high rates of lateral gene transfer events (Abby et al., 2012) which could be a contributing factor for the higher degree of divergence between *recA* and 16S rRNA trees observed in this group.

The phylogeny of *Deltaproteobacteria* based on *recA* and 16S rRNA genes is represented in Fig. 11.4. In general, the phylogenetic information provided by both trees was analogous, including the possibility of *Desulfobacterales* being a polyphyletic group. On the other hand, while the 16S rRNA gene tree suggested that *Desulphurellales* might represent a lineage distinct from the remaining *Deltaproteobacteria*, the same was not observed in the *recA* tree, in which *Desulphurellales* clustered together with *Bdellovibrionales*.

The phylogenetic trees of Firmicutes based on 16S rRNA and *recA* genes are represented in Fig 11.5. A general agreement in the phylogenetic information of both trees was also observed in the case of Firmicutes, including the clustering of the *Alicyclobacillaceae Alicyclobacillus acidocaldarius* and *Kyrpidia tusciae*, usually classified as *Bacilli*, within the *Clostridia* cluster. On the other hand, while the two representative *Negativicutes* sequences clustered together in the 16S rRNA gene tree, this did not occur in the *recA* tree.

recA *duplication and horizontal gene transfer*

The presence of more than one copy of the *recA* gene was detected in 28 out of the 1076 chromosomes analyzed (2.6 %) (Table 11.2). The identity between the two *recA* gene copies (median = 63.5 %) ranged from 41 % in *Lactococcus lactis* sp. *lactis* KF147 to 91 % in *Frankia* sp., which could indicate that, in general, the two genes are unlikely to have resulted from a recent duplication event. The presence of more than one *recA* copy in bacterial chromosomes had been previously described in *Myxococcus xanthus* and *Bacillus megaterium* DMS 319 (2 copies), as well as in the cyanobacterium *Acaryochloris marina* (3 copies) (Norioka et al., 1995; Nahrstedt et al., 2005; Swingley et al., 2008). The present work indicates that the duplication of the *recA* gene may be common in certain bacterial groups, particularly *Deltaproteobacteria* and Firmicutes.

Table 11.2. Bacterial genomes containing multiple copies of the *recA* gene and comparisons between different *recA* copies from the same genome.

Organism	Accession no.	Genome size (Mb)	Group	RecA1 size (aa)	RecA2 (aa)	RecA3 (aa)	Max id. between *recA* copies (%)
***Acaryochloris marina* MBIC11017**	CP000828	6.5	Cyanobacteria	356	350	349	80
***Frankia* sp. EAN1pec**[1]	CP000820	9.0	*Actinobacteria*	347	345		91
***Anaeromyxobacter dehalogenans* 2CP-1**	CP001359	5.0	*Deltaproteobacteria*	316	358		71
***A. dehalogenans* 2CP-C**	CP000251	5.0	*Deltaproteobacteria*	315	358		70
***Anaeromyxobacter* sp. Fw109-5**	CP000769	5.3	*Deltaproteobacteria*	358	340		73
***Anaeromyxobacter* sp. K**	CP001131	5.1	*Deltaproteobacteria*	358	343		74
***Haliangium ochraceum* DSM 14365**	CP001804	9.5	*Deltaproteobacteria*	375	379		72
***Myxococcus xanthus* DK 1622**	CP000113	9.1	*Deltaproteobacteria*	363	342		67
Myxococcus fulvus HW-1	CP002830	9.0	*Deltaproteobacteria*	341	290		53
Corallococcus coralloides DSM 2259	CP003389	10.1	*Deltaproteobacteria*	341	284	361	70
***Sorangium cellulosum* 'So ce 56'**[2]	AM746676	13.0	*Deltaproteobacteria*	350	395		65
***Stigmatella aurantiaca* DW4/3-1**[3]	CP002271	10.3	*Deltaproteobacteria*	360	293		49
***Pseudomonas mendocina* ymp**	CP000680	5.1	*Gammaproteobacteria*	347	348		70
***Bacillus megaterium* DSM 319**	CP001982	5.1	Firmicutes	345	345		75
***Bacillus megaterium* QM B1551**	CP001983	5.1	Firmicutes	341	345		76
***Bacillus megaterium* WSH-002**	CP003017	5.0	Firmicutes	345	343		75
***Lactobacillus casei* ATCC 334**	CP000423	2.9	Firmicutes	353	397		61
***Lactobacillus casei* BD-II**	CP002618	3.1	Firmicutes	353	397		60
***Lactobacillus casei* BL23**	FM177140	3.1	Firmicutes	353	397		62
***Lactobacillus casei* LC2W**	CP002616	3.0	Firmicutes	353	397		60
***Lactobacillus casei str.* Zhang**	CP001084	2.9	Firmicutes	353	397		61
***Lactobacillus rhamnosus* Lc 705**	FM179323	3.0	Firmicutes	350	381		60
***Lactobacillus rhamnosus* ATCC 8530**	CP003094	3.0	Firmicutes	350	395		60
***Lactobacillus rhamnosus* GG**	FM179322	3.0	Firmicutes	350	395		60
***Lactococcus lactis subsp. cremoris* A76**	CP003132	2.5	Firmicutes	387	346		53
***Moorella thermoacetica* ATCC 39073**	CP000232	2.6	Firmicutes	348	339		60
***Lactococcus lactis* sp. *lactis* KF147**[4]	CP001834	2.6	Firmicutes	303	200		41
Candidatus *Solibacter usitatus* Ellin6076	CP000473	10.0	Acidobacteria	248	355	224	51

[1] Additionally contains RecA domain protein annotated as "recombinase A" which corresponds to the C-terminal domain
[2] Contains additional gene fragment annotated as "recombinase A" with reduced homology to *recA* in database
[3] Contains additional protein annotated as "RecA bacterial DNA recombination family protein" that shows partial homology to the P-loop NTPase superfamily of Rad55. Second copy with reduced identity to sequences in database
[4] Second copy with homology to the C-terminal of the protein

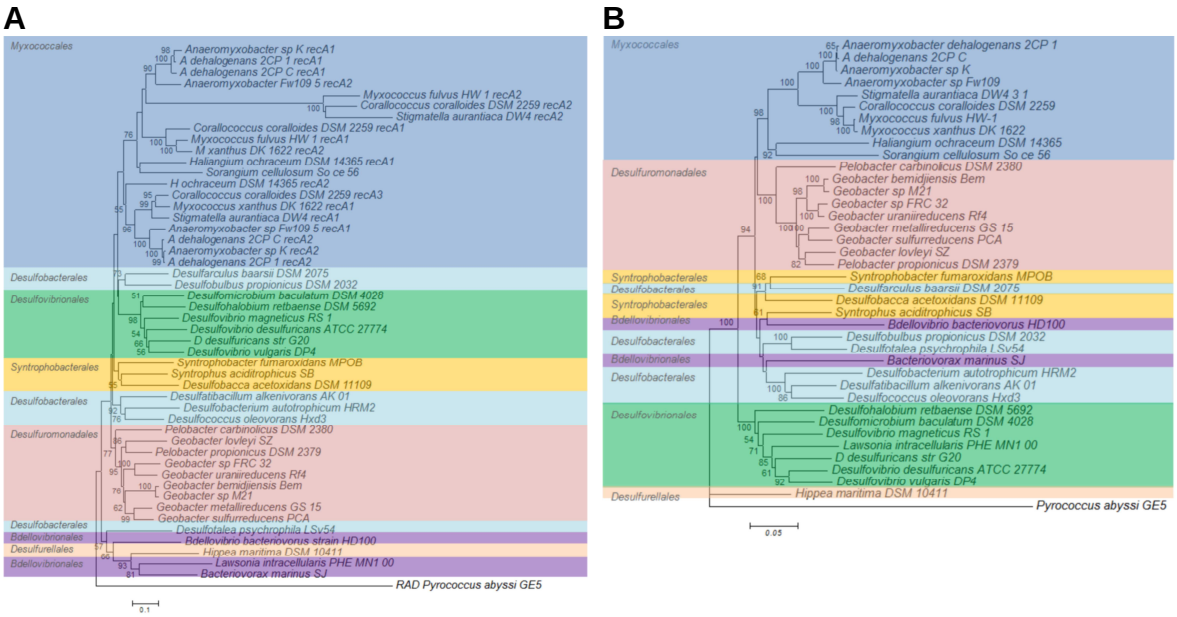

Fig. 11.4. Phylogenetic tree of *recA* (A) and 16S rRNA (B) genes in *Deltaproteobacteria.* Bootstrap values of 50 % or greater are shown at the appropriate nodes. Labels and colour shadings are used to put in evidence commonly used subdivisions.

recA duplication in *Deltaproteobacteria*

Two (and, in the case of *Corallococcus coralloides* DSM 2259, three) copies of the *recA* gene were found in all the available complete genome sequences of members of the *Myxococcales* order. The identity of the two copies ranged between 49 % in *Stigmatella aurantiaca* and 74 % in *Anaeromyxobacter* sp. K. When Karlin *et al.* (1995) first reported the presence of two *recA* genes in *M. xanthus*, the authors suggested that the higher amount of the RecA repair protein would allow this topsoil bacteria to withstand UV irradiation. The present observation of the widespread duplication of *recA* in myxobacteria inhabiting various environments suggests that UV radiation is not the only factor underlying the presence of additional copies of the *recA* gene.

Myxococcales typically display large genomes ranging from ~10 to 13 Mb, while anaerobic myxobacteria belonging to the genus *Anaeromyxobacter* have smaller genome sizes (~5 Mb). The typically large genome size of myxobacteria seems to be due to genome expansion as a result of duplications of specific categories of genes, particularly those involved in cell-cell signaling, small molecule sensing and multicomponent transcriptional control. Such genome expansion allowed the evolution of the complex molecular machinery required for the development of a multicellular lifestyle typical of myxobacteria (Goldman et al., 2006). As hypothesized for the cyanobacteria *Acaryochloris marina* (Swingley et al., 2008; Miller et al., 2011), it is possible that the presence of multiple copies of *recA* and related genes in a

myxobacteria ancestral could have mediated the gene duplication and/or integration of foreign genes that led to their genome expansion, and at the same time would allow genome stability, through its role in the DNA damage repair and DNA recombination. It is interesting to notice that in the case of Candidatus *Solibacter usitatus* (Phylum Acidobacteria), which also possesses a very large genome (10 Mb), there are also three annotated copies of the *recA* gene in the genome (though two of them are smaller than the expected size). Since not all large bacterial genomes display multiple copies of the *recA* gene, it is possible that *recA* duplication could have played an important role in the expansion of the genome of bacteria belonging to particular phylogenetic groups, such as the cyanobacterium *Acaryochloris marina*, myxobacteria and the Acidobacteria Candidatus *Solibacter usitatus*.

recA duplication in Firmicutes

Duplication of the *recA* gene was also detected in some Firmicutes genomes such as those of *Lactobacillus* and *Lactococcus* species and *Bacillus megaterium* which belong to *Bacilli*, and the *Clostridia Moorella thermoacetica* (Table 11.2). In the case of *M. thermoacetica* the second gene copy was found to be more similar to the homologs of *Bacilli* than *Clostridia* (Fig. 11.5). The identity between the two gene copies ranged between 41 % in *Lactococcus lactis* sp. *lactis* KF147 and 76 % in *Bacillus megaterium* QM B1551. The presence of two *recA* copies in *B. megaterium* had previously been reported and proposed to contribute to increase its ability for recombinational repair and enhance its resistance to DNA damage compared to other *Bacillus* species (Nahrstedt et al., 2005). The presence of two copies of the *recA* gene among members of Firmicutes of different phylogenetic lineages (*Clostridia* and *Bacilli*) could either be explained by horizontal acquisition of the extra *recA* gene or an ancient duplication event in a Firmicutes ancestor with subsequent loss of the gene in all other *Clostridia* except *M. thermoacetica*.

In order to address the possible horizontal acquisition of *recA* genes in Firmicutes, the G+C content of the gene and the respective genome was compared (Table 11.3). Among Firmicutes, *Lactococcus lactis* subsp. *cremoris* A76 and *Lactobacillus rhamnosus* Lc 705 displayed considerable differences between the G+C content of the second *recA* gene and the average genomic G+C content, by approximately 13 % and 10 %, respectively.

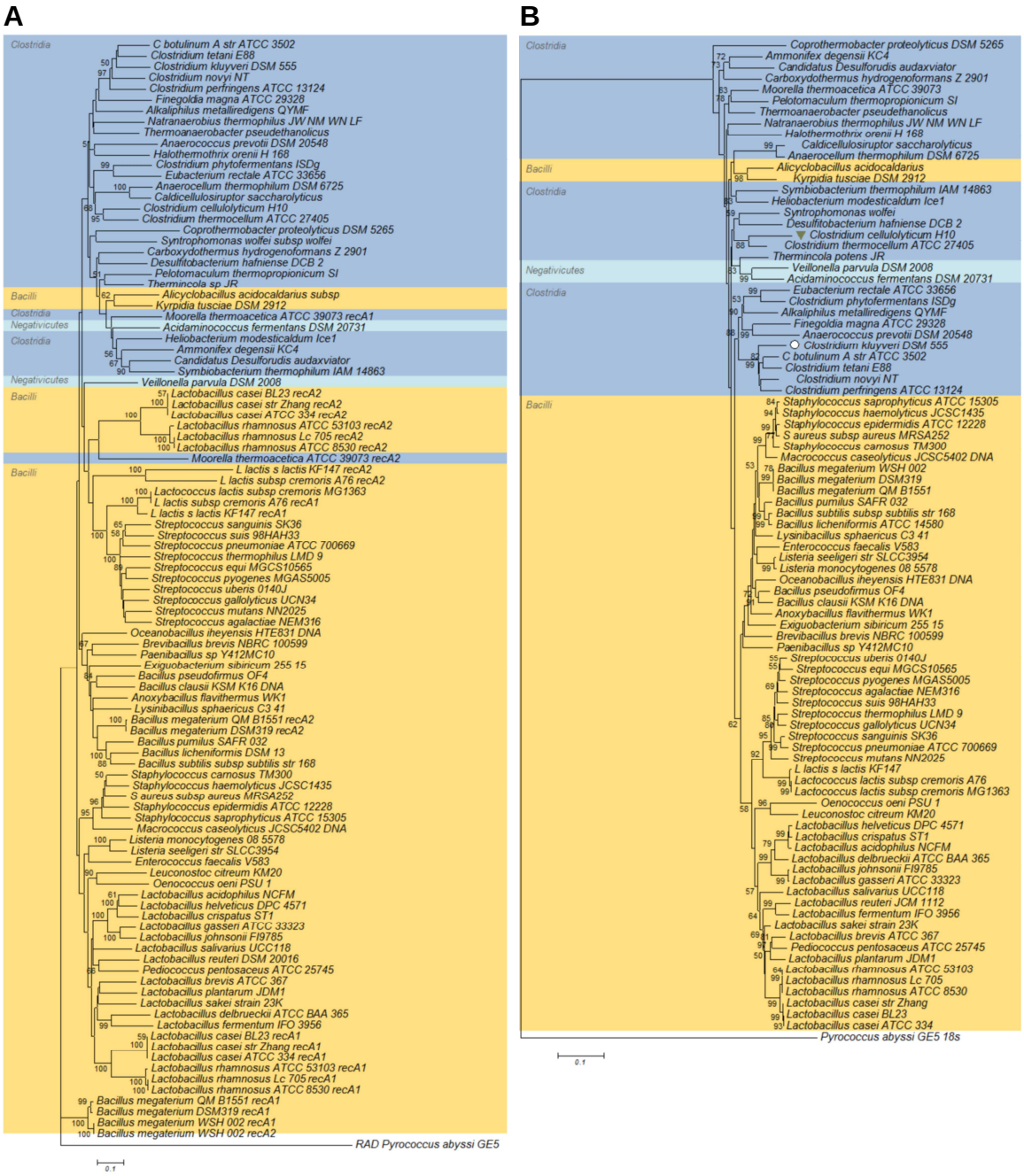

Fig. 11.5. Phylogenetic tree of *recA* (A) and 16S rRNA (B) genes in Firmicutes. Bootstrap values of 50 % or greater are shown at the appropriate nodes. Labels and colour shadings are used to put in evidence commonly used subdivisions.

Such difference could indicate an exogenous acquisition of the second *recA* copy in these organisms. Furthermore, in the case of *Lactococcus lactis* subsp. *cremoris* A76, BLASTP searches using the second RecA as a query revealed it was most related with the RecA homolog (RecAlp) from the plasmid pNP40 of *Lactococcus lactis*, raising the possibility of the mobility of the *recA* gene being mediated through mobile genetic elements.

Table 11.3. Bacterial genomes on which the G+C content of the *recA* gene showed relevant deviation (over 1.5 times the standard deviation of the genome) in relation to the G+C content of the whole genome. Values of G+C content of both genome and *recA* gene are presented, as well as the closest relative protein product. Avg – average. SD – standard deviation.

Organism	Accession no.	Group	Genomic G+C content (%) (Avg ± SD)	*recA* G+C content (%)	Maximum identity
***Borrelia burgdorferi* B31**	AE000783	Spirochaetes	28.4 ± 5.1	37.0	99 % (*Borrelia burgdorferi* JD1´)
***Corynebacterium diphtheriae gravis* NCTC 13129**	BX248353	*Actinobacteria*	53.9 ± 4.7	46.7	94 % (*Corynebacterium pseudotuberculosis* FRC41)
***Cytophaga hutchinsonii* ATCC 33406**	CP000383	Bacteroidetes/Chlorobi	38.9 ± 4.4	59.5	85 % (*Algoriphagus* sp. PR1)
***Cyanothece* sp PCC 7424**	CP001291	Cyanobacteria	39.2 ± 5.0	46.8	98 % (*Cyanothece* sp. PCC 7822)
***Lactobacillus rhamnosus* Lc 705 (recA2)**	FM179323	Firmicutes	47.2 ± 3.9	37.0	100 % (*Lactobacillus rhamnosus HN001*)
***Lactococcus lactis* subsp. *cremoris* A76 (recA2)**	CP003132	Firmicutes	35.9 ± 5.7	49.2	58 % (plasmid pNP40 of *Lactococcus lactis*)
***Mesorhizobium loti* MAFF303099**	BA000012	*Alphaproteobacteria*	62.7 ± 3.6	68.8	99 % (*Mesorhizobium ciceri biovar biserrulae* WSM1271)
***Pseudomonas mendocina* ymp (recA2)**	CP000680	*Gammaproteobacteria*	64.6 ± 4.3	51.7	77 % (*Shewanella* sp. MR-4)

The high similarity observed between *recA* copies in *Bacillus megaterium* strains (87 %) could be indicative of a recent duplication event. A much lower similarity of the two *recA* copies in *Lactobacillus* (60 %), *Lactococcus* (45 %) and *Moorella* (65 %), suggests that divergence between the copies could have taken place earlier in their evolution or eventually the second copy could have been acquired by horizontal gene transfer. Nevertheless, the concordance between *recA* and 16S rRNA trees suggests that potential gene transfer events have not obscured the phylogenetic relationships.

In *B. megaterium* both copies seem to be functional (Nahrstedt et al., 2005), while in the other Firmicutes members this is not known. The investigation of the functionality of the two *recA* copies among other Firmicutes could shed further light into the potential role of RecA in the evolution of these lineages. Speculations can only be made about the significance of the presence of the extra *recA* among these bacterial members. *Lactococcus* and *Lactobacillus* are microaerophilic organisms that under certain conditions can tolerate oxygen. However, oxygen consumption results in altered redox state with the formation of reactive oxygen species which can pose a significant threat (Duwat et al., 1995). The involvement of RecA in resistance to oxidative and thermal stress has been reported in *Lactococcus lactis*, in which it seems to play an important role in the repair of damage induced by the hydroxyl radical generated by the Fenton reaction (Duwat et al., 1995). Whether the presence of an extra *recA* gene confers a supplementary protection to DNA damage in these bacteria, is not known.

Moorella thermoacetica, on the other hand, is strictly anaerobic, making additional protection against oxidative stress as the explanation for the presence of a second *recA* copy paradoxical. However, previous investigations showed the presence in *M. thermoacetica* of a gene cluster coding for proteins involved in oxidative and nitrosative stress protection, including an aerobic type Fe/Mn superoxide dismutase (SOD) and catalase (Das et al., 2005). Based on these observations, one possible explanation for the presence of two *recA* copies in *M. thermoacetica* was the presence of the two *recA* genes in an ancestral common to *Bacilli* and *Clostridia* that was latter lost from the remaining *Clostridia* and then from most *Bacilli*. As before, whether this extra copy is functional and possesses a role in the fitness of this organism, is unknown and merits further research.

recA duplications in other bacterial groups

In the gammaproteobacterium *Pseudomonas mendocina* ymp, the second *recA* gene displayed a high deviation in its G+C content compared to the average of the genome (51.7 % versus 64.6 %, Table 11.3). The corresponding protein showed a maximum identity of 77 % with the RecA from *Shewanella* sp. MR-4. These observations indicate that the second *recA* gene of *Pseudomonas mendocina* ymp could have been acquired by a horizontal gene transfer event. Furthermore, analysis of the genomic context of the second *recA* copy revealed the presence of two genes coding for putative transposases immediately downstream. Genes encoding for the presence of transposases in the immediate vicinity of the *recA* gene were detected in other 22 genomes (supplementary information in Appendix), four of them associated to *recA* duplicates (*Lactococcus lactis* KF147, *Frankia* sp. EAMI1pec, *Moorella thermoacetica* ATCC 39073 and *Pseudomonas mendocina* ymp). In the case of the *Gammaproteobacteria Frankia* sp. EAMI1pec and *Pseudomonas mendocina* ymp the presence of putative transposases belonging to the same family (IS*4*) was observed. Whether these genetic elements could have played a role in the acquisition of the additional *recA*, is unknown.

Presence of *recA* in plasmids

The presence of *recA* homologs was detected in 31 plasmids deposited in the NCBI database (Table 11.4). The existence of plasmid-located *recA* genes was already reported in *Lactococcus lactis* (Garvey et al., 1997), *Vibrio* sp. (Hazen et al., 2007),

Acaryochloris marina (Swingley et al., 2008) and *Deinococcus deserti* (Dulermo et al., 2009). In the present work, plasmid-encoded *recA* genes were also detected in plasmids of members of the gammaproteobacterial genera *Escherichia*, *Serratia*, *Pseudomonas*, *Yersinia* and *Salmonella*, the Firmicutes *Paenibacillus* and the Chloroflexi *Thermomicrobium*. Inter-subspecies lateral gene transfer of *recA* has been demonstrated at least in *Salmonella* species (McQuiston et al., 2008), and our observations raise the possibility of the involvement of plasmids in the process.

In general, plasmid-encoded *recA* genes showed the highest identity with *recA* genes encoded in the chromosome of the host organism, but some exceptions were observed (Table 11.4). For example, the *recA* gene in plasmid pSM22 of *Serratia marcescens* strain B-6493 (*Enterobacteriales*) encoded a protein that showed its highest identity to the RecA of *Aggregatibacter aphrophilus* ATCC 33389 (*Pasteurellales*). In this case, a notable difference (7 %) was also observed between the G+C content of the plasmid-encoded *recA* gene and the G+C content of the plasmid, which could indicate an exogenous origin. It is also noteworthy the presence of a gene encoding a transposase in the vicinity of the plasmid-encoded *recA* (Fig. 11.6 A, B). The presence in the plasmid of a gene coding for DNA polymerase V subunit, which performs translesion DNA synthesis during the SOS response, immediately adjacent to the *recA* gene (Fig. 11.6 A, B) could suggest that this plasmid-encoded copy might fulfil a role in complementing the chromosomally elicited SOS response.

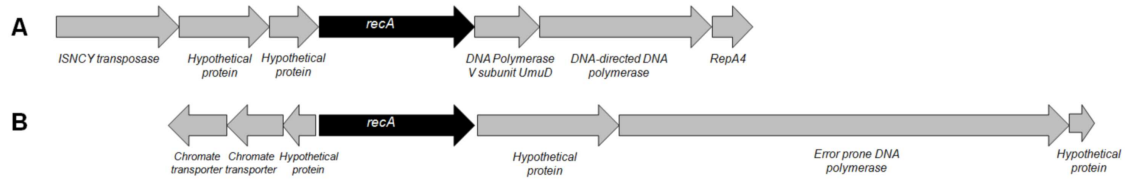

Fig. 11.6. Genomic context of *recA* in the plasmids of (A) *Serratia marcescens* strain B-6493 (plasmid pSM22) and (B) *Thermomicrobium roseum*. In both cases, DNA polymerases involved in error repair are present in the vicinity of the *recA* gene. The displayed length is proportional to the size of the corresponding open reading frame.

In the Chloroflexi *Thermomicrobium* the protein encoded by the plasmid *recA* gene showed a maximum identity (31 %) to the homologous of the alphaproteobacterium *Hyphomicrobium denitrificans* ATCC 51888.

Table 11.4. Plasmids encoding RecA homologs, with indication of the hosts and G+C content; the G+C content and size of the *recA* gene as well as the closest relative of its product are also presented.

Organism	Plasmid	Accession no.	Plasmid G+C content (%)	*recA* G+C content (%)	Size (aa)	% Maximum identity
***Vibrio* sp. 23023**	p23023	CP000755	44.7	44.5	364	79 % (*Vibrio angustum* S14)
***Deinococcus deserti* VCD115**	Plasmid 1	CP001115	60.7	63.3	344	Copies 100 % similar
***Deinococcus deserti* VCD115**	Plasmid 3	CP001117	61.4	63.5	344	81 % (*Deinococcus radiopugnans* ATCC 19172)
Pseudomonas putida	pW2	FJ948173	62.1	61.8	247	94 % (*P. aeruginosa* PAb1)
Lactococcus lactis	pNP40	DQ534432	32.3	36.2	341	99 % (*L. lactis* subsp. *lactis* CV56) 99 %
***Paenibacillus polymyxa* SC2**	pSC2	CP002214	37.6	43.7	348	74 % (*Paenibacillus vortex* V453)
***Acaryochloris marina* MBIC11017**	pREB1	CP000838	47.3	52.3	357	
***Acaryochloris marina* MBIC11017**	pREB 2	CP000839	45.3	49.1	357	94 % (each other)
***Acaryochloris marina* MBIC11017**	pREB4	CP000841	45.9	52.0	352	
***Acaryochloris marina* MBIC11017**	pREB5	CP000842	44.7	49.1	357	
***Lactococcus lactis* subsp. *lactis* CV56**	pCV56A	CP002366	32.1	36.3	341	58 % (*Lactococcus lactis* subsp. *cremoris* A76)
***Salmonella enterica* subsp. enterica serovar Typhi str. CT18**	pHCM2	AL513384	50.6	55.3	358	99 % (pMT plasmids of *Yersinia* strains)
***Yersinia pestis* Angola**	pMT-pPCP	CP000900	50.0	54.6	358	99 % (*Salmonella enterica* subsp. *enterica* serovar Typhi str. CT18) All RecA in plasmids of *Yersinia pestis* strains are 100 % equal except for one amino acid modification in *Yersinia pestis* KIM 10 plasmid pMT1
***Yersinia pestis* Antiqua**	pMT	CP000309	50.2	54.6	358	
***Yersinia pestis* biovar Medievalis str. Harbin 35**	pMT	CP001610	50.2	54.6	358	
***Yersinia pestis* biovar Microtus str. 91001**	pMT1	AE017045	50.3	54.6	358	
***Yersinia pestis* CA88-4125**	pMT1	CP000723	50.2	54.6	358	
***Yersinia pestis* CO92**	pMT1	AL117211	50.2	54.6	358	
***Yersinia pestis* D106004**	pMT1	CP001587	50.2	54.6	358	
***Yersinia pestis* D182038**	pMT1	CP001591	50.2	54.6	358	
***Yersinia pestis* KIM 10**	pMT1	AF053947	50.2	54.5	358	
***Yersinia pestis* Nepal516**	pMT	CP000306	50.2	54.6	358	
***Yersinia pestis* Pestoides F**	MT	CP000670	50.2	54.6	358	
Yersinia pestis	pG8786	AJ698720	50.2	54.6	358	
***Yersinia pestis* Z176003**	pMT1	CP001595	50.2	54.6	358	
***Yersinia pestis* A1122**	unnamed	CP002957	50.2	54.6	358	
***Yersinia pestis* KIM**	pMT-1	AF074611	50.2	54.6	358	
***Pseudomonas putida* OCT**	alk genes cluster	AJ245436	50.93	51.5	348	
***Serratia marcescens* strain B-6493**	pSM22	HQ896493	58.5	65.5	369	65 % (*Aggregatibacter aphrophilus* ATCC 33389)
***Thermomicrobium roseum* DSM 5159**	unnamed	CP001276	65.7	68.3	357	31 % (*Hyphomicrobium denitrificans* ATCC 51888)
***Escherichia coli* LF82**	unnamed	CU638872	46.2	48.5	779	97 % (*Escherichia coli* B354)

Also in this case, an error prone DNA polymerase was found upstream the plasmid *recA*, suggesting a role in the SOS response (Fig. 11.6 B). However, whether these plasmid-located *recA* genes are functional and actually contribute for the SOS response of the cell, or play any part in increasing the fitness of these organisms, is unknown and an interesting matter of research.

Conclusions

The *recA* gene is ubiquitous in eubacteria, being absent only in endosymbionts. In the latter the absence of this gene seems to confer genetic stability, which may be advantageous for the intracellular lifestyle. In some bacterial strains such as those belonging to the *Mycoplasma* genus, the *recA* gene is interrupted by intein-coding sequences with a homing endonuclease function. In some *Bacillus* and *Geobacillus* species *recA* is also interrupted by introns, which might have played an evolutionary role. In general, the phylogeny of the RecA protein supports the phyla defined on the basis of rRNA gene analysis demonstrating its high degree of conservation resulting from its fundamental housekeeping role in bacteria. *recA* and 16S rRNA trees of *Deltaproteobacteria* and Firmicutes were broadly in agreement. Results were more divergent in *Gammaproteobacteria*, suggesting that *recA* may not be a good molecular marker for this group. The presence of two copies of the *recA* gene seems to be a common feature of myxobacteria, where it could have mediated its genome expansion. *recA* duplication is also frequent among some Firmicutes. Further work is necessary to assess the functionality of the newly detected extra copies of *recA*. Additionally, our results point to the possibility of acquisition of extra *recA* genes by horizontal gene transfer with a possible involvement of plasmids in mediating the acquisition.

Acknowledgments

This work was supported by CESAM (Centre for Environmental and Marine Studies, University of Aveiro) and the Portuguese Foundation for Science and Technology (FCT) in the form of a PhD grant to A.L. Santos (SFRH/BD/40160/2007) and a post-Doctoral grant to I. Henriques (SFRH/BPD/63487/2009) and A. Moura (SFRH/BPD/72256/2010).

CHAPTER 12

DISCUSSION

The combined effects of global changes, such as ocean acidification and thermal stratification, and changes in solar UV fluxes are expected to result in enhanced exposure of aquatic organisms to damaging UV wavelengths over the course of the next decades, with far reaching ecological consequences (Andrady et al., 2010).

The effects of UV radiation are well known to be wavelength-dependent (Sundin and Jacobs, 1999; Qiu et al., 2004; Wilson et al., 2004; Qiu et al., 2005a; Bauermeister et al., 2009). A relatively large number of studies have addressed the effects of UV radiation, particularly in the UVB range, on natural bacterioplankton assemblages from various geographic locations (Bailey et al., 1983; Herndl et al., 1993; Müller-Niklas et al., 1995; Sommaruga et al., 1997; Pakulski et al., 1998; Alonso-Sáez et al., 2006; Langenheder et al., 2006; Hernández et al., 2007; Joux et al., 2009; Santos et al., 2011a; Santos et al., 2012a; Santos et al., 2012b).

In the environment, the interaction between UV radiation and microorganisms is complex and influenced by several factors, including species composition, environmental factors such as temperature, salinity and nutrients, as well as intrinsic properties, like DNA repair potential, cell size and growth phase (Berney et al., 2006c; Joux et al., 2009; Matallana-Surget et al., 2010). In the case of the UVB range, the effects on aquatic organisms are, at least in part, determined by the dose of harmful radiation to which an individual organism is exposed which, in turn, is affected by both the positioning of the organism in the water column and the optical characteristics (*i.e.* UVB transmittance) of the water body (Sommaruga, 2003).

Bacterioneuston as a model community for environmental photobiology studies

Located at the air-water interface, the surface microlayer (SML) represents a unique microbial niche (Norkrans, 1980) inhabited by a bacterial community, *i.e.* bacterioneuston, that is particularly exposed to high doses of solar UV radiation (Hardy, 1982). Despite these harmful conditions, the surface microlayer has been reported to contain higher abundances of microorganisms than underlying waters (UW) (Norkrans, 1980; Hardy, 1982; Agogué et al., 2004), suggesting that bacterioneuston might have

developed strategies to survive in this "extreme environment". Therefore, bacterioneuston emerges as an interesting model system for the assessment of UVB effects on aquatic organisms, which might provide valuable predictive information on the consequences of future changes in UV radiation levels in the underlying water column.

In the present work, the influence of the light history of bacterial communities to their UVB sensitivity was assessed on two levels (1) by studying and comparing the effects of UVB exposure on the bacterial communities of the SML and UW in terms of abundance, activity, phylogenetic and physiological diversity, and (2) by studying and comparing the photobiological responses of bacterial isolates retrieved from the SML and UW.

Effects of UVB radiation on bacterioneuston and bacterioplankton

Regarding experiments with communities from the SML and UW, irradiation was found to have a lower impact on the abundance of culturable and total bacteria in bacterioneuston than in bacterioplankton, suggesting the possibility of enhanced UVB resistance of bacterial communities from the SML. Decreases in cell abundance were accompanied by a reduction in the phylogenetic diversity of both bacterioneuston and bacterioplankton, revealed by DGGE fingerprinting, thus demonstrating the relevance of UVB radiation as a driver of the structure of bacterial communities. UVB-induced changes in bacterial community structure can mainly be attributed to (i) differences in UVB sensitivity among bacterial members (Joux et al., 1999; Arrieta et al., 2000; Agogué et al., 2005; Santos et al., 2011b) and/or (ii) selection for bacterial community members specialized on photochemically modified dissolved organic matter (DOM) compounds and resistant to oxidative stress induced by inhibitory photoproducts (Fisher et al., 2008). Using DGGE analysis and sequencing, two ribotypes affiliated to the UV-resistant *Gammaproteobacteria* class (Alonso-Sáez et al., 2006) were found to persist throughout the irradiation period in both bacterioneuston and bacterioplankton suggesting the occurrence of selection of resistant strains by UVR.

FISH analysis supported the qualitative information provided by DGGE, confirming *Gammaproteobacteria* as the dominant group in bacterioneuston (Franklin et al., 2005). Furthermore, FISH results revealed that the relative abundance of the UV-resistant *Gammaproteobacteria* class increased with UVB exposure, dominating both irradiated bacterioneuston and bacterioplankton. The observations made in the present

work indicate that UVB exposure might select photo-resistant members of the bacterial community. Furthermore, the dominance of the UV-resistant *Gammaproteobacteria* group in the original SML community suggests that bacterioneuston may contain a pool of UV-resistant bacteria. This hypothesis is in accordance with earlier suggestions that members of bacterioneuston may have adapted to cope with the stressful conditions of the SML (Hermansson et al., 1987). More recently, Stolle *et al.* (2011) also observed that the strongest differences between the active communities of the non-attached size fraction of bacterioneuston and bacterioplankton occurred in response to high radiation levels. The authors suggested that UV radiation altered the community composition of non-attached, active bacterioneuston members, particularly under low wind conditions, resulting in increased differences between bacterioneuston and bacterioplankton.

In general, UVB-induced inhibition of protein synthesis was higher in bacterioneuston, while DNA synthesis was more inhibited in bacterioplankton. However, the observation of a lower UVB-induced decrease in cell abundance (total and culturable) in bacterioneuston compared to bacterioplankton, suggests enhanced UV resistance of bacterioneuston. It is possible that reducing protein synthesis upon UVB exposure could be a metabolic strategy that contributes to enhance survival, as actively growing bacteria are more susceptible to stress (Fischer and Sauer, 2005). Such a hypothesis would also help to explain the consistently reported lower bacterial biomass productivity at the SML compared to UW (Obernosterer et al., 2008; Reinthaler et al., 2008; Stolle et al., 2010), though nutrients often concentrate at the air-water interface (Williams et al., 1986).

UVB also caused a shift in the physiological profiles of sole-carbon-source utilization of the communities, assessed by the Biolog EcoPlate™ approach. Though limited in assessing the functional diversity of bacterial assemblages, Biolog EcoPlates™ have been used in the study of carbon source use patterns in different environments (Christian and Lind, 2006). Biolog EcoPlates™ have also been used to assess changes induced by sea ice melting in the functional diversity of bacterioplankton (Sala et al., 2010) and, together with the present work, reveal the potential of this tool to study the impact of global changes in the functioning of aquatic microbial communities.

The use of Biolog EcoPlates™ also provided new insights into the biology of bacterioneuston, specifically, the existence of clearly distinctive metabolic profiles in bacterioneuston and bacterioplankton. The original bacterioneuston community was able to use 11 out of the 32 substrates provided, being α-ketobutyric acid (14.2 %) and

glucose-1-phosphate (13.4 %) the most used substrates. On the other hand, the original bacterioplankton community was able to use 4 out of the 32 substrates provided, being *i*-erythritol (41.6 %) the most used one. These observations suggest substantial differences in the function of these structurally similar communities. Such results are in accordance with previous reports of differences in the relative abundances of bacterial groups incorporating leucine, as well as differences in terms of functional traits associated with trace gas metabolism, in the two communities (Cunliffe et al., 2008; Obernosterer et al., 2008; Hörtnagl et al., 2010).

UVB exposure caused not only a decrease in the number of substrates used by both communities but also a shift in the type of substrate preferably used. In bacterioneuston, the observed overall trend was from a metabolism relying mostly on carbohydrates and amino acids in the original community to a metabolism mostly dependent on carbohydrates upon UVB exposure. In the case of bacterioplankton, the metabolism of the original community was heavily dependent on the use of phenolic compounds and relied mostly on the use of amino acids after irradiation.

UVB-induced shifts in metabolic profiles can be related to alterations in microbial community composition or adaptation of the prevalent community to UVB radiation (Insam and Goberna, 2004). In the latter case, changes in the profiles of carbon sources preferably used are expected to be a consequence of a shift from cellular growth to DNA repair and other processes to ameliorate UVB-induced damage. However, the meaning of the observed metabolic shifts is still difficult to explain, in light of current knowledge. Further studies using, for instance, a metabolomic approach will help to gain more insights into the metabolic events that follow UVB exposure and their biological and ecological consequences.

Experimental considerations

The effects of UVB radiation on the structural and functional diversity of bacterioneuston and bacterioplankton were studied using a microcosm setup under laboratorial conditions. The depth of the irradiated SML and UW samples was similar and corresponded to approximately the averaged depth of the SML described in the literature (Cunliffe et al., 2011). Clear effects of UVB on the abundance, diversity and activity of bacterioneuston and bacterioplankton were observed, and a potential for the SML to contain bacterial members adapted to cope with high UV levels emerged. However, the possibility that these effects were exacerbated by the experimental setup

used cannot be excluded, as it most likely limited natural avoidance mechanisms, such as vertical migration, and did not allow the diffusion of toxic by-products of DOM photodegradation (Sommaruga, 2003). Nevertheless, such biases were present in both SML and UW experimental setups and should not compromise the comparison of the responses of both communities.

Preliminary experiments indicated that the removal of neither zooplankton nor phytoplankton from water samples affected, with statistical significance, the photobiological responses of the two bacterial communities, in accordance to previous works (Alonso-Sáez et al., 2006). The possibility that the overall bacterial responses observed may have a contribution of the effects of UVB on other members of the SML and UW communities, namely virus, cannot be excluded, but this can actually help to contextualize bacterial photobiological responses in the context of the microbial food web.

Isolation of UV-resistant bacterioneuston and bacterioplankton

In order to gain further insights into the influence of the light history of bacterial communities on their photobiological responses, UVB-resistant bacteria were isolated from the surface microlayer and underlying waters of the estuarine system of Ria de Aveiro. The individual UVB sensitivity of the retrieved isolates was then assessed in terms of CFU numbers, activity (leucine and thymidine incorporation), sole-carbon source use profiles, repair potential (light-dependent and independent), and photoadaptation potential under different physiological conditions.

As observed with experiments conducted with communities, isolates from the SML were, on average, significantly more resistant to UVB-induced damage than those retrieved from the UW, as assessed from culturable counts. Leucine incorporation was more reduced in bacterioneuston isolates than in bacterioplankton isolates, while thymidine incorporation was equally inhibited by UVB exposure in both sets of isolates. A shift in the physiological profile of the bacterial isolates with UVB exposure, assayed using Biolog EcoPlates^{TM}, was also observed, in accordance with the results obtained in the experiments with bacterial communities. Such a shift was particularly considerable in bacterioneuston isolates, which displayed statistically significant decreases in the utilization of amines and amino acids with irradiation. This shift in the physiological profile could reflect an active transcriptional reaction of the cells to UVB stress, involving a change in metabolic resource allocation from growth to defence/repair,

and/or could be a consequence of metabolic restructuring to compensate for UV-induced damage to sensitive enzymes.

UV sensitivity and repair potential was found to be affected by the nutritional condition of the cell, with nutrient depleted cells displaying enhanced sensitivity to UVB radiation and enhanced inhibition of thymidine incorporation. This observation denotes modulation of UVB responses by the nutritional status of the cell. In bacterioneuston, but not in bacterioplankton, recovery from UVB-induced damage was enhanced under nutrient starvation, suggesting the possibility of an intrinsic adaptation of bacterioneuston to nutrient depletion. Dissolved organic compounds (*e.g.*, free amino acids) are known to accumulate at the SML (Williams et al., 1986). However, bacterioneuston seems to display consistently lower bacterial growth efficiencies than bacterioplankton, indicating differences in the physiological state of bacterioneuston and bacterioplankton (Kuznetsova and Lee, 2002; Reinthaler et al., 2008). Rapidly growing cells are often more susceptible to inactivation than slower growing ones, because of the shorter time for excision repair between rounds of replication (Harm, 1980; Jagger, 1985). The present work raises the possibility that natural differences in physiological state of bacterioneuston and bacterioplankton could influence their UV sensitivity and help to explain the enhanced UVB resistance of bacterioneuston.

New insights into the mechanisms of UV-induced damage

Though UV radiation of different wavelengths is well known to cause damage to cells, ultimately resulting in cell death (Moan and Peak, 1989), the cellular targets of UV radiation, particularly in the UVB range, in bacteria and the mechanisms whereby radiation elicits damage to the cell are still unclear.

In order to gain further insights into the mechanisms of UV-induced damage, a set of bacterial isolates with different UV sensitivities was used as biological models to study (1) the wavelength-dependence of the biological damage elicited by UV radiation, (2) the identity and targets of the ROS involved in UVB-induced damage, (3) the influence of transition metals in the oxidative damage elicited by UVB exposure and (4) the role of abiotic properties and bacterial growth conditions in UVB-induced damage.

Wavelength-dependence of UV-induced damage

Reduction in cell numbers and activity, as well as DNA damage, displayed a clear wavelength-dependent variation following exposure to UV radiation of different spectral regions (UVA, UVB and UVC), being highest under UVC and lowest under UVA. Intracellular ROS generation, lipid oxidation (TBARS) and protein carbonylation, showed an inverse pattern, being highest upon exposure to UVA irradiation. These observations are in good agreement with earlier observations denoting the indirect, oxidative nature of UVA-induced damage (Eisenstark, 1970; Webb and Lorenz, 1970; Reed, 1997) and the high genotoxic potential of UVC radiation (Moan and Peak, 1989).

Principal component analysis confirmed the involvement of the extent of the oxidative damage to lipids and proteins, as well as ROS levels, in separating UVA-treated samples from the remaining, while the extent of DNA damage, assessed as DNA strand breaks (DSB), contributed the most for the separation of UVC-treated samples. Effects of UVB were found to be intermediate between those of UVA and UVC, in accordance with previous observations (Qiu et al., 2005a).

In order to identify the main determinants of bacterial inactivation under the different UV wavelengths, multiple linear stepwise regression analysis was applied to the data set. Despite the fact that UVA-treated samples were differentiated from the remaining treatments by enhanced levels of ROS and protein and lipid oxidation, surprisingly the amount of DSB emerged as the major determinant of inactivation upon exposure to UVA. DNA does not have a strong absorption in the UVA range. Therefore, UVA-induced damage to DNA is usually considered to be a result of photodynamic reactions mediated by cellular chromophores (Cadet et al., 2005a). However, recent investigations conducted in eukaryotes have highlighted the high mutagenic potential of UVA (Rünger et al., 2012) and the role of cyclobutane pyrimidine dimers, rather than oxidative lesions, in UVA-induced damage (Ikehata et al., 2008). The most UVA sensitive strains displayed significantly higher levels of DSB and TBARS (1-way ANOVA, $p < 0.05$) than resistant ones. Taken together, these results suggest that the extent of oxidative damage to biomolecules underlies the variability in UVA susceptibility among different bacteria but, ultimately, it is the accumulation of DNA lesions that leads to cell death under this radiation regime.

Under UVB, the main determinants of inactivation were found to be oxidative damage to lipids (TBARS), accumulation of DNA damage, as well as loss of metabolic activity. These results indicate the involvement of changes in the integrity of membrane structure and functionality, besides DNA damage, in bacterial inactivation by UVB radiation. The most UVB sensitive strains displayed significantly higher levels of protein carbonyls than resistant ones (1-way ANOVA, $p < 0.05$), suggesting a role of protein oxidative damage in determining bacterial sensitivity to UVB radiation. Enhanced levels of protein chaperones were previously reported in *Sphingopyxis alaskensis* following UVB exposure (Matallana-Surget et al., 2009a), denoting the importance of maintaining proper protein structure and function upon irradiation under UVB.

Regression analysis revealed that ROS levels together with DNA damage were the best predictors of cell inactivation under UVC. The most UVC sensitive strains were characterized by significantly higher TBARS and carbonyls levels than resistant ones (1-way ANOVA, $p < 0.05$). These results suggest that the extent of ROS-mediated damage to lipids and proteins, probably by interfering with vital biological functions, is a critical component of UVC-induced inactivation (Krisko and Radman, 2010; Schenk et al., 2011). Unexpectedly, ROS levels were significantly higher in resistant strains than in sensitive ones (1-way ANOVA, $p < 0.05$). ROS are known to be involved in eliciting specific defence strategies in response to UVC exposure in cyanobacteria (Dillon et al., 2002) and plants (Murphy and Huerta, 1990). The present work raises the possibility that ROS might play a physiological role in mediating the responses of bacteria to UVC radiation that deserves further investigation.

In order to gain additional insights into the cellular targets of UV radiation of different wavelengths, the effects of irradiation on the lipids and proteins of two representative bacteria with distinct UV sensitivities were studied by mid-infrared spectroscopy. In general, exposure to UV radiation of different wavelengths resulted in an increase in lipid methylation, denoted by the increase in the intensity of mid-infrared bands at approximately 2950 cm^{-1}, 2870 cm^{-1}, 1460 cm^{-1} and 1370 cm^{-1}. Lipid methylation strongly affects the fluidity of cellular membranes and changes in membrane fluidity have been associated with cellular adaptation to stress in *Oenococcus oeni* (Delmas et al., 2001) and signal transduction in higher organisms (Sangwan et al., 2002). Whether such changes could be involved in eliciting the bacterial response to UV radiation, is unknown.

Additionally, changes in the intensity of methyl bands together with decreased intensity of bands associated with esters and glyco- and/or phospholipids were also observed, suggesting altered lipid composition upon UV exposure. Such changes could reflect a consequence of damage to enzymes involved in lipid metabolism. Alternatively, it could represent a metabolic strategy to preserve the resources of the cell for repair strategies, for example, by using less phosphorus for phospholipid synthesis, diverting it for DNA repair strategies that require ATP.

UV exposure also resulted in a general increase in the intensity of mid-infrared bands associated with lipid oxidation products, denoting the potential of UV radiation to induce lipid oxidation also suggested from the measurement of TBARS levels.

Mid-infrared analysis of proteins extracted from irradiated cells showed UV-induced changes in the frequency and/or intensity of the components of the mid-infrared amide I band centred at approximately 1650 cm^{-1}, thus suggesting altered protein conformation and/or composition with irradiation. The observed changes in protein conformation could be associated with (1) induction of repair strategies (Demple, 1991), (2) aggregation and/or oxidative modifications of amino acid side chains, also consistent with the observed decrease in intensity of the mid-infrared band of tyrosine at approximately 1518 cm^{-1} (Lasch et al., 2001), and (3) synthesis of proteins with different composition and/or conformations in response to UV radiation (Matallana-Surget et al., 2009a; Bosshard et al., 2010b).

Additionally, mid-infrared spectroscopy revealed that UV exposure was also accompanied by a substantial increase in the intensity of methylene/CH_2 (and to a lesser extent, methyl/CH_3) bands associated with proteins and/or amino acids. This observation can reflect changes in protein composition, specifically, an increase in the relative proportion of amino acids particularly rich in CH_2 groups, like proline, lysine, isoleucine or glutamine/glutamic acid, potentially involved in stress protection (Kováčik et al., 2010). Additionally, enhanced intensity of bands assigned to CH_3 and CH_2 stretching vibrations can arise as a result of the addition of these groups to proteins during the process of propionylation of lysine residues (Singh et al., 2012). Propionylation is involved in the regulation of the activity of some enzymes in bacteria (Garrity et al., 2007). Whether this process could play a role in the metabolic response of bacteria to UV-induced stress is unknown and an interesting matter of research.

Finally, UV exposure also resulted in a general decrease in intensity of mid-infrared bands associated with glycosylated and/or phosphorylated proteins in the region

between 1200-900 cm^{-1}. This observation could possibly denote a decrease in the phosphorylation level of proteins, which was previously observed in *Xanthomonas oryzae* following UVC exposure (Huang et al., 1995), and/or decreased protein glycosylation levels. Changes in protein glycosylation levels are known to be involved in the regulation of the activity of specific proteins, including the RecA protein coordinating the SOS response of bacteria (Fischer and Haas, 2004).

Whether the modifications observed by mid-infrared spectroscopy in bacterial lipids and proteins reflect UV-induced damage to biomolecules or could actually be involved in a UV stress response mechanism is unknown and warrants further research. Additional studies using complementary techniques, such as mass spectrometry-based lipidomics and proteomics, could help to address the specific questions raised during this investigation.

Identity and targets of ROS in UVB-induced damage

In order to identify the ROS involved in UVB-induced damage and their biological targets, bacterial suspensions were pre-treated with specific scavengers for different ROS (hydroxyl radical, hydrogen peroxide, singlet oxygen and superoxide radical) before irradiation and their photobiological responses compared with those of isolates not amended with the scavengers.

Amendment of cell suspensions with sodium azide, a singlet oxygen scavenger, enhanced survival during UVB exposure and conferred a statistically significant protective effect against lipid oxidation. These observations indicate that singlet oxygen might play a pivotal role in UVB-induced cell inactivation, previously identified in eukaryotic cells (Vile and Tyrrell, 1995).

The hydroxyl radical, on the other hand, might be involved in DNA damage, as suggested by the observation of statistically significant lower levels of DSB in mannitol-amended samples. Such observation is in accordance with previous reports of the contribution of the hydroxyl radical to DNA damage in human cells exposed to UV radiation (Peak and Peak, 1990). Mannitol also significantly attenuated protein carbonylation during UVB exposure, indicating the participation of the hydroxyl radical in oxidative damage to proteins during UVB exposure.

The addition of exogenous CAT and SOD significantly protected the capacity for glucose uptake and respiration, suggesting that superoxide and H_2O_2 potentially participate in the impairment of metabolic activity during UVB exposure.

However, in some cases amendment with ROS scavenger resulted in an exacerbation of the detrimental effect of UVB radiation on biological parameters. In particular, a statistically significant increase in the amount of DSB was observed upon pre-treatment of cells with SOD and CAT, suggesting that the activity of these enzymes can contribute to the oxidative damage of biomolecules during exposure to UVB. Such observation is in accordance with previous work reporting the ability of CAT activity to generate ROS during UVB exposure when the antioxidant capabilities of the cell are diminished (Heck et al., 2003; Heck et al., 2010). SOD can also contribute to enhance the oxidative burden of the cell since H_2O_2 generated from its activity is a more oxidant species than superoxide (Scott et al., 1989). Ultimately, depending on the intracellular oxidation status of the cell, the activity of these antioxidant enzymes in response to UVB radiation can be either protective or cytotoxic.

Role of metals in UVB-induced damage

Metals play a crucial catalytic role in the production of free radicals and oxidative stress. In recent years, research conducted in different biological models has highlighted the role of divalent cationic metals in protection against the detrimental effects of several stressors (Daly et al., 2004; Bagwell et al., 2008; Ghosh et al., 2011; Granger et al., 2011). However, the role of transition metals on the susceptibility of bacteria to environmentally relevant UVB radiation is unknown. This information is crucial to fully understand the effects UV radiation in bacterial communities in natural environments, where metals are frequently present and may represent an additional stress factor (Zhou, et al., 2008)

In general, UVB and metal amendment, most notably iron, copper and manganese, contributed synergistically to enhance bacterial inactivation. In particular, iron amendment exacerbated ROS generation, DNA damage and lipid oxidative damage during irradiation. Oxidative damage to lipids was also enhanced in cells pre-treated with copper and cobalt. Such observations are in accordance with the involvement of iron in promoting the generation of the powerful oxidant hydroxyl radical through the Fenton reaction (Buda et al., 2003). Copper can also participate in Haber-Weiss reactions that mediate the generation of the hydroxyl radical (Santo et al., 2011). Previous investigations have reported altered expression of genes and proteins involved in iron influx and storage, as well as iron-containing enzymes, in bacteria exposed to UV radiation (Qiu et al., 2005a; Qiu et al., 2005b; Matallana-Surget et al., 2009a). The

present work indicates that metal homeostasis during irradiation might be important in limiting oxidative stress associated with UVB exposure.

Amendment of cell suspensions with manganese resulted in a statistically significant reduction in protein carbonyl levels during UVB exposure in all the strains tested, as well as a reduction in ROS levels. High levels of intracellular manganese have also been shown to contribute for the resistance of bacteria to UVC radiation and ionizing radiation by mitigating protein oxidation (Daly et al., 2004; Ghosh et al., 2011; Granger et al., 2011). This protective effect results from the replacement of the iron present in the Fe-S clusters of enzymes by the Mn^{2+} ion, thereby preventing the formation of damaging hydroxyl radicals through the Fenton reaction (Anjem et al., 2009). Additionally, Mn^{2+} is also capable of forming complexes with metabolites which can scavenge superoxide, H_2O_2 and hydroxyl radicals (Daly et al., 2010).

Surprisingly, the protective effect of manganese against protein carbonylation and ROS levels was accompanied by a statistically significant reduction in survival during exposure to UVB, compared to non-amended controls and, in three of the strains tested, a significant increase in DNA damage levels. The reason for this detrimental effect is unclear in the face of current knowledge, but some speculations can be made. For example, the protective effect of Mn^{2+} is known to be dependent on the high expression of antioxidant enzymes, particularly catalase (Schellhorn et al., 1998), but CAT can be inactivated by UVB (Zigman et al., 1996). This could have contributed for the observed enhanced inactivation by UVB in the presence of manganese. On the other hand, it is possible that the Fe^{2+} that is displaced by Mn^{2+} in proteins could be able to participate in damage to DNA or lipids, thus overriding its protective effect against protein carbonylation.

Taken together, these results indicate that the toxicity of reactive oxygen species generated during UV exposure is mediated by intracellular metals and that metal homeostasis is decisive in limiting the detrimental effects of ROS generated during UVB exposure in bacteria. The corollary following these observations is that enhanced metal concentration in the environment might increase the sensitivity of bacteria to UVB-induced damage. Accordingly, photoreactions on cell surfaces have been proposed to contribute to the biological damage caused by copper in polluted ecosystems (Hayase and Zepp, 1991).

Factors influencing UVB-induced inactivation and their mechanisms of interaction

UV properties (wavelength, dose, mode of delivery), as well as environmental (temperature, salinity, nutrients) (Ogbebo and Ochs, 2008; Joux et al., 2009; Bullock and Jeffrey, 2010; Matallana-Surget et al., 2010) and biological (specific sensitivity, repair mechanisms, nutritional state, growth phase) (Berney et al., 2006c; Bucheli-Witschel et al., 2010) factors, influence the effects of UV exposure on bacteria.

In the present work, the influence of different extrinsic and intrinsic factors on the photobiological responses of bacteria was also studied.

Influence of nutrients and the suspension medium

Properties associated with the medium in which bacterial cells are suspended for irradiations can influence their UV sensitivity by affecting bacterial physiology, photodynamic reactions and/or light penetration through the medium (Muela et al., 2002; Steinberger et al., 2002; Arana et al., 2004).

In the present work, the influence of nutrient concentration on the photobiological responses of bacteria was studied by inoculating bacterial assemblages of different origins (bacterioneuston and bacterioplankton) in water containing different nutrient (nitrogen and phosphorus) content (high and low). UV-induced inhibition was generally attenuated upon inoculation of bacterial communities in high nutrient medium, compared to unamended conditions. Repair processes elicited in response to UVR require nitrogen for synthesis of proteins involved in DNA repair and ROS scavenging, and thus can potentially be inhibited by a limitation in nitrogen supply. These repair processes are also energy-dependent, requiring ATP, and are consequently susceptible to limitation in the supply of phosphorus (Beardall et al., 2009). The results obtained indicate that nutrient amendment potentially attenuates UV-induced inhibition of bacteria by providing the elements required for synthesis of proteins, including those involved in repair of UV-induced damage. These observations are in accordance with previous work reporting the ability of nutrient inputs to promote recovery from UV-induced damage in bacterioplankton (Pausz and Herndl, 2002; Joux et al., 2009).

The influence of the quality of the suspension medium on the UV-sensitivity responses of bacterial communities was studied by inoculating bacterioneuston and bacterioplankton samples of marine and brackish origin in cell-free water of different origin (surface and subsurface of marine and brackish origin). Their photobiological

responses in terms of culturable numbers and activity (leucine incorporation) were determined and compared to those observed upon inoculation in an artificial mineral solution (AMS).

In general, inoculation of bacterial communities in SML and UW water attenuated the inhibitory effects of radiation, compared to those observed upon inoculation in AMS. The UV protective effect of inoculation of bacterial communities in SML and/or UW compared to the AMS treatment can be attributed to stimulation of bacterial metabolism by low molecular weight compounds resulting from the photolytic cleavage of DOM present in the natural samples (Amador et al., 1989; Bushaw et al., 1996; Moran and Zepp, 1997; Bertilsson and Tranvik, 1998; Obernosterer et al., 1999) which could have compensated for the direct negative effects of irradiation. On the other hand, DOC present in the environmental samples can also exert a shield and quenching effect (Muela et al., 2000; Bracchini et al., 2005) that might have contributed to mitigate the detrimental effects of irradiation in samples diluted in SML and/or UW, compared to samples in AMS. Taken together, these results demonstrate that the media in which bacteria are suspended for irradiations influence the biological effects of UV radiation, thus pointing to the importance of the SML and UW abiotic environment in determining the UV responses of the corresponding bacterial communities.

Influence of light dose and growth conditions

In order to test the influence of growth conditions in UV-induced oxidative damage, a representative estuarine bacterial strain was grown to the mid-exponential, late-exponential or stationary phase at 15 ºC or 25 ºC under nutrient-rich (TSB) or nutrient-poor (M9 medium) conditions and irradiated up to a cumulative dose of 60 kJ m^{-2}. Cell numbers and markers of oxidative damage (lipid peroxidation, protein carbonylation, DNA strand breaks and DNA-protein cross-links) during irradiation were monitored.

In general, oxidative damage only followed a linear dose-dependence for low UVB doses ($\leq$ 10 kJ m^{-2}), suggesting that oxidative damage levels during irradiation result from a dynamic interaction between damage induction and repair. Another possibility is that, at high UVB doses, there is a saturation of oxidative damage as a result of consecutive molecule excitation by high UV fluences, which gives rise to a complex, non-linear dependence of oxidative damage on the irradiation dose (Byeong et al., 2007).

Stationary phase cells generally survived better and showed lower levels of oxidative damage than exponential phase cells, particularly at low and intermediate UVB doses. Enhanced survival of stationary phase cells to several stress factors has been attributed to the role of the alternative sigma factor RpoS or σ^{38}, encoded by the *rpoS* gene, that is active in the stationary phase of many bacteria and induces a number of mechanisms that ensure resistance to environmental stress (Loewen and Hengge-Aronis, 1994; Chen et al., 1996; Schellhorn et al., 1998; Hengge-Aronis, 1999).

Mid-exponential phase cells grown at 15 ºC survived better to UVB exposure and showed lower levels of oxidative damage than cells grown at 25 ºC, particularly at low UVB doses. These results suggest a potential temperature effect on ROS generation and/or ROS interaction with the cellular targets. UV-induced DNA damage, assessed by CPD and/or 6-4 PP quantification, was previously found to be enhanced at higher temperatures (Takeuchi et al., 1996; Waterworth et al., 2002; Li et al., 2004; Matallana-Surget et al., 2010). A possible influence of temperature on the conformational state of DNA (Li et al., 2002) and/or an indirect influence of temperature on DNA lesions, by affecting DNA-binding proteins (Matallana-Surget et al., 2010), could contribute for such a temperature trend. Furthermore, it is also possible that the chemical reactions involved in the interaction of ROS with their targets might be temperature-dependent (Li et al., 2002). The electron transport chain is a major source of ROS in the cell (Imlay and Fridovich, 1991; González-Flecha and Demple, 1995). It is possible that, by reducing oxygen consumption, lower temperatures might attenuate ROS production and the risk of oxidative damage (Borgeraas and Hessen, 2000).

Cells cultivated in nutrient-rich TSB generally survived better to medium-high UVB doses (> 10 kJ m^{-2}) than those grown in nutrient-poor M9 medium. Nutrient-rich TSB, but not M9, could possibly have provided sufficient amounts of the chemical elements required for the synthesis of macromolecules necessary to withstand high UVB doses (*e.g.*, enzymes involved in DNA repair and ROS scavenging), thus accounting for the enhanced UVB resistance of cells grown in TSB. These results are consistent with the enhanced UVB resistance of a set of bacterial isolates in nourished conditions, compared to their starved counterparts (Santos et al., 2012a), and enhanced UVB resistance of bacterioplankton and bacterioneuston upon amendment with high nutrient concentrations (Chapter 9).

These results reveal that growth conditions preceding irradiation are important determinants of survival and oxidative damage imposed by UVB exposure, potentially by affecting the temporal progression and the magnitude of biomolecule damage.

The role of RecA as an indicator of UV repair potential

The RecA protein is the primary regulator of dark repair mechanisms in bacteria (Miller and Kokjohn, 1990). Because the *recA* gene is itself regulated as part of the SOS gene expression system, measurement of the concentration of RecA protein in the cell allows monitoring of its repair capacity. Accordingly, RecA levels have been proposed as a barometer of the repair potential of bacterial isolates and communities in response to incident solar UV radiation (Booth et al., 2001a; Booth et al., 2001b). Transcriptomic and proteomics studies have supported the potential role of RecA as a biomarker of UV-induced damage (Courcelle et al., 2001; Qiu et al., 2005a; Qiu et al., 2005b; Berney et al., 2006a; Moeller et al., 2007b; Matallana-Surget et al., 2012).

Evidences suggest that structural or kinetic properties of RecA are also related to specific requirements of DNA damage repair systems in some species. For example, the RecA of the radiation-resistant *Deinococcus radiodurans* and that of *E. coli* show differences in terms of orientation and composition of the C-terminal domain involved in binding double-stranded DNA (Rajan and Bell, 2004). These observations raise the hypothesis that the ability to cope with DNA damage, particularly that induced by UV radiation, during the life history of microorganisms could be reflected in RecA phylogeny and/or in the number of its gene copies in the genome.

In the present work, it was investigated whether RecA phylogeny and *recA* frequency among fully sequenced genomes could reflect an adaptation to cope with UV-induced damage. Phylogenetic analysis of the RecA protein was, in general, coherent with the phyla defined by 16S rRNA gene analysis, demonstrating the high degree of conservation of RecA resulting from its fundamental housekeeping role in bacteria. Duplication of the *recA* gene was found to be widespread among myxobacteria (*Deltaproteobacteria*) and some Firmicutes members. Earlier work by Karlin *et al.* (1995) suggested that the presence of two *recA* genes in the myxobacteria *Myxococcus xanthus* could provide higher amounts of the RecA repair protein that would allow this topsoil bacteria to withstand UV irradiation. However, our observations of the widespread duplication of *recA* in myxobacteria inhabiting various environments

suggest that UV radiation is not the only factor underlying the presence of additional copies of the *recA* gene.

Duplication of the *recA* gene was also detected in several Firmicutes members. In *Bacillus megaterium*, both *recA* copies seem to be functional, and the second *recA* copy is known to complement the loss of *recA*1 in terms of UV sensitivity (Nahrstedt et al., 2005). The authors suggested that a greater amount of RecA might increase the capacity of the cell for recombinational repair. Whether this is applicable to the other Firmicutes members in which *recA* duplication was observed, is unknown.

Several new cases of plasmids encoding the *recA* gene that had not been previously reported in the literature were also identified by database mining. The presence of two *recA* ($recA_{P1}$ and $recA_{P3}$) in two different plasmids in *Deinococcus deserti*, in addition to the chromosomal *recA*, was proposed to provide higher levels of RecA protein for efficient error-free repair of DNA damage (Dulermo et al., 2009). In the present work, in some of the plasmids the presence of a gene coding for DNA polymerase V subunit, which performs translesion DNA synthesis during the SOS response, immediately after the *recA* gene was observed. This could suggest that the plasmid-encoded *recA* copy might fulfil a role in complementing the chromosomal *recA* in the SOS response, including during the response to UV exposure. However, further studies are necessary to clarify whether the newly detected plasmid-encoded RecA proteins are actually functional and can, in fact, complement the chromosomal RecA in the SOS response.

PÁGINA INTENCIONALMENTE DEIXADA EM BRANCO

CHAPTER 13

GENERAL CONCLUSIONS

The results of this thesis indicate that:

- **The light history of bacterial communities influences their UV sensitivity.** Results from community assays comparing the responses of bacterioneuston and bacterioplankton to UVB radiation revealed that bacterial abundance and DNA synthesis were more affected in bacterioplankton, while protein synthesis was more inhibited in bacterioneuston. UVB exposure seemed to select for UV-resistant *Gammaproteobacteria*, particularly abundant in bacterioneuston. Enhanced resistance of bacterioneuston to UVB radiation, in terms of abundance, was confirmed in investigations conducted with isolated bacterial strains. Furthermore, UVB irradiation was also found to be accompanied by a shift in sole-carbon source use profiles in bacterial isolates. Recovery from UVB-induced stress was enhanced in bacterioneuston, particularly under nutrient-depleted conditions. These results suggest that bacterioneuston may contain a pool of UV-resistant strains that, under appropriate meteorological conditions, may be selected upon UV exposure.
- **DNA damage, oxidative damage to lipids, and intracellular ROS levels account for bacterial inactivation under UVA, UVB and UVC wavelengths.** Using a combination of several UV-sensitivity tests and their statistical analysis, applied to a range of bacteria, new information regarding the process of UV-based inactivation was gained. Mid-infrared spectroscopy revealed an array of modifications in the lipids and proteins of bacteria following irradiation. These results provide new insights into the targets of different UV wavelengths in bacterial cells, as well as clues to the underlying common mechanisms involved in the inactivation of different bacteria. This information can contribute for a better understanding of the environmental effects of UV radiation and allow the optimization of UV-based disinfection strategies.
- **Singlet oxygen is pivotal in UVB-induced cell inactivation.** Using specific ROS scavengers, singlet oxygen was also found to be important in lipid peroxidation. The hydroxyl radical was found to participate in DNA strand breakage and protein carbonylation, while the impairment of glucose

incorporation and respiration during UVB exposure had a contribution of hydrogen peroxide and superoxide.

- **Metal amendment, particularly iron, copper and manganese, enhances bacterial inactivation during UVB exposure.** Amendment with iron exacerbated ROS generation, DNA damage and lipid peroxidation during irradiation. Copper and cobalt also enhanced lipid peroxidation. Despite attenuating the formation of protein carbonyls during irradiation, manganese amendment decreased bacterial survival. These results indicate that iron, copper, cobalt and manganese play a role in UVB-induced inactivation and that metal homeostasis is crucial in limiting the detrimental effects of ROS generated during UVB exposure.
- **The abiotic environment (nutrient content and quality of the suspension medium) influences the UVB sensitivity of bacterial communities.** In general, inoculation of bacterial communities in high nutrient medium attenuated UVB-induced inhibition of abundance and activity, compared to unamended conditions. Suspension in natural water resulted in less pronounced inhibitory effects of UVB exposure, compared to suspensions prepared in an artificial mineral solution.
- **Growth conditions preceding irradiation are crucial to the extent of the oxidative damage induced by UVB exposure.** In general, stationary phase cells survived better and showed lower levels of protein carbonyls than exponential phase cells. Oxidative damage to biomolecules was generally higher at 25 ºC than at 15 ºC, particularly in mid-exponential phase cells, pointing to a temperature effect on ROS generation and/or ROS interaction with the cellular targets. Growth conditions seemed to affect UVB sensitivity by influencing the temporal progression and the magnitude of the damage to biomolecules.
- **RecA phylogeny reflects the high degree of conservation of the protein, rather than particular adaptations to withstand stressful conditions.** Duplication of the *recA* gene was found to be widespread in myxobacteria and also frequent among Firmicutes. Several plasmids containing *recA* homologs not yet reported in the literature were identified. Gene context analysis suggested that plasmid-encoded *recA* genes could complement the activity of chromosome-encoded *recA* genes in the bacterial SOS response.

REFERENCES

Aas, P., Lyons, M. M., Pledger, R., Mitchell, D. L. & Jeffrey, W. H. 1996. Inhibition of bacterial activities by solar radiation in nearshore waters and the Gulf of Mexico. *Aquatic Microbial Ecology,* 11, 229-238.

Abboudi, M., Surget, S. M., Rontani, J. F., Sempéré, R. & Joux, F. 2008. Physiological alteration of the marine bacterium *Vibrio angustum* S14 exposed to simulated sunlight during growth. *Current Microbiology,* 57, 412-417.

Abby, S. S., Tannier, E., Gouy, M. & Daubin, V. 2012. Lateral gene transfer as a support for the tree of life. *Proceedings of the National Academy of Sciences of the United States of America,* 109, 4962-4967.

Abu-ghararah, Z. H. 1994. Effect of temperature on the kinetics of wastewater disinfection using ultraviolet radiation. *Journal of Environmental Science and Health - Part A Environmental Science and Engineering,* 29, 585-603.

Agogué, H., Casamayor, E. O., Joux, F., Obernosterer, I., Dupuy, C., Lantoine, F., Catala, P., Weinbauer, M. G., Reinthaler, T., Herndl, G. J. & Lebaron, P. 2004. Comparison of samplers for the biological characterization of the sea surface microlayer. *Limnology and Oceanography: Methods,* 2, 213-225.

Agogué, H., Joux, F., Obernosterer, I. & Lebaron, P. 2005. Resistance of marine bacterioneuston to solar radiation. *Applied and Environmental Microbiology,* 71, 5282-5289.

Aller, J. Y., Kuznetsova, M. R., Jahns, C. J. & Kemp, P. F. 2005. The sea surface microlayer as a source of viral and bacterial enrichment in marine aerosols. *Journal of Aerosol Science,* 36, 801-812.

Almeida, M. A., Cunha, M. A. & Alcântara, F. 2001. Physiological responses of marine and brackish water bacterial assemblages in a tidal estuary (Ria de Aveiro, Portugal). *Aquatic Microbial Ecology,* 25, 113-125.

Alonso-Sáez, L., Gasol, J. M., Lefort, T., Hofer, J. & Sommaruga, R. 2006. Effect of natural sunlight on bacterial activity and differential sensitivity of natural bacterioplankton groups in Northwestern Mediterranean coastal waters. *Applied and Environmental Microbiology,* 72, 5806-5813.

Altschul, S. F., Gish, W., Miller, W., Myers, E. W. & Lipman, D. J. 1990. Basic local alignment search tool. *Journal of Molecular Biology,* 215, 403-410.

Amador, J. A., Alexander, M. & Zika, R. G. 1989. Sequential photochemical and microbial degradation of organic molecules bound to humic acid. *Applied and Environmental Microbiology,* 55, 2843-2849.

Amann, R. I., Krumholz, L. & Stahl, D. A. 1990. Fluorescent-oligonucleotide probing of whole cells for determinative, phylogenetic, and environmental studies in microbiology. *Journal of Bacteriology,* 172, 762-770.

Anderl, J. N., Zahller, J., Roe, F. & Stewart, P. S. 2003. Role of nutrient limitation and stationary-phase existence in *Klebsiella pneumoniae* biofilm resistance to ampicillin and ciprofloxacin. *Antimicrobial Agents and Chemotherapy,* 47, 1251-1256.

Andersen, B. M., Bånrud, H., Bøe, E., Bjordal, O. & Drangsholt, F. 2006. Comparison of UV C light and chemicals for disinfection of surfaces in hospital isolation units. *Infection Control and Hospital Epidemiology,* 27, 729-734.

Anderson, J., Russell Iii, J. M., Solomon, S. & Deaver, L. E. 2000. Halogen Occultation Experiment confirmation of stratospheric chlorine decreases in accordance with the Montreal Protocol. *Journal of Geophysical Research D: Atmospheres,* 105, 4483-4490.

Andolfi, A., Cimmino, A., Lo Cantore, P., Iacobellis, N. S. & Evidente, A. 2008. Bioactive and structural metabolites of *Pseudomonas* and *Burkholderia* species causal agents of cultivated mushrooms diseases. *Perspectives in Medicinal Chemistry,* 2008, 81-112.

Andrady, A., Aucamp, P. J., Bais, A. F., Ballare, C. L., Bjorn, L. O., Bornman, J. F., Caldwell, M., Cullen, A. P., Erickson, D. J., deGruijl, F. R., Häder, D. P., Ilyas, M.,

Kulandaivelu, G., Kumar, H. D., Longstreth, J., McKenzie, R. L., Norval, M., Paul, N., Redhwi, H. H., Smith, R. C., Solomon, K. R., Sulzberger, B., Takizawa, Y., Tang, X., Teramura, A. H., Torikai, A., van der Leun, J. C., Wilson, S. R., Worrest, R. C. & Zepp, R. G. 2010. Environmental effects of ozone depletion and its interactions with climate change: progress report, 2009. *Photochem Photobiol Sci,* 9, 275-94.

Anesio, A. M. & Granéli, W. 2003. Increased photoreactivity of DOC by acidification: Implications for the carbon cycle in humic lakes. *Limnology and Oceanography,* 48, 735-744.

Anesio, A. M., Theil-Nielsen, J. & Granéli, W. 2000. Bacterial growth on photochemically transformed leachates from aquatic and terrestrial primary producers. *Microbial Ecology,* 40, 200-208.

Anjem, A., Varghese, S. & Imlay, J. A. 2009. Manganese import is a key element of the OxyR response to hydrogen peroxide in *Escherichia coli*. *Molecular Microbiology,* 72, 844-858.

Apel, K. & Hirt, H. 2004. Reactive oxygen species: Metabolism, oxidative stress, and signal transduction. *Annual Review of Plant Biology,* 55, 373-399.

Arana, I., Seco, C., Epelde, K., Muela, A., Fernández-Astorga, A. & Barcina, I. 2004. Relationships between *Escherichia coli* cells and the surrounding medium during survival processes. *Antonie van Leeuwenhoek, International Journal of General and Molecular Microbiology,* 86, 189-199.

Aranda, J., Bardina, C., Beceiro, A., Rumbo, S., Cabral, M. P., Barbé, J. & Bou, G. 2011. *Acinetobacter baumannii* RecA protein in repair of DNA damage, antimicrobial resistance, general stress response, and virulence. *Journal of Bacteriology,* 193, 3740-3747.

Archibald, F. S. & Duong, M. N. 1986. Superoxide dismutase and oxygen toxicity defenses in the genus *Neisseria*. *Infection and Immunity,* 51, 631-641.

Arrieta, J. M., Weinbauer, M. G. & Herndl, G. J. 2000. Interspecific variability in sensitivity to UV radiation and subsequent recovery in selected isolates of marine bacteria. *Applied and Environmental Microbiology,* 66, 1468-1473.

Azam, F., Fenchel, T., Field, J. G., Gray, J. S., Meyer, L. A. & Thingstad, F. 1983. The ecological role of water column microbes in the sea. *Marine Ecology Progress Series,* 10, 257-263.

Azam, F. & Malfatti, F. 2007. Microbial structuring of marine ecosystems. *Nature Reviews Microbiology,* 5, 782-791.

Azevedo, J. S. N., Ramos, I., Araújo, S., Oliveira, C. S., Correia, A. & Henriques, I. S. 2012. Spatial and temporal analysis of estuarine bacterioneuston and bacterioplankton using culture-dependent and culture-independent methodologies. *Antonie van Leeuwenhoek, International Journal of General and Molecular Microbiology,* 1-17.

Bagwell, C. E., Milliken, C. E., Ghoshroy, S. & Blom, D. A. 2008. Intracellular copper accumulation enhances the growth of *Kineococcus radiotolerans* during chronic irradiation. *Applied and Environmental Microbiology,* 74, 1376-1384.

Baier, J., Maisch, T., Maier, M., Engel, E., Landthaler, M. & Bäumler, W. 2006. Singlet Oxygen Generation by UVA Light Exposure of Endogenous Photosensitizers. *Biophysical Journal,* 91, 1452-1459.

Bailey, C. A., Neihof, R. A. & Tabor, P. S. 1983. Inhibitory Effect of Solar Radiation on Amino Acid Uptake in Chesapeake Bay Bacteria. *Applied and Environmental Microbiology,* 46, 44-49.

Bais, A. F., Tourpali, K., Kazantzidis, A., Akiyoshi, H., Bekki, S., Braesicke, P., Chipperfield, M. P., Dameris, M., Eyring, V., Garny, H., Iachetti, D., Jöckel, P., Kubin, A., Langematz, U., Mancini, E., Michou, M., Morgenstern, O., Nakamura, T., Newman, P. A., Pitari, G., Plummer, D. A., Rozanov, E., Shepherd, T. G., Shibata, K., Tian, W. & Yamashita, Y. 2011. Projections of UV radiation changes in the 21st century: Impact of ozone recovery and cloud effects. *Atmospheric Chemistry and Physics,* 11, 7533-7545.

Baker, A. & Kanofsky, J. R. 1992. Quenching of Singlet Oxygen by Biomolecules from L1210 Leukemia Cells. *Photochemistry and Photobiology*, 55, 523-528.

Ballaré, C. L., Caldwell, M. M., Flint, S. D., Robinson, S. A. & Bornman, J. F. 2011. Effects of solar ultraviolet radiation on terrestrial ecosystems. Patterns, mechanisms, and interactions with climate change. *Photochemical and Photobiological Sciences*, 10, 226-241.

Bancroft, B. A., Baker, N. J. & Blaustein, A. R. 2007. Effects of UVB radiation on marine and freshwater organisms: A synthesis through meta-analysis. *Ecology Letters*, 10, 332-345.

Barnese, K., Gralla, E. B., Cabelli, D. E. & Selverstone Valentine, J. 2008. Manganous Phosphate Acts as a Superoxide Dismutase. *Journal of the American Chemical Society*, 130, 4604-4606.

Barras, F. & Fontecave, M. 2011. Cobalt stress in *Escherichia coli* and *Salmonella enterica*: molecular bases for toxicity and resistance. *Metallomics*, 3, 1130-1134.

Barros, A. 1999. *Contribution à la sélection et la comparaison de variables caractéristiques.* PhD Thesis, Institut National Agronomique Paris-Grignon.

Barth, A. 2000. The infrared absorption of amino acid side chains. *Progress in Biophysics and Molecular Biology*, 74, 141-173.

Bast, A., Haenen, G. R. M. M. & Doelman, C. J. A. 1991. Oxidants and antioxidants: State of the art. *American Journal of Medicine*, 91, 3C-2S-3C-13S.

Batty, D. P. & Wood, R. D. 2000. Damage recognition in nucleotide excision repair of DNA. *Gene*, 241, 193-204.

Bauermeister, A., Bentchikou, E., Moeller, R. & Rettberg, P. 2009. Roles of PprA, IrrE, and RecA in the resistance of *Deinococcus radiodurans* to germicidal and environmentally relevant UV radiation. *Archives of Microbiology*, 191, 913-918.

Baumstark-Khan, C. & Horneck, G. 2007. Results from the "Technical Workshop on Genotoxicity Biosensing" on the micro-scale fluorometric assay of deoxyribonucleic acid unwinding. *Analytica Chimica Acta*, 593, 75-81.

Baxter, R. M. & Carey, J. H. 1983. Evidence for photochemical generation of superoxide ion in humic waters. *Nature*, 306, 575-576.

Beak, S. M., Lee, Y. S. & Kim, J. A. 2004. NADPH oxidase and cyclooxygenase mediate the ultraviolet B-induced generation of reactive oxygen species and activation of nuclear factor-κB in HaCaT human keratinocytes. *Biochimie*, 86, 425-429.

Beardall, J., Sobrino, C. & Stojkovic, S. 2009. Interactions between the impacts of ultraviolet radiation, elevated CO_2, and nutrient limitation on marine primary producers. *Photochemical and Photobiological Sciences*, 8, 1257-1265.

Becker-Hapak, M., Troxtel, E., Hoerter, J. & Eisenstark, A. 1997. RpoS dependent overexpression of carotenoids from *Erwinia herbicola* in OxyR deficient *Escherichia coli*. *Biochemical and Biophysical Research Communications*, 239, 305-309.

Becker, M. M. & Wang, Z. 1989. Origin of ultraviolet damage in DNA. *Journal of Molecular Biology*, 210, 429-438.

Beers, R. F. J. & Sizer, I. W. 1952. A spectrophotometric method for measuring the breakdown of hydrogen peroxide by catalase. *Journal of Biological Chemistry*, 195, 133-140.

Behrenfeld, M., Hardy, J., Gucinski, H., Hanneman, A., Lee Ii, H. & Wones, A. 1993. Effects of ultraviolet-B radiation on primary production along latitudinal transects in the South Pacific ocean. *Marine Environmental Research*, 35, 349-363.

Benner, R. & Biddanda, B. 1998. Photochemical transformations of surface and deep marine dissolved organic matter: Effects on bacterial growth. *Limnology and Oceanography*, 43, 1373-1378.

Benov, L. & Fridovich, I. 1999. Why superoxide imposes an aromatic amino acid auxotrophy on *Escherichia coli*: The transketolase connection. *Journal of Biological Chemistry*, 274, 4202-4206.

Berlett, B. S., Chock, P. B., Yim, M. B. & Stadtman, E. R. 1990. Manganese(II) catalyzes the bicarbonate-dependent oxidation of amino acids by hydrogen peroxide and the amino

acid-facilitated dismutation of hydrogen peroxide. *Proceedings of the National Academy of Sciences of the United States of America,* 87, 389-393.

Berlett, B. S. & Stadtman, E. R. 1997. Protein oxidation in aging, disease, and oxidative stress. *Journal of Biological Chemistry,* 272, 20313-20316.

Berney, M., Weilenmann, H.-U. & Egli, T. 2006a. Gene expression of *Escherichia coli* in continuous culture during adaptation to artificial sunlight. *Environmental Microbiology,* 8, 1635-1647.

Berney, M., Weilenmann, H. U. & Egli, T. 2006b. Flow-cytometric study of vital cellular functions in *Escherichia coli* during solar disinfection (SODIS). *Microbiology,* 152, 1719-1729.

Berney, M., Weilenmann, H. U., Ihssen, J., Bassin, C. & Egli, T. 2006c. Specific growth rate determines the sensitivity of *Escherichia coli* to thermal, UVA, and solar disinfection. *Applied and Environmental Microbiology,* 72, 2586-2593.

Berney, M., Weilenmann, H. U., Simonetti, A. & Egli, T. 2006d. Efficacy of solar disinfection of *Escherichia coli, Shigella flexneri, Salmonella* Typhimurium and *Vibrio cholerae*. *Journal of Applied Microbiology,* 101, 828-836.

Bertilsson, S. & Tranvik, L. J. 1998. Photochemically produced carboxylic acids as substrates for freshwater bacterioplankton. *Limnology and Oceanography,* 43, 885-895.

Beyer, W. F., Jr. & Fridovich, I. 1991. *In vivo* competition between iron and manganese for occupancy of the active site region of the manganese-superoxide dismutase of *Escherichia coli*. *Journal of Biological Chemistry,* 266, 303-308.

Bhandari, R. & Sharma, P. 2011. Photosynthetic and biochemical characterization of pigments and UV-absorbing compounds in *Phormidium tenue* due to UV-B radiation. *Journal of Applied Phycology,* 23, 283-292.

Bianco, P. R., Tracy, R. B. & Kowalczykowski, S. C. 1998. DNA strand exchange proteins: a biochemical and physical comparison. *Frontiers in Bioscience,* 17, D570-603.

Bligh, E. G. & Dyer, W. J. 1959. A rapid method of total lipid extraction and purification. *Canadian Journal of Biochemistry and Physiology,* 37, 911-917.

Boles, B. R. & Horswill, A. R. 2008. The Cyclization of Peptides and Proteins with Inteins. *In:* Lutz, S. & Bornscheuer, U. T. (eds.) *Protein Engineering Handbook.* Weinheim, Germany: Wiley-VCH Verlag GmbH & Co. KGaA.

Bolton, N. F., Cromar, N. J., Hallsworth, P. & Fallowfield, H. J. 2010. A review of the factors affecting sunlight inactivation of micro-organisms in waste stabilisation ponds: Preliminary results for enterococci.

Booth, M. G., Hutchinson, L., Brumsted, M., Aas, P., Coffin, R. B., Downer Jr, R. C., Kelley, C. A., Lyons, M. M., Pakulski, J. D., Holder Sandvik, S. L., Jeffrey, W. H. & Miller, R. V. 2001a. Quantification of *recA* gene expression as an indicator of repair potential in marine bacterioplankton communities of Antarctica. *Aquatic Microbial Ecology,* 24, 51-59.

Booth, M. G., Jeffrey, W. H. & Miller, R. V. 2001b. RecA expression in response to solar UVR in the marine bacterium *Vibrio natriegens*. *Microbial Ecology,* 42, 531-539.

Borgeraas, J. & Hessen, D. O. 2000. UV-B induced mortality and antioxidant enzyme activities in *Daphnia magna* at different oxygen concentrations and temperatures. *Journal of Plankton Research,* 22, 1167-1183.

Bose, B. & Chatterjee, S. N. 1995. Correlation between UVA-induced changes in microviscosity, permeability and malondialdehyde formation in liposomal membrane. *Journal of Photochemistry and Photobiology B: Biology,* 28, 149-153.

Bosshard, F., Berney, M., Scheifele, M., Weilenmann, H. U. & Egli, T. 2009. Solar disinfection (SODIS) and subsequent dark storage of *Salmonella typhimurium* and *Shigella flexneri* monitored by flow cytometry. *Microbiology,* 155, 1310-1317.

Bosshard, F., Bucheli, M., Meur, Y. & Egli, T. 2010a. The respiratory chain is the cell's Achilles' heel during UVA inactivation in *Escherichia coli*. *Microbiology,* 156, 2006-2015.

Bosshard, F., Riedel, K., Schneider, T., Geiser, C., Bucheli, M. & Egli, T. 2010b. Protein oxidation and aggregation in UVA-irradiated *Escherichia coli* cells as signs of accelerated cellular senescence. *Environmental Microbiology,* 12, 2931-2945.

Boulikas, T. 1992. Evolutionary consequences of nonrandom damage and repair of chromatin domains. *Journal of Molecular Evolution,* 35, 156-180.

Bourdon, E. & Blache, D. 2001. The importance of proteins in defense against oxidation. *Antioxid Redox Signal,* 3, 293-311.

Bowden, G. H. & Li, Y. H. 1997. Nutritional influences on biofilm development. *Advances in Dental Research,* 11, 81-99.

Bracchini, L., Dattilo, A. M., Falcucci, M., Loiselle, S. A., Hull, V., Arena, C. & Rossi, C. 2005. Spatial and temporal variations of the inherent and apparent optical properties in a shallow coastal lake. *Journal of Photochemistry and Photobiology B: Biology,* 80, 161-177.

Bradford, M. M. 1976. A rapid and sensitive method for the quantitation of microgram quantities of protein utilizing the principle of protein dye binding. *Analytical Biochemistry,* 72, 248-254.

Braun, V., Hantke, K. & Koster, W. 1998. Bacterial iron transport: mechanisms, genetics, and regulation. *Metal Ions in Biological Systems,* 35, 67-145.

Bucheli-Witschel, M., Bassin, C. & Egli, T. 2010. UV-C inactivation in *Escherichia coli* is affected by growth conditions preceding irradiation, in particular by the specific growth rate. *Journal of Applied Microbiology,* 109, 1733-1744.

Bucher, J. R., Tien, M. & Aust, S. D. 1983. The requirement for ferric in the initiation of lipid peroxidation by chelated ferrous iron. *Biochemical and Biophysical Research Communications,* 111, 777-784.

Buda, F., Ensing, B., Gribnau, M. C. M. & Baerends, E. J. 2003. O_2 evolution in the Fenton reaction. *Chemistry - A European Journal,* 9, 3436-3444.

Buettner, G. R., Ng, C. F., Wang, M., Rodgers, V. G. J. & Schafer, F. Q. 2006. A New Paradigm: Manganese Superoxide Dismutase Influences the Production of H_2O_2 in Cells and Thereby Their Biological State. *Free Radical Biology and Medicine,* 41, 1338-1350.

Bullock, A. K. & Jeffrey, W. H. 2010. Temperature and solar radiation interactions on ^{3}H-leucine incorporation by bacterioplankton in a subtropical estuary. *Photochemistry and Photobiology,* 86, 593-599.

Buma, A. G. J., Boelen, P. & Jeffrey, W. H. 2003. UVR-induced DNA damage in aquatic organisms. *In:* Helbling, E. W. & Zagarese, H. E. (eds.) *UV Effects in Aquatic Organisms and Ecosystems.* Cambridge, UK: Royal Society of Chemistry.

Buma, A. G. J., De Boer, M. K. & Boelen, P. 2001. Depth distributions of DNA damage in antarctic marine phyto and bacterioplankton exposed to summertime UV radiation. *Journal of Phycology,* 37, 200-208.

Bushaw, K. L., Zepp, R. G., Tarr, M. A., Schulz-Jander, D., Bourbonniere, R. A., Hodson, R. E., Miller, W. L., Bronk, D. A. & Moran, M. A. 1996. Photochemical release of biologically available nitrogen from aquatic dissolved organic matter. *Nature,* 381, 404-407.

Byeong, H. Y., Young, A. L., Kim, S. K., Kuzmin, V., Kolbanovskiy, A., Dedon, P. C., Geacintov, N. E. & Shafirovich, V. 2007. Photosensitized oxidative DNA damage: From hole injection to chemical product formation and strand cleavage. *Journal of the American Chemical Society,* 129, 9321-9332.

Cabiscol, E., Tamarit, J. & Ros, J. 2000. Oxidative stress in bacteria and protein damage by reactive oxygen species. *International Microbiology,* 3, 3-8.

Cadet, J., Courdavault, S., Ravanat, J. L. & Douki, T. 2005a. UVB and UVA radiation-mediated damage to isolated and cellular DNA. *Pure and Applied Chemistry,* 77, 947-961.

Cadet, J., Sage, E. & Douki, T. 2005b. Ultraviolet radiation-mediated damage to cellular DNA. *Mutation Research,* 571, 3-17.

Caldwell, M. M., Ballaré, C. L., Bornman, J. F., Flint, S. D., Björn, L. O., Teramura, A. H., Kulandaiveli, G. & Tevini, M. 2003. Terrestrial ecosystems, increased solar ultraviolet radiation and interactions with other climatic change factors. *Photochemical and Photobiological Sciences,* 2, 29-38.

Caldwell, M. M., Björn, L. O., Bornman, J. F., Flint, S. D., Kulandaivelu, G., Teramura, A. H. & Tevini, M. 1998. Effects of increased solar ultraviolet radiation on terrestrial ecosystems. *Journal of Photochemistry and Photobiology B: Biology,* 46, 40-52.

Caldwell, M. M., Bornman, J. F., Ballaré, C. L., Flint, S. D. & Kulandaivelu, G. 2007. Terrestrial ecosystems, increased solar ultraviolet radiation, and interactions with other climate change factors. *Photochemical and Photobiological Sciences,* 6, 252-266.

Calleja, M. L., Duarte, C. M., Navarro, N. & Agustí, S. 2005. Control of air-sea CO_2 disequilibria in the subtropical NE Atlantic by planktonic metabolism under the ocean skin. *Geophys. Res. Lett.,* 32, L08606.

Canuto, V. M., Levine, J. S., Augustsson, T. R. & Imhoff, C. L. 1982. UV radiation from the young Sun and oxygen and ozone levels in the prebiological palaeoatmosphere. *Nature,* 296, 816-820.

Carlson, D. J. 1982. Surface microlayer phenolic enrichments indicate sea surface slicks. *Nature,* 296, 426-429.

Carrillo, P., Medina-Sánchez, J. M. & Villar-Argaiz, M. 2002. The interaction of phytoplankton and bacteria in a high mountain lake: Importance of the spectral composition of solar radiation. *Limnology and Oceanography,* 47, 1294-1306.

Chamberlain, J. & Moss, S. H. 1987. LIPID PEROXIDATION AND OTHER MEMBRANE DAMAGE PRODUCED IN Escherichia coli K1060 BY NEAR-UV RADIATION AND DEUTERIUM OXIDE. *Photochemistry and Photobiology,* 45, 625-630.

Chatila, K., Demers, S., Mostajir, B., Gosselin, M., Chanut, J. P. & Monfort, P. 1999. Bacterivory of a natural heterotrophic protozoan community exposed to different intensities of ultraviolet-B radiation. *Aquatic Microbial Ecology,* 20, 59-74.

Chatila, K., Demers, S., Mostajir, B., Gosselin, M., Chanut, J. P., Monfort, P. & Bird, D. 2001. The responses of a natural bacterioplankton community to different levels of ultraviolet-B radiation: A food web perspective. *Microbial Ecology,* 41, 56-68.

Chee, G. J. & Takami, H. 2005. Housekeeping *recA* gene interrupted by group II intron in the thermophilic *Geobacillus kaustophilus*. *Gene,* 363, 211-220.

Chen, C. Y. I., Eckmann, L., Libby, S. J., Fang, F. C., Okamoto, S., Kagnoff, M. F., Fierer, J. & Guiney, D. G. 1996. Expression of *Salmonella typhimurium rpoS* and *rpoS*-dependent genes in the intracellular environment of eukaryotic cells. *Infection and Immunity,* 64, 4739-4743.

Choksi, K. B., Nuss, J. E., DeFord, J. H. & Papaconstantinou, J. 2008. Age-related alterations in oxidatively damaged proteins of mouse skeletal muscle mitochondrial electron transport chain complexes. *Free Radical Biology and Medicine,* 45, 826-838.

Christian, B. W. & Lind, O. T. 2006. Key issues concerning Biolog use for aerobic and anaerobic freshwater bacterial community-level physiological profiling. *International Review of Hydrobiology,* 91, 257-268.

Christopherson, M. R., Suen, G., Bramhacharya, S., Jewell, K. A., Aylward, F. O., Moeller, J. A., Munk, A. C., Goodwin, L. A., Currie, C. R., Mead, D. & Brumm, P. J. 2012. The Complete Genomes of *Cellulomonas fimi* and *Cellvibrio gilvus* ATCC 13127 Reveal Two Cellulolytic Bacteria and the Reclassification of *Cellulomonas gilvus* comb. nov. *Seventh Annual DOE Joint Genome Institute User Meeting.* Walnut Creek, California.

Chróst, R. J. & Faust, M. A. 1999. Consequences of solar radiation on bacterial secondary production and growth rates in subtropical coastal water (Atlantic Coral Reef off Belize, Central America). *Aquatic Microbial Ecology,* 20, 39-48.

Chrzanowski, T. H. & Kyle, M. 1996. Ratios of carbon, nitrogen and phosphorus in *Pseudomonas fluorescens* as a model for bacterial element ratios and nutrient regeneration. *Aquatic Microbial Ecology,* 10, 115-122.

Chun, H., Kim, J., Chung, K., Won, M. & Song, K. B. 2009. Inactivation kinetics of *Listeria monocytogenes*, *Salmonella enterica* serovar Typhimurium, and *Campylobacter jejuni* in ready-to-eat sliced ham using UV-C irradiation. *Meat Science,* 83, 599-603.

Ciccarelli, F. D., Doerks, T., Von Mering, C., Creevey, C. J., Snel, B. & Bork, P. 2006. Toward automatic reconstruction of a highly resolved tree of life. *Science,* 311, 1283-1287.

Conan, P., Joux, F., Torréton, J. P., Pujo-Pay, M., Douki, T., Rochelle-Newall, E. & Mari, X. 2008. Effect of solar ultraviolet radiation on bacterio- and phytoplankton activity in a large coral reef lagoon (southwest New Caledonia). *Aquatic Microbial Ecology,* 52, 83-98.

Coohill, T. P. & Sagripanti, J.-L. 2008. Overview of the Inactivation by 254 nm Ultraviolet Radiation of Bacteria with Particular Relevance to Biodefense. *Photochemistry and Photobiology,* 84, 1084-1090.

Coohill, T. P. & Sagripanti, J.-L. 2009. Bacterial Inactivation by Solar Ultraviolet Radiation Compared with Sensitivity to 254 nm Radiation. *Photochemistry and Photobiology,* 85, 1043-1052.

Cooper, W. J., Zika, R. G., Petasne, R. G. & Fischer, A. M. 1988. Sunlight-Induced Photochemistry of Humic Substances in Natural Waters: Major Reactive Species. *In:* Suffet, I. H. & MacCarthy, P. (eds.) *Aquatic Humic Substances.* American Chemical Society.

Costechareyre, D., Rhouma, A., Lavire, C., Portier, P., Chapulliot, D., Bertolla, F., Boubaker, A., Dessaux, Y. & Nesme, X. 2010. Rapid and Efficient Identification of *Agrobacterium Species* by *recA* Allele Analysis. *Microbial Ecology,* 60, 862-872.

Cottrell, M. T. & Kirchman, D. L. 2000. Community composition of marine bacterioplankton determined by 16S rRNA gene clone libraries and fluorescence *in situ* hybridization. *Applied and Environmental Microbiology,* 66, 5116-5122.

Courcelle, J., Khodursky, A., Peter, B., Brown, P. O. & Hanawalt, P. C. 2001. Comparative Gene Expression Profiles Following UV Exposure in Wild-Type and SOS-Deficient *Escherichia coli*. *Genetics,* 158, 41-64.

Cox, M. M. 2007. Motoring along with the bacterial RecA protein. *Nature Reviews Molecular Cell Biology,* 8, 127-138.

Creed, D. 1984. The photophysics and photochemistry of the near-UV absorbing amino acids, I: tryptophan and its simple derivatives. *Photochemistry and Photobiology,* 39, 537-562.

Crossley, R. A., Gaskin, D. J. H., Holmes, K., Mulholland, F., Wells, J. M., Kelly, D. J., van Vliet, A. H. M. & Walton, N. J. 2007. Riboflavin Biosynthesis Is Associated with Assimilatory Ferric Reduction and Iron Acquisition by *Campylobacter jejuni*. *Applied and Environmental Microbiology,* 73, 7819-7825.

Crutzen, P. J. 1970. The influence of nitrogen oxides on the atmospheric ozone content. *Quarterly Journal of the Royal Meteorological Society,* 96, 320-325.

Cullen, J. J. & Neale, P. J. 1994. Ultraviolet radiation, ozone depletion, and marine photosynthesis. *Photosynthesis Research,* 39, 303-320.

Cunliffe, M., Engel, A., Frka, S., Gašparović, B., Guitart, C., Murrell, J. C., Salter, M., Stolle, C., Upstill-Goddard, R. & Wurl, O. 2013. Sea surface microlayers: A unified physicochemical and biological perspective of the air–ocean interface. *Progress In Oceanography,* 109, 104-116.

Cunliffe, M. & Murrell, J. C. 2009. The sea-surface microlayer is a gelatinous biofilm. *ISME Journal,* 3, 1001-1003.

Cunliffe, M., Schäfer, H., Harrison, E., Cleave, S., Upstill-Goddard, R. & Murrell, J. C. 2008. Phylogenetic and functional gene analysis of the bacterial and archaeal communities associated with the surface microlayer of an estuary. *ISME Journal,* 2, 776-789.

Cunliffe, M., Upstill-Goddard, R. C. & Murrell, J. C. 2011. Microbiology of aquatic surface microlayers. *FEMS Microbiology Reviews,* 35, 233-246.

Curatolo, W. 1987. Glycolipid function. *BBA - Reviews on Biomembranes,* 906, 137-160.

Curtis, T. P., Mara, D. D. & Silva, S. A. 1992. Influence of pH, oxygen, and humic substances on ability of sunlight to damage fecal coliforms in waste stabilization pond water. *Applied and Environmental Microbiology*, 58, 1335-1343.

D'Angelo, S., Ingrosso, D., Perfetto, B., Baroni, A., Zappia, M., Lobianco, L. L., Tufano, M. A. & Galletti, P. 2001. UVA irradiation induces L-isoaspartyl formation in melanoma cell proteins. *Free Radical Biology and Medicine*, 31, 1-9.

Dagan, T., Roettger, M., Bryant, D. & Martin, W. 2010. Genome networks root the tree of life between prokaryotic domains. *Genome Biology and Evolution*, 2, 379-392.

Daims, H., Brühl, A., Amann, R., Schleifer, K. H. & Wagner, M. 1999. The domain-specific probe EUB338 is insufficient for the detection of all bacteria: Development and evaluation of a more comprehensive probe set. *Systematic and Applied Microbiology*, 22, 434-444.

Daly, M. J., Gaidamakova, E. K., Matrosova, V. Y., Kiang, J. G., Fukumoto, R., Lee, D.-Y., Wehr, N. B., Viteri, G. A., Berlett, B. S. & Levine, R. L. 2010. Small-Molecule Antioxidant Proteome-Shields in *Deinococcus radiodurans*. *PLoS ONE*, 5, e12570.

Daly, M. J., Gaidamakova, E. K., Matrosova, V. Y., Vasilenko, A., Zhai, M., Leapman, R. D., Lai, B., Ravel, B., Li, S.-M. W., Kemner, K. M. & Fredrickson, J. K. 2007. Protein oxidation implicated as the primary determinant of bacterial radioresistance. *PLoS Biol*, 5, e92.

Daly, M. J., Gaidamakova, E. K., Matrosova, V. Y., Vasilenko, A., Zhai, M., Venkateswaran, A., Hess, M., Omelchenko, M. V., Kostandarithes, H. M., Makarova, K. S., Wackett, L. P., Fredrickson, J. K. & Ghosal, D. 2004. Accumulation of Mn(II) in *Deinococcus radiodurans* facilitates gamma-radiation resistance. *Science*, 306, 1025-1028.

Dantur, K. I. & Pizarro, R. A. 2004. Effect of growth phase on the *Escherichia coli* response to ultraviolet-A radiation: Influence of conditioned media, hydrogen peroxide and acetate. *Journal of Photochemistry and Photobiology B: Biology*, 75, 33-39.

Das, A., Silaghi-Dumitrescu, R., Ljungdahl, L. G. & Kurtz Jr, D. M. 2005. Cytochrome bd oxidase, oxidative stress, and dioxygen tolerance of the strictly anaerobic bacterium *Moorella thermoacetica*. *Journal of Bacteriology*, 187, 2020-2029.

Davies-Colley, R. J., Bell, R. G. & Donnison, A. M. 1994. Sunlight inactivation of enterococci and fecal coliforms in sewage effluent diluted in seawater. *Applied and Environmental Microbiology*, 60, 2049-2058.

Davies, M. J. 2003. Singlet oxygen-mediated damage to proteins and its consequences. *Biochemical and Biophysical Research Communications*, 305, 761-770.

Davis, E. O., Thangaraj, H. S., Brooks, P. C. & Colston, M. J. 1994. Evidence of selection for protein introns in the RecAs of pathogenic mycobacteria. *EMBO Journal*, 13, 699-703.

De La Vega, U. P., Rettberg, P., Douki, T., Cadet, J. & Horneck, G. 2005. Sensitivity to polychromatic UV-radiation of strains of *Deinococcus radiodurans* differing in their DNA repair capacity. *International Journal of Radiation Biology*, 81, 601-611.

De Lange, H. J., Morris, D. P. & Williamson, C. E. 2003. Solar ultraviolet photodegradation of DOC may stimulate freshwater food webs. *Journal of Plankton Research*, 25, 111-117.

Delmas, F., Pierre, F., Coucheney, F., Divies, C. & Guzzo, J. 2001. Biochemical and physiological studies of the small heat shock protein Lo18 from the lactic acid bacterium *Oenococcus oeni*. *Journal of Molecular Microbiology and Biotechnology*, 3, 601-610.

Demidova, T. N. & Hamblin, M. R. 2004. Photodynamic therapy targeted to pathogens. *International Journal of Immunopathology and Pharmacology*, 17, 245-254.

Demple, B. 1991. Regulation of bacterial oxidative stress genes. *Annual Review of Genetics*, 25, 315-337.

Di Capua, C., Bortolotti, A., Farías, M. E. & Cortez, N. 2011. UV-resistant *Acinetobacter* sp. isolates from Andean wetlands display high catalase activity. *FEMS Microbiology Letters*, 317, 181-189.

Diffey, B. L. 1991. Solar ultraviolet radiation effects on biological systems. *Physics in Medicine and Biology,* 36, 299-328.

Dillon, J. G., Tatsumi, C. M., Tandingan, P. G. & Castenholz, R. W. 2002. Effect of environmental factors on the synthesis of scytonemin, a UV-screening pigment, in a cyanobacterium (*Chroococcidiopsis* sp.). *Archives of Microbiology,* 177, 322-331.

DiRuggiero, J. & Robb, F. T. 2004. Early evolution of DNA repair mechanisms. *In:* Ribas de Pouplana, L. (ed.) *The Genetic Code and the Origin of Life*. Austin, TX: Landes Biosciences.

Dixon, J. L. & Nightingale, P. D. 2012. Fine-scale variability in methanol uptake and oxidation: From the microlayer to 1000 m. *Biogeosciences,* 9, 2961-2972.

Dobretsov, S. V., Gosselin, L. & Qian, P. Y. 2010. Effects of solar PAR and UV radiation on tropical biofouling communities. *Marine Ecology Progress Series,* 402, 31-43.

Dodd, C. E. R., Sharman, R. L., Bloomfield, S. F., Booth, I. R. & Stewart, G. S. A. B. 1997. Inimical processes: Bacterial self-destruction and sub-lethal injury. *Trends in Food Science and Technology,* 8, 238-241.

Dodson, M. L., Michaels, M. L. & Lloyd, R. S. 1994. Unified catalytic mechanism for DNA glycosylases. *Journal of Biological Chemistry,* 269, 32709-32712.

Dorrell, N., Davies, D. J. G. & Moss, S. H. 1995. Evidence of photoenzymatic repair due to the *phrA* gene in a *phrB* mutant of *Escherichia coli* K-12. *Journal of Photochemistry and Photobiology B: Biology,* 28, 87-92.

Douki, T. 2006. Effect of denaturation on the photochemistry of pyrimidine bases in isolated DNA. *Journal of Photochemistry and Photobiology B: Biology,* 82, 45-52.

Dukan, S. & Nyström, T. 1999. Oxidative Stress Defense and Deterioration of Growth-arrested *Escherichia coli* Cells. *Journal of Biological Chemistry,* 274, 26027-26032.

Dulermo, R., Fochesato, S., Blanchard, L. & De Groot, A. 2009. Mutagenic lesion bypass and two functionally different RecA proteins in *Deinococcus deserti*. *Molecular Microbiology,* 74, 194-208.

Duwat, P., Ehrlich, S. D. & Gruss, A. 1995. The *recA* gene of *Lactococcus lactis*: Characterization and involvement in oxidative and thermal stress. *Molecular Microbiology,* 17, 1121-1131.

Dybvig, K., Hollingshead, S. K., Heath, D. G., Clewell, D. B., Sun, F. & Woodard, A. 1992. Degenerate oligonucleotide primers for enzymatic amplification of *recA* sequences from gram-positive bacteria and mycoplasmas. *Journal of Bacteriology,* 174, 2729-2732.

Egorov, S. Y., Kamalov, V. F., Koroteev, N. I., Krasnovsky Jr, A. A., Toleutaev, B. N. & Zinukov, S. V. 1989. Rise and decay kinetics of photosensitized singlet oxygen luminescence in water. Measurements with nanosecond time-correlated single photon counting technique. *Chemical Physics Letters,* 163, 421-424.

Eisen, J. A. 1995. The RecA protein as a model molecule for molecular systematic studies of bacteria: Comparison of trees of RecAs and 16S rRNAs from the same species. *Journal of Molecular Evolution,* 41, 1105-1123.

Eisenstark, A. 1970. Sensitivity of *Salmonella typhimurium* recombinationless (rec) mutants to visible and near-visible light. *Mutation Research/Fundamental and Molecular Mechanisms of Mutagenesis,* 10, 1-6.

Eisenstark, A. 1998. Bacterial gene products in response to near-ultraviolet radiation. *Mutation Research/Fundamental and Molecular Mechanisms of Mutagenesis,* 422, 85-95.

Eisenstark, A., Calcutt, M. J., Becker-Hapak, M. & Ivanova, A. 1996. Role of *Escherichia coli rpoS* and associated genes in defense against oxidative damage. *Free Radical Biology and Medicine,* 21, 975-993.

Eker, A. P. M., Formenoy, L. & de Wit, L. E. A. 1991. Photoreactivation in the extreme halophilic archaebacterium *Halobacterium cutirubrum*. *Photochemistry and Photobiology,* 53, 643-651.

Elasri, M. O. & Miller, R. V. 1998. A *Pseudomonas aeruginosa* biosensor responds to exposure to ultraviolet radiation. *Applied Microbiology and Biotechnology,* 50, 455-458.

Elasri, M. O. & Miller, R. V. 1999. Study of the response of a biofilm bacterial community to UV radiation. *Applied and Environmental Microbiology,* 65, 2025-2031.

Espeland, E. M. & Wetzel, R. G. 2001. Complexation, stabilization, and UV photolysis of extracellular and surface-bound glucosidase and alkaline phosphatase: Implications for biofilm microbiota. *Microbial Ecology,* 42, 572-585.

Esterbauer, H., Jurgens, G., Quehenberger, O. & Koller, E. 1987. Autoxidation of human low density lipoprotein: Loss of polyunsaturated fatty acids and vitamin E and generation of aldehydes. *Journal of Lipid Research,* 28, 495-509.

Esterbauer, H., Schaur, R. J. & Zollner, H. 1991. Chemistry and Biochemistry of 4-hydroxynonenal, malonaldehyde and related aldehydes. *Free Radical Biology and Medicine,* 11, 81-128.

Falkowski, P. G. 2006. Tracing oxygen's imprint on earth's metabolic evolution. *Science,* 311, 1724-1725.

Fantino, J.-R., Py, B., Fontecave, M. & Barras, F. 2010. A genetic analysis of the response of *Escherichia coli* to cobalt stress. *Environmental Microbiology,* 12, 2846-2857.

Farman, J. C., Gardiner, B. G. & Shanklin, J. D. 1985. Large losses of total ozone in Antarctica reveal seasonal ClOx/NOx interaction. *Nature,* 315, 207-210.

Ferenci, T. 1999. Regulation by nutrient limitation. *Current Opinion in Microbiology,* 2, 208-213.

Fernández Murga, M. L., Cabrera, G. M., De Valdez, G. F., Disalvo, A. & Seldes, A. M. 2000. Influence of growth temperature on cryotolerance and lipid composition of *Lactobacillus acidophilus*. *Journal of Applied Microbiology,* 88, 342-348.

Fernández Zenoff, V., Heredia, J., Ferrero, M., Siñeriz, F. & Farías, M. 2006a. Diverse UV-B Resistance of Culturable Bacterial Community from High-Altitude Wetland Water. *Current Microbiology,* 52, 359-362.

Fernández Zenoff, V., Siñeriz, F. & Farías, M. E. 2006b. Diverse responses to UV-B radiation and repair mechanisms of bacteria isolated from high-altitude aquatic environments. *Applied and Environmental Microbiology,* 72, 7857-7863.

Ferreri, C. & Chatgilialoglu, C. 2009. Membrane lipidomics and the geometry of unsaturated fatty acids from biomimetic models to biological consequences. *Methods in molecular biology (Clifton, N.J.),* 579, 391-411.

Fischer, E. & Sauer, U. 2005. Large-scale *in vivo* flux analysis shows rigidity and suboptimal performance of *Bacillus subtilis* metabolism. *Nature Genetics,* 37, 636-640.

Fischer, W. & Haas, R. 2004. The RecA Protein of *Helicobacter pylori* Requires a Posttranslational Modification for Full Activity. *Journal of Bacteriology,* 186, 777-784.

Fisher, M. B., Keenan, C. R., Nelson, K. L. & Voelker, B. M. 2008. Speeding up solar disinfection (SODIS): Effects of hydrogen peroxide, temperature, pH, and copper plus ascorbate on the photoinactivation of *E. coli*. *Journal of Water and Health,* 6, 35-51.

Fleischmann, E. M. 1989. The measurement and penetration of ultraviolet radiation into tropical marine water. *Limnology and Oceanography,* 34, 1623-1629.

Foote, C. S. 1987. Type I and Type II Mechanisms of Photodynamic Action. *Light-Activated Pesticides.* American Chemical Society.

Foote, C. S. 1991. Definition of type I and type II photosensitized oxidation. *Photochemistry and Photobiology,* 54, 659.

Franklin, M. P., McDonald, I. R., Bourne, D. G., Owens, N. J. P., Upstill-Goddard, R. C. & Murrell, J. C. 2005. Bacterial diversity in the bacterioneuston (sea surface microlayer): the bacterioneuston through the looking glass. *Environmental Microbiology,* 7, 723-736.

Frederick, J. E. & Lubin, D. 1988. The budget of biologically active ultraviolet radiation in the Earth- atmosphere system. *Journal of Geophysical Research,* 93, 3825-3832.

Fredriksson, Å., Ballesteros, M., Dukan, S. & Nyström, T. 2005. Defense against Protein Carbonylation by DnaK/DnaJ and Proteases of the Heat Shock Regulon. *Journal of Bacteriology,* 187, 4207-4213.

Fridovich, I. 1995. Superoxide radical and superoxide dismutases. *Annual Review of Biochemistry,* 64, 97-112.

Friedberg, E. C. 1985. *DNA repair*, New York, W. H. Freeman and Company.

Friedberg, E. C., McDaniel, L. D. & Schultz, R. A. 2004. The role of endogenous and exogenous DNA damage and mutagenesis. *Current Opinion in Genetics and Development,* 14, 5-10.

Friedberg, E. C., Walker, G. C. & Siede, W. 1995. *DNA Repair and Mutagenesis,* Washington, D. C., American Society of Microbiology Press.

Froidevaux, L., Livesey, N. J., Read, W. G., Salawitch, R. J., Waters, J. W., Drouin, B., MacKenzie, I. A., Pumphrey, H. C., Bernath, P., Boone, C., Nassar, R., Montzka, S., Elkins, J., Cunnold, D. & Waugh, D. 2006. Temporal decrease in upper atmospheric chlorine. *Geophysical Research Letters,* 33.

Fuhrman, J. A. & Azam, F. 1982. Thymidine incorporation as a measure of heterotrophic bacterioplankton production in marine surface waters: Evaluation and field results. *Marine Biology,* 66, 109-120.

Futsaether, C. M., Kjeldstad, B. & Johnsson, A. 1995. Intracellular pH changes induced in *Propionibacterium acnes* by UVA radiation and blue light. *Journal of Photochemistry and Photobiology B: Biology,* 31, 125-131.

Gaballa, A. & Helmann, J. D. 2002. A peroxide-induced zinc uptake system plays an important role in protection against oxidative stress in *Bacillus subtilis*. *Molecular Microbiology,* 45, 997-1005.

Galkin, V. E., Yu, X., Bielnicki, J., Ndjonka, D., Bell, C. E. & Egelman, E. H. 2009. Cleavage of Bacteriophage λ cI Repressor Involves the RecA C-Terminal Domain. *Journal of Molecular Biology,* 385, 779-787.

Garcia-Pichel, F. 1994. A model for internal self-shading in planktonic organisms and its implications for the usefulness of ultraviolet sunscreens. *Limnology and Oceanography,* 39, 1704-1717.

Garland, J. L. & Mills, A. L. 1991. Classification and characterization of heterotrophic microbial communities on the basis of patterns of community-level sole-carbon-source utilization. *Applied and Environmental Microbiology,* 57, 2351-2359.

Garmyn, M. & Yarosh, D. B. 2007. The molecular and genetic effects of ultraviolet radiation exposure on skin cells. *In:* Lim, H. W., Honigsman, H. & Hawk, J. (eds.) *Principles and practice of photodermatology.* New York, NY: Informa Healthcare.

Garrity, J., Gardner, J. G., Hawse, W., Wolberger, C. & Escalante-Semerena, J. C. 2007. N-Lysine Propionylation Controls the Activity of Propionyl-CoA Synthetase. *Journal of Biological Chemistry,* 282, 30239-30245.

Garvey, P., Rince, A., Hill, C. & Fitzgerald, G. F. 1997. Identification of a RecA homolog (RecA(LP)) on the conjugative lactococcal phage resistance plasmid pNP40: Evidence of a role for chromosomally encoded RecA(L) in abortive infection. *Applied and Environmental Microbiology,* 63, 1244-1251.

Gault, N., Rigaud, O., Poncy, J.-L. & Lefaix, J.-L. 2005. Infrared microspectroscopy study of γ-irradiated and H_2O_2-treated human cells. *International Journal of Radiation Biology,* 81, 767-779.

Gayán, E., Monfort, S., Álvarez, I. & Condón, S. 2011. UV-C inactivation of *Escherichia coli* at different temperatures. *Innovative Food Science & Emerging Technologies,* 12, 531-541.

Ghosh, S., Ramirez-Peralta, A., Gaidamakova, E., Zhang, P., Li, Y. Q., Daly, M. J. & Setlow, P. 2011. Effects of Mn levels on resistance of *Bacillus megaterium* spores to heat, radiation and hydrogen peroxide. *Journal of Applied Microbiology,* 111, 663-670.

Girotti, A. W. 1985. Mechanisms of lipid peroxidation. *Journal of Free Radicals in Biology and Medicine,* 1, 87-95.

Girotti, A. W. 1998. Lipid hydroperoxide generation, turnover, and effector action in biological systems. *Journal of Lipid Research,* 39, 1529-1542.

Girotti, A. W. 2001. Photosensitized oxidation of membrane lipids: Reaction pathways, cytotoxic effects, and cytoprotective mechanisms. *Journal of Photochemistry and Photobiology B: Biology,* 63, 103-113.

Girotti, A. W. & Giacomoni, P. U. 2007. Lipid and protein damage provoked by ultraviolet radiation: mechanisms of indirect photooxidative damage. *In:* Giacomoni, P. U. (ed.) *Biophysical and physiological effects of solar radiation on human skin.* Amsterdam: Elsevier.

Glaeser, S. P., Grossart, H.-P. & Glaeser, J. 2010. Singlet oxygen, a neglected but important environmental factor: short-term and long-term effects on bacterioplankton composition in a humic lake. *Environmental Microbiology,* 12, 3124-3136.

Glöckner, F. O., Fuchs, B. M. & Amann, R. 1999. Bacterioplankton compositions of lakes and oceans: A first comparison based on fluorescence *in situ* hybridization. *Applied and Environmental Microbiology,* 65, 3721-3726.

Gocke, K. 1977. Comparison of methods for determining the turnover times of dissolved organic compounds. *Marine Biology,* 42, 131-141.

Goldblatt, C., Lenton, T. M. & Watson, A. J. 2006. Bistability of atmospheric oxygen and the Great Oxidation. *Nature,* 443, 683-686.

Goldman, B. S., Nierman, W. C., Kaiser, D., Slater, S. C., Durkin, A. S., Eisen, J., Ronning, C. M., Barbazuk, W. B., Blanchard, M., Field, C., Halling, C., Hinkle, G., Iartchuk, O., Kim, H. S., Mackenzie, C., Madupu, R., Miller, N., Shvartsbeyn, A., Sullivan, S. A., Vaudin, M., Wiegand, R. & Kaplan, H. B. 2006. Evolution of sensory complexity recorded in a myxobacterial genome. *Proceedings of the National Academy of Sciences of the United States of America,* 103, 15200-15205.

Gomes, A. A., Silva-Júnior, A. C. T., Oliveira, E. B., Asad, L. M. B. O., Reis, N. C. S. C., Felzenszwalb, I., Kovary, K. & Asad, N. R. 2005. Reactive oxygen species mediate lethality induced by far-UV in *Escherichia coli* cells. *Redox Report,* 10, 91-95.

Gonzaga, M. L. C., Ricardo, N. M. P. S., Heatley, F. & Soares, S. d. A. 2005. Isolation and characterization of polysaccharides from *Agaricus blazei* Murill. *Carbohydrate Polymers,* 60, 43-49.

González-Flecha, B. & Demple, B. 1995. Metabolic sources of hydrogen peroxide in aerobically growing *Escherichia coli*. *Journal of Biological Chemistry,* 270, 13681-13687.

Goodman, M. F. 2002. Error-prone repair DNA polymerases in prokaryotes and eukaryotes. *Annual Review of Biochemistry,* 71, 17-50.

Gophna, U., Doolittle, W. F. & Charlebois, R. L. 2005. Weighted genome trees: Refinements and applications. *Journal of Bacteriology,* 187, 1305-1316.

Gorman, A. A. & Rodgers, M. A. 1992. Current perspectives of singlet oxygen detection in biological environments. *Journal of Photochemistry and Photobiology. B, Biology,* 14, 159-176.

Gourmelon, M., Cillard, J. & Pommepuy, M. 1994. Visible light damage to *Escherichia coli* in seawater: Oxidative stress hypothesis. *Journal of Applied Bacteriology,* 77, 105-112.

Granger, A. C., Gaidamakova, E. K., Matrosova, V. Y., Daly, M. J. & Setlow, P. 2011. Effects of Mn and Fe levels on *Bacillus subtilis* spore resistance and effects of Mn^{2+}, other divalent cations, orthophosphate, and dipicolinic acid on protein resistance to ionizing radiation. *Applied and Environmental Microbiology,* 77, 32-40.

Grasshoff, K., Ehrhardt, M. & Kremling, K. 1983. *Methods of seawater analysis,* New York, Verlag Chemie.

Gustavson, K., Garde, K., Wängberg, S. A. & Selmer, J. S. 2000. Influence of UV-B radiation on bacterial activity in coastal waters. *Journal of Plankton Research,* 22, 1501-1511.

Häder, D.-P. & Sinha, R. P. 2005. Solar ultraviolet radiation-induced DNA damage in aquatic organisms: potential environmental impact. *Mutation Research/Fundamental and Molecular Mechanisms of Mutagenesis,* 571, 221-233.

Häder, D.-P. & Worrest, R. C. 1991. Effects of enhanced solar ultraviolet radiation on aquatic ecosystems. *Photochemistry and Photobiology,* 53, 717-725.

Häder, D. P. 2001. Ultraviolet radiation and aquatic microbial ecosystems. *In:* Cockell, C. S. & Blaustein, A. R. (eds.) *Ecosystems, Evolution, and Ultraviolet Radiation.* New York: Springer-Verlag.

Häder, D. P., Helbling, E. W., Williamson, C. E. & Worrest, R. C. 2011. Effects of UV radiation on aquatic ecosystems and interactions with climate change. *Photochemical and Photobiological Sciences,* 10, 242-260.

Häder, D. P., Kumar, H. D., Smith, R. C. & Worrest, R. C. 1998. Effects on aquatic ecosystems. *Journal of Photochemistry and Photobiology B: Biology,* 46, 53-68.

Häder, D. P., Kumar, H. D., Smith, R. C. & Worrest, R. C. 2003. Aquatic ecosystems: Effects of solar ultraviolet radiation and interactions with other climatic change factors. *Photochemical and Photobiological Sciences,* 2, 39-50.

Häder, D. P., Kumar, H. D., Smith, R. C. & Worrest, R. C. 2007. Effects of solar UV radiation on aquatic ecosystems and interactions with climate change. *Photochemical and Photobiological Sciences,* 6, 267-285.

Häder, D. P., Worrest, R. C., Kumar, H. D. & Smith, R. C. 1995. Effects of increased solar ultraviolet radiation on aquatic ecosystems. *Ambio,* 24, 174-180.

Halliwell, B. 2006. Reactive species and antioxidants. Redox biology is a fundamental theme of aerobic life. *Plant Physiology,* 141, 312-322.

Halliwell, B. & Gutteridge, J. M. C. 1999. *Free Radicals in Biology and Medicine (3rd Ed.),* Oxford, Oxford Univ. Press.

Harada, E., Iida, K. I., Shiota, S., Nakayama, H. & Yoshida, S. I. 2010. Glucose metabolism in *Legionella pneumophila*: Dependence on the Entner-Doudoroff pathway and connection with intracellular bacterial growth. *Journal of Bacteriology,* 192, 2892-2899.

Hardy, J. T. 1982. The sea surface microlayer: Biology, chemistry and anthropogenic enrichment. *Progress In Oceanography,* 11, 307-328.

Harm, W. 1980. *Biological effects of ultraviolet radiation,* Cambridge, UK, Cambridge University Press.

Hartke, A., Giard, J. C., Laplace, J. M. & Auffray, Y. 1998. Survival of *Enterococcus faecalis* in an oligotrophic microcosm: Changes in morphology, development of general stress resistance, and analysis of protein synthesis. *Applied and Environmental Microbiology,* 64, 4238-4245.

Harvey, G. W. & Burzell, L. A. 1972. A simple microlayer method for small samples. *Limnology and Oceanography,* 17, 156-157.

Haugen, P., Simon, D. M. & Bhattacharya, D. 2005. The natural history of group I introns. *Trends in Genetics,* 21, 111-119.

Hayase, K. & Zepp, R. G. 1991. Photolysis of copper(II)-amino acid complexes in water. *Environmental Science & Technology,* 25, 1273-1279.

Hayes, C. S., Illades-Aguiar, B., Casillas-Martinez, L. & Setlow, P. 1998. *In vitro* and *in vivo* oxidation of methionine residues in small, acid- soluble spore proteins from *Bacillus* species. *Journal of Bacteriology,* 180, 2694-2700.

Hayes, C. S., Peng, Z. Y. & Setlow, P. 2000. Equilibrium and kinetic binding interactions between DNA and a group of novel, nonspecific DNA-binding proteins from spores of *Bacillus* and *Clostridium* species. *Journal of Biological Chemistry,* 275, 35040-50.

Hayes, C. S. & Setlow, P. 1997. Analysis of deamidation of small, acid-soluble spore proteins from *Bacillus subtilis in vitro* and *in vivo*. *Journal of Bacteriology,* 179, 6020-6027.

Hazen, T. H., Wu, D., Eisen, J. A. & Sobecky, P. A. 2007. Sequence characterization and comparative analysis of three plasmids isolated from environmental *Vibrio* spp. *Applied and Environmental Microbiology,* 73, 7703-7710.

He, Y. Y. & Häder, D. P. 2002. UV-B-induced formation of reactive oxygen species and oxidative damage of the cyanobacterium *Anabaena* sp.: Protective effects of ascorbic acid and N-acetyl-L-cysteine. *Journal of Photochemistry and Photobiology B: Biology,* 66, 115-124.

Heck, D. E., Shakarjian, M., Kim, H. D., Laskin, J. D. & Vetrano, A. M. 2010. Mechanisms of oxidant generation by catalase. *Annals of the New York Academy of Sciences,* 1203, 120-125.

Heck, D. E., Vetrano, A. M., Mariano, T. M. & Laskin, J. D. 2003. UVB light stimulates production of reactive oxygen species - Unexpected role for catalase. *Journal of Biological Chemistry,* 278, 22432-22436.

Hegglin, M. I. & Shepherd, T. G. 2009. Large climate-induced changes in ultraviolet index and stratosphere-to-troposphere ozone flux. *Nature Geoscience,* 2, 687-691.

Helbling, E. W., Villafane, V., Ferrario, M. & Holm-Hansen, O. 1992. Impact of natural ultraviolet radiation on rates of photosynthesis and on specific marine phytoplankton species. *Marine Ecology Progress Series,* 80, 89-100.

Helbling, E. W., Villafañe, V. & Holm-Hansen, O. 1994. Effects of ultraviolet radiation on Antarctic marine phytoplankton photosynthesis with particular attention to the influence of mixing. *In:* Weiler, C. S. & Penhale, P. A. (eds.) *Ultraviolet Radiation in Antarctica: Measurements and Biological Effects.* Washington, DC: AGU.

Hélène, C. 1987. Excited states and photochemical reactions in DNA, DNA-photosensitizer, and DNA-protein complexes. A review. *In:* Favre, A., Tyrrell, R. & Cadet, J. (eds.) *From Photophysics to Photobiology* Amsterdam, The Netherlands: Elsevier.

Hengge-Aronis, R. 1999. Interplay of global regulators and cell physiology in the general stress response of *Escherichia coli*. *Current Opinion in Microbiology,* 2, 148-152.

Hengge-Aronis, R. 2002. Recent insights into the general stress response regulatory network in *Escherichia coli*. *Journal of Molecular Microbiology and Biotechnology,* 4, 341-346.

Henriques, I. S., Alves, A., Tacão, M., Almeida, A., Cunha, A. & Correia, A. 2006a. Seasonal and spatial variability of free-living bacterial community composition along an estuarine gradient (Ria de Aveiro, Portugal). *Estuarine, Coastal and Shelf Science,* 68, 139-148.

Henriques, I. S., Fonseca, F., Alves, A., Saavedra, M. J. & Correia, A. 2006b. Occurrence and diversity of integrons and β-lactamase genes among ampicillin-resistant isolates from estuarine waters. *Research in Microbiology,* 157, 938-947.

Hermansson, M., Jones, G. W. & Kjelleberg, S. 1987. Frequency of antibiotic and heavy metal resistance, pigmentation, and plasmids in bacteria of the marine air-water interface. *Applied and Environmental Microbiology,* 53, 2338-2342.

Hernandez, E. A., Ferreyra, G. A. & Mac Cormack, W. P. 2006. Response of two Antarctic marine bacteria to different natural UV radiation doses and wavelengths. *Antarctic Science,* 18, 205-212.

Hernández, K. L., Quiñones, R. A., Daneri, G., Farias, M. E. & Helbling, E. W. 2007. Solar UV radiation modulates daily production and DNA damage of marine bacterioplankton from a productive upwelling zone (36°S), Chile. *Journal of Experimental Marine Biology and Ecology,* 343, 82-95.

Hernández, K. L., Quiñones, R. A., Daneri, G. & Helbling, E. W. 2006. Effects of solar radiation on bacterioplankton production in the upwelling system off central-southern Chile. *Marine Ecology Progress Series,* 315, 19-31.

Herndl, G. J., Brugger, A., Hager, S., Kaiser, E., Obernosterer, I., Reitner, B. & Slezak, D. 1997. Role of ultraviolet-B radiation on bacterioplankton and the availability of dissolved organic matter. *Plant Ecology,* 128, 43-51.

Herndl, G. J., Muller-Niklas, G. & Frick, J. 1993. Major role of ultraviolet-B in controlling bacterioplankton growth in the surface layer of the ocean. *Nature,* 361, 717-719.

Hertwig, B., Streb, P. & Feierabend, J. 1992. Light dependence of catalase synthesis and degradation in leaves and the influence of interfering stress conditions. *Plant Physiology,* 100, 1547-1553.

Hobbie, J. E., Daley, R. J. & Jasper, S. 1977. Use of nuclepore filters for counting bacteria by fluorescence microscopy. *Applied and Environmental Microbiology,* 33, 1225-1228.

Hoerter, J. D., Arnold, A. A., Kuczynska, D. A., Shibuya, A., Ward, C. S., Sauer, M. G., Gizachew, A., Hotchkiss, T. M., Fleming, T. J. & Johnson, S. 2005a. Effects of sublethal UVA irradiation on activity levels of oxidative defense enzymes and protein oxidation in *Escherichia coli*. *Journal of Photochemistry and Photobiology B: Biology,* 81, 171-180.

Hoerter, J. D., Arnold, A. A., Ward, C. S., Sauer, M., Johnson, S., Fleming, T. & Eisenstark, A. 2005b. Reduced hydroperoxidase (HPI and HPII) activity in the Δ*fur* mutant contributes to increased sensitivity to UVA radiation in *Escherichia coli*. *Journal of Photochemistry and Photobiology B: Biology,* 79, 151-157.

Hogg, N., Darley-Usmar, V. M., Wilson, M. T. & Moncada, S. 1992. Production of hydroxyl radicals from the simultaneous generation of superoxide and nitric oxide. *Biochemical Journal,* 281, 419-424.

Høibye, L., Clauson-Kaas, J., Wenzel, H., Larsen, H. F., Jacobsen, B. N. & Dalgaard, O. 2008. Sustainability assessment of advanced wastewater treatment technologies. *Water Science and Technology,* 58, 963-968.

Holland, H. D. 2006. The oxygenation of the atmosphere and oceans. *Philosophical Transactions of the Royal Society B: Biological Sciences,* 361, 903-915.

Hollósy, F. 2002. Effects of ultraviolet radiation on plant cells. *Micron,* 33, 179-197.

Hörtnagl, P., Pérez, M. T. & Sommaruga, R. 2010. Living at the border: A community and single-cell assessment of lake bacterioneuston activity. *Limnology and Oceanography,* 55, 1134-1144.

Hörtnagl, P., Pérez, M. T. & Sommaruga, R. 2011. Contrasting effects of ultraviolet radiation on the growth efficiency of freshwater bacteria. *Aquatic Ecology,* 45, 125-136.

Howden, P. J. & Faux, S. P. 1996. Fibre-induced lipid peroxidation leads to DNA adduct formation in *Salmonella typhimurium* TA104 and rat lung fibroblasts. *Carcinogenesis,* 17, 413-419.

Huang, H.-j., Lin, S.-h., Yang, B.-c., Cheng, C.-m., Yang, C.-c. & Kuo, T.-t. 1995. Rapid inhibition of protein histidine phosphorylation by UV-irradiation in *Xanthomonas oryzae* pv. *oryzae*. *FEMS Microbiology Letters,* 134, 189-194.

Hunter, M. I. S., Olawoye, T. L. & Saynor, D. A. 1981. The effect of temperature on the growth and lipid composition of the extremely halophilic coccus, *Sarcina marina*. *Antonie van Leeuwenhoek, International Journal of General and Molecular Microbiology,* 47, 25-40.

Ihssen, J. & Egli, T. 2004. Specific growth rate and not cell density controls the general stress response in *Escherichia coli*. *Microbiology,* 150, 1637-1648.

Ikehata, H., Kawai, K., Komura, J. I., Sakatsume, K., Wang, L., Imai, M., Higashi, S., Nikaido, O., Yamamoto, K., Hieda, K., Watanabe, M., Kasai, H. & Ono, T. 2008. UVA1 genotoxicity is mediated not by oxidative damage but by cyclobutane pyrimidine dimers in normal mouse skin. *Journal of Investigative Dermatology,* 128, 2289-2296.

Imlay, J. A. 2003. Pathways of oxidative damage. *Annual Review of Microbiology,* 57, 395-418.

Imlay, J. A. 2006. Iron-sulphur clusters and the problem with oxygen. *Molecular Microbiology,* 59, 1073-1082.

Imlay, J. A. 2008. Cellular defenses against superoxide and hydrogen peroxide. *Annual Review of Biochemistry* 77, 755-776.

Imlay, J. A., Chin, S. M. & Linn, S. 1988. Toxic DNA damage by hydrogen peroxide through the Fenton reaction *in vivo* and *in vitro*. *Science,* 240, 640-642.

Imlay, J. A. & Fridovich, I. 1991. Assay of metabolic superoxide production in *Escherichia coli*. *Journal of Biological Chemistry,* 266, 6957-6965.

Insam, H. & Goberna, M. 2004. Use of Biolog for the community level physiological profiling (CLPP) of environmental samples. *In:* Akkermans, A. D. L., van Elsas, J. D., DeBrujin, F. J., Head, I. M. & Kowalchuck, G. A. (eds.) *Molecular Microbial Ecology Manual.* Dordrecht, The Netherlands: Kluwer Academic Publishers.

Iqbal, M. 1983. *Introduction to Solar Radiation,* Toronto, Canada, Academic Press.

Jacobs, J. L. & Sundin, G. W. 2001. Effect of Solar UV-B Radiation on a Phyllosphere Bacterial Community. *Applied and Environmental Microbiology,* 67, 5488-5496.

Jagger, J. 1985. *Solar UV Actions on Living Cells,* New York, Praeger Publishing.

Jeffrey, W. H., Aas, P., Lyons, M. M., Coffin, R. B., Pledger, R. J. & Mitchell, D. L. 1996a. Ambient solar radiation-induced photodamage in marine bacterioplankton. *Photochemistry and Photobiology,* 64, 419-427.

Jeffrey, W. H., Pledger, R. J., Aas, P., Hager, S., Coffin, R. B., Von Haven, R. & Mitchell, D. L. 1996b. Diel and depth profiles of DNA photodamage in bacterioplankton exposed to ambient solar ultraviolet radiation. *Marine Ecology Progress Series,* 137, 283-291.

Jewett, M. C., Miller, M. L., Chen, Y. & Swartz, J. R. 2009. Continued protein synthesis at low [ATP] and [GTP] enables cell adaptation during energy limitation. *Journal of Bacteriology,* 191, 1083-1091.

Joshi, S. G., Cooper, M., Yost, A., Paff, M., Ercan, U. K., Fridman, G., Friedman, G., Fridman, A. & Brooks, A. D. 2011. Nonthermal dielectric-barrier discharge plasma-induced inactivation involves oxidative DNA damage and membrane lipid peroxidation in *Escherichia coli*. *Antimicrobial Agents and Chemotherapy,* 55, 1053-1062.

Joux, F., Agogué, H., Obernosterer, I., Dupuy, C., Reinthaler, T., Herndl, G. J. & Lebaron, P. 2006. Microbial community structure in the sea surface microlayer at two contrasting coastal sites in the northwestern Mediterranean Sea. *Aquatic Microbial Ecology,* 42, 91-104.

Joux, F., Jeffrey, W. H., Abboudi, M., Neveux, J., Pujo-Pay, M., Oriol, L. & Naudin, J. J. 2009. Ultraviolet radiation in the Rhône river lenses of low salinity and in marine waters of the northwestern mediterranean sea: Attenuation and effects on bacterial activities and net community production. *Photochemistry and Photobiology,* 85, 783-793.

Joux, F., Jeffrey, W. H., Lebaron, P. & Mitchell, D. L. 1999. Marine bacterial isolates display diverse responses to UV-B radiation. *Applied and Environmental Microbiology,* 65, 3820-3827.

Jozefczuk, S., Klie, S., Catchpole, G., Szymanski, J., Cuadros-Inostroza, A., Steinhauser, D., Selbig, J. & Willmitzer, L. 2010. Metabolomic and transcriptomic stress response of *Escherichia coli*. *Molecular Systems Biology,* 6.

Jürgens, K. & Jeppesen, E. 2000. The impact of metazooplankton on the structure of the microbial food web in a shallow, hypertrophic lake. *Journal of Plankton Research,* 22, 1047-1070.

Kaiser, E. & Herndl, G. J. 1997. Rapid recovery of marine bacterioplankton activity after inhibition by UV radiation in coastal waters. *Applied and Environmental Microbiology,* 63, 4026-4031.

Kammler, M., Schön, C. & Hantke, K. 1993. Characterization of the ferrous iron uptake system of *Escherichia coli*. *Journal of Bacteriology,* 175, 6212-6219.

Kanehisa, M. 2002. The KEGG database. *Novartis Foundation Symposium,* 247, 91-101.

Kankaanpää, P., Yang, B., Kallio, H., Isolauri, E. & Salminen, S. 2004. Effects of polyunsaturated fatty acids in growth medium on lipid composition and on physicochemical surface properties of lactobacilli. *Applied and Environmental Microbiology,* 70, 129-136.

Karentz, D. 1994. Ultraviolet tolerance mechanisms in Antarctic marine organisms. *In:* Weiler, C. S. & Penhale, P. A. (eds.) *Ultraviolet Radiation in Antarctica: Measurements and Biological Effects.* Washington, DC: AGU.

Karentz, D., Bothwell, M. L., Coffin, R. B., Hanson, A., Herndl, G. J., Kilham, S. S., Lesser, M. P., Lindell, M., Moeller, R. E., Morris, D. P., Neale, P. J., Sanders, R. W., Weiler, C. S. & Wetzel, R. G. 1994. Impact of UV-B radiation on pelagic ecosystems: report of working group on bacteria and phytoplankton. *Archiv für Hydrobiologie–Beiheft Ergebnisse der Limnologie,* 43, 31-69.

Karentz, D., Cleaver, J. E. & Mitchell, D. L. 1991. Cell survival characteristics and molecular responses of Antarctic phytoplankton to ultraviolet-B radiation. *Journal of Phycology,* 27, 326-341.

Kehrer, J. P. 2000. The Haber-Weiss reaction and mechanisms of toxicity. *Toxicology,* 149, 43-50.

Kidambi, S. P., Booth, M. G., Kokjohn, T. A. & Miller, R. V. 1996. *recA*-dependence of the response of *Pseudomonas aeruginosa* to UVA and UVB irradiation. *Microbiology,* 142, 1033-40.

Kieber, D. J., McDaniel, J. & Mopper, K. 1989. Photochemical source of biological substrates in sea water: Implications for carbon cycling. *Nature,* 341, 637-639.

Kim, S. T., Malhotra, K., Smith, C. A., Taylor, J. S. & Sancar, A. 1994. Characterization of (6-4) photoproduct DNA photolyase. *Journal of Biological Chemistry,* 269, 8535-8540.

King, B., Kesavan, J. & Sagripanti, J.-L. 2011. Germicidal UV Sensitivity of Bacteria in Aerosols and on Contaminated Surfaces. *Aerosol Science and Technology,* 45, 645-653.

Klančnik, A., Guzej, B., Jamnik, P., Vučković, D., Abram, M. & Možina, S. S. 2009. Stress response and pathogenic potential of *Campylobacter jejuni* cells exposed to starvation. *Research in Microbiology,* 160, 345-352.

Kligman, L. H., Akin, F. J. & Kligman, A. M. 1985. The contributions of UVA and UVB to connective tissue damage in hairless mice. *Journal of Investigative Dermatology,* 84, 272-276.

Ko, M., Choi, H. & Park, C. 2002. Group I self-splicing intron in the *recA* gene of *Bacillus anthracis*. *Journal of Bacteriology,* 184, 3917-3922.

Kohen, E., Santus, R. & Hirschberg, J. G. 1995. Photochemistry of biological molecules. *Photobiology*. Amsterdam: Academic Press.

Kokjohn, T. A. & Miller, R. V. 1985. Molecular cloning and characterization of the *recA* gene of *Pseudomonas aeruginosa* PAO. *Journal of Bacteriology,* 163, 568-72.

Kokjohn, T. A. & Miller, R. V. 1994. IncN plasmids mediate UV resistance and error-prone repair in *Pseudomonas aeruginosa* PAO. *Microbiology,* 140, 43-8.

Koppenol, W. H. 2001. The Haber-Weiss cycle - 70 years later. *Redox Report,* 6, 229-234.

Korbashi, P., Katzhendler, J., Saltman, P. & Chevion, M. 1989. Zinc protects *Escherichia coli* against copper-mediated paraquat-induced damage. *Journal of Biological Chemistry,* 264, 8479-8482.

Kováčik, J., Klejdus, B. & Bačkor, M. 2010. Physiological Responses of *Scenedesmus quadricauda* (Chlorophyceae) to UV-A and UV-C Light. *Photochemistry and Photobiology,* 86, 612-616.

Kraemer, K. H., Lee, M. M. & Scotto, J. 1987. Xeroderma pigmentosum. Cutaneous, ocular, and neurologic abnormalities in 830 published cases. *Archives of Dermatology,* 123, 241-250.

Kramer, G. F., Norman, H. A., Krizek, D. T. & Mirecki, R. M. 1991. Influence of UV-B radiation on polyamines, lipid peroxidation and membrane lipids in cucumber. *Phytochemistry,* 30, 2101-2108.

Krasnovsky Jr, A. A. 1981. Quantum yield of photosensitized luminescence and radiative lifetime of singlet (1Δg) molecular oxygen in solutions. *Chemical Physics Letters,* 81, 443-445.

Kripke, M. L. 1988. Impact of ozone depletion on skin cancers. *Journal of Dermatologic Surgery and Oncology,* 14, 853-857.

Krisko, A. & Radman, M. 2010. Protein damage and death by radiation in *Escherichia coli* and *Deinococcus radiodurans*. *Proceedings of the National Academy of Sciences of the United States of America,* 107, 14373-14377.

Kuzminov, A. 1999. Recombinational repair of DNA damage in *Escherichia coli* and bacteriophage λ. *Microbiology and Molecular Biology Reviews,* 63, 751-813.

Kuznetsova, M. & Lee, C. 2002. Dissolved free and combined amino acids in nearshore seawater, sea surface microlayers and foams: Influence of extracellular hydrolysis. *Aquatic Sciences,* 64, 252-268.

Landeta, G., Reverón, I., Carrascosa, A. V., Rivas, B. D. L. & Muñoz, R. 2011. Use of *recA* gene sequence analysis for the identification of *Staphylococcus equorum* strains predominant on dry-cured hams. *Food Microbiology,* 28, 1205-1210.

Lane, D. J. 1991. 16S/23S rRNA sequencing. *In:* Stackebrandt, E. & Goodfellow, M. (eds.) *Nucleic Acid Techniques in Bacterial Systematics*. New York: John Wiley and Sons

Langenheder, S., Sobek, S. & Tranvik, L. J. 2006. Changes in bacterial community composition along a solar radiation gradient in humic waters. *Aquatic Sciences,* 68, 415-424.

Lasch, P., Petras, T., Ullrich, O., Backmann, J., Naumann, D. & Grune, T. 2001. Hydrogen Peroxide-induced Structural Alterations of RNase A. *Journal of Biological Chemistry*, 276, 9492-9502.

Le Dréau, Y., Dupuy, N., Gaydou, V., Joachim, J. & Kister, J. 2009. Study of jojoba oil aging by FTIR. *Analytica Chimica Acta*, 642, 163-170.

Lesk, A. M. 1973. On hypothesized selective pressure by u.v. on DNA base compositions. *J Theor Biol*, 40, 201-2.

Lesser, M. P. & Shick, J. M. 1989. Effects of irradiance and ultraviolet radiation on photoadaptation in the zooxanthellae of *Aiptasia pallida*: primary production, photoinhibition, and enzymic defenses against oxygen toxicity. *Marine Biology*, 102, 243-255.

Li, S., Paulsson, M. & Björn, L. O. 2002. Temperature-dependent formation and photorepair of DNA damage induced by UV-B radiation in suspension-cultured tobacco cells. *Journal of Photochemistry and Photobiology B: Biology*, 66, 67-72.

Li, S. S., Wang, Y. & Björn, L. O. 2004. Effects of temperature on UV-B-induced DNA damage and photorepair in *Arabidopsis thaliana*. *Journal of Environmental Sciences*, 16, 173-176.

Lindell, M. & Edling, H. 1996. Influence of light on bacterioplankton in a tropical lake. *Hydrobiologia*, 323, 67-73.

Lindell, M. J., Granéli, H. W. & Tranvik, L. J. 1996. Effects of sunlight on bacterial growth in lakes of different humic content. *Aquatic Microbial Ecology*, 11, 135-141.

Lindell, M. J., Graneli, W. & Tranvik, L. J. 1995. Enhanced bacterial growth in response to photochemical transformation of dissolved organic matter. *Limnology and Oceanography*, 40, 195-199.

Lindroos, A., Szabo, H. M., Nikinmaa, M. & Leskinen, P. 2011. Comparison of sea surface microlayer and subsurface water bacterial communities in the Baltic Sea. *Aquatic Microbial Ecology*, 65, 29-42.

Liochev, S. I. & Fridovich, I. 2002. The Haber-Weiss cycle - 70 years later: An alternative view [1]. *Redox Report*, 7, 55-57.

Liss, P. S. 1975. Chemistry of the sea-surface microlayer. *In:* Riley, J. P. & Skirrow, G. (eds.) *Chemical Oceanography (2nd ed.)*. London: Academic Press.

Lister, K. N., Lamare, M. D. & Burritt, D. J. 2010. Sea ice protects the embryos of the Antarctic sea urchin *Sterechinus neumayeri* from oxidative damage due to naturally enhanced levels of UV-B radiation. *The Journal of Experimental Biology*, 213, 1967-1975.

Loewen, P. C. & Hengge-Aronis, R. 1994. The role of the sigma factor σ(S) (*katF*) in bacterial global regulation. *Annual Review of Microbiology*, 48, 53-80.

López-Lara, I. M., Gao, J.-L., Soto, M. J., Solares-Pérez, A., Weissenmayer, B., Sohlenkamp, C., Verroios, G. P., Thomas-Oates, J. & Geiger, O. 2005. Phosphorus-Free Membrane Lipids of *Sinorhizobium meliloti* Are Not Required for the Symbiosis with Alfalfa but Contribute to Increased Cell Yields Under Phosphorus-Limiting Conditions of Growth. *Molecular Plant-Microbe Interactions*, 18, 973-982.

Ludwig, W. 2010. Molecular phylogeny of microorganisms: is rRNA still a useful marker? *In:* Oren, A. & Papke, R. T. (eds.) *Molecular phylogeny of microorganisms*. Norfolk: Caister Academic Press.

Ludwig, W. & Klenk, H.-P. 2001. Overview: A phylogenetic backbone and taxonomic framework for prokaryotic systematics. *In:* Boone, D. R. & Castenholz, R. W. (eds.) *Bergey's Manual of Systematic Bacteriology*. Berlin Springer-Verlag.

Luksiene, Z. 2003. Photodynamic therapy: mechanism of action and ways to improve the efficiency of treatment. *Medicina (Kaunas, Lithuania)*, 39, 1137-1150.

Luksiene, Z. 2005. New approach to inactivation of harmful and pathogenic microorganisms by photosensitization. *Food Technology and Biotechnology*, 43, 411-418.

Lusetti, S. L., Wood, E. A., Fleming, C. D., Modica, M. J., Korth, J., Abbott, L., Dwyer, D. W., Roca, A. I., Inman, R. B. & Cox, M. M. 2003. C-terminal Deletions of the *Escherichia coli* RecA Protein. *Journal of Biological Chemistry*, 278, 16372-16380.

Lyamichev, V. 1991. Unusual conformation of (dA)n·(dT)n-tracts as revealed by cyclobutane thymine – thymine dimer formation. *Nucleic Acids Research,* 19, 4491-4496.

Lyons, M. M., Aas, P., Pakulski, J. D., Van Waasbergen, L., Miller, R. V., Mitchell, D. L. & Jeffrey, W. H. 1998. DNA damage induced by ultraviolet radiation in coral-reef microbial communities. *Marine Biology,* 130, 537-543.

Macomber, L., Rensing, C. & Imlay, J. A. 2007. Intracellular copper does not catalyze the formation of oxidative DNA damage in *Escherichia coli*. *Journal of Bacteriology,* 189, 1616-1626.

Mäder, J. A., Staehelin, J., Peter, T., Brunner, D., Rieder, H. E. & Stahel, W. A. 2010. Evidence for the effectiveness of the Montreal Protocol to protect the ozone layer. *Atmospheric Chemistry and Physics,* 10, 12161-12171.

Magnani, D. & Solioz, M. 2007. How bacteria handle copper. *In:* Nies, D. H. & Silver, S. (eds.) *Molecular microbiology of heavy metals.* Heidelberg, Germany: Springer.

Maki, J. S. 1993. The air-water interface as an extreme environment. *In:* Ford, T. E. (ed.) *Aquatic microbiology - an ecological approach.* Boston: Blackwell Scientific.

Maloy, S. R., Cronan, J. E. & Freifelder, D. 1994. *Microbial genetics, 2nd Edition,* Sudbury, Mass., USA, Jones and Bartlett.

Manney, G. L., Santee, M. L., Rex, M., Livesey, N. J., Pitts, M. C., Veefkind, P., Nash, E. R., Wohltmann, I., Lehmann, R., Froidevaux, L., Poole, L. R., Schoeberl, M. R., Haffner, D. P., Davies, J., Dorokhov, V., Gernandt, H., Johnson, B., Kivi, R., Kyrö, E., Larsen, N., Levelt, P. F., Makshtas, A., McElroy, C. T., Nakajima, H., Parrondo, M. C., Tarasick, D. W., Von Der Gathen, P., Walker, K. A. & Zinoviev, N. S. 2011. Unprecedented Arctic ozone loss in 2011. *Nature,* 478, 469-475.

Manrique, J. M., Calvo, A. Y., Halac, S. R., Villafañe, V. E., Jones, L. R. & Walter Helbling, E. 2012. Effects of UV radiation on the taxonomic composition of natural bacterioplankton communities from Bahía Engaño (Patagonia, Argentina). *Journal of Photochemistry and Photobiology B: Biology,* 117, 171-178.

Manz, W., Amann, R., Ludwig, W., Vancanneyt, M. & Schleifer, K. H. 1996. Application of a suite of 16S rRNA-specific oligonucleotide probes designed to investigate bacteria of the phylum cytophaga-flavobacter-bacteroides in the natural environment. *Microbiology,* 142, 1097-1106.

Maranger, R., Del Giorgio, P. A. & Bird, D. F. 2002. Accumulation of damaged bacteria and viruses in lake water exposed to solar radiation. *Aquatic Microbial Ecology,* 28, 213-227.

Martin, A., Hall, J. & Ryan, K. 2009. Low Salinity and High-Level UV-B Radiation Reduce Single-Cell Activity in Antarctic Sea Ice Bacteria. *Applied and Environmental Microbiology,* 75, 7570-7573.

Matallana-Surget, S., Douki, T., Meador, J. A., Cavicchioli, R. & Joux, F. 2010. Influence of growth temperature and starvation state on survival and DNA damage induction in the marine bacterium *Sphingopyxis alaskensis* exposed to UV radiation. *Journal of Photochemistry and Photobiology B: Biology,* 100, 51-56.

Matallana-Surget, S., Joux, F., Raftery, M. J. & Cavicchioli, R. 2009a. The response of the marine bacterium *Sphingopyxis alaskensis* to solar radiation assessed by quantitative proteomics. *Environmental Microbiology,* 11, 2660-2675.

Matallana-Surget, S., Joux, F., Wattiez, R. & Lebaron, P. 2012. Proteome Analysis of the UVB-Resistant Marine Bacterium *Photobacterium angustum* S14. *PLoS ONE,* 7, e42299.

Matallana-Surget, S., Meador, J. A., Joux, F. & Douki, T. 2008. Effect of the GC content of DNA on the distribution of UVB-induced bipyrimidine photoproducts. *Photochemical & Photobiological Sciences,* 7, 794-801.

Matallana-Surget, S. M., Douki, T., Cavicchioli, R. & Joux, F. 2009b. Remarkable resistance to UVB of the marine bacterium *Photobacterium angustum* explained by an unexpected role of photolyase. *Photochemical and Photobiological Sciences,* 8, 1313-1320.

McCord, J. M. & Fridovich, I. 1969. Superoxide dismutase. An enzymic function for erythrocuprein (hemocuprein). *Journal of Biological Chemistry,* 244, 6049-6055.

McCormick, J. P., Fischer, J. R., Eisenstark, A. & Pachlatko, J. P. 1976. Characterization of a cell lethal product from the photooxidation of tryptophan: hydrogen peroxide. *Science,* 191, 468-469.

McEwan, A. G. 2009. New insights into the protective effect of manganese against oxidative stress: MicroCommentary. *Molecular Microbiology,* 72, 812-814.

McNaughton, R. L., Reddi, A. R., Clement, M. H. S., Sharma, A., Barnese, K., Rosenfeld, L., Gralla, E. B., Valentine, J. S., Culotta, V. C. & Hoffman, B. M. 2010. Probing in vivo Mn^{2+} speciation and oxidative stress resistance in yeast cells with electron-nuclear double resonance spectroscopy. *Proceedings of the National Academy of Sciences of the United States of America,* 107, 15335-15339.

McQuiston, J. R., Herrera-Leon, S., Wertheim, B. C., Doyle, J., Fields, P. I., Tauxe, R. V. & Logsdon Jr, J. M. 2008. Molecular phylogeny of the salmonellae: relationships among *Salmonella* species and subspecies determined from four housekeeping genes and evidence of lateral gene transfer events. *Journal of Bacteriology,* 190, 7060-7067.

Meador, J., Jeffrey, W. H., Kase, J. P., Pakulski, J. D., Chiarello, S. & Mitchell, D. L. 2002. Seasonal fluctuation of DNA photodamage in marine plankton assemblages at Palmer Station, Antarctica. *Photochemistry and Photobiology,* 75, 266-271.

Medina-Sánchez, J. M., Villar-Argaiz, M. & Carrillo, P. 2002. Modulation of the bacterial response to spectral solar radiation by algae and limiting nutrients. *Freshwater Biology,* 47, 2191-2204.

Merle, C., Laugel, C. & Baillet-Guffroy, A. 2010. Effect of UVA or UVB irradiation on cutaneous lipids in films or in solution. *Photochemistry and Photobiology,* 86, 553-562.

Miller, R. V. 2000. *recA*: The gene and its protein product. *In:* Luria, S. (ed.) *Encyclopedia of Microbiology, 2nd Ed.* San Diego: Academic Press.

Miller, R. V. & Kokjohn, T. A. 1990. General Microbiology of *recA* : Environmental and Evolutionary Significance. *Annual Review of Microbiology,* 44, 365-394.

Miller, S. R., Wood, A. M., Blankenship, R. E., Kim, M. & Ferriera, S. 2011. Dynamics of gene duplication in the genomes of chlorophyll d-producing cyanobacteria: implications for the ecological niche. *Genome Biology and Evolution,* 3, 601-13.

Mishra, Y., Chaurasia, N. & Rai, L. C. 2009. AhpC (alkyl hydroperoxide reductase) from *Anabaena* sp. PCC 7120 protects *Escherichia coli* from multiple abiotic stresses. *Biochemical and Biophysical Research Communications,* 381, 606-611.

Misiaszek, R., Crean, C., Joffe, A., Geacintov, N. E. & Shafirovich, V. 2004. Oxidative DNA damage associated with combination of guanine and superoxide radicals and repair mechanisms via radical trapping. *Journal of Biological Chemistry,* 279, 32106-32115.

Mitchell, D. L. 1995. DNA damage and repair. *In:* Horspool, W. & Song, P. S. (eds.) *A handbook of organic photochemistry and photobiology.* London: CRC Press.

Mitchell, D. L. & Karentz, D. 1993. The induction and repair of DNA photodamage in the environment. *In:* Young, A. R., Bjorn, L. O., Moan, J. & Nultsch, W. (eds.) *Environmental UV Photobiology* New York: Plenum Press.

Mitsch, W. J. & Gosselink, J. G. 2000. *Wetlands (3rd Ed.),* New York, Van Nostrand Reinhold

Miyamoto, S., Ronsein, G. E., Prado, F. M., Uemi, M., Corrêa, T. C., Toma, I. N., Bertolucci, A., Oliveira, M. C. B., Motta, F. D., Medeiros, M. H. G. & Mascio, P. D. 2007. Biological hydroperoxides and singlet molecular oxygen generation. *IUBMB Life,* 59, 322-331.

Moan, J., Dahlback, A. & Setlow, R. B. 1999. Epidemiological support for an hypothesis for melanoma induction indicating a role for UVA radiation. *Photochemistry and Photobiology,* 70, 243-247.

Moan, J. & Peak, M. J. 1989. Effects of UV radiation on cells. *Journal of Photochemistry and Photobiology B: Biology,* 4, 21-34.

Moeller, R., Douki, T., Cadet, J., Stackebrandt, E., Nicholson, W. L., Rettberg, P., Reitz, G. & Horneck, G. 2007a. UV-radiation-induced formation of DNA bipyrimidine photoproducts in *Bacillus subtilis* endospores and their repair during germination. *International Microbiology,* 10, 39-46.

Moeller, R., Douki, T., Rettberg, P., Reitz, G., Cadet, J., Nicholson, W. & Horneck, G. 2010. Genomic bipyrimidine nucleotide frequency and microbial reactions to germicidal UV radiation. *Archives of Microbiology,* 192, 521-529.

Moeller, R., Stackebrandt, E., Douki, T., Cadet, J., Rettberg, P., Mollenkopf, H. J., Reitz, G. & Horneck, G. 2007b. DNA bipyrimidine photoproduct repair and transcriptional response of UV-C irradiated *Bacillus subtilis*. *Archives of Microbiology,* 188, 421-431.

Molina, M. J. & Rowland, F. S. 1974. Stratospheric sink for chlorofluoromethanes: chlorine atom catalysed destruction of ozone. *Nature,* 249, 810-812.

Mols, M., van Kranenburg, R., van Melis, C. C. J., Moezelaar, R. & Abee, T. 2010. Analysis of acid-stressed *Bacillus cereus* reveals a major oxidative response and inactivation-associated radical formation. *Environmental Microbiology,* 12, 873-885.

Montzka, S. A., Butler, J. H., Myers, R. C., Thompson, T. M., Swanson, T. H., Clarke, A. D., Lock, L. T. & Elkins, J. W. 1996. Decline in the tropospheric abundance of halogen from halocarbons: Implications for stratospheric ozone depletion. *Science,* 272, 1318-1322.

Moolenaar, G. F., Herron, M. F. P. a., Monaco, V., van der Marel, G. A., van Boom, J. H., Visse, R. & Goosen, N. 2000. The Role of ATP Binding and Hydrolysis by UvrB during Nucleotide Excision Repair. *Journal of Biological Chemistry,* 275, 8044-8050.

Moorhouse, C. P., Halliwell, B., Grootveld, M. & Gutteridge, J. M. C. 1985. Cobalt(II) ion as a promoter of hydroxyl radical and possible 'crypto-hydroxyl' radical formation under physiological conditions. Differential effects of hydroxyl radical scavengers. *Biochimica et Biophysica Acta - General Subjects,* 843, 261-268.

Moran, M. A. & Zepp, R. G. 1997. Role of photoreactions in the formation of biologically labile compounds from dissolved organic matter. *Limnology and Oceanography,* 42, 1307-1316.

Moran, M. A. & Zepp, R. G. 2000. UV radiation effects on microbes and microbial processes. *In:* Kirchman, D. L. (ed.) *Microbial ecology of the oceans.* New York.

Moriarty, D. J. W. 1986. Measurement of bacterial growth rates and production of biomass in aquatic environments. *In:* Grigorova, R. & Norris, J. R. (eds.) *Methods in microbiology.* Cambridge, UK: Academic Press.

Morris, R. M., Rappé, M. S., Connon, S. A., Vergin, K. L., Siebold, W. A., Carlson, C. A. & Giovannoni, S. J. 2002. SAR11 clade dominates ocean surface bacterioplankton communities. *Nature,* 420, 806-810.

Moss, S. H. & Smith, K. C. 1981. Membrane damage can be a significant factor in the inactivation of *Escherichia coli* by near-ultraviolet radiation. *Photochemistry and Photobiology,* 33, 203-210.

Mostajir, B., Demers, S., De Mora, S., Belzile, C., Chanut, J. P., Gosselin, M., Roy, S., Villegas, P. Z., Fauchot, J., Bouchard, J., Bird, D., Monfort, P. & Levasseur, M. 1999. Experimental test of the effect of ultraviolet-B radiation in a planktonic community. *Limnology and Oceanography,* 44, 586-596.

Mudhoo, A., Garg, V. K. & Wang, S. 2012. Heavy Metals: Toxicity and Removal by Biosorption. *In:* Lichtfouse, E., Schwarzbauer, J. & Robert, D. (eds.) *Environmental Chemistry for a Sustainable World.* Springer Netherlands.

Muela, A., García-Bringas, J., Arana, I. & Barcina, I. 2000. Humic materials offer photoprotective effect to *Escherichia coli* exposed to damaging luminous radiation. *Microbial Ecology,* 40, 336-344.

Muela, A., García-Bringas, J. M., Seco, C., Arana, I. & Barcina, I. 2002. Participation of oxygen and role of exogenous and endogenous sensitizers in the photoinactivation of *Escherichia coli* by photosynthetically active radiation, UV-A and UV-B. *Microbial Ecology,* 44, 354-364.

Müller-Niklas, G., Heissenberger, A., Puskaric, S. & Herndl, G. J. 1995. Ultraviolet-B radiation and bacterial metabolism in coastal waters. *Aquatic Microbial Ecology,* 9, 111-116.

Murakami, K., Tsubouchi, R., Fukayama, M., Ogawa, T. & Yoshino, M. 2006. Oxidative inactivation of reduced NADP-generating enzymes in *E. coli*: Iron-dependent inactivation with affinity cleavage of NADP-isocitrate dehydrogenase. *Archives of Microbiology,* 186, 385-392.

Murphy, T. M. & Huerta, A. J. 1990. Hydrogen peroxide formation in cultured rose cells in response to UV-C radiation. *Physiologia Plantarum,* 78, 247-253.

Nadtochenko, V. A., Rincon, A. G., Stanca, S. E. & Kiwi, J. 2005. Dynamics of *E. coli* membrane cell peroxidation during TiO2 photocatalysis studied by ATR-FTIR spectroscopy and AFM microscopy. *Journal of Photochemistry and Photobiology A: Chemistry,* 169, 131-137.

Nahrstedt, H., Schröder, C. & Meinhardt, F. 2005. Evidence for two *recA* genes mediating DNA repair in *Bacillus megaterium*. *Microbiology,* 151, 775-787.

Nair, S. & Finkel, S. E. 2004. Dps Protects Cells against Multiple Stresses during Stationary Phase. *Journal of Bacteriology,* 186, 4192-4198.

Nguyen, K. L., Steryo, M., Kurbanyan, K., Nowitzki, K. M., Butterfield, S. M., Ward, S. R. & Stemp, E. D. A. 2000. DNA−Protein Cross-Linking from Oxidation of Guanine via the Flash−Quench Technique. *Journal of the American Chemical Society,* 122, 3585-3594.

Niki, E., Yoshida, Y., Saito, Y. & Noguchi, N. 2005. Lipid peroxidation: Mechanisms, inhibition, and biological effects. *Biochemical and Biophysical Research Communications,* 338, 668-676.

Nolan, C. V. & Amanatidis, G. T. 1995. European commission research on the fluxes and effects of environmental UVB radiation. *Journal of Photochemistry and Photobiology B: Biology,* 31, 3-7.

Nord, D., Torrents, E. & Sjöberg, B. M. 2007. A functional homing endonuclease in the *Bacillus anthracis nrdE* group I intron. *Journal of Bacteriology,* 189, 5293-5301.

Norioka, N., Hsu, M. Y., Inouye, S. & Inouye, M. 1995. Two *recA* genes in *Myxococcus xanthus*. *Journal of Bacteriology,* 177, 4179-4182.

Norkrans, B. 1980. Surface microlayers in aquatic environments. *In:* Alexander, M. (ed.) *Advances in microbial ecology.* New York: Plenum Press.

Norris, T. B., McDermott, T. R. & Castenholz, R. W. 2002. The long-term effects of UV exclusion on the microbial composition and photosynthetic competence of bacteria in hot-spring microbial mats. *FEMS Microbiology Ecology,* 39, 193-209.

Norval, M., Lucas, R. M., Cullen, A. P., De Gruijl, F. R., Longstreth, J., Takizawa, Y. & Van Der Leun, J. C. 2011. The human health effects of ozone depletion and interactions with climate change. *Photochemical and Photobiological Sciences,* 10, 199-225.

Notley, L. & Ferenci, T. 1996. Induction of RpoS-dependent functions in glucose-limited continuous culture: What level of nutrient limitation induces the stationary phase of *Escherichia coli*? *Journal of Bacteriology,* 178, 1465-1468.

Nowis, D. & Golab, J. 2008. Photodynamic therapy and oxidative stress. *In:* Hamblin, M. R. & Mroz, P. (eds.) *Advances in photodynamic therapy: basic, translational, and clinical.* Boston, MA: Artech House.

Nunez, M., Forgan, B. & Roy, C. 1994. Estimating ultraviolet radiation at the earth's surface. *International Journal of Biometeorology,* 38, 5-17.

Nyström, T. 2004. Stationary-phase physiology. *Annual Review of Microbiology,* 58, 161-181.

Nyström, T. 2005. Role of oxidative carbonylation in protein quality control and senescence. *EMBO Journal,* 24, 1311-1317.

Nyström, T., Olsson, R. M. & Kjelleberg, S. 1992. Survival, stress resistance, and alterations in protein expression in the marine *Vibrio* sp. strain S14 during starvation for different individual nutrients. *Applied and Environmental Microbiology,* 58, 55-65.

Obernosterer, I., Catala, P., Lami, R., Caparros, J., Ras, J., Bricaud, A., Dupuy, C., Van Wambeke, F. & Lebaron, P. 2008. Biochemical characteristics and bacterial community structure of the sea surface microlayer in the South Pacific Ocean. *Biogeosciences,* 5, 693-705.

Obernosterer, I., Catala, P., Reinthaler, T., Herndl, G. J. & Lebaron, P. 2005. Enhanced heterotrophic activity in the surface microlayer of the Mediterranean Sea. *Aquatic Microbial Ecology,* 39, 293-302.

Obernosterer, I., Reitner, B. & Herndl, G. J. 1999. Contrasting effects of solar radiation on dissolved organic matter and its bioavailability to marine bacterioplankton. *Limnology and Oceanography,* 44, 1645-1654.

Obernosterer, I., Sempéré, R. & Herndl, G. J. 2001. Ultraviolet radiation induces reversal of the bioavailability of DOM to marine bacterioplankton. *Aquatic Microbial Ecology,* 24, 61-68.

Ogbebo, F. E. & Ochs, C. 2008. Bacterioplankton and phytoplankton production rates compared at different levels of solar ultraviolet radiation and limiting nutrient ratios. *Journal of Plankton Research,* 30, 1271-1284.

Ojanen, T., Helander, I. M., Haahtela, K., Korhonen, T. K. & Laakso, T. 1993. Outer Membrane Proteins and Lipopolysaccharides in Pathovars of *Xanthomonas campestris*. *Applied and Environmental Microbiology,* 59, 4143-4151.

Oppezzo, O. J. 2012. Intermediaries and Targets of the Oxidative Stress Induced by Natural Sunlight in *Escherichia coli*. *Journal of Life Sciences,* 6, 130-136.

Oppezzo, O. J., Costa, C. S. & Pizarro, R. A. 2011. Influence of *rpoS* mutations on the response of *Salmonella enterica* serovar Typhimurium to solar radiation. *Journal of Photochemistry and Photobiology B: Biology,* 102, 20-25.

Ordoñez, O., Flores, M., Dib, J., Paz, A. & Farías, M. 2009. Extremophile Culture Collection from Andean Lakes: Extreme Pristine Environments that Host a Wide Diversity of Microorganisms with Tolerance to UV Radiation. *Microbial Ecology,* 58, 461-473.

Ortega-Retuerta, E., Pulido-Villena, E. & Reche, I. 2007. Effects of dissolved organic matter photoproducts and mineral nutrient supply on bacterial growth in Mediterranean inland waters. *Microbial Ecology,* 54, 161-169.

Pajares, S., Bonilla-Rosso, G., Travisano, M., Eguiarte, L. & Souza, V. 2012. Mesocosms of Aquatic Bacterial Communities from the Cuatro Cienegas Basin (Mexico): A Tool to Test Bacterial Community Response to Environmental Stress. *Microbial Ecology,* 64, 346-358.

Pakker, H., Martins, R. S. T., Boelen, P., Buma, A. G. J., Nikaido, O. & Breeman, A. M. 2000. Effects of temperature on the photoreactivation of ultraviolet-B-induced DNA damage in *Palmaria palmata* (Rhodophyta). *Journal of Phycology,* 36, 334-341.

Pakulski, J. D., Aas, P., Jeffrey, W., Lyons, M., Van Waasbergen, L. G., Mitchell, D. & Coffin, R. 1998. Influence of light on bacterioplankton production and respiration in a subtropical coral reef. *Aquatic Microbial Ecology,* 14, 137-148.

Pakulski, J. D., Baldwin, A., Dean, A. L., Durkin, S., Karentz, D., Kelley, C. A., Scott, K., Spero, H. J., Wilhelm, S. W., Amin, R. & Jeffrey, W. H. 2007. Responses of heterotrophic bacteria to solar irradiance in the eastern Pacific Ocean. *Aquatic Microbial Ecology,* 47, 153-162.

Panagopoulos, I., Bornman, J. F. & Björn, L. O. 1990. Effects of ultraviolet radiation and visible light on growth, fluorescence induction, ultraweak luminescence and peroxidase activity in sugar beet plants. *Journal of Photochemistry and Photobiology, B: Biology,* 8, 73-87.

Park, J. W. & Floyd, R. A. 1992. Lipid peroxidation products mediate the formation of 8-hydroxydeoxyguanosine in DNA. *Free Radical Biology and Medicine,* 12, 245-250.

Parsons, T. R., Maita, Y. & Lalli, C. M. 1984. *A manual of chemical and biological methods for seawater analysis (1st Ed.),* New York, NY, Pergamon Press.

Pattison, D. I. & Davies, M. J. 2006. Actions of ultraviolet light on cellular structures. *EXS.*, 131-157.

Paul, N. D. & Gwynn-Jones, D. 2003. Ecological roles of solar UV radiation: Towards an integrated approach. *Trends in Ecology and Evolution,* 18, 48-55.

Pausz, C. & Herndl, G. J. 1999. Role of ultraviolet radiation on phytoplankton extracellular release and its subsequent utilization by marine bacterioplankton. *Aquatic Microbial Ecology,* 18, 85-93.

Pausz, C. & Herndl, G. J. 2002. Role of nitrogen versus phosphorus availability on the effect of UV radiation on bacterioplankton and their recovery from previous UV stress. *Aquatic Microbial Ecology,* 29, 89-95.

Payne, G. W., Vandamme, P., Morgan, S. H., LiPuma, J. J., Coenye, T., Weightman, A. J., Jones, T. H. & Mahenthiralingam, E. 2005. Development of a *recA* gene-based identification approach for the entire *Burkholderia* genus. *Applied and Environmental Microbiology,* 71, 3917-3927.

Payne, J. L., Boyer, A. G., Brown, J. H., Finnegan, S., Kowalewski, M., Krause, R. A., Lyons, S. K., McClain, C. R., McShea, D. W., Novack-Gottshall, P. M., Smith, F. A., Stempien, J. A. & Wang, S. C. 2008. Two-phase increase in the maximum size of life over 3.5 billion years reflects biological innovation and environmental opportunity. *Proceedings of the National Academy of Sciences*.

Peak, J. G. & Peak, M. J. 1990. Ultraviolet light induces double-strand breaks in DNA of cultured human P3 cells as measured by neutral filter elution. *Photochemistry and Photobiology,* 52, 387-393.

Pelletier, É., Sargian, P., Payet, J. & Demers, S. 2006. Ecotoxicological effects of combined UVB and organic contaminants in coastal waters: A review. *Photochemistry and Photobiology,* 82, 981-993.

Pérez, J. M., Arenas, F. A., Pradenas, G. A., Sandoval, J. M. & Vásquez, C. C. 2008. *Escherichia coli* YqhD Exhibits Aldehyde Reductase Activity and Protects from the Harmful Effect of Lipid Peroxidation-derived Aldehydes. *Journal of Biological Chemistry,* 283, 7346-7353.

Pérez, J. M., Calderón, I. L., Arenas, F. A., Fuentes, D. E., Pradenas, G. A., Fuentes, E. L., Sandoval, J. M., Castro, M. E., Elías, A. O. & Vásquez, C. C. 2007. Bacterial toxicity of potassium tellurite: Unveiling an ancient enigma. *PLoS ONE,* 2.

Pérez, M. T. & Sommaruga, R. 2007. Interactive effects of solar radiation and dissolved organic matter on bacterial activity and community structure. *Environmental Microbiology,* 9, 2200-2210.

Pernthaler, J., Glöckner, F. O., Schönhuber, W. & Amann, R. 2001. Fluorescence *in situ* hybridization (FISH) with rRNA-targeted oligonucleotide probes.

Pfeifer, G. P. 1997. Formation and Processing of UV Photoproducts: Effects of DNA Sequence and Chromatin Environment. *Photochemistry and Photobiology,* 65, 270-283.

Piccini, C., Conde, D., Pernthaler, J. & Sommaruga, R. 2009. Alteration of chromophoric dissolved organic matter by solar UV radiation causes rapid changes in bacterial community composition. *Photochemical and Photobiological Sciences,* 8, 1321-1328.

Pinhassi, J., Sala, M. M., Havskum, H., Peters, F., Guadayol, Ò., Malits, A. & Marrasé, C. 2004. Changes in bacterioplankton composition under different phytoplankton regimens. *Applied and Environmental Microbiology,* 70, 6753-6766.

Piquet, A. M. T., Bolhuis, H., Davidson, A. T. & Buma, A. G. J. 2010. Seasonal succession and UV sensitivity of marine bacterioplankton at an Antarctic coastal site. *FEMS Microbiology Ecology,* 73, 68-82.

Pizarro, R. A. & Orce, L. V. 1988. Membrane damage and recovery associated with growth delay induced by near-UV radiation in *Escherichia coli* K-12. *Photochemistry and Photobiology,* 47, 391-397.

Plane, J. M. C., Blough, N. V., Ehrhardt, M. G., Waters, K. J., Zepp, R. G. & Zika, R. G. 1997. Report Group 3 - Photochemistry in the sea-surface microlayer. *In:* Liss, P. S. & Duce, R. A. (eds.) *The Sea Surface and Global Change*. Cambridge, UK: Cambridge University Press.

Ploug, H. 2008. Cyanobacterial surface blooms formed by *Aphanizomenon* sp. and *Nodularia spumigena* in the Baltic Sea: Small-scale fluxes, pH, and oxygen microenvironments. *Limnology and Oceanography,* 53, 914-921.

Poole, L. B. 2005. Bacterial defenses against oxidants: mechanistic features of cysteine-based peroxidases and their flavoprotein reductases. *Archives of Biochemistry and Biophysics,* 433, 240-254.

Qiu, X., Sundin, G. W., Chai, B. & Tiedje, J. M. 2004. Survival of *Shewanella oneidensis* MR-1 after UV radiation exposure. *Applied and Environmental Microbiology,* 70, 6435-6443.

Qiu, X., Sundin, G. W., Wu, L., Zhou, J. & Tiedje, J. M. 2005a. Comparative analysis of differentially expressed genes in *Shewanella oneidensis* MR-1 following exposure to UVC, UVB, and UVA radiation. *Journal of Bacteriology,* 187, 3556-3564.

Qiu, X., Tiedje, J. M. & Sundin, G. W. 2005b. Genome-wide examination of the natural solar radiation response in *Shewanella oneidensis* MR-1. *Photochemistry and Photobiology,* 81, 1559-1568.

Rademaker, J. L. W., Louws, F. J., Versalovic, J. & Bruijn, F. J. 2004. Characterization of the diversity of ecologically important microbes by rep-PCR genomic fingerprinting. *In:* Akkermans, A. D. L., van Elsas, J. D. & de Bruijn, F. J. (eds.) *Molecular Microbial Ecology Manual II, suppl. 3.* Dordrecht: Kluwer.

Radman, M. 1975. SOS repair hypothesis: phenomenology of an inducible DNA repair which is accompanied by mutagenesis. *Basic Life Sciences,* 355-67.

Rajan, R. & Bell, C. E. 2004. Crystal structure of RecA from *Deinococcus radiodurans*: Insights into the structural basis of extreme radioresistance. *Journal of Molecular Biology,* 344, 951-963.

Ranquet, C., Ollagnier-de-Choudens, S., Loiseau, L., Barras, F. & Fontecave, M. 2007. Cobalt Stress in *Escherichia coli*. *Journal of Biological Chemistry,* 282, 30442-30451.

Rastogi, V. K., Wallace, L. & Smith, L. S. 2007. Disinfection of *Acinetobacter baumannii*-contaminated surfaces relevant to medical treatment facilities with ultraviolet C light. *Military Medicine,* 172, 1166-1169.

Rattray, A. J. & Strathern, J. N. 2003. Error-prone DNA polymerases: when making a mistake is the only way to get ahead. *Annual Review of Genetics,* 37, 31-66.

Ravanat, J. L., Douki, T. & Cadet, J. 2001. Direct and indirect effects of UV radiation on DNA and its components. *Journal of Photochemistry and Photobiology B: Biology,* 63, 88-102.

Reardon, J. T. & Sancar, A. 2005. Nucleotide Excision Repair. *Progress in Nucleic Acid Research and Molecular Biology* 79, 183-235.

Reed, R. H. 1997. Solar inactivation of faecal bacteria in water: the critical role of oxygen. *Letters in Applied Microbiology,* 24, 276-280.

Rees, C. E. D. 1995. The significance of bacteria in stationary phase to food microbiology. *International Journal of Food Microbiology,* 28, 263-275.

Reinthaler, T., Sintes, E. & Herndl, G. J. 2008. Dissolved organic matter and bacterial production and respiration in the sea-surface microlayer of the open Atlantic and the western Mediterranean Sea. *Limnology and Oceanography,* 53, 122-136.

Requena, J. R., Chao, C. C., Levine, R. L. & Stadtman, E. R. 2001. Glutamic and aminoadipic semialdehydes are the main carbonyl products of metal-catalyzed oxidation of proteins. *Proceedings of the National Academy of Sciences of the United States of America,* 98, 69-74.

Riemann, L., Steward, G. F. & Azam, F. 2000. Dynamics of bacterial community composition and activity during a mesocosm diatom bloom. *Applied and Environmental Microbiology,* 66, 578-587.

Robinson, N. E. & Robinson, A. B. 2001. Molecular clocks. *Proceedings of the National Academy of Sciences,* 98, 944-949.

Roca, A. I. & Cox, M. M. 1990. The RecA Protein: Structure and function. *Critical Reviews in Biochemistry and Molecular Biology,* 25, 415-456.

Rodier, J. 1996. *L'analyse de l'eau: eaux naturelles, eaux résiduaires, eau de mer (8th Ed),* Paris, Dunod.

Rothschild, K. J., DeGrip, W. J. & Sanches, R. 1980. Fourier transform infrared study of photoreceptor membrane. I. Group assignments based on rhodopsin delipidation and reconstitution. *Biochimica et Biophysica Acta,* 596, 338-351.

Roy, S. 2000. Strategies for the minimization of UV-induced damage. *In:* de Mora, S., Demers, S. & Vernet, M. (eds.) *The Effects of UV Radiation in the Marine Environment.* Cambridge, UK: Cambridge University Press.

Rünger, T. M., Farahvash, B., Hatvani, Z. & Rees, A. 2012. Comparison of DNA damage responses following equimutagenic doses of UVA and UVB: A less effective cell cycle arrest with UVA may render UVA-induced pyrimidine dimers more mutagenic than UVB-induced ones. *Photochemical and Photobiological Sciences,* 11, 207-215.

Ruiz-González, C., Lefort, T., Galí, M., Montserrat Sala, M., Sommaruga, R., Simó, R. & Gasol, J. M. 2012. Seasonal patterns in the sunlight sensitivity of bacterioplankton from Mediterranean surface coastal waters. *FEMS Microbiology Ecology,* 79, 661-674.

Sagan, C. 1973. Ultraviolet selection pressure on the earliest organisms. *Journal of Theoretical Biology,* 39, 195-200.

Sakumi, K. & Sekiguchi, M. 1990. Structures and functions of DNA glycosylases. *Mutation Research,* 236, 161-172.

Sala, M. M., Arrieta, J. M., Boras, J. A., Duarte, C. M. & Vaqué, D. 2010. The impact of ice melting on bacterioplankton in the Arctic Ocean. *Polar Biology,* 33, 1683-1694.

Salcedo, I., Andrade, J. A., Quiroga, J. M. & Nebot, E. 2007. Photoreactivation and dark repair in UV-treated microorganisms: Effect of temperature. *Applied and Environmental Microbiology,* 73, 1594-1600.

Salmon, S., Maziere, J. C., Santus, R., Morliere, P. & Bouchemal, N. 1990. UVB-induced photoperoxidation of lipids of human low and high density lipoproteins. A possible role of tryptophan residues. *Photochemistry and Photobiology,* 52, 541-545.

Sancar, A. 1994. Structure and function of DNA photolyase. *Biochemistry,* 33, 2-9.

Sancar, A. 1996. No 'end of history' for photolyases. *Science,* 272, 48-49.

Sangwan, V., Örvar, B. L., Beyerly, J., Hirt, H. & Dhindsa, R. S. 2002. Opposite changes in membrane fluidity mimic cold and heat stress activation of distinct plant MAP kinase pathways. *The Plant Journal,* 31, 629-638.

Santo, C. E., Lam, E. W., Elowsky, C. G., Quaranta, D., Domaille, D. W., Chang, C. J. & Grass, G. 2011. Bacterial Killing by Dry Metallic Copper Surfaces. *Applied and Environmental Microbiology,* 77, 794-802.

Santos, A. L., Baptista, I., Lopes, S., Henriques, I., Gomes, N. C. M., Almeida, A., Correia, A. & Cunha, A. 2012a. The UV responses of bacterioneuston and bacterioplankton isolates depend on the physiological condition and involve a metabolic shift. *FEMS Microbiology Ecology,* 80, 646-658.

Santos, A. L., Henriques, I., Gomes, N. C. M., Almeida, A., Correia, A. & Cunha, A. 2011a. Effects of ultraviolet radiation on the abundance, diversity and activity of bacterioneuston and bacterioplankton: Insights from microcosm studies. *Aquatic Sciences,* 73, 63-77.

Santos, A. L., Lopes, S., Baptista, I., Henriques, I., Gomes, N. C. M., Almeida, A., Correia, A. & Cunha, Â. 2011b. Diversity in UV sensitivity and recovery potential among bacterioneuston and bacterioplankton isolates. *Letters in Applied Microbiology,* 52, 360-366.

Santos, A. L., Mendes, C., Gomes, N. C. M., Henriques, I., Correia, A., Almeida, A. & Cunha, Â. 2009. Short-term variability of abundance, diversity and activity of estuarine bacterioneuston and bacterioplankton. *Journal of Plankton Research,* 31, 1545-1555.

Santos, A. L., Oliveira, V., Baptista, I., Henriques, I., Gomes, N. C. M., Almeida, A., Correia, A. & Cunha, A. 2012b. Effects of UV-B radiation on the structural and physiological diversity of bacterioneuston and bacterioplankton. *Applied and Environmental Microbiology,* 78, 2066-2069.

Santos, A. L., Oliveira, V., Baptista, I., Henriques, I., Gomes, N. C. M., Almeida, A., Correia, A. & Cunha, Â. 2013. Wavelength dependence of biological damage induced by UV radiation on bacteria. *Archives of Microbiology,* 195, 63-74.

Santos, L., Santos, A. L., Coelho, F. J. R. C., Gomes, N. C. M., Dias, J. M., Cunha, Â. & Almeida, A. 2011c. Relation between bacterial activity in the surface microlayer and estuarine hydrodynamics. *FEMS Microbiology Ecology,* 77, 636-646.

Schellhorn, H. E., Audia, J. P., Wei, L. I. C. & Chang, L. 1998. Identification of conserved, RpoS-dependent stationary-phase genes of *Escherichia coli*. *Journal of Bacteriology,* 180, 6283-6291.

Schenk, M., Raffellini, S., Guerrero, S., Blanco, G. A. & Alzamora, S. M. 2011. Inactivation of *Escherichia coli*, *Listeria innocua* and *Saccharomyces cerevisiae* by UV-C light: Study of cell injury by flow cytometry. *LWT- Food Science and Technology,* 44, 191-198.

Schimel, J., Balser, T. C. & Wallenstein, M. 2007. Microbial stress-response physiology and its implications for ecosystem function. *Ecology,* 88, 1386-1394.

Schlacher, K. & Goodman, M. F. 2007. Lessons from 50 years of SOS DNA-damage-induced mutagenesis. *Nature Reviews Molecular Cell Biology,* 8, 587-594.

Scholz, H. C., Al Dahouk, S., Tomaso, H., Neubauer, H., Witte, A., Schloter, M., Kämpfer, P., Falsen, E., Pfeffer, M. & Engel, M. 2008. Genetic diversity and phylogenetic relationships of bacteria belonging to the *Ochrobactrum–Brucella* group by *recA* and 16S rRNA gene-based comparative sequence analysis. *Systematic and Applied Microbiology,* 31, 1-16.

Schrope, M. 2000. Successes in fight to save ozone layer could close holes by 2050. *Nature,* 408, 627.

Sciacca, F., Rengifo-Herrera, J. A., Wéthé, J. & Pulgarin, C. 2010. Dramatic enhancement of solar disinfection (SODIS) of wild *Salmonella* sp. in PET bottles by H_2O_2 addition on natural water of Burkina Faso containing dissolved iron. *Chemosphere,* 78, 1186-1191.

Scott, C., Rawsthorne, H., Upadhyay, M., Shearman, C. A., Gasson, M. J., Guest, J. R. & Green, J. 2000. Zinc uptake, oxidative stress and the FNR-like proteins of *Lactococcus lactis*. *FEMS Microbiology Letters,* 192, 85-89.

Scott, M. D., Meshnick, S. R. & Eaton, J. W. 1989. Superoxide dismutase amplifies organismal sensitivity to ionizing radiation. *Journal of Biological Chemistry,* 264, 2498-2501.

Scully, N. M., Tranvik, L. J. & Cooper, W. J. 2003. Photochemical effects on the interaction of enzymes and dissolved organic matter in natural waters. *Limnology and Oceanography,* 48, 1818-1824.

Searles, P. S., Flint, S. D. & Caldwell, M. M. 2001. A meta-analysis of plant field studies simulating stratospheric ozone depletion. *Oecologia,* 127, 1-10.

Seckmeyer, G., Pissulla, D., Glandorf, M., Henriques, D., Johnsen, B., Webb, A., Siani, A. M., Bais, A., Kjeldstad, B., Brogniez, C., Lenoble, J., Gardiner, B., Kirsch, P., Koskela, T., Kaurola, J., Uhlmann, B., Slaper, H., Den Outer, P., Janouch, M., Werle, P., Gröbner, J., Mayer, B., De La Casiniere, A., Simic, S. & Carvalho, F. 2008. Variability of UV irradiance in Europe. *Photochemistry and Photobiology,* 84, 172-179.

Seeberg, E., Eide, L. & Bjørås, M. 1995. The base excision repair pathway. *Trends in Biochemical Sciences,* 20, 391-397.

Semchyshyn, H., Bagnyukova, T., Storey, K. & Lushchak, V. 2005. Hydrogen peroxide increases the activities of *soxRS* regulon enzymes and the levels of oxidized proteins and lipids in *Escherichia coli*. *Cell Biology International,* 29, 898-902.

Sepe, A., Barbieri, P., Peduzzi, R. & Demarta, A. 2008. Evaluation of *recA* sequencing for the classification of *Aeromonas* strains at the genotype level. *Letters in Applied Microbiology,* 46, 439-444.

Severin, B. F., Suidan, M. T. & Engelbrecht, R. S. 1983. Effects of temperature on ultraviolet light disinfection. *Enironmental Science and Technology,* 17, 717-721.

Shannon, A. E. & Weaver, W. 1963. *The Mathematical Theory of Communication,* Urbana. IL, University Illinois Press.

Sharples, G. J. 2009. For absent friends: life without recombination in mutualistic γ-proteobacteria. *Trends in Microbiology,* 17, 233-242.

Shick, J. M. & Dunlap, W. C. 2002. Mycosporine-like amino acids and related gadusols: Biosynthesis, accumulation, and UV-protective functions in aquatic organisms. *Annual Review of Physiology,* 64, 223-262.

Shinohara, A. & Ogawa, T. 1995. Homologous recombination and the roles of double-strand breaks. *Trends in Biochemical Sciences,* 20, 387-391.

Siebeck, O., Vail, T., Williamson, C. E., Vetter, R., Hessen, D., Zagarese, H., Little, E., Balseiro, E., Modenutti, B., Seva, J. & Shumate, A. 1994. Impact of UV-B radiation on zooplankton and fish in pelagic freshwater ecosystems. *Archiv fur Hydrobiologie Ergebnisse Limnologie,* 43, 101-114.

Silipo, A., Lanzetta, R., Garozzo, D., Lo Cantore, P., Iacobellis, N. S., Molinaro, A., Parrilli, M. & Evidente, A. 2002. Structural determination of lipid A of the lipopolysaccharide from *Pseudomonas reactans*. *European Journal of Biochemistry,* 269, 2498-2505.

Silver, S. & Phung, L. 2005. A bacterial view of the periodic table: genes and proteins for toxic inorganic ions. *Journal of Industrial Microbiology and Biotechnology,* 32, 587-605.

Simon, M. & Azam, F. 1989. Protein content and protein synthesis rates of planktonic marine bacteria. *Marine Ecology Progress Series,* 51, 201-214.

Simonson, C. S., Kokjohn, T. A. & Miller, R. V. 1990. Inducible UV repair potential of *Pseudomonas aeruginosa* PAO. *Journal of General Microbiology,* 136, 1241-9.

Singer, C. E. & Ames, B. N. 1970. Sunlight ultraviolet and bacterial DNA base ratios. *Science,* 170, 822-826.

Singh, B., Boopathy, S., Somasundaram, K. & Umapathy, S. 2012. Fourier transform infrared microspectroscopy identifies protein propionylation in histone deacetylase inhibitor treated glioma cells. *Journal of Biophotonics,* 5, 230-239.

Singh, S. K., Grass, G., Rensing, C. & Montfort, W. R. 2004. Cuprous Oxidase Activity of CueO from *Escherichia coli*. *Journal of Bacteriology,* 186, 7815-7817.

Sinton, L. W., Hall, C. H., Lynch, P. A. & Davies-Colley, R. J. 2002. Sunlight inactivation of fecal indicator bacteria and bacteriophages from waste stabilization pond effluent in fresh and saline waters. *Applied and Environmental Microbiology,* 68, 1122-1131.

Slade, D. & Radman, M. 2011. Oxidative stress resistance in *Deinococcus radiodurans*. *Microbiology and Molecular Biology Reviews,* 75, 133-191.

Smith, B. T. & Walker, G. C. 1998. Mutagenesis and more: *umuDC* and the *Escherichia coli* SOS response. *Genetics,* 148, 1599-610.

Smith, D. C. & Azam, F. 1992. A simple, economical method for measuring bacterial protein synthesis rates in seawater using tritiated-leucine. *Marine Microbial Food Webs,* 6, 107–114.

Smith, R. C. 1989. Ozone, Middle Ultraviolet Radiation and the Aquatic Environment. *Photochemistry and Photobiology,* 50, 459-468.

Smith, R. C., Baker, K. S., Holm-Hansen, O. & Olson, R. 1980. Photoinhibition of photosynthesis in natural waters. *Photochemistry and Photobiology,* 31, 585-592.

Smith, R. C., Prézelin, B. B., Baker, K. S., Bidigare, R. R., Boucher, N. P., Coley, T., Karentz, D., Macintyre, S., Matlick, H. A., Menzies, D., Ondrusek, M., Wan, Z. & Waters, K. J. 1992. Ozone depletion: Ultraviolet radiation and phytoplankton biology in Antarctic waters. *Science,* 255, 952-959.

Sobota, J. M. & Imlay, J. A. 2011. Iron enzyme ribulose-5-phosphate 3-epimerase in *Escherichia coli* is rapidly damaged by hydrogen peroxide but can be protected by manganese. *Proceedings of the National Academy of Sciences of the United States of America,* 108, 5402-5407.

Sokal, R. R. & Rolf, F. J. 1995. *Biometry (3rd Ed.),* New York, NY, W. H. Freeman and Company.

Solomon, S. 1999. Stratospheric ozone depletion: A review of concepts and history. *Reviews of Geophysics*, 37, 275-316.

Sommaruga, R. 2003. UVR and its effects on species interactions. *In:* Helbling, E. W. & Zagarese, H. E. (eds.) *UV Effects in Aquatic Organisms and Ecosystems.* Cambridge, UK: The Royal Society of Chemistry and Springer Verlag.

Sommaruga, R., Oberleiter, A. & Psenner, R. 1996. Effect of UV radiation on the bacterivory of a heterotrophic nanoflagellate. *Applied and Environmental Microbiology*, 62, 4395-4400.

Sommaruga, R., Obernosterer, I., Herndl, G. J. & Psenner, R. 1997. Inhibitory effect of solar radiation on thymidine and leucine incorporation by freshwater and marine bacterioplankton. *Applied and Environmental Microbiology*, 63, 4178-4184.

Sommers, C. H., Cooke, P. H., Fan, X. & Sites, J. E. 2009. Ultraviolet Light (254 nm) Inactivation of *Listeria monocytogenes* on Frankfurters That Contain Potassium Lactate and Sodium Diacetate. *Journal of Food Science*, 74, M114-M119.

Spiro, S. & D'Autreaux, B. 2012. Non-Heme Iron Sensors of Reactive Oxygen and Nitrogen Species. *Antioxid Redox Signal*, 8, 8.

Stadtman, E. R. 1992. Protein oxidation and aging. *Science*, 257, 1220-1224.

Stadtman, E. R., Berlett, B. S. & Chock, P. B. 1990. Manganese-dependent disproportionation of hydrogen peroxide in bicarbonate buffer. *Proceedings of the National Academy of Sciences*, 87, 384-388.

Steinberger, R. E., Allen, A. R., Hansma, H. G. & Holden, P. A. 2002. Elongation correlates with nutrient deprivation in *Pseudomonas aeruginosa* - Unsaturated biofilms. *Microbial Ecology*, 43, 416-423.

Stochel, G., Brindell, M., Macyk, W., Stasicka, Z. & Szaciłowski, K. 2009. Photoenzymes. *Bioinorganic Photochemistry*. John Wiley & Sons, Ltd.

Stolle, C., Nagel, K., Labrenz, M. & Jürgens, K. 2010. Bacterial activity in the sea-surface microlayer: In situ investigations in the Baltic Sea and the influence of sampling devices. *Aquatic Microbial Ecology*, 58, 67-78.

Sundin, G. W. & Jacobs, J. L. 1999. Ultraviolet radiation (UVR) sensitivity analysis and UVR survival strategies of a bacterial community from the phyllosphere of field-grown peanut (*Arachis hypogeae* L.). *Microbial Ecology*, 38, 27-38.

Sundin, G. W. & Murillo, J. 1999. Functional analysis of the *Pseudomonas syringae rulAB* determinant in tolerance to ultraviolet B (290-320 nm) radiation and distribution of *rulAB* among *P. syringae* pathovars. *Environmental Microbiology*, 1, 75-87.

Swingley, W. D., Chen, M., Cheung, P. C., Conrad, A. L., Dejesa, L. C., Hao, J., Honchak, B. M., Karbach, L. E., Kurdoglu, A., Lahiri, S., Mastrian, S. D., Miyashita, H., Page, L., Ramakrishna, P., Satoh, S., Sattley, W. M., Shimada, Y., Taylor, H. L., Tomo, T., Tsuchiya, T., Wang, Z. T., Raymond, J., Mimuro, M., Blankenship, R. E. & Touchman, J. W. 2008. Niche adaptation and genome expansion in the chlorophyll d-producing cyanobacterium *Acaryochloris marina*. *Proceedings of the National Academy of Sciences of the United States of America*, 105, 2005-2010.

Szweda, L. I., Uchida, K., Tsai, L. & Stadtman, E. R. 1993. Inactivation of glucose-6-phosphate dehydrogenase by 4-hydroxy-2-nonenal. Selective modification of an active-site lysine. *Journal of Biological Chemistry*, 268, 3342-3347.

Takeuchi, Y., Murakami, M., Nakajima, N., Kondo, N. & Nikaido, O. 1996. Induction and repair of damage to DNA in cucumber cotyledons irradiated with UV-B. *Plant and Cell Physiology*, 37, 181-187.

Tamarit, J., Cabiscol, E. & Ros, J. 1998. Identification of the major oxidatively damaged proteins in *Escherichia coli* cells exposed to oxidative stress. *Journal of Biological Chemistry*, 273, 3027-3032.

Tamura, K., Peterson, D., Peterson, N., Stecher, G., Nei, M. & Kumar, S. 2011. MEGA5: Molecular evolutionary genetics analysis using maximum likelihood, evolutionary distance, and maximum parsimony methods. *Molecular Biology and Evolution*, 28, 2731-2739.

Tang, X., Wilson, S. R., Solomon, K. R., Shao, M. & Madronich, S. 2011. Changes in air quality and tropospheric composition due to depletion of stratospheric ozone and interactions with climate. *Photochemical and Photobiological Sciences,* 10, 280-291.

Tank, S. E., Xenopoulos, M. A. & Hendzel, L. L. 2005. Effect of ultraviolet radiation on alkaline phosphatase activity and planktonic phosphorus acquisition in Canadian boreal shield lakes. *Limnology and Oceanography,* 50, 1345-1351.

Taranto, M. P., Perez-Martinez, G. & Font de Valdez, G. 2006. Effect of bile acid on the cell membrane functionality of lactic acid bacteria for oral administration. *Research in Microbiology,* 157, 720-725.

Tark, M., Tover, A., Tarassova, K., Tegova, R., Kivi, G., Hõrak, R. & Kivisaar, M. 2005. A DNA Polymerase V Homologue Encoded by TOL Plasmid pWW0 Confers Evolutionary Fitness on *Pseudomonas putida* under Conditions of Environmental Stress. *Journal of Bacteriology,* 187, 5203-5213.

Taylor, H. R., West, S. K., Rosenthal, F. S., Munoz, B., Newland, H. S., Abbey, H. & Emmett, E. A. 1988. Effect of ultraviolet radiation on cataract formation. *New England Journal of Medicine,* 319, 1429-1433.

Tedetti, M. & Sempéré, R. 2006. Penetration of ultraviolet radiation in the marine environment. A review. *Photochemistry and Photobiology,* 82, 389-397.

Thoma, F. 1999. Light and dark in chromatin repair: Repair of UV-induced DNA lesions by photolyase and nucteotide excision repair. *EMBO Journal,* 18, 6585-6598.

Thomas, C. E., Morehouse, L. A. & Aust, S. D. 1985. Ferritin and superoxide-dependent lipid peroxidation. *Journal of Biological Chemistry,* 260, 3275-3280.

Thomas, P., Swaminathan, A. & Lucas, R. M. 2012. Climate change and health with an emphasis on interactions with ultraviolet radiation: A review. *Global Change Biology*.

Thompson, C. C., Thompson, F. L., Vandemeulebroecke, K., Hoste, B., Dawyndt, P. & Swings, J. 2004. Use of *recA* as an alternative phylogenetic marker in the family Vibrionaceae. *International Journal of Systematic and Evolutionary Microbiology,* 54, 919-924.

Thompson, J. D., Gibson, T. J., Plewniak, F., Jeanmougin, F. & Higgins, D. G. 1997. The CLUSTAL X windows interface: Flexible strategies for multiple sequence alignment aided by quality analysis tools. *Nucleic Acids Research,* 25, 4876-4882.

Thorgersen, M. P. & Downs, D. M. 2007. Cobalt targets multiple metabolic processes in *Salmonella enterica*. *Journal of Bacteriology,* 189, 7774-7781.

Torriani, S., Felis, G. E. & Dellaglio, F. 2001. Differentiation of *Lactobacillus plantarum, L. pentosus,* and *L. paraplantarum* by *recA* Gene Sequence Analysis and Multiplex PCR Assay with *recA* Gene-Derived Primers. *Applied and Environmental Microbiology,* 67, 3450-3454.

Tranvik, L. & Kokalj, S. 1998. Decreased biodegradability of algal DOC due to interactive effects of UV radiation and humic matter. *Aquatic Microbial Ecology,* 14, 301-307.

Tranvik, L. J. & Bertilsson, S. 2001. Contrasting effects of solar UV radiation on dissolved organic sources for bacterial growth. *Ecology Letters,* 4, 458-463.

Tyrrell, R. M. 1973. Induction of pyrimidine dimers in bacterial DNA by 365 nm radiation. *Photochemistry and Photobiology,* 17, 69-73.

Ubomba-Jaswa, E., Navntoft, C., Polo-López, M. I., Fernandez-Ibáñez, P. & McGuigan, K. G. 2009. Solar disinfection of drinking water (SODIS): An investigation of the effect of UV-A dose on inactivation efficiency. *Photochemical and Photobiological Sciences,* 8, 587-595.

Upstill-Goddard, R. C., Frost, T., Henry, G. R., Franklin, M., Murrell, J. C. & Owens, N. J. P. 2003. Bacterioneuston control of air-water methane exchange determined with a laboratory gas exchange tank. *Global Biogeochemical Cycles,* 17, 19-1.

Urbach, F. 1969. Geographic Pathology of Skin Cancer. *In:* Urbach, F. (ed.) *The Biologic Effects of Ultraviolet Radiation.* Oxford (NY): Pergamon Press Ltd.

Vähätalo, A. V., Aarnos, H., Hoikkala, L. & Lignell, R. 2011. Photochemical transformation of terrestrial dissolved organic matter supports hetero- and autotrophic production in coastal waters. *Marine Ecology Progress Series,* 423, 1-14.

Valko, M., Rhodes, C. J., Moncol, J., Izakovic, M. & Mazur, M. 2006. Free radicals, metals and antioxidants in oxidative stress-induced cancer. *Chemico-Biological Interactions,* 160, 1-40.

Van Hannen, E. J., Veninga, M., Bloem, J., Gons, H. J. & Laanbroek, H. J. 1999. Genetic changes in the bacterial community structure associated with protistan grazers. *Archiv fur Hydrobiologie,* 145, 25-38.

Van Waasbergen, L. G., Balkwill, D. L., Crocker, F. H., Bjornstad, B. N. & Miller, R. V. 2000. Genetic diversity among *Arthrobacter* species collected across a heterogeneous series of terrestrial deep-subsurface sediments as determined on the basis of 16s rRNA and *recA* gene sequences. *Applied and Environmental Microbiology,* 66, 3454-3463.

Van Wambeke, F., Tedetti, M., Duhamel, S. & Sempéré, R. 2009. Diel variability of heterotrophic bacterial production and underwater UV doses in the eastern South Pacific. *Marine Ecology Progress Series,* 387, 97-108.

Velders, G. J. M., Andersen, S. O., Daniel, J. S., Fahey, D. W. & McFarland, M. 2007. The importance of the Montreal Protocol in protecting climate. *Proceedings of the National Academy of Sciences of the United States of America,* 104, 4814-4819.

Vernet, M., Brody, E. A., Holm-Hansen, O. & Mitchell, B. G. 1994. The response of Antarctic phytoplankton to ultraviolet radiation: Absorption, photosynthesis, and taxonomic composition. *In:* Weiler, C. S. & Penhale, P. A. (eds.) *Ultraviolet Radiation in Antarctica: Measurements and Biological Effects.* Washington, DC: AGU.

Versalovic, J., Schneider, M., De Bruijn, F. J. & Lupski, J. R. 1994. Genomic fingerprinting of bacteria using repetitive sequence-based polymerase chain reaction. *Methods in Molecular and Cellular Biology,* 5, 25-40.

Vile, G. F. & Tyrrell, R. M. 1995. UVA radiation-induced oxidative damage to lipids and proteins *in vitro* and in human skin fibroblasts is dependent on iron and singlet oxygen. *Free Radical Biology and Medicine,* 18, 721-730.

Vincent, W. F. & Neale, P. J. 2000. Mechanism of UV damage to aquatic organisms. *In:* de Mora, S., Demers, S. & Vernet, M. (eds.) *The Effects of UV Radiation in the Marine Environment.* Cambridge, UK: Cambridge University Press.

Visser, P. M., Poos, J. J., Scheper, B. B., Boelen, P. & Van Duyl, F. C. 2002. Diurnal variations in depth profiles of UV-induced DNA damage and inhibition of bacterioplankton production in tropical coastal waters. *Marine Ecology Progress Series,* 228, 25-33.

Visser, P. M., Snelder, E., Kop, A. J., Boelen, P., Buma, A. G. J. & Van Duyl, F. C. 1999. Effects of UV radiation on DNA photodamage and production in bacterioplankton in the coastal Caribbean Sea. *Aquatic Microbial Ecology,* 20, 49-58.

W.M.O. 1988. Report of the International Ozone Trends Panel - 1988. *Global Ozone Research and Monitoring Project.* Geneva.

W.M.O. 1991. Report of the International Ozone Trends Panel - 1991. *Global Ozone Research and Monitoring Project.* Geneva.

Walker, G. C. 1984. Mutagenesis and inducible responses to deoxyribonucleic acid damage in *Escherichia coli*. *Microbiological Reviews,* 48, 60-93.

Walker, J. C. G., Margulis, L. & Rambler, M. 1976. Reassessment of roles of oxygen and ultraviolet light in Precambrian evolution. *Nature,* 264, 620-624.

Wängberg, S. Å., Andreasson, K. I. M., Gustavson, K., Reinthaler, T. & Henriksen, P. 2008. UV-B effects on microplankton communities in Kongsfjord, Svalbard - A mesocosm experiment. *Journal of Experimental Marine Biology and Ecology,* 365, 156-163.

Wängberg, S. A., Selmer, J. S. & Gustavson, K. 1998. Effects of UV-B radiation on carbon and nutrient dynamics in marine plankton communities. *Journal of Photochemistry and Photobiology B: Biology,* 45, 19-24.

Wardman, P. & Candeias, L. P. 1996. Fenton chemistry: An introduction. *Radiation Research,* 145, 523-531.

Warnecke, F., Sommaruga, R., Sekar, R., Hofer, J. S. & Pernthaler, J. 2005. Abundances, identity, and growth state of *Actinobacteria* in mountain lakes of different UV transparency. *Applied and Environmental Microbiology,* 71, 5551-5559.

Waterworth, W. M., Jiang, Q., West, C. E., Nikaido, M. & Bray, C. M. 2002. Characterization of *Arabidopsis* photolyase enzymes and analysis of their role in protection from ultraviolet-B radiation. *Journal of Experimental Botany,* 53, 1005-1015.

Webb, R. B. & Lorenz, J. R. 1970. Oxygen dependence and repair of lethal effects of near ultraviolet and visible light. *Photochemistry and Photobiology,* 12, 283-289.

Wegelin, M., Canonica, S., Mechsner, K., Fleischmann, T., Pesaro, F. & Metzler, A. 1994. Solar water disinfection: Scope of the process and analysis of radiation experiments. *Aqua: Journal of Water Supply Research and Technology,* 43, 154-169.

Wells, R. L. & Han, A. 1984. Action spectra for killing and mutation of Chinese hamster cells exposed to mid- and near-ultraviolet monochromatic light. *Mutation Research,* 129, 251-258.

Weng, F. Y., Chiou, C. S., Lin, P. H. P. & Yang, S. S. 2009. Application of *recA* and *rpoB* sequence analysis on phylogeny and molecular identification of *Geobacillus* species. *Journal of Applied Microbiology,* 107, 452-464.

Wetzel, R. G., Hatcher, P. G. & Bianchi, T. S. 1995. Natural photolysis by ultraviolet irradiance of recalcitrant dissolved organic matter to simple substrates for rapid bacterial metabolism. *Limnology and Oceanography,* 40, 1369-1380.

White, D. 1995. *The Physiology and Biochemistry of Prokaryotes, 2nd Edition,* New York, Oxford Univ. Press.

Whitehead, K. & Vernet, M. 2000. Influence of mycosporine-like amino acids (MAAs) on UV absorption by particulate and dissolved organic matter in La Jolla Bay. *Limnology and Oceanography,* 45, 1788-1796.

Whitehead, R. F., de Mora, S. J. & Demers, S. 2000. Enhanced UV radiation - a new problem for the marine environment. *In:* de Mora, S., Demers, S. & Vernet, M. (eds.) *The Effects of UV Radiation in the Marine Environment.* Cambridge, UK: Cambridge University Press.

Williams, K. P., Gillespie, J. J., Sobral, B. W. S., Nordberg, E. K., Snyder, E. E., Shallom, J. M. & Dickerman, A. W. 2010. Phylogeny of *Gammaproteobacteria*. *Journal of Bacteriology,* 192, 2305-2314.

Williams, P. M., Carlucci, A. F., Henrichs, S. M., Van Vleet, E. S., Horrigan, S. G., Reid, F. M. H. & Robertson, K. J. 1986. Chemical and microbiological studies of sea-surface films in the Southern Gulf of California and off the West Coast of Baja California. *Marine Chemistry,* 19, 17-98.

Wilson, C., Caton, T. M., Buchheim, J. A., Buchheim, M. A., Schneegurt, M. A. & Miller, R. V. 2004. DNA-Repair Potential of *Halomonas* spp. from the Salt Plains Microbial Observatory of Oklahoma. *Microbial Ecology,* 48, 541-549.

Wilson, S. R., Solomon, K. R. & Tang, X. 2007. Changes in tropospheric composition and air quality due to stratospheric ozone depletion and climate change. *Photochemical and Photobiological Sciences,* 6, 301-310.

Winter, C., Moeseneder, M. M. & Herndl, G. J. 2001. Impact of UV radiation on bacterioplankton community composition. *Applied and Environmental Microbiology,* 67, 665-672.

WMO 1985. Scientific Assessment of Ozone Depletion: 1985. *Global Ozone Research and Monitoring Project – Report No. 16.* Geneva.

Woese, C. R. 1987. Bacterial evolution. *Microbiological Reviews,* 51, 221-271.

Wong, H. C. & Wang, P. 2004. Induction of viable but nonculturable state in *Vibrio parahaemolyticus* and its susceptibility to environmental stresses. *Journal of Applied Microbiology,* 96, 359-366.

Wood, J. M. & Schallreuter, K. U. 2006. UVA-irradiated pheomelanin alters the structure of catalase and decreases its activity in human skin. *Journal of Investigative Dermatology,* 126, 13-14.

Worrest, R. C. & Häder, D. P. 1989. Effects of stratospheric ozone depletion on marine organisms. *Environmental Conservation*, 16, 261-263.

Xenopoulos, M. A. & Schindler, D. W. 2003. Differential responses to UVR by bacterioplankton and phytoplankton from the surface and the base of the mixed layer. *Freshwater Biology*, 48, 108-122.

Yentsch, C. S. & Menzel, D. W. 1963. A method for the determination of phytoplankton chlorophyll and phaeophytin by fluorescence. *Deep-Sea Research and Oceanographic Abstracts*, 10, 221-231.

Yuan, M., Chen, M., Zhang, W., Lu, W., Wang, J., Yang, M., Zhao, P., Tang, R., Li, X., Hao, Y., Zhou, Z., Zhan, Y., Yu, H., Teng, C., Yan, Y., Ping, S., Wang, Y. & Lin, M. 2012. Genome Sequence and Transcriptome Analysis of the Radioresistant Bacterium *Deinococcus gobiensis*: Insights into the Extreme Environmental Adaptations. *PLoS ONE*, 7, e34458.

Zeeshan, M. & Prasad, S. M. 2009. Differential response of growth, photosynthesis, antioxidant enzymes and lipid peroxidation to UV-B radiation in three cyanobacteria. *South African Journal of Botany*, 75, 466-474.

Zeigler, D. R. 2003. Gene sequences useful for predicting relatedness of whole genomes in bacteria. *International Journal of Systematic and Evolutionary Microbiology*, 53, 1893-1900.

Zepp, R. G., Callaghan, T. V. & Erickson, D. J. 1998. Effects of enhanced solar ultraviolet radiation on biogeochemical cycles. *Journal of Photochemistry and Photobiology B: Biology*, 46, 69-82.

Zepp, R. G., Erickson III, D. J., Paul, N. D. & Sulzberger, B. 2007. Interactive effects of solar UV radiation and climate change on biogeochemical cycling. *Photochemical and Photobiological Sciences*, 6, 286-300.

Zepp, R. G., Erickson III, D. J., Paul, N. D. & Sulzberger, B. 2011. Effects of solar UV radiation and climate change on biogeochemical cycling: Interactions and feedbacks. *Photochemical and Photobiological Sciences*, 10, 261-279.

Zhang, S. & Sundin, G. W. 2004. Mutagenic DNA repair potential in *Pseudomonas* spp., and characterization of the *rulABPc* operon from the highly mutable strain *Pseudomonas cichorii* 302959. *Canadian Journal of Microbiology*, 50, 29-39.

Zhang, Y.-M. & Rock, C. O. 2008. Membrane lipid homeostasis in bacteria. *Nature Reviews Microbiology*, 6, 222-233.

Zhou, Q., Zhang, J., Fu, J., Shi, J. & Jiang, G. 2008. Biomonitoring: An appealing tool for assessment of metal pollution in the aquatic ecosystem. *Analytica Chimica Acta*, 606, 135-150.

Zigman, S., Reddan, J., Schultz, J. B. & McDaniel, T. 1996. Structural and functional changes in catalase induced by near-UV radiation. *Photochemistry and Photobiology*, 63, 818-824.

Zouine, M., Sculo, Q. & Labedan, B. 2002. Correct assignment of homology is crucial when genomics meets molecular evolution. *Comparative and Functional Genomics*, 3, 488-493.

PÁGINA INTENCIONALMENTE DEIXADA EM BRANCO

APPENDIX

Supplementary tables to Chapter 2

Supplementary Table 2.1. Physical, chemical and biological properties of the original samples from the SML and UW used in the microcosms (average ± standard deviation). POC – particulate organic carbon. cDOM – chromophoric dissolved organic matter, expressed as fluorescence intensity (F) calibrated in quinine sulfate units (QSU). DIN – dissolved inorganic nitrogen. TPA – total prokaryote abundance. SML – surface microlayer. UW – underlying water. n.s. – not significant. Physical, chemical and biological parameters were determined using standard procedures.

Parameter	SML	UW	p value (n = 9)
Salinity (PSU)	28.0 ± 2.5	28.5 ± 2.6	n.s.
pH	7.5 ± 0.3	7.4 ± 0.3	n.s.
Temperature (ºC)	17.8 ± 0.9	17.7 ± 0.9	n.s.
DIN (µM)	29.6 ± 0.9	28.4 ± 0.9	n.s.
Phosphate (µM)	14.5 ± 0.5	10.2 ± 0.4	0.000
Silicates (µM)	13.8 ± 0.5	17.3 ± 0.6	0.001
Ammonium (µM)	0.7 ± 0.1	0.6 ± 0.0	0.008
Chlorophyll a (µg L^{-1})	3.5 ± 0.2	3.3 ± 0.2	n.s.
POC (mg L^{-1})	21.5 ± 1.9	6.7 ± 0.6	0.000
cDOM (F/QSU)	8.9 ± 0.7	8.4 ± 0.4	n.s.
TPA (cells mL^{-1})	$1.7x10^6 \pm 1.5x10^5$	$1.0\ x10^6 \pm 1.0\ x10^5$	0.003
Leucine Incorporation Rate (pM leucine h^{-1} $cell^{-1}$)	3.5 ± 0.1	12.0 ± 0.3	0.000
Thymidine Incorporation Rate (pM thymidine h^{-1} $cell^{-1}$)	2.9 ± 0.1	11.6 ± 0.4	0.000

Supplementary Table 2.2. Phylogenetic affiliation of cloned DGGE band sequences determined after BLAST analysis.

Band number	Accession no.	Origin	Closest relative (accession no.)	Affiliation	% similarity
1	JF699648	N0	Uncultured Flavobacteria bacterium clone SIMO-2669 (DQ189644.1)	Bacteroidetes-Chlorobi	100
2	JF699632	N0	*Staphylococcus* sp. 09BS3-3 (HM565997.1)	Firmicutes	99
3	JF699646	N0	Uncultured marine bacterium clone A-Alg131 (HM437364.1)	*Gammaproteobacteria*	100
4	JF699642	N0	*Vibrio splendidus* strain Mj82 (GQ455013.1)	*Gammaproteobacteria*	100
5	JF699650	N0	Uncultured marine bacterium clone B-SW10 (HM437577.1)	*Gammaproteobacteria*	100
6	JF699649	P0	*Vibrio* sp. 09BSKS-1 (HM565999.1)	*Gammaproteobacteria*	98
7	JF699640	P0	*Pseudoalteromonas marina* strain DHY3 (GU198498.1)	*Gammaproteobacteria*	98
8	JF699651	N12	*Staphylococcus* sp. 09BS3-3 (HM565997.1)	Firmicutes	99
9	JF699643	N12	Uncultured marine bacterium clone A-Alg131 (HM437364.1)	*Gammaproteobacteria*	97
10	JF699638	N24	Uncultured bacterium clone ncd493d12c1 (HM316088.1)	Bacteroidetes-Chlorobi	99
11	JF699635	N24	Uncultured Burkholderiaceae (FM211915.1)	*Betaproteobacteria*	96
12	JF699644	N24	Uncultured *Lactococcus* sp. isolate DGGE gel band 13 (GU363938.1)	Firmicutes	100
13	JF699634	P36	Uncultured Burkholderiaceae (FM211915.1)	*Betaproteobacteria*	96
14	JF699633	N48	*Staphylococcus* sp. 09BS3-3 (HM565997.1)	Firmicutes	100
15	JF699637	P48	*Pseudoalteromonas* sp. strain B201 (FN295770.1)	*Gammaproteobacteria*	96
16	JF699652	P48	Uncultured bacterium clone 1C226941 (EU799354.1)	Chloroplast	100
17	JF699636	N60	Uncultured *Rubrobacter* (FN689575.1)	*Actinobacteria*	100
18	JF699645	P60	Uncultured marine bacterium clone A-Alg131 (HM437364.1)	*Gammaproteobacteria*	98
19	JF699641	P60	Uncultured bacterium clone 12mt8_07 (GU249433.1)	*Gammaproteobacteria*	99
20	JF699639	P60	*Vibrio splendidus* strain Mj82 (GQ455013.1)	*Gammaproteobacteria*	99
21	JF699647	P60	Uncultured bacterium clone MuztB30-61 (GU246972.1)	*Betaproteobacteria*	99

Supplementary figures to Chapter 2

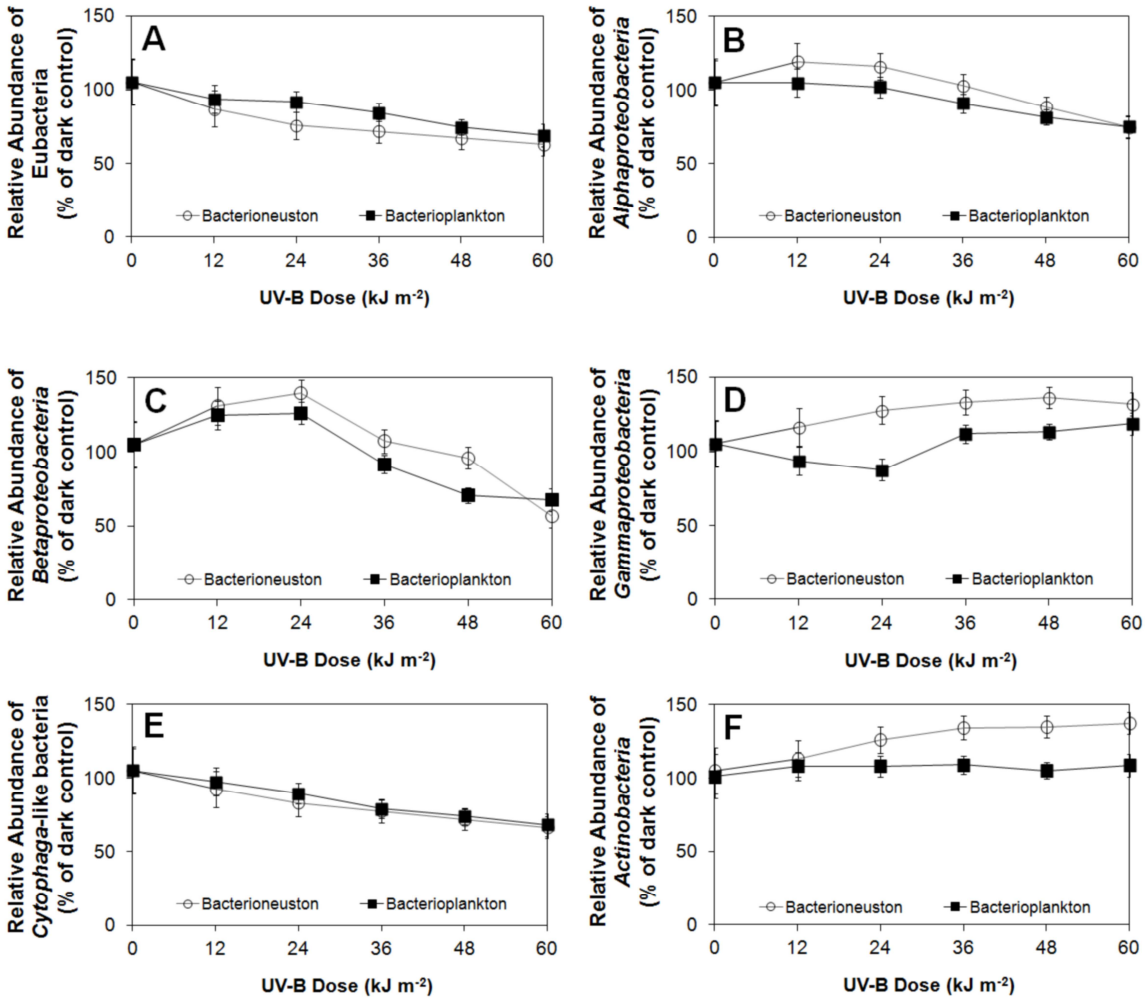

Supplementary Figure 2.1. UVB dose-dependent variation of the relative abundance of (A) Eubacteria, (B) *Alphaproteobacteria*, (C) *Betaproteobacteria*, (D) *Gammaproteobacteria*, (E) *Cytophaga*-like bacteria and (F) *Actinobacteria* as detected by Fluorescence *in situ* hybridization (FISH). Results are expressed as % of the dark controls. Mean values (n = 27) were plotted. Error bars represent standard deviations. Absence of error bars indicates that standard deviations are too small to see on the scale used.

Supplementary tables to Chapter 11

Supplementary Table 11.1. Organisms and genome sequences from which sequences annotated as *recA* were excluded; reasons for exclusion are presented.

Organism	Accession Number	Reason for exclusion
***Robiginitalea biformata* HTCC2501**	NC_013222.1	Sequence annotated as "recombinase A" but that does not contain an ORF
***Onion yellows phytoplasma* OY-M**	NC_005303.2	3 *recA/radA recombinase* pseudogenes
***Fusobacterium nucleatum* subsp. *nucleatum* ATCC 25586**	NC_003454.1	Sequence annotated as additional *recA* gene revealed homology to NMT1_2 superfamily
***Gemmatimonas aurantiaca* T-27**	NC_012489.1	Sequence annotated as additional *recA* gene revealed no homology to conserved domains
***Brucella melitensis* biovar abortus 2308**	NC_007618.1	Sequence annotated as "DNA recombination protein RecA" revealed identity with urease accessory protein UREG
***Vibrio vulnificus* CMCP6**	NC_004459.3	Sequence annotated as RecA/RadA recombinase revealed homology with SulA superfamily
***Vibrio vulnificus* MO6-24/O**	NC_014965.1	Sequence annotated as RecA/RadA recombinase revealed homology with SulA superfamily
***Stenotrophomonas maltophilia* D457**	HE798556	Sequence annotated as RecA/RadA recombinase revealed homology with SulA superfamily
***Acidithiobacillus caldus* SM-1**	NC_015850.1	Sequence annotated as RecA/RadA recombinase revealed homology with SulA superfamily
***Vibrio* sp. Ex25**	NC_013456.1	Sequence annotated as RecA/RadA recombinase revealed homology with SulA superfamily
***Alteromonas macleodii* str. 'Deep ecotype'**	NC_011138.2	Sequence annotated as RecA/RadA recombinase revealed homology with SulA superfamily
***Collimonas fungivorans* Ter331**	NC_015856.1	Sequence annotated as RecA/RadA recombinase revealed homology with SulA superfamily

Supplementary Table 11.2. Bacterial genomes containing transposases in the immediate vicinity of the *recA* gene. Phylogenetic affiliation of the organisms, sequence accession number, and annotated family of the transposase are presented. The genetic context of the *recA* gene is presented on the diagrams of the left column, with transposase genes represented as grey shadowed arrows; the length of each open reading frame is proportional to the its size.

Organism	Accession no.	Annotated IS family	Genetic context
Pseudomonas mendocina ymp	CP000680	IS*204*/IS*1001*/IS*1096*/IS*1165* IS*4* IS*204*/IS*1001*/IS*1096*/IS*1165*	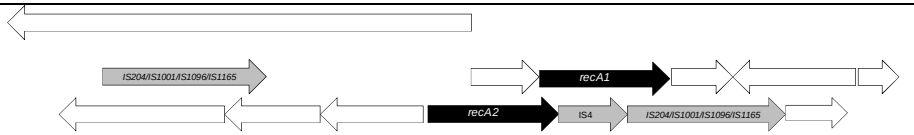
Serratia marcescens plasmid pSM22	HQ896493	IS*NCY*	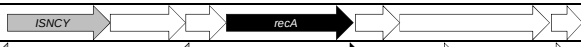
Lactococcus lactis subsp. KF147	CP001834	IS*LL6*	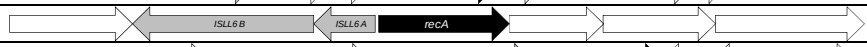
Ammonifex degensii KC4	CP001785	IS*605* OrfB	
'Desulforudis audaxviator' MP104C	CP000860	IS*605* OrfB family	
Corynebacterium aurimucosum ATCC 700975	CP001601	-	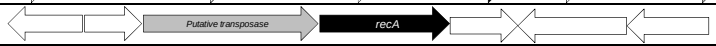
Edwardsiella ictaluri 93 146	CP001600	IS*256* Mutator family	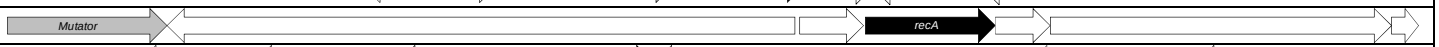
Frankia EAN1pec *recA2*	CP000820	IS*4*	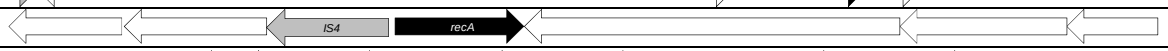
Leptospira borgpetersenii serovar *Hardjo- bovis* JB197	CP000350	IS*110*	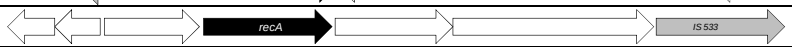
L. borgpetersenii serovar *Hardjo-bovis* L550	CP000348	IS*110*	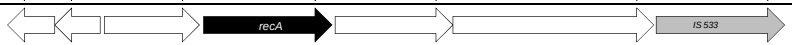
Moorella thermoacetica ATCC 39073	CP000232	IS3/IS*911*	
Microcystis aeruginosa NIES 843	AP009552	IS*As1*	
Mycoplasma gallisepticum str R low	AE015450	Mutator family Mutator family	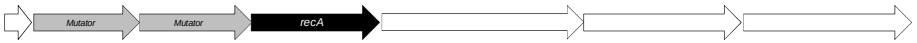
Neisseria meningitidis serogroup C FAM18	AM421808	IS*1655*	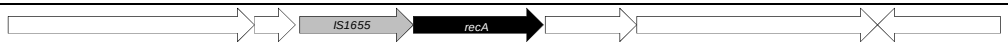
Nitrobacter winogradskyi Nb 255	CP000115	IS*4*	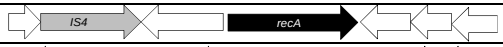
Porphyromonas gingivalis ATCC 33277	AP009380	IS*Pg3*	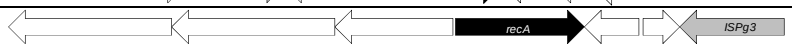
Rhodopseudomonas palustris BisB18[5]	CP000301	-	
Shewanella denitrificans OS217	CP000302	IS*4*	
Shewanella sediminis HAW EB3	CP000821	IS*116*/IS*110*/IS*902*	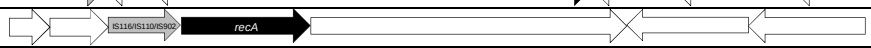

[5] The blue bars in the genetic context denote gcvT elements.

Supplementary Table 11.2. (*continued*)

Organism	Accession no.	Annotated IS family	Genetic context
Streptococcus equi subsp *zooepidemicus* MGCS10565	CP001129	IS*861* orfB IS*861* orfA IS*Sth1* orfA IS*Sth1* orfB	
Wolbachia sp. wRi	CP001391	IS*5*	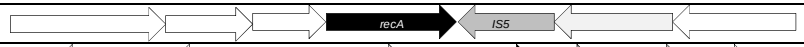
Yersinia enterocolitica subsp *enterocolitica* 8081[6]	AM286415	IS*1329* transposase A IS*1329* transposase B	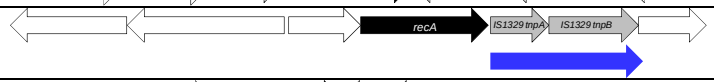
Yersinia pestis Angola	CP000901	IS*285*	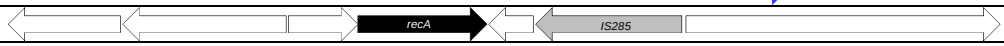

[6] The blue arrow in the genetic context denotes a repeat region encompassing the annotated transposases.

PÁGINA INTENCIONALMENTE DEIXADA EM BRANCO